• U C • FCTUC FACULDADE DE CIÊNCIAS E TECNOLOGIA UNIVERSIDADE DE COIMBRA

Interplay between the Ubiquitin-Proteasome System and mechanisms of neurodegeneration in the context of Machado-Joseph disease

Márcio Paulo Simões Baptista

Departamento de Ciências da Vida da Faculdade de Ciências e Tecnologia da Universidade de Coimbra

Tese de Doutoramento em Biologia, especialidade em Biologia Celular

Trabalho efectuado sob a orientação da

Professora Doutora Patrícia Espinheira de Sá Maciel
Professora Associada
da Escola de Ciências da Saúde,
Universidade do Minho, Braga, Portugal.

e co-orientação do

Professor Doutor Carlos Bandeira Duarte
Professor Associado com Agregação
da Faculdade de Ciências e Tecnologia,
Universidade de Coimbra, Coimbra, Portugal

Setembro de 2013

À Ana Maria e ao Humberto

Agradecimentos/Acknowledgments

À Professora Patrícia Maciel por me ter aceite no seu laboratório, pelo apoio, paciência e por ter sempre uma atitude positiva e construtiva comigo! Pela liberdade de escolha que me deu quando cheguei ao seu laboratório e pela disponibilidade para ouvir novas ideias e deixar que elas se concretizem.

Ao Professor Carlos Duarte pela sua constante presença ao longo dos últimos anos, principalmente nos momentos mais difíceis, pela inspiração e motivação que sempre me transmitiu.

À Professora Sandra Ribeiro por me ter recebido no seu laboratório e pelo apoio e disponibilidade.

Aos meus pais, a Ana Maria e o Humberto, e ao meu irmão Miguel porque serão sempre a minha grande inspiração e a quem dedico esta tese.

To all my labmates in Bristol: Tex, Matt, Anna, Dan, Minos, Ellen, Keri, Tom, Nadia. For all the help in the lab, and also for helping the old guy to easily adapt to a new country.

A todos os colegas do ICVS de Braga pelo apoio, companhia e incentivo: Sofia, Anabela, Andreia Carvalho, Sara Silva, Diogo e Carlos Bessa. Ao Miguel pelo seu contributo para o meu trabalho, e por ser um bom amigo.

Aos colegas das *C. elegans:* Adriana, Ana Jalles e Bruno pelo apoio, companheirismo e boa disposição e também por me deixarem ouvir rádio que não a rádio comercial de vez quando!

À Andreia Castro pela inspiração e apoio que sempre me deu, e pela sua disponibilidade!

Aos colegas do Porto (alguns também de Braga) pelo apoio, por me terem recebido bem no IBMC e pelo companheirismo que sempre tiveram: Joaninha Fraga, Vanessa, Zsuzsa, Sara, Joana, Diogo, Miguel, Nandinho, Xana. Bruno obrigado pelo companheirismo e apoio que sempre deste. Ana obrigado pelo apoio e paciência!

À Rita que foi sempre uma grande inspiração para mim e que contribui para que isto se concretizasse!

À minha família pela companhia dos domingos e por estarem sempre ao meu lado. Ao meu avô José Eduardo e á minha Avó Lena pelo carinho que sempre me deram!

Aos amigos de sempre e também aos que fui fazendo por continuarem por perto e me ajudarem a levar tudo por diante!

Interplay between the Ubiquitin-Proteasome System and mechanisms of neurodegeneration in the context of Machado-Joseph disease

Abstract

The Ubiquitin-Proteasome System is a major intracellular pathway for regulated protein turnover. This system is essential for maintaining cellular homeostasis and signaling. Varying the ubiquitin linkage type and chain length influences the fate of ubiquitylated substrates. Substrate ubiquitylation can be reversed by the action of Deubiquitylating Enzymes (DUBs). DUBs act by editing or disassembling polyubiquitin chains, and are responsible for cleaving ubiquitin precursors, avoid target substrate degradation, editing of the ubiquitin chain at proteasome entrance and for the generation of free ubiquitin pools.

The role of the UPS in nervous system disease has been characterized over the last years, and in particular concerning polyQ disorders has been extensively described, starting with evidence that components of the UPS were consistently found in misfolded protein aggregates. Ataxin-3 (ATXN3) is a DUB present in all or most tissues in humans and mice. Functions of ATXN3 range from the editing of polyubiquitylated proteins, sequestering aggregated proteins in aggresomes and modulating E3 ubiquitin ligases, to regulating protein degradation and stress response, determining cell adhesion and cytoskeletal structure, modulating cell differentiation and regulating transcription. Expansion of a polyglutamine tract in ATXN3 results in the development of the neurodegenerative disease Machado-Joseph disease (MJD), also called spinocerebellar ataxia type 3, the most common dominantly inherited ataxia worldwide.

The aims of this work were the identification of the putative roles of the UPS in neurodegeneration, namely through the identification of a new binding partner for ATXN3, the characterization of the influence of another DUB (UCH-L1) in MJD, and the role of the UPS in Glutamic Acid Decarboxylase (GAD) cleavage upon calcium deregulation/excitotoxicity.

In this study we identified a new molecular partner for ATXN3, the molecular chaperone HSP60. The interaction is direct and through the catalytically active domain of ATXN3, the Josephin domain. ATXN3 was able to interact with both the monomeric HSP60 as with the heptameric form of HSP60. This interaction might unravel new aspects of the interplay between molecular chaperones and the UPS and, with the second determining proteins' fate after the recognition of altered proteostasis by the first.

Ubiquitin C-terminal Hydrolase 1 (UBH-1) is the *C. elegans* orthologue of vertebrate ubiquitin carboxyl-terminal hydrolase 1, an enzyme that besides its deubiquitylating activity also works

as a monoubiquitin stabilizer, and ubiquitin-ligase. This DUB has been described to be involved in the etiology of Parkinson Disease due to altered enzymatic activity, and is also described as an essential component of the synapse. Restoring UCH-L1 protein levels lead to improvements in synaptic transmission in Alzheimer's disease models. The upregulation of proinflammatory genes and the overload of reactive oxygen species are a known hallmark in most neurodegenerative diseases and also in MJD. Cyclopentenone prostaglandins are metabolites of prostaglandin D2 (PGD2), some of which, such as 15-deoxy-Δ12,14-PGJ2 (15d-PGJ2), have been described as modulators of UCH-L1 activity, also leading to its unfolding and aggregation and also as inducers of the production of intracellular reactive oxygen species. In our work we evaluated the specific contribution of UBH-1 (*Caenorhabditis elegans* homologue of UCH-L1) as a possible modifier of MJD in a nematode model of the disease. We found that upon 15d-PGJ2 treatment, that was able to induce oxidative stress in our reporter strains, no alterations in terms of animal motility or ATXN3 aggregation were observed. These results might be related with the redundancy in functions that UCH-L1 shares with the close related UCH-L3.

The characteristic neurodegeneration in MJD is characterized by molecular alterations that interfere with transcriptional regulation, protein aggregation and clearance, perturb UPS function and deregulate calcium homeostasis. In MJD calcium deregulation is relevant, as expanded ATXN3 binds aberrantly to type 1 inositol 1,4,5-trisphosphate receptor (InsP3R1), a calcium channel involved in diverse cellular functions, and induces calcium release by sensitizing the receptor to its natural ligand (InsP3). Consistently, treatment with a specific inhibitor of calcium release from the sarcoplasmic reticulum in skeletal muscles improves the behavior of MJD mice.

The activity of the proteasome has been shown to be downregulated in ischemia and inhibition of the proteasome has proven to be protective in focal brain ischemia, situations where calcium deregulation is critical. More recently, it was described that excitotoxic stimulation leads to the disassembly of the 26S proteasome in its subunits, and activation of extrasynaptic N-methyl-D-aspartate receptors (NMDA) is responsible for toxicity. We wanted to evaluate the contribution of the UPS to calcium deregulation and specifically to the described cleavage of Glutamic Acid Decarboxylase, the enzyme responsible for γ-Amino Butyric Acid (GABA) synthesis, the main inhibitory neurotransmitter in neuronal transmission. We found that excitotoxic stimulation with glutamate of cultured hippocampal neurons from rat lead to a time-dependent cleavage of the two enzyme forms (GAD65 and GAD67) leading to altered distribution in neurites. This cleavage was inhibited in the presence of proteasome and E1 activating enzyme inhibitors, thus indicating a role for the UPS in the calpain-mediated processing of GADs.

In summary, this work has contributed for the discovery of new links between UPS components and neurodegenerative processes.

Keywords: Ubiquitin-Proteasome System; Neurodegeneration; Machado-Joseph disease

Interacção entre o Sistema Ubiquitina-Proteosoma e mecanismos de neurodegenerescência no contexto da doença de Machado-Joseph

Resumo

O Sistema Ubiquitina-Proteosoma (SUP) é um dos maiores sistemas de degradação regulada de proteínas. O sistema é essencial para a manutenção da homeostase e sinalização celulares. O tipo de ligação entre ubiquitinas e o seu comprimento vão definir o destino dos substratos ubiquitinados. A ubiquitinação de substratos pode ser revertida pela acção das enzimas desubiquitinadoras (DUBs). As DUBs podem actuar através da edição ou desmontagem das cadeias de poli-ubiquitina, são responsáveis pela clivagem dos precursores de ubiquitina, por evitar a degradação de substratos-alvo, pela edição das cadeias de ubiquitina à entrada do proteossoma e também pela manutenção das reservas celulares de ubiquitina livre.

O papel do SUP nas doenças do sistema nervoso tem sido caracterizado ao longo dos últimos anos, e em particular nas doença de expansão de poliglutaminas, tendo começado por evidências de que componentes do SUP faziam parte dos agregados de proteínas desnaturadas. A ataxina 3 (ATXN3) é uma DUB presente em todos ou quase todos os tecidos do corpo humano e do murganho. As funções da ATXN3 vão desde a edição das proteínas poli-ubiquitinadas, ao sequestro de proteínas agregadas em agregossomas, à regulação da degradação proteica e resposta ao stress, à determinação da adesão celular e da estrutura do citoesqueleto, à modulação da diferenciação celular, até à regulação da transcrição. A expansão de um tracto de poliglutaminas na ATXN3 resulta no desenvolvimento de uma doença neurodegenerativa, a Doença de Machado-Joseph (DMJ), também chamada Ataxia Espinocerebelosa Tipo 3, uma das ataxias mais comuns no mundo.

Os objectivos deste trabalho foram a identificação de possíveis pontos de envolvimento do SUP em processos de neurodegenerescência, nomeadamente através da identificação da interacção entre a ATXN3 e uma chaperone molecular, a caracterização da influência de uma outra DUB (UCH-L1) na DMJ, e o papel do SUP na clivagem da Descarboxilase do Ácido Glutâmico (DAG) em situações de desregulação do cálcio celular/excitoxicidade.

Neste estudo foi identificado um novo parceiro molecular da ATXN3, a chaperone molecular HSP60. A interacção é mediada pelo domínio catalítico activo, o domínio Josefina. A ATXN3 interactuou tanto com a forma monomérica como com a forma heptamérica da HSP60. Esta interacção pode levar à descoberta de novos mecanismos na interligação entre as chaperonas

moleculares e o SPU, com o último a determinar o destino das proteínas depois do reconhecimento pelas primeiras da alteração na proteostase.

A Hidrolase de Ubiquitina do terminal Carboxílico 1 (UBH-1) é o ortólogo da UCH-L1 dos vertebrados, uma enzima que para além da sua actividade de DUB também funciona como estabilizador de mono-ubiquitina, e como ligase de ubiquitna. Esta DUB tem sido descrita como estando envolvida na etiologia da Doença de Parkinson devido a alterações na sua actividade enzimática, e está descrita também como sendo um componente essencial da sinapse. A restauração dos níveis proteicos de UCH-L1 leva a um melhoramento na transmissão sináptica em modelos da Doença de Alzheimer. A sobre-expressão de genes pró-inflamatórios e a sobrecarga de espécies reactivas de oxigénio são uma marca reconhecida na maioria das doenças neurodegenerativas e também na DMJ. As Prostaglandinas (PGs) Ciclopentenonas são metabolitos da Prostaglandina D2 (PGD2), algumas das quais, como a 15-desoxi-Δ12,14-PGJ2 (15d-PGJ2), tem sido descrita como modulador da actividade da UCH-L1, também provocando a sua desnaturação e agregação. Neste trabalho avaliámos a contribuição específica da UBH-1 (a homóloga em *C. elegans* da UCH-L1) como possível modificador da DMJ num modelo de nemátode da doença. Verificámos que, sob tratamento com 15d-PGJ2, que foi capaz de induzir stresse oxidativo em estirpes repórter, não houve alterações em termos de motilidade ou agregação da ATXN3 nos animais. Estes resultados podem estar relacionados com a redundância funcional que a UCH-L1 partilha com a relacionada UCH-L3.

A neurodegeneração característica na DMJ é caracterizada por alterações moleculares que interferem com a regulação da transcrição, agregação proteica, perturbam a função do SUP e desregulação da homeostasia do cálcio. Na DMJ a desregulação do cálcio é relevante, dado que a ATXN3 expandida se liga anormalmente ao receptor do tipo 1 de inositol 1,4,5-trifosfato (InsP3R1), um canal de cálcio envolvido em diversas funções celulares, e induz a libertação de cálcio pela sensitização do receptor ao seu ligando natural (InsP3). Em concordância, o tratamento com um inibidor de cálcio específico para o reticulo sarcoplasmático nos músculos esqueléticos melhora o comportamento de murganhos com DMJ.

Tem sido demonstrado que a actividade do proteossoma é diminuída em situações de isquémia e a inibição do proteossoma tem provado ser protectora em isquémia cerebral, situações onde a desregulação do cálcio é critica. Mais recentemente, foi descrito que a estimulação excitotóxica leva ao desmembramento do proteosoma 26S nas suas subunidades, sendo a activação dos receptores N-metil-D-aspartato extra-sinápticos a responsável pela toxicidade. Assim, quisemos avaliar a contribuição do SUP para a desregulação do cálcio celular e especificamente para a clivagem da DAG, a enzima responsável pela síntese do ácido amino-butírico γ (GABA), o principal neurotransmissor inibitório na transmissão neuronal.

Descobrimos que o estímulo excitotóxico com glutamato em culturas primárias de hipocampo de rato leva a uma clivagem dependente do tempo das duas enzimas (GAD65 e GAD67) levando a uma alteração na distribuição das GADs nas neurites. Esta clivagem foi inibida na presença de ininbidores do proteosoma e da enzima activadora de ubiquitina E1, indicando um papel para o SUP no processameento das GADs mediado pelas calpaínas.

Em sumário, este trabalho contribuiu para a descoberta de novas interacções entre componentes do SUP e processos de neurodegenerescência.

Palavras-chave: Sistema Ubiquitina-Proteosoma; Neurodegenerecência; Doença de Machado-Joseph

Table of Contents:

Thesis outline

In this work we focus on the interplay between the UPS and the mechanisms of neurodegeneration, particularly in the context of Machado-Joseph disease.

The Ubiquitin-Proteasome System plays a particularly relevant role in the nervous system, and in the etiology and pathology of neurodevelopmental and neurodegenerative diseases. In this thesis the role of the UPS in normal and diseased nervous system is explored in the Introduction. A role for the UPS in the clearance of misfolded or unfolded proteins in normal or diseased conditions is well established. For the identification of proteins in these conditions, the cooperation with other molecular systems is required, namely with the molecular chaperones, which are responsible for the recognition of nonnative proteins conformation. The cooperation between the UPS and chaperones is thus essential when the last are not able to help proteins reach their native state. We tested the interaction between the deubiquitylase involved in the etiology of Machado-Joseph disease – ataxin-3 – and a molecular chaperone that plays a fundamental role in mitochondrial proteostasis - Heat Shock Protein 60 (HSP60). Another relevant player in neurodegeneration is calcium signaling and homeostasis, and also here the UPS can act as a downstream effector, since its components are directly regulated by calcium [1–4]. We wanted to specifically evaluate the contribution of the UPS in the cleavage of Glutamic Acid Decarboxylase (GAD), the key enzyme in the synthesis of γ-aminobutiric acid (GABA) which is the main inhibitory neurotransmitter in the vertebrate nervous systems, with relevance for excitotoxicity [5]. One relevant component of the UPS, particularly in the brain where it represents 1-2% of the total soluble protein [6], is Ubiqutin carboxy-terminal hydrolase L1 (UCH-L1). This deubiquitylase [7] has other putative roles in cells, acting also as a monoubiquitin stabilizer [8] and as an ubiquitin ligase [9]. Its role in neurodegeneration, namely the close association with Parkinson Disease, and the potential demonstrated in the improvement of synaptic transmission in Alzheimer´s Disease [10], could be indicative of a broader implication in neurodegeneration and our objective was to assess the effects of deletion or modulation of UBH-1 (UCH-L1 *C. elegans* homologue) by prostaglandins in our *Caenorhabditis elegans* model of Machado-Joseph disease [11].

Chapter 1

General Introduction

This chapter is partially based on the published (peer-reviewed) review article:

Baptista M, Duarte C and Maciel P. "Role of the ubiquitin-proteasome system in nervous system function and disease: using *C. elegans* as a dissecting tool". Cellular and Molecular Life Sciences, 69(16):2691-715, 2012.

General Introduction

The UPS is an evolutionarily conserved and tightly regulated biochemical pathway that modulates the levels of critical proteins in specific cellular contexts and is responsible for the degradation of irreversibly damaged proteins. Ubiquitylation can also be uncoupled from proteasomal degradation, regulating protein location and activity. Although the relevance of this system in neuronal function and in several disorders of the nervous system is becoming increasingly evident, in most cases the identity of the molecular players and the detailed mechanisms of UPS regulation remain to be clarified.

1. The ubiquitin-proteasome system

Degradation of proteins via UPS involves two steps: (1) covalent attachment of ubiquitin to the target protein and (2) degradation of the ubiquitin-tagged protein by the 26S proteasome, with release of re-usable ubiquitin, by the action of deubiquitylating enzymes (DUBs). Two main structures are part of the 26S proteasome: the core or 20S particle, responsible for protein hydrolysis, and the 19S regulatory particle, which is involved in the recognition of the substrate [12]. The *C. elegans* 26S has 14 conserved subunits in the 20S core and 18 conserved subunits in the 19S core. The interactions between subunits within the 26S complex have been identified recurring to two-hybrid-based protein interaction mapping [13].

The tagging of a protein for degradation is regulated by consecutive action of three classes of enzymes: E1, E2 and E3. First, ubiquitin is adenylated by an ubiquitin-activating enzyme (E1) and transferred to a cysteine residue in the E1, in an ATP-dependent reaction. Two mammalian E1 enzymes were described until now [14,15], in contrast with *C. elegans,* where the *uba-1* gene encodes the sole E1 enzyme [16,17]. Activated ubiquitin is then transferred to a cysteine residue on the ubiquitin-conjugating enzyme (E2) through formation of a thioester bond with the glycine 76 of ubiquitin. Members of the E2 family have a highly conserved ubiquitin-conjugating catalytic fold (UBC), which is responsible for the binding to activated ubiquitin, to E1s and ubiquitin ligases (E3s) [18]. A total of 35 E2s have been described until now in humans [19], whereas in *C. elegans* there are 22 proteins with homology to ubiquitin-conjugating enzymes, based on the criteria of having a UBC motif and the catalytic cysteine residue that accepts activated ubiquitin. Furthermore, three variant E2s exist in *C. elegans* that lack the cysteine residue but share the UBC fold [16,20]. After conjugation, ubiquitin-loaded E2s selectively interact with E3s that recruit and bind specific substrates. Ubiquitin is transferred from the E2 to a

cysteine residue located in the active site of the E3 prior to transfer to a lysine residue on the target protein. There are about 617 putative E3s in humans, as described in a genome-wide screen based on the presence of specific catalytic domains [21]. Although the number of E3s present in *C. elegans* is not yet very clear, until now a few hundreds were suggested [22,23]. Ubiquitin ligases are classified in three classes according to the characteristics of their catalytic domain: RING finger, U-Box or HECT. RING domain are the most abundant E3s and may exist as monomeric RING fingers or as complexes. In the latter E3s the RING domain binds E2 but the other subunit is responsible for the interaction with the substrate [24,25]. Through the use of ubiquitin fusion degradation substrate – Ubi-GST – it was found that in the presence of solely E1, E2 and E3 enzymes, the majority of ubiquitin-protein conjugates contained only one to three ubiquitins. For efficient further elongation an extra enzyme was needed - UFD2 – that was termed an E4 [26]. E4s constitute an extra class of enzymes in the UPS that are necessary in specific contexts for efficient transition from mono to polyubiquitylation [27].

Ubiquitin is covalently attached to the target protein via an isopeptide bond between its C-terminal glycine and a lysine in the target protein. After the attachment of the first ubiquitin others can bind to the target protein, since a substrate can be multi-ubiquitylated in several lysine residues, or polyubiquitylated at a single residue. In the latter case, E3s can elongate the ubiquitin chain by creating ubiquitin-ubiquitin isopeptide bonds. Ubiquitin has seven lysine residues (Lys6, Lys11, Lys27, Lys29, Lys33, Lys48 and Lys63) and the assembly of a chain with at least four ubiquitins linked through their Lys48 targets the protein for proteasome degradation [28,29]. Proteins that are monoubiquitylated or containing Lys63-linked ubiquitin chains are known to be directed to the regulation of intracellular traffic or transcription, and to DNA repair [30,31]. In some instances, monoubiquitylation also enhances protein activity [30,32]. Although the UPS can negatively regulate transcription by downregulating the levels of transcriptional activators [33], monoubiquitylation often leads to increased potency of these activators [34,35]. This occurs because proteasomal ATPase destabilizes activator-promotor complexes [36] and activator monoubiquitylation protects it from this destabilization [37].

Recent evidence show that unconventional ubiquitin chains, linked through different lysines - Lys6, Lys11, Lys27, Lys29, Lys33 - can also direct proteins to proteasomal degradation, both in *S. cerevesiae* [38] and in 26S knockout mice [39]. Whether Lys63-linked chains may also target proteins to proteasomal degradation is still controversial [40,41]. The conflicting results that have been published may arise from the fact that proteins targeted with Lys63 chains are degraded by the proteasome less efficiently, due to reduced accessibility and increased deubiquitylation rates [42]. There are also polyubiquitin chains formed by the ligation of more than one lysine

residue, referred as mixed-linkage chains [41]; these are relevant for protein endocytosis and to promote or avoid protein degradation [43–45]. Although ubiquitylation is emerging as a very important mode of regulation of protein activity in cells, akin to phosphorylation and involving an equivalent amount of molecular players (as described below), the "ubiquitin code", i.e. the correspondence between the type of ubiquitin chain bound to a given protein and its effect, remains to be fully clarified.

Polyubiquitin chains can be totally removed or their length reduced, disassembly occurring through the action of DUBs. These play an important role in cell homeostasis, on the one hand regenerating free ubiquitin for re-use by the UPS, and on the other facilitating substrate entrance into the proteasome since the removal of poly-ubiquitin chains by proteasome-associated DUBs precedes the access of unfolded proteins to the proteolytic chamber of the 20S proteasome. DUBs can also protect Lys48-linked polyubiquitin-conjugated proteins from degradation at the proteasome [46,47]. A chain-editing activity for DUBs has also been described, as highlighted by the *in vitro* studies of human ataxin-3 by Winborn and co-workers [48]. Another recent study further supports this notion by demonstrating that *C. elegans* ataxin-3 is also involved in ubiquitin chain editing, producing chains of three to four ubiquitins (that might promote protein degradation), revealing an evolutionarily conserved mechanism of action for this DUB [49].

DUBs can be sub-divided in five classes: four are cysteine proteases while the other class comprises metalloproteases (jab1/MPN domain-associated metalloisopeptidase class (JAMM)). Based on their ubiquitin protease domain cysteine proteases can be further divided in ubiquitin C-terminal hydrolases (UCHs), ubiquitin-specific proteases (USPs), otubain proteases (OTUs) and Machado-Joseph disease proteases (MJDs). Mammalian genomes encode approximately 100 DUBs [50], while in *C. elegans* there are predictions of 53 putative DUBs [22].

The UPS is responsible for the vast majority of regulated protein degradation. It is involved in the degradation of regulatory, short-lived and aberrant proteins, playing a critical role in the maintenance of cellular homeostasis. Regulation of cell cycle, intracellular signaling, DNA damage response and transcription are major known roles of the UPS [51–55]. In addition to assuring that basic cell function is preserved, the UPS also contributes to the response to insults such as ischemia, oxidative stress, DNA damage, inflammation and others [56–59].

The UPS assumes a particularly important role in the context of the nervous system. The fact that neurons in the adult nervous system do not have the capacity to divide makes the machinery responsible for protein quality control particularly relevant. In addition, UPS

degradation of key components seems to be necessary for axonal pathfinding, synaptogenesis, synaptic plasticity, and other neuron-specific activities. In the next sections we will give examples of the contribution of the UPS for nervous system physiology.

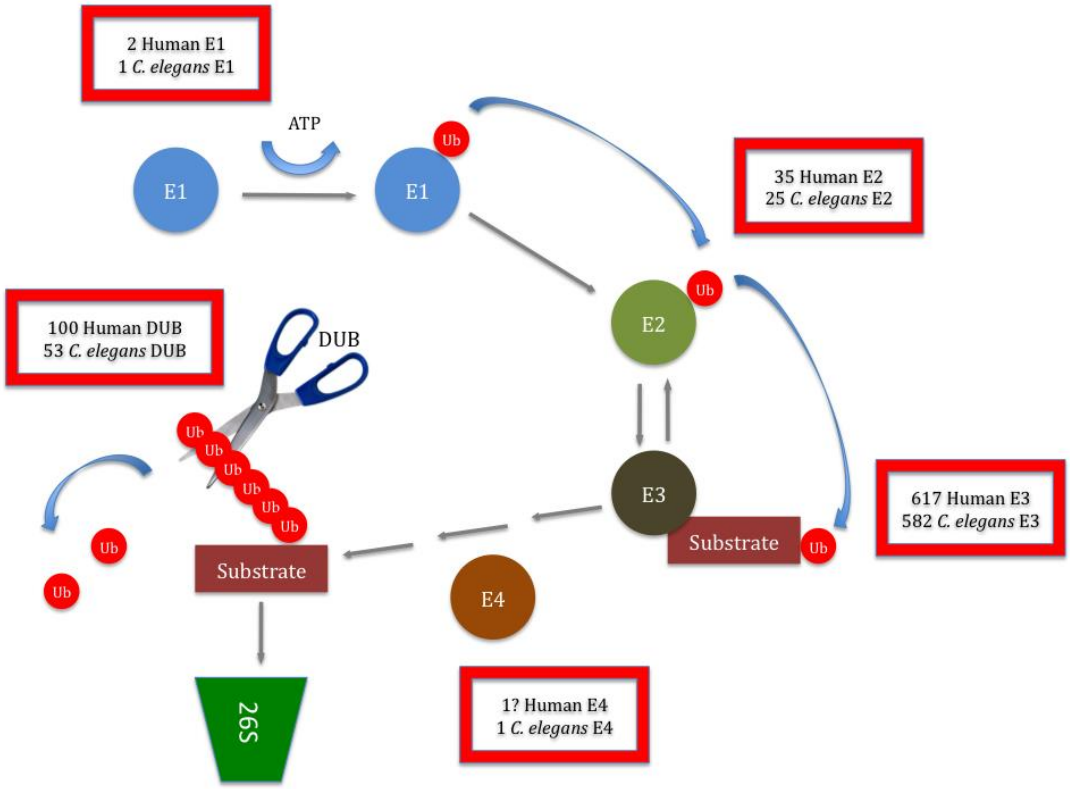

Fig. 1. Comparison of the UPS between humans and in *C. elegans*. E1s for both species are already identified and characterized. *C. elegans* E2s were identified based on the criteria of having a UBC motif and the catalytic cysteine residue that accepts activated ubiquitin, and their function has been determined recurring to RNAi studies; Human E2s were identified through sequence homology using E2 protein sequences from *C. elegans* and *Arabidopsis thaliana* as an initial set. Predictions for E3s number in humans and *C. elegans* were made based in a genome-wide screen based on the presence of specific catalytic domains. One E4 was described and characterized until now in each species, although it is possible that many more exist.

1.1- The UPS in the developing nervous system

The function of the nervous system relies on its precise connectivity. The formation of the neuronal networks present in the adult nervous system is a highly dynamic and tightly regulated process, involving the development of neurons with polarised morphology, axon pathfinding and the establishment of an intricate network of synaptic connections. The UPS has emerged as a crucial component in the regulation of the developing nervous system [60] by controlling the proliferation of neuronal precursors and cell specification [61–65] neuronal migration [66,67], neuritogenesis [68–74] and synaptic pruning [75–77]. E3 ligases are particularly relevant during the development of the nervous system, selecting key regulators for posterior proteasomal degradation or directing these proteins for specific signalling cascades. The E3 ligases involved in the processes of neural development are listed in table 1.

Axons must then find their target in an environment of negative and positive cues. The axons that fail to hit a target must be dismantled whereas those that reach their target form functional synaptic contacts [78–80]. Given the key role of the UPS in the regulation of the protein content in the cytoplasm and in the nucleus, it is not surprising that it also contributes to this and other aspects of neuronal development. Thus, during the establishment of neuronal polarity in cultured rat hippocampal neurons the degradation of Rap1b-GTPase by the UPS, mediated by E3 Smad ubiquitylation regulatory factors 1 and 2 (Smurf1 and Smurf2), defines which neurites become the axon and which are dismantled; only neurites with an accumulation of active Rap1B-GTP are viable [71].

The axon guidance cues netrin-1 and semaphorin 3A are involved in the regulation of growth cone guidance both in *Xenopus* [81,82] as well as in mammals [83]. The growth cone collapse inducer L-α-lysophosphatidic acid (LPA) is also involved in this regulation [84], and both netrin-1 and LPA upregulate the amount of ubiquitin conjugates in growth cones. Inhibition of the proteasome was shown to abolish the attraction of retinal growth cones towards a netrin-1 gradient [85] showing a role for the UPS in the tightly regulated control of protein synthesis/degradation necessary for correct axon guidance.

Major contributions to the understanding of nervous system formation came from studies using *C. elegans* as a model organism. This is illustrated by the studies of Shen and co-workers to discover how precise synapse connectivity is established during development. This group first identified the SYG-1 protein (homologous to vertebrates' NEPH1) as a relevant player in synaptic specificity [86], and additional studies showed SYG-1 as a partner of SKR-1, the core

component of Skip1-cullin-F-Box (SCF) E3, during the establishment of hermaphrodite-specific motor neuron (HSNL) synapses. This interaction interferes with the assembly of the SCF complex and as a consequence there is a decrease in synapse elimination in the area where synapses are formed in the adult animal, the primary synapse region (PSR). In these studies it was suggested that the SCF is rate-limiting for synapse elimination in a proteasome-dependent manner. In the area surrounding the PSR – the secondary synapse region - synapses are more likely to be eliminated due to the absence of SYG-1 and consequent presence of more functional E3 [77].

Another E3 that has been implicated in neuronal development, the Regulator of Pre-synaptic Morphology-1 (RPM-1), is localized to pre-synaptic terminals in *C. elegans* neurons [87]. In *rpm-1 C. elegans* mutants the extension and stabilization of synaptic branches are disrupted and an alteration in synaptic vesicle localization is also observed. Furthermore, in this model the neurons do not form correct mature synapses at the right time and place [88]. More recent evidence identified the specific partners of this E3 in the regulation of axon outgrowth: RPM-1 seems to act by negatively regulating UNC-5/UNC-5 and SAX-3/robo-mediated axon outgrowth-promoting activity [89]. Another target of RPM-1 regulation is GLO-4, a Rab guanine nucleotide exchange factor. The interaction between these proteins is thought to activate the GLO pathway with RPM-1 acting as a positive regulator, promoting vesicular trafficking essential for correct axon termination and synaptogenesis in mechanosensory neurons [90]. RPM-1 forms a SCF-like complex E3 ligase with the F-box protein FSN-1 , the SKP1 ortholog SKR-1 and the Cullin CUL-1 [91] and besides its role in the regulation of axon outgrowth RPM-1 also acts as a negative modulator of a MAP kinase cascade that regulates pre-synaptic architecture, including the Dual-Leucine zipper Kinase MAPKKK (DLK-1), MKK-4, and the p38 MAPK ortholog, PMK-3 [75].

In the context of nervous system development, DUBs also play an important role, with relevant examples in most DUB classes. Repressor element 1-silencing transcription factor (REST) plays a key role as a transcriptional repressor of neuronal differentiation-associated genes [92]. REST is targeted for proteasomal degradation by the E3 SCF-β-TrCP. The ubiquitin-specific protease Herpesvirus-Associated Ubiquitin-Specific Protease (HAUSP) - also termed ubiquitin-specific protease 7 (USP7) - negatively regulates REST ubiquitylation, promoting REST stabilization and thus preventing neural precursor cell differentiation [93].

Ubiquitin C-terminal hydrolase 37 (Uch37*)* was identified as essential for early nervous system development in mouse. The complete deletion of Uch37 resulted in prenatal lethality resultant from deficient formation of the telencephalon, mesencephalon and metencephalon [94]. In the group of metalloprotease DUBs, associated molecule with the SH3 domain of STAM (AMSH) [95]

was identified as essential for postnatal development in mice. *AMSH* deficient mice generated by gene targeting are normal at birth but have postnatal growth retardation and die prematurely. These mice show significant loss of CA1 hippocampal neurons at day 6. Hippocampal neurons cultured *in vitro* were unable to survive without the presence of AMSH while other cell types were able to survive, further suggesting a role for this DUB in the normal development of these neurons. Also, neuron numbers in the cerebral cortex were significantly reduced in sixteen day old AMSH $^{-/-}$ mice, revealing an important role for this DUB in the neuronal cell survival in the hippocampus and cerebral cortex [96].

UPS component	**Mechanism of action**	**References**
Neural stem and progenitor cells		
SCF-bTRCP	REST/NSFR is a master repressor of neural gene expression; SCF-bTRCP is responsible for UPS-mediated REST degradation, allowing derepression of pro-neural REST targets	[61]
HUWE1	HUWE1 supression of a N-Myc-DLL3 cascade, setting cell-cycle withdrawal and neuronal differentiation, restrains proliferation and enables neuronal differentiation	[64]
BTBD6	BTBD6 acts as an adaptor protein in the SCF E3 ligase complex and targets the transcriptional repressor and neurogenesis inhibitor Plzf for degradation	[65]
MIB1	RING-type E3 MIB1 expressing cells generate Notch signalling in neighboring radial glial cells to maintan their stemness and correct differentiation	[63]
TRIM11	TRIM11 mediates the degradation of the development regulator transcription factor Pax6	[62]
Neural cell migration		
E3 ligase complex containing cullin 5	Cul5 auxiliates Dab1 dgradation in target neurons after a signalling cascade that involves VLDR and ApoE receptors, directing the speed and correct migration of neuronal populations	[66,67]
Axonal growth		
RPM-1	RPM-1 E3 ligase negatively regulates axon outgrowth by the guidance receptors SAX-3/robo and UNC-5/UNC-5	[89]
CDH1-APC complex	Ubiquitin ligase CDH1-APC operates in the nucleus of neurons to inhibit axon	[69,70]

	growth through the promotion of transcription factors SnoN and Id2 degradation	
NEDD4	NEDD4 acts as a positive regulator of dendrite extension and arborization through the ubiquitination of RAP2A and PTEN downregulation	[72,73]
SMURF1	SMURF1 enhances neurite outgrowth ubiquitinating RhoA	[68]
SMURF2	SMURF2 ubiquitinates RAP1B directing it to proteasomal degradation, assuring that only one neurite will become an axon	[71]
Synaptic prunning		
DIAP1	E3 ligase DIAP1 degradation, mediated by UBCD1 conjugating enzyme, leads to a caspase-dependent efficient prunning of C4da neuron in *Drosophila*	[76]
RPM-1	RPM-1 E3 ligase negatively regulates a p38 MAPK pathway contibuting to the correct formation of mature synapses in *C. Elegans*	[75]
SKR1	SKR-1, a core component of SCF E3 contibutes to synapse elimination in a proteasoem-dependent mannerin HSNL	[77]

Table 1 – List of E3 ligases involved in the processes of neural development.

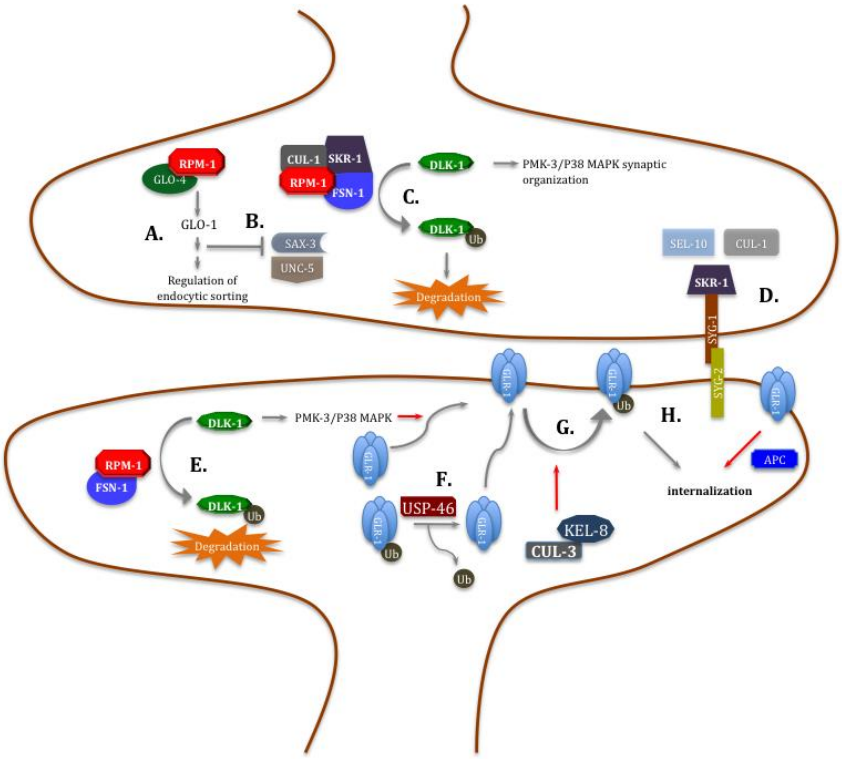

Fig. 2. Major contributions of *C. elegans* to the current understanding of the role of the UPS in the synapse. a) RPM-1 a RING finger domain protein regulates pre-synaptic differerentiation by interacting with GLO-4 (Rab GEF), that promotes vesicule-specific membrane proteins trafficking through GLO-1 and AP-3; this pathway is involved in the regulation of axon termination and synaptogenesis. **b)** RPM-1 co-ordinates axon outgrowth by negatively regulating SAX-3 and UNC-5 guidance receptors; this is achieved by controlling vesicular trafficking via the GLO-4 pathway**. c)** RPM-1 contributes to regulate pre-synaptic architecture by forming, with FSN-1 and SKR-1, an SCF complex ubiquitin ligase that leads to DLK-1 ubiquitination and consequent downregulation, thus inhibiting the MAP kinase cascade that includes MKK-4 and PMK-3, known to be involved in synaptic organization. **d)** The transmembrane adhesive molecule SYG-1 determines synaptic sites by preventing SCF^{SEL-10} ubiquitin ligase complex assembly and synapse elimination, through its interaction with SKR-1. **e)** RPM-1 and FSN-1, working as an E3, negatively regulate DLK-1 and consequently the p38MAPK pathway thus leading to GLR-1 accumulation in neurites. **f)** The deubiquitylase USP-46 cleaves ubiquitin from GLR-1 receptors thus promoting GLR-1 surface membrane expression and preventing its degradation in the lysosome. **g)** Post-synaptic ubiquitylation of GLR-1, in a mechanism that requires KEL-8, negatively regulates its levels in the membrane by promoting internalization and posterior degradation by the lysosome. **h)** APC E3 ligase promotes loss of GLR-1 containing synapses possibly through the ubiquitination of a scaffold protein associated with GLR-1. Red arrows represent mechanisms/pathways still not fully elucidated.

1.2- The UPS in the mature nervous system

In addition to its function in neurodevelopment, the UPS also plays a critical role in the mature nervous system, namely in pre- and post-synaptic regulation, and in synaptic plasticity [97].

The first evidence of the involvement of the UPS in synaptic function came from studies in *Aplysia* demonstrating that the degradation of Protein Kinase A (PKA) subunits, an event necessary for long-term facilitation, was mediated through the UPS [98]. Not surprisingly, additional studies showed that the UPS is also essential for Long-Term Synaptic Depression in this organism [99].

Studies in *Drosophila* neuromuscular junction demonstrated unequivocally for the first time that UPS components were part of the presynaptic terminal [100]. Chen and co-workers, using rat brain synaptosomes, showed that the influx of calcium following membrane depolarization is rapidly coupled to a general downregulation of ubiquitin-conjugated proteins, and that this effect was reversible [1].

At the presynaptic terminal the influx of calcium is coupled to the release of neurotransmitters by exocytosis of synaptic vesicles. The synapse-localized ubiquitin ligase SCRAPPER was shown to be an E3 for Rab3-interacting molecule 1 (RIM1), a Rab-3 effector involved in exocytosis [101] and known to be part of a calcium sensor complex [102]. Studies using *scrapper*-knockout and *scrapper*-transgenic mice overexpressing the protein in the hippocampus showed that this E3 regulates the levels of RIM1 thus affecting presynaptic vesicle release [103]. Loss of this E3 increased the frequency of miniature excitatory postsynaptic currents (mEPSCs) and reduced paired pulse facilitation in hippocampal neurons, as a consequence of the increased release probability. This led to anxiety and altered contextual fear-conditioning in heterozygous SCR KO mice [104].

In *Drosophila*, the E3 anaphase-promoting complex (APC), besides its role in cell cycle regulation [105], is also involved in the regulation of synaptic growth in neuromuscular junctions, with Liprin-α as effector and possible substrate. APC mutants showed increased levels of the alpha-amino-3-hydroxy-5-methyl-4-isoxazolepropionic acid receptor (AMPAr) subunit GluA2 at the post-synaptic level, which increased the sensitivity to the neurotransmitter glutamate [106].

The activation of post-synaptic receptors by neurotransmitters released from nerve terminals induces several downstream signaling cascades. These events alter the composition of the post-synaptic compartment, and the UPS is required for these changes. The use of *C. elegans* as a model organism provided significant contributions in the elucidation of some of these

mechanisms, including the first reports of ubiquitylation of AMPAr, of great relevance for the current understanding of synaptic plasticity mechanisms. Burbea and co-workers demonstrated *in vivo* the ubiquitylation of GLR-1, the *C. elegans* non-NMDA receptor subunit most similar to mammalian AMPAr [107] resulting in removal of the receptors from the synapse [108]. The mechanism of GluA1 AMPA receptor endocytosis was recently described in vertebrates and it was demonstrated that ubiquitylation is also required for internalization of surface AMPA receptors in response to AMPAr agonist [109]. Studies conducted in *C. elegans* also showed that the internalization of GLR-1 is mediated by KEL-8 and that this protein forms a complex with the CUL-3 subunit of the CDL3 ubiquitin ligase [110]. Other E3s specifically involved in this regulation were also identified in *C. elegans*. Temperature-sensitive mutants in APC E3 ligase subunits showed an increase in GLR-1::GFP puncta in the ventral nerve cord at restrictive temperature. This effect was not observed when blocking endocytosis, suggesting that APC regulates the local recycling of GLR-1 [111].

Besides its role on the organization of the pre-synaptic bouton in *C. elegans* motor neurons [87], RPM-1 is also involved in the regulation of post-synaptic abundance of GLR-1. This mechanism involves the p38 MAPK pathway and is most likely related to the E3 ubiquitin ligase activity of RPM-1, since loss of FSN-1 (the RPM-1 partner in the E3 complex) also results in the same phenotype [112]. LIN-23 is the substrate-binding subunit of a SCF E3 – SCF^{LIN-23}. *lin-23* mutants have increased GLR-1 expression in the ventral nerve cord and in these an increase in the cytosolic pool of β-catenin homolog BAR-1 was observed. In *bar-1*;*lin-23* double mutants a smaller increase in GLR -1 puncta was observed compared with *bar-1* single mutants, suggesting that the effect of LIN-23 on GLR-1 levels is partially mediated through BAR-1. Another Wnt signalling target, the TCF/Lef transcription factor homolog POP-1, was found to mediate the effects of BAR-1 in GLR-1 levels, since *pop-1* mutants significantly decreased the increase of GLR-1::GFP puncta intensity in animals expressing dominant-negative LIN-23. These results suggest an involvement of the Wnt signalling in GLR-1 regulation [113]. A list of the major E3s involved in the regulation of the post-synapse is presented in table 2.

More recently, a DUB was identified that might be regulating AMPAr trafficking in the synapse. The ubiquitin-specific protease 46 (USP-46), homologue to mammalian USP-46, is expressed in *C. elegans* nervous system and regulates the abundance of GLR-1 in ventral nerve cord neurons by deubiquitylating the receptor and thus preventing its internalization [114]. Recent studies showed that the ubiquitin-conjugating enzyme variant UEV1 is also essential for AMPAr endocytosis in *C. elegans* [115]. The ubiquitin C-terminal hydrolase 1 (UCH-L1) is another example of a DUB with a relevant role in the maintenance of nervous system function. Besides its DUB activity [50,116] the enzyme also functions as an E3 ligase in the dimeric form [9] and as a stabilizer

of mono-ubiquitin, the last not requiring enzymatic activity [8]. The expression of AP-Uch (UCH-L1 ortholog) in *Aplysia* increases in sensory neurons after long-term facilitation (LTF) *in vivo* and LTF is inhibited upon AP-Uch blockade [117,118]. In mice, Gong and co-workers discovered that UCH-L1 inhibition reduced both basal synaptic transmission and long term potentiation (LTP) [119]. Moreover, both in APP/PS1 Alzheimer's mice model hippocamapal slices or in amyloid-β treated hippocampal slices UCH-L1 perfusion led to improvement in synaptic function [119]. The fact that treatment with amyloid-β led to a decrease of 70% of mono-ubiquitin levels and that infusion of slices with UCH-L1 prior to amyloid-β treatment blocks this decrease [119] points to UCH-L1 as a critical regulator of mono-ubiquitin availability in the synapse.

E3 ligases	Mechanism of action	References
UBE3A	Neuronal activity promotes UBE3A expression and consequent downregulation of the substrate ARC, known to be involved in AMPAr endocytosis	120,121
APC	APC E3 recruits CDC20 co-factor and regulates the abundance of GLR-1 receptors on the post-synaptic compartment in C. elegans; In Drosophila APC/C is involved in the regulation of synaptic size in NMJ and also in the regulation of pos-synaptic GluA2 levels	106,111,122
PDZRN3A	PDZRN3A synapse-associated RING finger E3 binds to MuSK and downregulates its surface levels thus regulating the post-synaptic dvelopment of the NMJ	123
SCF/LIN23	SCF E3 containing F-box protein LIN-23 regulates GLR-1 abundance in C. elegans ventral cord through the ubiquitination of BAR-1	113
KEL-8/CUL3	KEL-8 binds CUL3 forming a E3 ubiquitin ligase complex that is required for synaptic removal of GLR-1 in C. elegans	110
RPM-1	RPM-1 forms a E3 SCF complex with FSN-1, SKR-1 and CUL-1; RPM-1 inhibits p30 MAPK signaling inducing GLR-1 endocytosis in *C. elegans* synapses	112
MDM2	MDM2 E3 ligase ubiquitinates the scaffolding protein PSD95 upon NMDA activation, leading to its proteasomal degradation thus regulating AMPA receptors synaptic levels	124
FBX2/CHIP	FBX2, a component of SCF E3 ligase complex, binds CHIP E3, and the interaction facilitates GluN1/2 NMDA receptor subunit degradation	125
MIB2	MIB2 ubiquitinates GluN2A and NMDA receptor activity is downregulated by MIB2 in a ubiquitin-proteasome dependent manner	126
TRIM3	Upon neuronal activity the RING-finger-containing E# TRIM3 promotes ubiquitination and proteasome-dependent degradation of the PSD protein GKAP acting as na inhibitor of dendritic spine growth in hippocampal neurons	127
SCRAPPER	SCRAPPER is the F-box component of a SCF E3; SCRAPPER ubiquitinates RIM-1 regulating its levels and controling synaptic vesicle release	103

Table 2. List of E3 ligases involved in the regulation of the post-synapse.

1.3- The UPS in neurological disease

Given the role of the UPS as a major intracellular pathway for degradation of proteins and a critical regulator of neuronal function, as described above, it is not surprising that its dysfunction is associated with several neurological disorders [128,129].

1.3.1- The UPS in neurodevelopmental disorders

Dysfunction of the UPS is associated with several neurodevelopmental disorders resulting from genetic mutations, epigenetic modifications and environmental factors that disturb the normal development, with onset during periods of ongoing maturation. Defects that occur during the establishment of the neuronal networks, either related to migration of neurons and/or to errors in neuronal connections are key factors in the etiology of these diseases [130].

Probably the best-known example of a neurodevelopmental disorder related with the UPS is Angelman Syndrome which, in most cases, is associated with the lack of a functional (and transcriptionally active) copy of the *UBE3A* gene [131]. Ube3A is a E3 found at the synapse and the loss of the maternal *Ube3a* allele leads to synaptic dysfunction in mice [120]. Activity-regulated cytoskeleton-associated protein (Arc), a substrate of Ube3A, is involved in AMPAr endocytosis and acts on the consolidation of LTP through regulation of actin dynamics [132]. Transfection of neurons with a Ube3A shRNA was found to decrease AMPAr expression at the membrane, and this effect was mediated by Arc [121]. The cognitive deficits observed in Angelman Syndrome patients [133] correlate well with the compromised synaptic function and with the cognitive and behavioural deficits in transgenic mouse models of the disease [134–137].

Point mutations and deletions in the UBE2A/HR6A/UBC2 gene, which encodes a E2, were described to be the cause of an X-linked syndrome characterized by intellectual disability, seizures, obesity, marked hirsutism and a characteristic facial appearance [138–141]. Although the function of UBE2A is not fully understood, it has been suggested to play a role in ubiquitin-dependent N-end rule targeting, i.e. the cleavage of proteins with destabilizing N-terminal residues (bulky hydrophobic or basic amino acids), through interaction with UBR1, the E3 binding N-end rule target proteins [142]. Interestingly, UBE2A activity is induced in PC12 cells by treatment with nerve growth factor (NGF) and necessary for the induction of neurite outgrowth by this neurotrophin [143]. The fact that proteasome inhibition also lead to a diminished neurite outgrowth lead to the concept that this E2 plays an active role in the promotion of neurite extension in response to NGF, through enhanced rates of synthesis of ubiquitin-protein conjugates, but by mechanisms other than targeting them for proteasome

degradation. The knockdown of UBE2B (a UBE2A paralogue gene with 80% homology but less abundant in cells) using siRNA also reduced Nerve Growth Factor-induced neurite lengthening in PC12 cells [144]. UBE2B is known to be involved in chromatin structure modification and transcription regulation [122,145], namely through the ubiquitylation of histone H2B, an activity that is shared by UBE2A. Recently, UBE2A (together with the proteasome subunit Psmd6 and the ubiquitin hydrolase Usp33) was also proposed to be at the core of a gene network playing a key role in fear-conditioning in mice, suggesting a role for this protein in learning and memory [146].

Intriguingly, mutations in UBR1, the RING finger E3 that cooperates with UBE2A/HR6A in N-end rule targeting [142,147], have been associated with the Johanson-Blizzard Syndrome which is characterized by intellectual disability as a key feature [148–151]. Patients with this genetic syndrome suffer from congenital exocrine pancreatic insufficiency, growth retardation, hypothyroidism, hearing loss and multiple malformations, such as nasal wing aplasia, oligodontia, cardiac anomalies, scalp defects and imperforate anus, and frequently developmental delay/intellectual disability. UBR1 is a member of the N-recognin class of E3s, proteins that label N-end rule substrates via covalent linkage to ubiquitin, allowing the subsequent substrate delivery to the 26S proteasome. The yeast homologue of Ubr1 is involved in the degradation of misfolded cytosolic proteins and in the regulation of the leucine-mTOR signaling pathway [152–155]. Mice lacking Ubr1 are viable but have defects that include pancreatic insufficiency, whereas mice lacking both Ubr1 and its paralogue Ubr2 die in mid-gestation, with severe disruption of nervous system and cardiovascular development. In the nervous system, cell proliferation, migration and differentiation appeared to be affected [156].

A link between UPS dysfunction and neurodevelopment disease was also found in other subtypes of intellectual disability. An alteration in the *CUL4B* gene was first identified in eight of the 250 families studied in a large project to identify genes causing X-linked intellectual disability [157]. CUL4B forms a complex that functions as an E3 ubiquitin ligase, known to be involved in cell proliferation and regulation of numerous nuclear processes, such as DNA damage response, DNA replication, and chromatin remodeling, through its action as a regulator of proteins involved in these processes, namely chromatin licensing and DNA replication factor 1 (CDT-1) in cell cycle regulation [158,159]. CUL4A and CUL4B were also shown to be components of a conserved Wnt-induced proteasome targeting complex that regulates p27(KIP1) levels and cell cycle progression in mammalian cells [160]. Cells from patients with CUL4B loss of function mutations exhibit sensitivity to camptothecin (CPT), increased Topo I-induced DNA breaks and impaired CPT-induced topoisomerase I (Topo I) degradation and

ubiquitylation, suggesting Topo I to be a novel Cul4-dependent substrate [161]. Cells from these patients also displayed overexpression of other known CUL4-dependent substrates, such as Cdt1 and p21, but how these biochemical findings are linked to the neurophsychological findings in the patients remains unknown.

The Williams–Beuren syndrome is characterized by a recognizable pattern of malformations, that include growth delay, cognitive disabilities and altered social behaviour (hypersociability), among other deficits [162]. The disease results from hemizygosity of more than twenty genes, one of which, Trim50, encodes a E3 ubiquitin ligase, opening the possibility of UPS involvement also in this disease [163].

Froyen and colleagues identified mutations in the *HUWE1* gene in three unrelated families with X-linked syndromic mental retardation [164]. *HUWE1* encodes a HECT domain E3 ligase known to interact with the proteasome [165], namely in the brain [166]. Interestingly, prolonged neuronal activity induced 26S disassembly and dissociation of HUWE1, among other proteins, from the proteasome [166] and this change in UPS composition might be relevant for synaptic plasticity. HUWE1 is known to ubiquitylate histones H1, H2A, H2B, H3 and H4 [167], and to modulate transcription of the preprodynorphin gene [168]. Furthermore, it targets CDC6 (involved in the regulation of DNA replication at the initiation step) [169], MCL-1 (regulating apoptosis)[170,171] and c-MYC [64,172]. In particular, c-MYC targeting appears essential in neurodevelopment, allowing neural precursors to arrest proliferation and enter neurogenesis [64,172]. HUWE1 is also relevant for neuron-radial glia interactions that are key to the proper migration and spatial arrangement of the cerebellar cortex [173]. Accordingly, conditional KO mice lacking HUWE1 in cerebellar granule neuron precursors and radial glia show a high rate of postnatal lethality and profound cerebellar abnormalities, resulting from aberrant proliferation and impaired differentiation of the progenitor cell population, as well as from layering aberrations, with persistence of ectopic clusters of granule neurons, due to severe granule neuron migration defects. Although this has been demonstrated for the cerebellum, a parallel role in other parts of the brain may exist.

Using whole genome copy number variant assessment, in a sample of more than 800 cases of individuals with Autism spectrum disorders (ASDs), mutations were found in four UPS-related genes previously unrelated with the disease: *UBE3A* – the ubiquitin ligase also related to Angelman Syndrome, *PARK2* – a ubiquitin ligase also related to Parkinson's disease (PD), *RFWD2* and *FBXO40* – also ubiquitin ligases. These genes were reported as ASDs candidate genes with altered copy number variants in the patients [174].

A region on chromosome 15q24 vulnerable to both deletions and duplications has been previously implicated in a range of phenotypes including autism, Asperger's syndrome, delayed

development, and mild to severe mental retardation [175]. Recent studies allowed narrowing the critical region and identification of ubiquitin-like 7 as a key gene [176,177]. This protein, also designated BMSC-UbP, contains a UBQ domain at its N-terminus and a ubiquitin-associated domain at its C-terminus. Its role in the nervous system remains unknown.

Overactivation of the UPS in the brain cortex has also been proposed to play a role in Down syndrome (DS), the most common genetic form of intellectual disability, caused by complete or partial trisomy of chromosome 21 [178]. Chymotrypsin and peptidyl-glutamyl peptide-hydrolyzing (PGPH)-like activities of the proteasome are upregulated in the frontal cortex of hAPP-YAC tg mice, which model the overexpression of one of the genes triplicated in DS patients. These proteasome activities were augmented by cholinergic stimulation in control mice, but not in hAPP-YAC tg mice, and a similar up-regulation of the UPS activities was detected in the frontal cortex of DS and Alzheimer's disease (AD) patients. Another link between the UPS and DS comes from the evidence that the tetratricopeptide repeat domain 3 gene, *TTC3*, located in the DS critical region of chromosome 21, encodes an E3 ligase that targets phosphorylated Akt, facilitating its polyubiquitylation and degradation, and inhibits neuronal differentiation through modulation of the Rho A small GTPase pathway. TTC3 physically interacts with Citron kinase (CIT-K) and Citron N (CIT-N), two Rho A effectors known to be involved in neuronal proliferation and differentiation. In PC12 cells, TTC3 overexpression leads to strong inhibition of neurite extension, which can be prevented by CIT-K RNAi [179]. Therefore, the upregulation of TTC3 may contribute to some of the pathological findings, namely the cognitive deficits, present in DS patients. Ubiquitin-specific protease 25 (USP-25) has also been related to DS, with the protein being overexpressed in human DS fetal brains [180].

The role of the UPS in the development of the nervous system, and its clear involvement in neurodevelopmental diseases, opens a whole new field of research concerning the outcomes of a perturbed UPS. As the system becomes better characterized and its involvement in disease increasingly known, its components may become important targets for pharmacological treatment [181–184], as is happening already in the cancer field [185,186].

	Disease	Components of the UPS	*C. elegans* homologue	*C. elegans* neuronal expression	References
Neurodevelopmental	Angelman Syndrome	UBE3A	Y48G8AL.1	expression still not defined	[121,131]
	Williams-Beuren Syndrome	TRIM50	Not described	expression still not defined	[163]
	Intellectual disability non otherwise specified	CUL4B	cul-4	no evidences	[157,187,188]
		HUWE1	eel-1	yes	
	Autism Spectrum Disorders	UBE3A	Y48G8AL.1	expression still not defined	[174,189]
		PARK2	pdr-1	yes	
		RFWD2	Not described	expression still not defined	
		FBXO40	C10E2.2	expresion still not defined	
	Johanson-Blizzard Syndrome	UBR1	C32E8.11	expresion still not defined	[151]
	Down Syndrome	TTC3	Not described	yes	[179]
		USP-25	Not described	expression still not defined	
Neurodegenerative	Parkinson's disease	PARK	pdr-1	yes	[190–195]
		UCH-L1	ubh-1	expresion still not defined	
		DJ-1	djr-1.1, djr-1.2	expresion still not defined	
		ATP13A2	catp-6	expresion still not defined	
	Machado-Joseph Disease	ATXN3	atx-3	yes	[196,197]
	Ataxia	USP-14	usp-14	expresion still not defined	[198]

Table 3. List of neurodevelopmental and neurodegenerative diseases for which a component of the UPS is known to be involved in the etiology of the disease and their *C. elegans* homologues.

1.3.2- The UPS in neurodegenerative disorders

The accumulation of misfolded protein aggregates is observed in a range of neurological diseases, which includes PD, AD, amyotrophic lateral sclerosis, frontotemporal dementia and polyglutamine (polyQ) expansion disorders, among others [199–204]. These aggregates are often immunoreactive for components of the UPS, namely ubiquitin [205–207]. The exact significance of this phenomenon is still a matter of debate.

The concept that UPS dysfunction leads to accumulation of misfolded proteins in neurodegenerative diseases is reasonable and may be supported by the available evidence, as described below. However, it is not possible to exclude that protein aggregation is an earlier step in the etiology of the disease that leads itself to UPS dysfunction, even before inclusion body formation [208]. Alternatively, the observed accumulation of UPS components in aggregates may constitute an adaptation, a cellular response to the aggregation phenomenon. In this process, UPS components may become trapped into the protein aggregates, which act simultaneously as the cause of UPS impairment and its consequence, in a positive-feedback mechanism [209]. In normal aging brains there are reports of protein aggregation [210], decreased activity of the UPS [211,212] and activation of the "immunoproteasome" [213]. These studies suggest a direct contribution of the UPS dysfunction for age-related neurological disorders. This is certainly the case for PD, where the most common familial disease form, autosomal recessive-juvenile Parkinsonism, results from mutations in parkin, a RING E3 ligase [190]. A mutation in the gene coding for UCH-L1 was also associated with familial forms of the disease, thought to be due to a decrease in the activity of this enzyme [191]. Six of the nine PD genes known to date, α-synuclein being the exception, have an identified *C. elegans* orthologue, including the UPS components, UCH-L1 and parkin [192]. Springer and co-workers identified the *C. elegans* parkin homolog, PDR-1, and contributed to elucidate the mechanisms by which parkin is involved in the disease. The nematode strain expressing an in-frame deletion allele of pdr-1 was more prone to protein aggregation and more sensitive to ER stress, suggesting that expressing the mutant form of the enzyme may be more useful to understand the neurotoxicity in the disease than completely abolishing its expression [189], a concept that may be relevant for the study of other diseases.

In polyQ disorders, including Huntington's disease (HD), spinocerebellar ataxias, Kennedy's disease and dentatorubropallidoluysian atrophy, a CAG triplet repeat expansion encodes an expanded polyQ stretch, and the resulting mutant proteins misfold, often forming protein

inclusions [214]. An important role for the UPS is suggested in these disorders, namely through the observation that the presence of ubiquitin-positive protein intranuclear inclusions is a common feature [215,216].

In HD UPS dysfunction was demonstrated in several models [208,217], and ubiquitin-positive polyQ inclusions were found in the brain of HD as in other neurodegenerative diseases such as MJD, spinocerebellar ataxia type 7 (SCA7) and dentatorubral-pallidoluysian atrophy patients [215,218,219]. However, the question of whether the UPS dysfunction is the cause or a consequence in neurodegenerative diseases is still under debate. In a transversal study using cell lines, HD mice and *post-mortem* brains of HD patients, it was suggested that accumulation of N-terminal fragments of mutant huntingtin (htt), which may be toxic and drive the formation of aggregates through "seeding" effects, were a consequence of age-related UPS dysfunction rather than its cause [220]. A recent study also suggested that toxic htt forms do not impair the proteasome and that, instead, the impairment of the UPS arises from the accumulation of N-terminal fragments [221]. Supporting this model, an HD mouse study showed no global impairment of UPS activities, and the forms of polyubiquitylated proteins accumulated in this model were of a different nature than those found upon proteasome inhibition [222]. In contrast, impairment of the UPS was demonstrated in transfected HEK293 cells upon polyQ aggregation, even before inclusion body formation [208]. A recent report reconciles apparently different models, demonstrating a poly-Q-induced global UPS impairment *in vivo* in a mouse model of HD [217]. These authors attributed the discrepancy between the results obtained in different models to the early onset of the disease in transgenic animals, which are therefore exposed to mutant htt for longer periods. This may lead to adaptation and formation of inclusion bodies, restoring of the UPS function, and this was suggested in the earlier studies to be beneficial in the context of the disease [223]. Recent reports trying to further unravel the mechanisms through which the UPS might be related to the disease showed that mutant htt interferes with the degradation of β-catenin, leading to its toxic accumulation [224].

The loss of the de-ubiquitylating enzyme Usp14 due to the ax^J mutation in *ataxia* mice was suggested to lead to a decrease in the availability of monomeric ubiquitin [225] and to synaptic transmission defects [226], which may be due to a dysfunction in the Usp14-regulated gamma-aminobutyric acid type A ($GABA_A$) receptor turnover [198]. Neuronal expression of Usp-14 was able to rescue the motor system defects observed in mice carrying the ax^J mutation [227], showing that the function of this DUB is highly relevant in neurons. Intriguingly, recent work has described inhibition of ubiquitin-protein conjugate degradation, *in vitro* and *in vivo*, by USP-14. This occurs through the trimming of substrate-bound ubiquitin chains on the proteasome. A specific inhibitor of USP-14 was described, 1-[1-(4-fluorophenyl)-2,5-

dimethylpyrrol-3-yl]-2-pyrrolidin-1-ylethanone, that can potentially be used to enhance proteasome function, and to improve clearance of misfolded proteins in neurodegenerative diseases [228].

Alzheimer's disease, the most common neurodegenerative disease in humans, is characterized by the accumulation of extracellular amyloid-β plaques and intracellular neurofibrillary tangles [229]. As in other neurodegenerative diseases, the identification of ubiquitin immunoreactivity in histological lesions suggested the link between UPS and disease [206]. A more direct link was established with the finding of a mutant form of ubiquitin in AD patients, ubiquitin-B+1 (UBB+1). This aberrant ubiquitin has a 19-amino-acid C-terminal extension that lacks the C-terminal glycine essential for substrate ubiquitylation, and was detected in the cortex in brain sections of AD patients, as well as in elderly controls whenever plaques and tangles were also present [230]. Accumulation of UBB+1 leads to neuritic beading, mitochondrial stress and neuronal degeneration in primary cultures of cortical neurons. UBB+1 is a UPS-substrate itself, being degraded at low levels; however, at high expression levels it inhibits the proteasome [231]. Table 3 shows examples of components of the UPS involved in nervous system diseases and their homologues in *C. elegans.*

1.3.2.1 - The UPS in Machado-Joseph disease

Machado-Joseph disease (MJD) or spinocerebellar ataxia type 3 is a polyQ disorder, polyglutamine tract expansion in ataxin-3 leads to the development of the disease [196].

Ataxin-3 (ATXN3) is a deubiquitylase (DUB) present in all or most tissues in humans and mice [232,233]. It is a component of the Ubiquitin Proteasome System (UPS) that acts as a deubiquitylating enzyme [48,232] having several described functions ranging from: sequestering aggregated proteins in aggresomes [234,235], modulating E3 ubiquitin ligases [236,237], to regulate protein degradation and stress response [49,238,239], to determining cell adhesion and cytoskeletal structure [238,240], modulating cell differentiation [240] and regulating transcription [11,49,238]. Until now ataxin-3 deubiquitylating activity has been described towards to Carboxy Terminus of Hsc70 Interacting Protein (CHIP) [48,237] and to the Parkinson Disease related E3 parkin [236,241].

Although polyQ diseases are thought to result predominantly from a gain of toxic function, due to the presence of the expansion of the polyQ tract, it is nevertheless intriguing that the protein involved in this particular disease has been reported to possess DUB and de-NEDDylase activity [242–244], and interacts with valosin-containing protein (VCP) [245,246], HHR23A and B [247], parkin [241], C terminus of Hsc70-interacting protein (CHIP) [237] as well as with components of the

proteasome [248]. In the search for physiological roles of ataxin-3 and for the mechanisms of pathogenicity, Pittman and colleagues suggested that ataxin-3 with an expanded polyQ tract displays increased affinity to VCP, preventing the assembly of the complex - VCP/Ufd1-Npl4 - responsible for the retranslocation of proteins from the endoplasmatic reticulum to the cytosol where ubiquitylated proteins are degraded by the proteasome – the endoplasmatic reticulum-associated degradation (ERAD) [249].

The *C. elegans* orthologue of ataxin-3 (ATX-3) also has DUB activity and interacts with the worm homologue of VCP and with UBXN-5, a VCP adapter thought to be involved in the transport of specific substrates to the proteasome [250]. The ubiquitin ligase CHIP, that interacts with chaperones to promote the degradation of misfolded proteins [251], has been previously described to interact with ataxin-3 [252], but the functional meaning of this interaction was unknown. Scaglione and co-workers identified the ubiquitin–conjugating enzyme Ube2w as responsible for CHIP mono-ubiquitylation and showed that this ubiquitylation stabilizes the interaction of CHIP with ataxin-3. In this complex, ataxin-3 is responsible for the editing of the ubiquitin chains of substrates associated to CHIP promoting their turnover. Ataxin-3 is also able to deubiquitylate CHIP upon the accumulation of polyubiquitylated substrates. This dynamic process is disturbed in the context of expanded-polyQ ataxin-3, since the altered form of the enzyme shows an approximately 6-fold increase in the affinity for CHIP. The functional meaning of this increased affinity is still not known but in this study it was observed that SCA3 mice (model of MJD) showed a significant decrease in CHIP levels compared with wild-type animals [237], which suggests that the increased affinity of ataxin-3 for CHIP results in CHIP degradation with the consequent deregulation of protein quality control mechanisms. Another contribution to the understanding of the disease came from a recent study demonstrating that ataxin-3 and parkin – an E3 ligase responsible for a familial form of PD [190] – interact both *in vitro* and in cells, and that ataxin-3 has DUB activity towards parkin. The expanded-polyQ version of ataxin-3 deubiquitylates parkin more efficiently and is also responsible for increased parkin degradation through the autophagy degradation pathway [241], and this correlates with decreased parkin levels in a transgenic mouse model of the disease [253]. Taking into account the neuroprotective role of parkin [254–256] the fact that expanded-polyQ ataxin-3-induced parkin clearance is altered might contribute to neurodegeneration in MJD.

Intriguingly, and perhaps counter-intuitively, ATX-3 knock-out *C. elegans* strains show an improved response to heat stress, with higher expression of chaperones [238], suggesting a negative regulatory role for this protein in the stress response or perhaps an adaptation of the knock-out strains to a permanent proteotoxic stress. Another insight to the ATX-3- mediated mechanisms of lifespan regulation was given by the finding that CDC48 and ATX-3

synergistically cooperate in ubiquitin-mediated proteolysis and in ageing regulation. Worms deficient in both ATX-3 and CDC48 have extended lifespan and it was suggested that this was mediated by the regulation of ubiquitylation of substrates involved in the insulin-IGF-1 signalling [49]. How the normal function of ataxin-3 can be related to disease in this context remains to be further clarified.

1.4 - The UPS in calcium homeostasis deregulation

The deregulation of calcium homeostasis is a common feature not only in neurodegenerative diseases but also in the cases of brain injury and epilepsy with the consequent excessive release of glutamate, also here the UPS plays a relevant role. Infusion of rats infused with 6-hydroxydopamine (6-OHDA), a known inducer of a PD-like phenotype lead to a significant increase of glutamate in cerebral cortex of injected animals, and also to an upregulation of the N-methyl-D-aspartate (NMDA) type glutamate receptors [257]. A reduction in the expression of the GLAST glutamate transporter, involved in the reuptake of extracellular glutamate and in maintaining physiological extracellular glutamate concentrations [258], was also observed [257]. All these alterations are consistent with a deregulation of calcium homeostasis in PD with an excessive activation of glutamate receptors and consequent excitotoxicity. According with previous studies that described enhancement of glutamate receptor activation and compromised calcium homeostasis in Huntington´s disease (HD) [259–261], a study recurring to the yeast artificial chromosome (YAC) mouse model of Huntington's disease (YAC128 - that develops motor abnormalities, age-dependent striatal atrophy and neuronal loss) described a significant increase in the binding of glutamate to its NMDA, AMPA and metabotropic receptors. This was due to an increase in the glutamate receptors present in the synaptic membranes and not due to alterations in mRNA [262]. The mislocalization of glutamate receptors might explain some of the altered calcium homeostasis mechanisms identified previously. Another study pinpoints that disturbed calcium signaling plays a pivotal role in the degeneration of medium spiny striatal neurons (MSN) characteristic of HD, and that the expanded form of huntingtin is involved in this disregulation [263]. Along with the other autosomal dominant spinocerebellar ataxias (SCAs), evidence point that related to the characteristic neurodegeneration in these diseases are molecular alterations that interference with transcriptional regulation, protein aggregation and clearance, alter the ubiquitin-proteasome system and deregulate calcium homeostasis [264,265]. Alterations in calcium homeostasis, its role in apoptosis and disarrangement of correct calcium

compartmentalization have long been related to cytotoxicity [266]. In MJD the expanded ataxin-3, opposite to WT ataxin-3, has been described to bind to type 1 inositol 1,4,5-trisphosphate receptor (InsP3R1), a calcium channel involved in diverse cellular functions and that is activated by InsP3 [267]. Mutant ataxin-3 binds specifically this receptor and induces calcium release through sensitizing the receptor to the natural ligand (InsP3), while treatment with a specific inhibitor of calcium release from the sarcoplasmic reticulum in skeletal muscles improves the behavior of SCA3 mice (mouse model of MJD). Calcium inhibitors also decreased neuronal loss in pontine nuclei and substantia nigra, which are among the most affected brain areas in the disease [268].

Brain damage in traumatic brain injury, epilepsy, and consequent hypoxia-ischemia, excessive release of the neurotransmitter glutamate is known to lead to an excessive calcium accumulation and consequent neuronal death [269–271]. The specific contribution of the UPS to the mechanisms of excitotoxicity, namely the contribution to the cleavage of the Gamma-Amino Butyric Acid (GABA) synthesis responsible enzyme – Glutamic Acid Decarboxylase (GAD) was, however, still not evaluated. GAD occurs in two isoforms, GAD65 and GAD67[272], while the first is responsible for the synthesis of the synaptic vesicles GABA [273–275], the second, besides constitutively active, produces the cytosolic pool of GABA and is responsible for the fine tuning of inhibitory transmission [276–280]. Under excitotoxic conditions, activation of calcium-dependent proteases occurs, and cleavage of both isoforms can be prevented with calpain inhibitors [281–285]. Also cathepsin inhibitors were able to inhibit GADs [284], suggesting the involvement of multiple proteolytic enzymes in GADs cleavage under calcium deregulation. The activity of the proteasome has been demonstrated to be downregulated in ischemia [286] and inhibition of the proteasome has proven to be protective in focal brain ischemia [287–289], more recently it was described that excitotoxic stimulation leads to the disassembly of the 26S proteasome in its subunits, and activation of extrasynaptic N-methyl-D-aspartate receptors (NMDA) is responsible for toxicity [290]. The role of the UPS in the cleavage of GAD enzymes is relevant because it contributes to the understanding of the specific roles of the UPS when calcium signaling in deregulated in cells, and to the understanding of GABA metabolism in these conditions.

1.5 - Targeting the UPS in disease

Combating neurodegenerative disorders by targeting the UPS is an attractive therapeutic approach [181–184], taking in consideration the significant involvement of UPS components in these disorders, as described above. Perhaps the most challenging aspect of this strategy is to define which step of UPS activity should be interfered with. The first drug used to target the UPS was the proteasome inhibitor bortezomib that is now used in the treatment of multiple myeloma under the approval of Food and Drug Administration in 2003 [291]. Recently this proteasome inhibitor was tested in rats subjected to ischemic reperfusion. The mRNA levels for inflammatory mediators such as Inducible nitric oxide synthase (iNOS), intercellular adhesion molecule (ICAM-1) and monocyte chemoattractant protein 1 (MCP-1) were downregulated in bortezomib-treated animals. Other protective outcomes were the decrease in the levels of NF-κB p65 subunit and the diminished apoptosis in IR animals [292]. These effects observed under proteasome blocking reinforce the major role of the UPS under ischemic conditions, and particularly in calcium deregulation situations. The protective effect of inhibiting the proteasome and the fact that under these conditions the proteasome is already compromised [290] might seem contradictory, but some studies conclude that only a temporary proteasome inhibition in the acute phase is protective while longer inhibition can be deleterious [293]. As substrate selection in the UPS is driven by the ubiquitin ligases, targeting E3s in the conjugation step would confer more specificity to the therapeutics. In the context of cancer treatment some neurodegenerative disease-related E3s have been successfully drug targeted. The E6-associated protein (E6-AP), that is involved in the etiology of Angelman´s syndrome, has its mRNA downregulated in cervical cancer cells treated with mRNA decay factor tristetraprolin (TTP), with the last showing an effective inhibition of this E3 [294]. Anyhow, successful strategies interfering with E3s are still not easy to devise due to enzyme complexity and lack of knowledge on mechanisms of catalysis [295], but with the increasing number of neurodegenerative disease-related E3s this will be a pathway to further explore [296,297]. The inhibition of neurodegenerative disease-related DUBs has been pursued. Inhibition of USP-14 might be relevant for the clearance of misfolded proteins according to the study that postulates that USP14 inhibits the degradation of ubiquitin-protein conjugates. Inhibition of USP14 by 1-[1-(4-fluorophenyl)-2,5-dimethylpyrrol-3-yl]-2-pyrrolidin-1-ylethanone (IU1), lead to increased proteolysis of neurodegenerative-related proteins, namely overexpressed Tau in murine embryonic fibroblasts was substantially more degraded upon USP14 inhibition, and the MJD-related protein ataxin-3 both in the WT and expanded polyQ form was downregulated

upon IU1 treatment [228]. Caution must be taken about the implications of this approach, since it can-not be ignored that decreased levels of USP-14 in USP14 *ax*^{J} mice also lead to redistributed membrane expression of $GABA_A$ receptors and consequent altered synaptic transmission, resulting in ataxia [198]. Another approach is to facilitate substrate degradation by the UPS; this can be achieved, amongst other possibilities, by induction of heat shock protein expression. This has been attempted with Geranylgeranylacetone [298,299], 17-(Allylamino)-17-demethoxygeldanamycin (17-AAG) and 17-(Dimethylaminoethylamino)-17-demethoxygeldanamycin (17-DMAG), among other molecules [300]. Taking into account the deleterious effects that disturbing such a widespread system evoke, the combinatorial use of UPS modifiers might be the greatest promise for the research in this field.

Chapter 2

HSP60: a new ataxin-3 interactor.

HSP60: a new ataxin-3 interactor.

Márcio S. Baptista[1,2], Andreia Teixeira-Castro[1,2], Miguel Oliveira[1,2], Bruno Almeida[3], Ana C. Figueiredo[3], Zsuzsa Sárkány[3], Andreia Neves-Carvalho[1,2], Sandra Macedo-Ribeiro[3] and Patrícia Maciel[1,2*]

1. Life and Health Sciences Research Institute (ICVS), School of Health Sciences, University of Minho, Braga, Portugal
2. ICVS/3B's - PT Government Associate Laboratory, Braga/Guimarães, Portugal
3. Instituto de Biologia Molecular e Celular, Universidade do Porto, Porto, Portugal

*Corresponding author:

Patrícia Maciel, PhD

Life and Health Sciences Research Institute (ICVS); School of Health Sciences; University of Minho; Campus de Gualtar; 4710-057 Braga, Portugal

e-mail: pmaciel@ecsaude.uminho.pt

Tel: +351 253 604 824 Fax: +351 253 604 820

Abstract

Heath shock protein 60 (HSP60) is a molecular chaperone predominantly located in the mitochondria but also present in other sub-cellular compartments. It is present in mammalian cells in monomeric, heptameric and tetradecameric forms and besides its protein folding role it is also involved in the regulation of many physiological processes such as modulating post-translation modifications, transcription regulation and acting as a ligand to modulate signaling cascades. In this study we demonstrate for the first time that HSP60, both in the monomeric and heptameric forms, is able to interact with the Machado-Joseph disease-related protein Ataxin-3 (ATXN3). We defined the interaction as being direct and identified the Josephin

domain of ATXN3 as the responsible for this interaction; furthermore, we show that the interaction takes place in differentiated neuronal cells, thus opening the possibility that it may be of relevance for proteostasis in this cell type and for its unbalance in MJD.

Introduction

The HSP family consists of high and low molecular weight chaperones, first identified as proteins induced upon heat shock treatment. Molecular chaperones are highly conserved specialized proteins which occur in all organisms and play a key role in cell maintenance and survival. Their role is to facilitate correct folding of newly synthesized (nascent) or denaturated (misfolded) proteins, preventing their loss of function and/or aggregation [301–303]. Type I chaperonins are molecular chaperones of the HSP60 family found in bacteria, mitochondria and chloroplasts [304]. The 60-kDa heat shock protein (HSP60) is a resident of the mitochondrial matrix, also present in the cytoplasm and nucleus, and is a vital cellular complex that mediates the folding of unfolded or misfolded mitochondrial proteins [305–308]. It is a homologue of GroEL (prokaryotic chaperone) and complexes with HSP10, a homologue of the prokaryotic GroES [309]. The mechanism of action of this complex has been described in *E. coli*. A misfolded or unfolded protein binds to the surface of one GroEL ring, followed by ATP-dependent GroES binding to that ring which causes an increase in the cavity size formed by GroEL, together with a switch from hydrophobic to hydrophilic environment inside the cavity. These conformational changes allow release of the substrate to the interior of the cavity, where the protein can fold correctly [310–312].

Ataxin-3 (ATXN3) is a deubiquitylase (DUB) present in all or most tissues in humans and mice [50,232]. Functions of ATXN3 range from the editing of ubiquitinated proteins [48,232], sequestering aggregated proteins in aggresomes [234,235], and modulating E3 ubiquitin ligases [236,237], to regulate protein degradation and stress response [49,238,239], to determining cell adhesion and cytoskeletal structure [238,240], modulating cell differentiation [240] and regulating transcription [11,49,238]. Expansion of a polyglutamine tract in ATXN3 results in the development of the neurodegenerative disease Machado-Joseph disease (MJD), also called spinocerebellar ataxia type 3 [196]. MJD is the most common dominantly inherited ataxia worldwide, and is a protein conformational disease defined by the accumulation of proteins with altered conformations [313].

Unchecked protein aggregation and misfolding are major features of age-related neurodegenerative diseases [314]. Polyglutamine diseases arise when proteins bearing an expanded polyglutamine tract adopt non-native conformation that favors their aggregation and the formation of protein aggregates. Misfolding and aggregation of these proteins results in gained cytotoxicity promoting inappropriate interactions that are detrimental to the cell or may confer loss of function to those proteins [315,316]. The cooperative action of molecular chaperones allows proteins to avoid aggregation, and this has been described for several diseases [317–319]. Specifically in the case of HSP60, inactivation of chaperonin has been demonstrated to be the cause for neurodegenerative diseases. In hereditary spastic paraplegia (SPG13) the V98I point mutation leads to decreased ATPase activity [320,321], and consequently a deficiency in the folding capacity of HSP60. In MitCHAP60 disease the mutant protein D3G destabilizes the oligomeric native form of HSP60 and is suggested that this leads to decreased activity of the enzyme and consequent deficit in folding capacity [322,323].

In the current study we describe the interaction of HSP60 with ATXN3. Given the important role of HSP60 in preventing protein aggregation and the involvement in the neurodegenerative diseases described above, this new interaction might undercover new molecular pathways that are likely to be relevant for cellular homeostasis. By using an array of techniques we were able to purify the oligomeric form of HSP60 and demonstrate that it interacts directly with ATXN3; this interaction occurs both *in vivo* (in neurons) and *in vitro*. The physiological relevance of the interaction was still not clarified, and further studies will be needed to undercover the potential role of HSP60 in the pathogenesis of MJD.

Experimental Procedures

Expression plasmids and recombinant proteins

GST and GST-NEDD8 expression clones were previously produced in our laboratory using a human cDNA library [244]; DNA constructs for expression of His_6 -tagged ATXN3-var1.1 (full-length of ataxin-3 variant 1.1 with three UIMs-ubiquitin interacting motifs) and His_6 -tagged Josephin domain (only the Josephin domain-JD) were produced as described [324]; DNA for His_6 -tagged D1 (JD plus two UIMs) and GST-HSP60 DNA was previously produced in our laboratory [244].

Generation of pET_GB1-HSP60 was performed by amplification of GST-HSP60 DNA with the primers HSP60_NcoI (5'-CCGGCCATGGGGCTTCGGTTACCCACAGTC-3') and HSP60_Acc65 (5'-CCGGGGTACCTTAGAACATGCCACCTCCCATAC.3') and inserted in the pET_GB1 vector between the restriction sites for NcoI and Acc65I.

Generation of His_6 -tagged mature HSP60

The nucleotide sequence encoding the mature form of human mHsp60 was amplified from pET_GB1-HSP60 DNA and inserted between restriction sites for NcoI and Acc65I into a modified pET using mHSP60_NcoI (5'-CCGGCCATGGGGGCCAAAGATGTAAAATTTGG-3') and mHSP60_Acc65I (5'-CCGGGGTACCTTAGAACATGCCACCTCCCATAC-3') primers.

Expression of recombinant proteins

Expression of GST, GST-NEDD8, GST-HSP60, pET_GB1-HSP60, pET_GB1-mHSP60 and all the His_6-tagged versions of Ataxin-3 was induced in *Escherichia coli* strain BL21(DE3) (Invitrogen), whereas expression of GST-HSP60 was induced in BL21(DE3)-SI cells (Invitrogen) using 300 mM NaCl. After inoculation of one colony of interest in 50 ml of LB broth medium supplemented with the appropriate antibiotic – ampicillin 50 µg/µl or kanamycin 100 µg/µl – cells were let to grow overnight. The overnight culture was diluted 1:10 in 2 litres of Luria Broth (Formedium) medium with (GST, GST-NEDD8, pET_GB1-HSP60 and pET_GB1-mHSP60) or without (GST-HSP60) NaCl (10g/l), ampicillin 50 µg/µl or kanamycin 100 µg/µl was added and cells were grown at 37°C until the OD_{600}~0.5. Temperature was adjusted to 37°C during 30 minutes and protein expression was then induced with IPTG (1 mM) or NaCl (300 mM) 3 hours at 37°C. Expression was evaluated by SDS-PAGE analysis after lysate preparation.

Cells were then collected through centrifugation (4000 rpm; 30 minutes) and lysed at 4 ºC in 20 mM Sodium Phophate, 10 mM imidazole, 500 mM NaCl at pH 7.5 in the presence of lysozyme (50 µg/mL), phenylmethylsulfonyl fluoride (0.5 mM) and $MgCl_2$ (10 mM) followed by sonication (4 minute with a 50% duty cycle). The protein extract was then centrifuged (20000 rpm; 30 minutes) and the supernatant was recovered.

Purification of GST-tagged recombinant proteins

Protein extracts were filtered (0.45 µm Low Protein Binding Durapore®, Millex®, Millipore) and loaded onto a 5ml Glutathione Sepharose 4B column (Amersham Biosciences) pre-equilibrated in lysis buffer. The extract was allowed to recirculate in the column during 1 hour at 2 ml/min using a peristaltic pump (EP-1 Econo Pump, Bio-Rad). After being washed extensively with PBS, the recombinant protein was eluted with 10 mM L-Glutathione reduced (Sigma). Recombinant proteins were kept in lysis buffer plus 5% glycerol and 1mM dithiothreitol (DTT) and frozen in liquid nitrogen. Fractions suitable for further purification were selected by SDS-PAGE analysis and then applied to a gel filtration column (Superdex 200 10/300 – GE Healthcare) powered by an ÄKTA FPLC system (ÄKTA Prime Plus, GE Healthcare) and previously equilibrated in sample buffer (20 mM HEPEs, pH 7.5; 200 mM NaCl; 5% glycerol; 1 mM DTT) for further separation of the GST-tagged recombinant proteins. After SDS-PAGE evaluation of the fractions collected by gel filtration, the purest fraction was concentrated on 15 ml concentrators (Amicon® Ultra-4, Millipore). Protein concentration was evaluated using a NanoDrop® ND1000 Spectrophotometer (Thermo Scientific) and subsequently proteins were liquid nitrogen frozen and stored at - 80°C.

Purification of His_6 -tagged recombinant proteins

His_6-tagged versions of Ataxin-3 - ATXN3-var1.1, Josephin domain and D1 – were purified previously in our laboratory as described [324]. Cell lysates of pET_GB1-HSP60 expression were collected by centrifugation and lysed in Buffer A (20 mM NaH_2PO_4/Na_2HPO_4; 300 mM NaCl; 10 mM Imidazole) supplemented with lysozyme (50 µg/mL), PMSF (0.5 mM) and $MgCl_2$ (10 mM) followed by sonication (4 minute with a 50% duty cycle). Extracts were than centrifuged (20000 rpm; 30 minutes) and supernatant was recovered. Protein extracts were filtered, loaded onto a 5 mL HisTrap HP column (GE Healthcare) previously equilibrated on Buffer A and let recirculate for 1 hour at 1 ml/min on a peristaltic pump. Recombinant protein was eluted in three steps by addition of increasing concentrations of Buffer B (50 mM NaH_2PO_4/Na_2HPO_4 pH 7.5; 300 mM NaCl; 500 mM Imidazole) with a flow rate of 1ml/min. Evaluation and concentration of purified protein were performed as described for GST-tagged recombinant proteins.

To further separate the isolated proteins, fractions were supplemented with 2mM EDTA, 1mM DTT and 10 mM $MgCl_2$ and applied to Superdex 200 10/300 previously equilibrated in 50 mM

NaH_2PO_4/Na_2HPO_4, pH 7.5; 300 mM NaCl; 2 mM EDTA; 1 mM DTT and 10 mM $MgCl_2$. Selected fractions were fractionated on a Superose 12 10/300 GL column (GE Healthcare) at a flow rate of 0,5 ml/min. Following fraction collection these were analyzed by SDS-PAGE and stored at -80°C after liquid nitrogen freezing.

Reconstitution of oligomeric HSP60 with mature form of the protein

Cell lysates of pET_GB1-mHSP60 expression were collected by centrifugation and lysed in lysis buffer (50 mM Tris-HCl pH 7.5; 100 mM NaCl; 10 mM Imidazole) supplemented with lysozyme (50 µg/mL), PMSF (0.5 mM) and $MgCl_2$ (10 mM) followed by sonication (4 minute with a 50% duty cycle); the supernatant was recovered after centrifugation (20000 rpm; 30 minutes). Protein extracts were filtered, loaded onto a 5 mL HisTrap HP column (GE Healthcare) previously equilibrated on Buffer A (50 mM Tris-HCl pH 7.5; 500 mM NaCl; 10 mM Imidazole) and let to recirculate for 1 hour at 1ml/min on a peristaltic pump. Recombinant protein was eluted in three steps by addition of increasing concentrations (10%, 40% and 70%) of Buffer B (50 mM Tris-HCl pH 7.5; 500 mM NaCl; 500 mM Imidazole) with a flow rate of 1ml/min. Enriched protein fraction (~20 ml) was incubated with Tobacco Etch Virus (TEV) in an enzyme/substrate molecular ratio of 1:2 during 2 hours at room temperature plus overnight incubation at 4°C, and at the same time dialyzed against Dialysis Buffer (50 mM Tris-HCl pH 7.5; 200 mM NaCl; 10 mM Imidazole; 2.5 mM β-mercaptoethanol). Mature HSP60 (mHSP60) was purified by removing the histidine tag previously associated with the protein and present in solution, through incubation during 2 hours on nickel agarose beads (Jena Biosciences) that were previously equilibrated on dialysis buffer. Flowthrough corresponding to mHSP60 was recovered and concentrated, during the concentration buffer was changed to eliminate imidazole so protein could be liquid nitrogen frozen. Concentrated protein was diluted approximately 20 times in buffer without NaCl (50 mM Tris-HCl pH 7.5; 2.5 mM β-mercaptoethanol) so that a concentration of ~10 mM NaCl could be reached. Diluted protein was loaded onto an anion-exchange chromatography column - 1 ml Mono Q 5/50 GL column (GE Healthcare), and eluted with a 10-column volume linear gradient of 10 mM – 1000 mM NaCl. Fractions forming the major peak containing mature HSP60 (monomeric form) were pooled and concentrated to approximately 40 µg/µl so oligomerization protocol (3) could be applied. Protein was supplemented with glycerol (5% v/v), DTT (2.5 mM), and NaCl concentration was adjusted to 300 mM. To 200 µl concentrated protein (~40 µg/µl) was added: KCl (20 mM); $Mg(CH_3COO)_2$ (20 mM); Adenosine-5'-triphosphate (ATP) pH 7.5 (4 mM)

and 350 µl of Oligomerization Buffer (50 mM Tris-HCl pH 7.7; 300 mM NaCl; 10 mM $MgCl_2$) following 90 minutes incubation at 30°C. Resultant protein forms were kept at 25°C and then loaded onto an gel-filtration column (Superose 6 10/300 GL, GE Healthcare) equilibrated in S6 Buffer (10 mM HEPEs pH 7.4; 160 mM NaCl; 50 µM Ethylenediaminetetraacetic acid (EDTA)). During all the process proteins were not subjected to temperature lower than 25°C, since this is crucial to maintain stable the oligomeric form of HSP60 [325]. The main peak fractions corresponding to low molecular weight HSP60 species or oligomers of HSP60 were pooled and concentrated and immediately kept at -80°C after liquid nitrogen frozen.

Calibration of Superose 6 analytical size-exclusion chromatography column

Superose 6 column (GE Healthcare) was assembled into an ÄKTA purifier 10 system (GE Healthcare) and equilibrated with buffer S6 (150mM NaCl, 5% (v/v) glycerol, 5 mM $MgCl_2$, 1mM EDTA, 1mM DTT, 20 mM Tris-HCl, pH 7,5). Blue dextran 2000 was used for determination of the void volume and albumin (67 kDa), aldolase (158 kDa), catalase (232 kDa), ferritin (440 kDa) and thyroglobulin (669 kDa) were used for column calibration (all proteins except ferritin – 1 mg/ml - were loaded at 10 mg/ml concentration). 100 µg of low molecular weight HSP60 species before oligomerization protocol or oligomeric HSP60 isolated after the oligomerization protocol samples were loaded into the column. The calibration curve was prepared by measuring the elution volumes of the standard proteins, calculating their corresponding K_{av} values and plotting them versus the logarithm of their respective molecular weight. The K_{av} parameter was determined according to the equation:

$$K_{av} = \frac{V_e - V_0}{V_t - V_0}$$

where V_e represents the elution volume,V_0 the void volume of the column, and V_t the total bed volume.

Dynamic Light Scattering (DLS)

Molecular size measurements were carried out recurring to Zeta sizer Nano Zs DLS system (Malvern Instruments). Samples of monomeric and oligomeric mature HSP60 at concentration of 1 mg/ml in buffer H (10 mM HEPEs pH 7.5; 160 mM NaCl; 50 µM EDTA) were centrifuged at 100,000 rpm for 30 minutes at 4 ºC in an AirfugeTM airdriven ultracentrifuge (Beckman Coulter). Three independent measurements were obtained using a 45 µL DTS 2112 cuvette at 25°C for each sample. All data was then analyzed using DTS (nano) 6.01, the software of the instrument (Zetasizer Nano Series *User Manual*. *MAN0317 Issue2. 1 July 2004* http://www.nbtc.cornell.edu/facilities/downloads/Zetasizer%20Manual.pdf)

Transmission Electron Microscopy (TEM)

For visualization by TEM, oligomeric species of mature HSP60 were adsorbed onto glow-discharged, carbon-coated collotion film supported on 200-mesh cupper grids and negatively stained with 2% (w/v) uranyl acetate to which was added NaOH (300 mM). HSP60 oligomers were diluted in H2O from an initial concentration of 9.8 mg/ml to a final concentration of 0,6 mg/ml and immediately adsorbed the copper grids. Grids were visualized using a Transmission Electron Microscope (model JEM-1400, Zeiss) at an accelerating voltage of 80 kV. The experiment was repeated three times.

SH-SY5Y cell culture

The human neuroblastoma SH-SY5Y cell line (ATCC number CRL-2266) was cultured in a 1:1 mixture Dulbecco's Modified Eagle Medium and Ham's F12 nutrient (Invitrogen) supplemented with 10% (v/v) fetal bovine serum, 2mM glutaMAX (Invitrogen), 100U/mL penicillin, 100µg/mL streptomycin and 25ng/mL puromycin (Sigma Aldrich). The cells were incubated in a humidified 37ºC/95%-air/5%-CO2 incubator. The medium was changed every two days. Differentiation was induced by 0.1µM all-trans-retinoic acid (Sigma Aldrich) in opti-MEM (Invitrogen) supplemented with 0.5% fetal bovine serum and penicillin/streptomycin during 7 days. Medium was replaced every two days.

Immunofluorescence and Immunoprecipitation assays

SH-SY5Y cells were grown on coverslips and after differentiation were stained for mitochondria using MitoTracker® Deep Red FM (Invitrogen); media was replaced and cells were incubated for thirty minutes with 50 nM of MitoTracker® in fresh media in the incubator. Cells were then fixed for 10 minutes in freshly prepared 4% p-formaldehyde (Sigma) in phosphate-buffered saline (PBS), permeabilized with PBS/0,1% Triton X-100 for 5min, washed in PBS 3 times and blocked with PBS/5% BSA for 30 minutes at RT. Hsp60 was detected after 1-hour incubation with anti-hsp60 (SPA-828; Stressgen) at 1:200 in PBS/1% BSA, ATXN3 was detected with anti-SCA3 (1H9, Chemicon). Fluorescent secondary antibodies (Alexa Fluor 488 rabbit anti-goat and Alexa Fluor 568 rabbit anti-mouse, Molecular Probes) were used at 1:500 during 1-hour incubation. DNA was stained using DAPI (Sigma) at 1 μg/ml during 10 minutes at RT. Cells were visualized in a Olympus FV100 confocal microscope (Olympus, Tokyo, Japan). For quantification of colocalization specific regions of singly labeled cells were selected first to set the thresholds. Then selected regions of interest were used for pixel quantification. Colocalization was calculated using Olympus FV1-ASW software, which calculates overlap and colocalization coefficient as derived from Mander's article based on Pearson's correlation coefficient.

Overlap coefficient: $[\Sigma(Ch1i)(Ch2i)]/[\sqrt{(sum(Ch1i)2(Ch2i)2)}]$

The values for the overlap coefficient range from 0 to 1. An overlap coefficient of 1 represents perfectly colocalized pixels.

Pearson's correlation: $[\Sigma(Ch1i - Ch1avg)(Ch2i)(Ch2avg)]/[\sqrt{(sum(Ch1i - Ch1avg)2\ (Ch2i - Ch2avg)2)}]$

Because each pixel is subtracted by the average pixel intensity, the value for Correlation R can average from -1 to 1. A value of 1 would mean that the patterns are perfectly similar (colocalized), while a value of -1 would mean that the patterns are perfectly opposite.

For immunoprecipitation SH-SY5Y differentiated cells were lysed in lysis buffer(50 mM Tris-HCl pH 7.5; 150 mM NaCl; 0.5 % (v/v) NP-40; 1mM EDTA) plus protease inhibitors (Roche) and briefly sonicated. The lysates were then pre-cleared with Protein-G Sepharose (GE Healthcare) for 1 hour at 4°C and then incubated with 4 μl of HSP60 antibody for 1 hour at 4°C. The immunocomplexes were precipitated with 50 μl of Protein-G sepharose for 2 hours at 4°C. Sepharose beads were washed 4 times in lysis buffer and finally eluted in 30 μl of 2X SDS

sample buffer. The eluted proteins were analysed by immunoblot with anti-ATXN3 antibody (MJD 1.1).

GST pull-down

The purified GST or GST-tagged proteins (2 μg) were incubated with 30 μl of Glutathione Sepharose beads 4B (GE Healthcare) for 1 hour at 4°C in 100 μl of binding buffer (50 mM Tris-HCl pH 7.5; 150 mM NaCl; 1% Triton X-100; 10% glycerol; 1 mM DTT; 1mM EDTA) and thoroughly washed after with binding buffer. ATXN3 was then added (2μg) and incubated for 2 hours at 4°C in a rotating wheel. Incubations of GST, GST-Hsp60 and GST-NEDD8 were performed in 3% BSA. Bound fractions were washed 4 times in 500 μl binding buffer without glycerol and with 300 mM NaCl, eluted in 30 μl 2X SDS sample buffer and then were analysed by SDS-PAGE. Immunoblots were performed using goat anti-GST (1:7500, GE Healthcare), or rabbit anti-MJD 1.1 (1:25000) antibodies, all diluted in 1% SM/PBS-T (1% skimmed milk in PBS/Tween20 0,05%). Secondary HRP-conjugated antibody incubations were as follows: anti-goat (Santa Cruz Biotechnology) at 1:10000 in 1% SM/PBS-T and anti-rabbit (Santa Cruz Biotechnology) 1:25000 in 1% SM/PBS-T. Detection was carried with ECL (GE Healthcare).

Surface Plasma Resonance

The Biacore apparatus from GE Healthcare, Biacore X100 system (Uppsala,Sweden) was used. All experiments were carried out at 10 °C. His6 -tagged ATXN3 was linked to the surface of a flow cell on a research grade NTA (nitriloacetic acid) sensor chip (Biacore). The NTA surface was saturated with nickel (500 μM) at 10 μl/min flow rate and washed extensively with A buffer (10 mM HEPES, pH 7.4, 150 mM NaCl, 50 μM EDTA, 0.05% Tween). The binding kinetics of HSP60 to immobilized ATXN3_His6 was determined by increasing HSP60 concentration (0 - 1000 nM) in P buffer at a flow rate of 30 μl/min. The sensor chip surface was regenerated by Regeneration Buffer (0.01 M HEPES, pH 8.3, 0.15 M NACl, 0.35 M EDTA, 0.05% Tween) at a flow rate of 30 μl/min. Unspecific binding was evaluated using another flow cell of the same sensor that was treated as above but in the absence of HSP60 (Flow Cell 1). The kinetic parameters of the binding reactions were determined using Biacore T100 evaluation software

(Biacore). The final sensorgram was calculated by substracting the signal of the control (Flow Cell 1) from that of the test (Flow Cell 2), and results expressed in resonance units.

Results

HSP60 interacts with ATXN3 *in vivo*

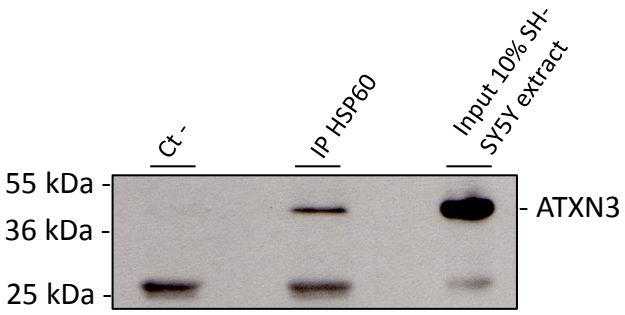

Figure 1 – Endogenous ATXN3 interacts with HSP60. SH-SY5Y differentiated cells were harvested and the supernatants pre-cleared with protein-G sepharose beads. Supernantants were then incubated for 1 hour with or without (Ct -) anti-hsp60 antibody (Stratagen); immunocomplexes were subsequently separated by SDS-PAGE and immunoblotted with anti-SCA3 antibody.

In order to investigate if endogenous HSP60 and ATXN3 proteins were able to interact in the context of mammalian brain cells we performed immunoprecipitation using extracts of differentiated SH-SY5Y neuroblastoma cells. These cells are able to synthesize proteins unique to a neuronal phenotype [326] and are routinely used, after differentiation with all-trans-retinoic acid, in studies to understand molecular pathways in neurons [327–330], and also in the context of neurological diseases [331,332], namely in the formation of polyglutamine aggregates [333], thus being a good model to study the possible interaction of HSP60 and ATXN3 in the nervous system. Extracts of differentiated SH-SY5Y cells were subjected to immunoprecipitation with an anti-HSP60 antibody. Immunoblotting with specific antibody against ATXN3 showed that a fraction of this protein co-precipitated with HSP60 (Figure 1), indicating that the two proteins are able to interact *in vivo* in neuronal cells. To further verify the interaction between the two proteins and their subcellular localization we performed confocal microscopy in differentiated SH-SY5Y cells (Figure 2). HSP60 displayed a cytoplasmic and mostly mitochondrial localization,

as shown by the quantification of the co-localization (82% of the pixels for HSP60 in the selected region of interest co-localize with Mitotracker® pixels), and in accordance with previously described observations [308,334]. ATXN3 had a more widespread localization being present both in the cytoplasm and nucleus according to previous results in these cells [335], and also a showed a strong co-localization with the mitochondria (70% co-localization). Merged images of single stack images showed strong co-localization of ATXN3 with HSP60 (90% co-localization), especially in the mitochondria. This result reinforces that HSP60 and ATXN3 are binding partners in neuronal cells.

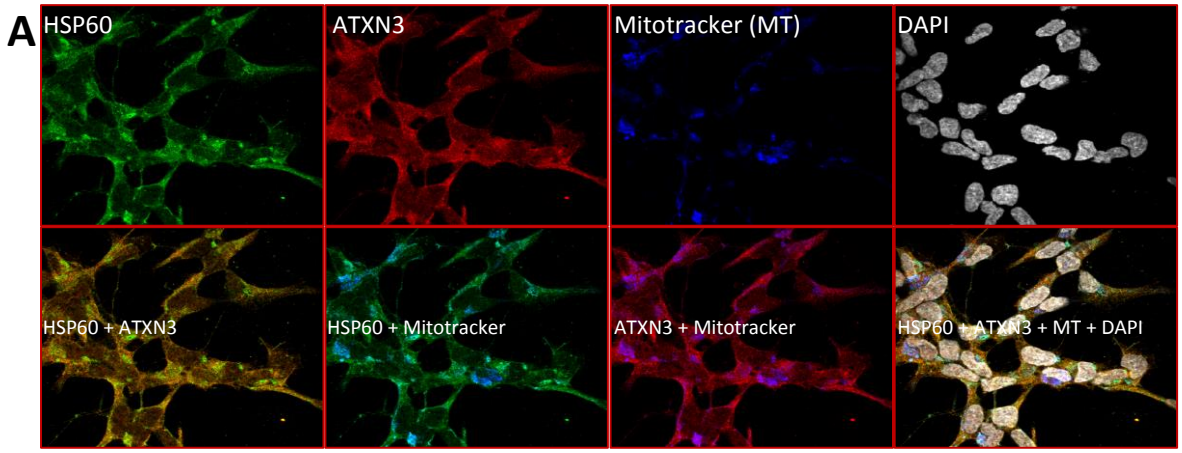

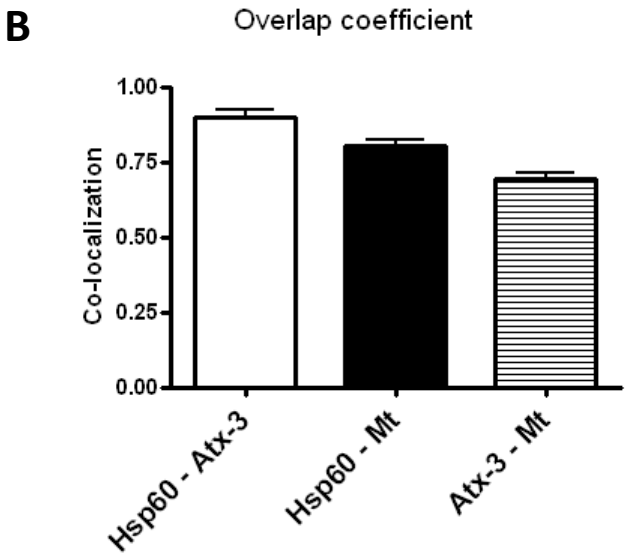

Figure 2 – Endogenous Hsp60 and ataxin-3 co-localize in SHSY5Y cells. *A*, The human neuroblastoma SH-SY5Y cell line was differentiated during 7 days using all-trans-retinoic acid, stained for the different proteins and subcellular compartments and images were visualized using confocal immunofluorescence microscopy . *A*, Single staining for: HSP60 (green); ataxin-3 (red); mitochondria (blue) and nuclei (white). Co-localization of the different pairs of proteins/compartments, merged image of: hsp60 plus ataxin-3; hsp60 plus mitochondria; ataxin-3 plus mitochondria and merged image of all stainings. *B*, Analysis of co-localization using overlap coefficient of designated areas (ROI – regions of interest) for HSP60ATXN3; HSP60/mitochondria and ATXN3/mitochondria; co-localization was calculated using Olympus FV1-ASW software.

ATXN3 and HSP60 interact directly *in vitro*

To investigate if the interaction of ATXN3 with HSP60 was direct and not the result of the interaction with other proteins, we initially expressed and purified GST and a GST-tagged version HSP60 and a His_6-tagged version of ATXN3 ^{324}. As observed in Figure 5 the recombinant protein containing GST fused to HSP60 bound purified ATXN3. ATXN3 was also pulled down by GST-NEDD8, used here as a positive control, since the interaction between NEDD8 and HSP60 has been previously described ^{244}. In contrast, GST was not able to pull-down ATXN3 indicating that HSP60 interacts directly and specifically with ATXN3 in these conditions. This result has additional functional significance, since we have confirmed through TEM and size-exclusion chromatography (data not shown) that the purified GST-HSP60 protein does not form native oligomeric structures, thus indicating that ATXN3 is able to interact with monomeric HSP60 and not just with the native functional active oligomeric state of the protein.

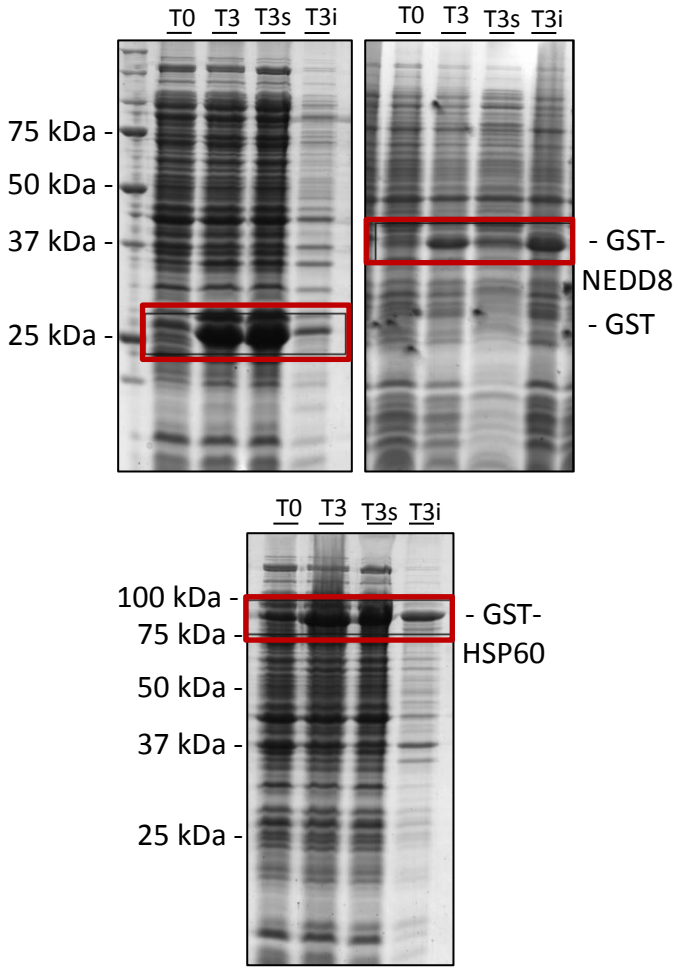

Figure 3 – Protein expression of GST, GST-NEDD8 in *Escherichia coli* strain BL21(DE3) and GST-HSP60 in BL21(SI). SDS-PAGE illustrating the protein expression profile; T0 – protein expression at time 0, before the induction of expression with IPTG; T3 – protein expression profile 3 hours after induction with IPTG; T3s – soluble fraction of the total protein after 3 hours of expression; T3i – insoluble fraction of the total protein expressed.

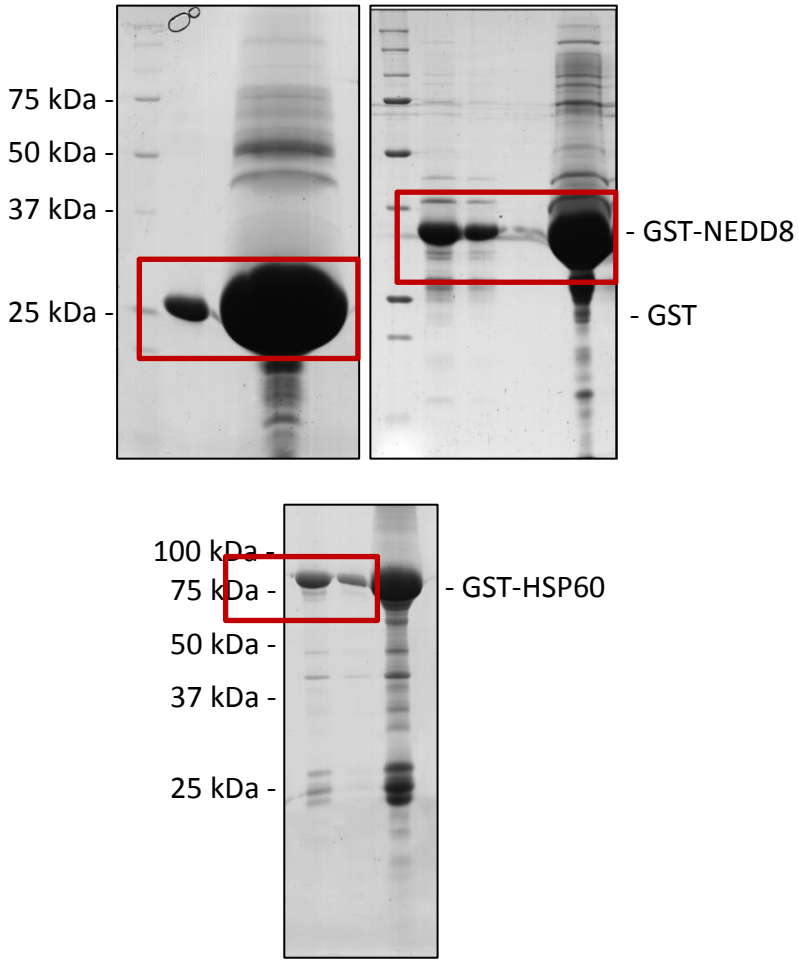

Figure 4 – Coomassie Blue-stained SDS–PAGE (10 % acrylamide) representing GST, GST-NEDD8 and GST-HSP60 purified proteins. Recombinant proteins after purification using Glutathione Sepharose B column and further purification using gel filtration column (Superdex 200 10/300) as described in "Experimental procedures".

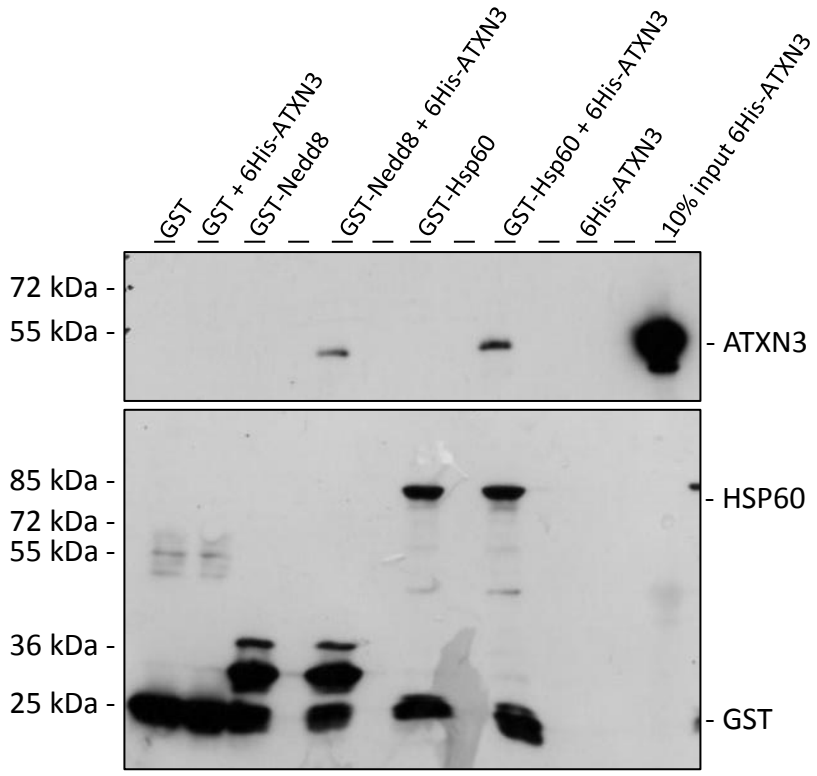

Figure 5 – ATXN3 interacts directly with HSP60 *in vitro*. The GST pull-down assay shows direct interaction between ATXN3 and HSP60. Recombinant proteins used in this assay: His_6-ATXN3 represents the full length of ATXN3 variant 1.1; GST; GST-NEDD8; GST-HSP60 and GST. Purified GST, GST-NEDD8 or GST-HSP60 were incubated with full length ATXN3 and NEDD8. A – NEDD8 and ATXN3 were able to pull-down HSP60 while GST alone (negative control) failed to pull-down HSP60.

Expression and purification of oligomeric mitochondrial HS

The folding of misfolded or unfolded proteins by chaperonins is performed by the coordinated action of two oligomeric proteins, HSP60 (homologue of prokaryotic GroEL) and its co-chaperone HSP10 (GroES in bacteria). GroEL is composed of fourteen identical subunits or monomers, disposed in two heptameric rings that form a barrel-shape cavity that allows the entrance of proteins [336,337]. GroES is composed of seven subunits that form a dome-like structure that, in the presence of ATP and Mg^{2+}, binds to GroES [338,339]. Due to the ease with which GroEL and GroES can be purified and to the stability of these bacterial oligomeric proteins, most of the knowledge about HSP60 and HSP10 comes from bacterial studies. Opposite to bacterial GroEL, HSP60 can function as a single heptameric ring [340,341] and occurs in

solution in a dynamic equilibrium between monomers, heptamers and tetradecamers [342–344]. Our objective was to reconstitute oligomeric HSP60 in its heptameric form to observe if in its native form HSP60 was able to interact with ATXN3.

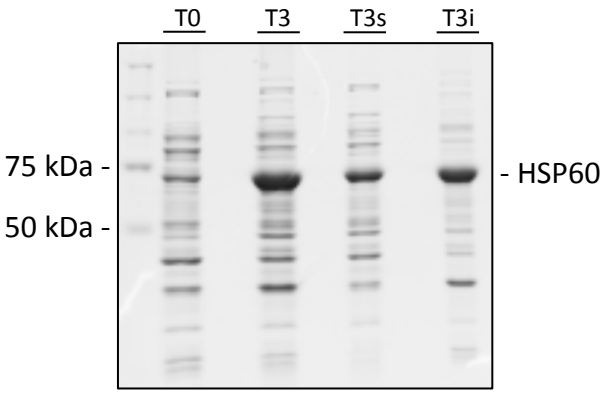

Figure 6 – Protein expression of mature HSP60 in *Escherichia coli* strain BL21(DE3). SDS-PAGE illustrating the protein expression profile; T0 – protein expression at time 0, before the induction of expression with IPTG; T3 – protein expression profile 3 hours after induction with IPTG; T3s – soluble fraction of the total protein after 3 hours of expression; T3i – insoluble fraction of the total protein expressed.

HSP60 is encoded by nuclear DNA, synthesized as a large precursor form containing an N-terminal targeting sequence necessary for its mitochondrial import and is cleaved during the processing to the mature form in the mitochondrial matrix [345]. We started by cloning the mature form of HSP60 [323] so we would be able to purify the oligomeric form of HSP60. Expression of pET_GB1-mHSP60 was performed in BL21(DE3) cells (Figure 6) and the protein was isolated from the cell extract recurring to a His-Trap purification column (Figure 7). To prepare oligomeric form of HSP60 the protein tag was removed through incubation with TEV (Figure 8), so HSP60 monomers were able to oligomerise to the native structure. To confirm the nature of HSP60 protein species isolated, purified untagged protein was passed through an ion-exchange chromatography column, chromatogram and SDS-PAGE confirmed the presence of HSP60 in a single form (Figure 9). These forms of HSP60 isolated in this initial step were tested in an analytical size-exclusion chromatography column (superpose 6 10/300) that later was also used to separate the oligomeric from the low molecular weight species of HSP60 (Figure 10). An oligomerization protocol (OP) [325] was applied and resultant proteins were separated using an ion-exchange chromatography column, the same used to analyse HSP60 species after His_6-tag removal (Figure 9). On panel A of figure 11 two analytical chromatograms are superimposed, in red the correspondent to isolation of low molecular weight forms of HSP60 isolated after His_6 tag removal, and in blue the correspondent to the

HSP60 species isolated after OP. Peak number 3 corresponds to a component of the OP buffer since no protein was detected in the samples collected from this peak (Figure 11, panel B). Peaks number 1 and 2 correspond to different molecular weight forms of HSP60. To identify the nature of both protein species further characterization studies were carried out.

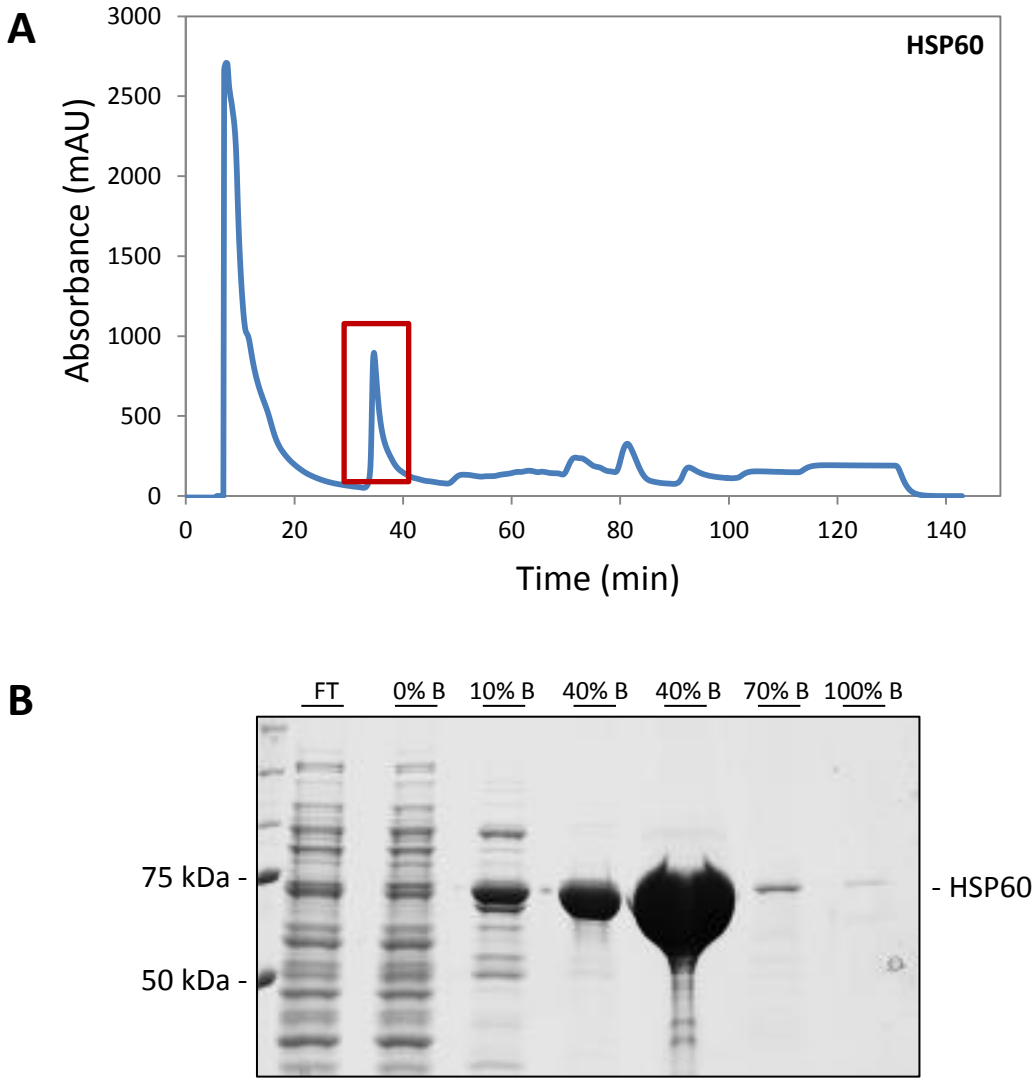

Figure 7 – HisTrap to purify His-tagged HSP60. *A*, Analytical HisTrap chromatography profile for the separation of His-tagged HSP60; red box indicates the fraction isolated from the total expressed protein, that was eluted in 40% Buffer B (50 mM NaH2PO4/Na2HPO4 pH 7.5; 300 mM NaCl; 500 mM Imidazole) and 60% of Buffer A (20 mM NaH2PO4/Na2HPO4; 300 mM NaCl; 10 mM Imidazole). *B*, Coomassie Blue-stained SDS–PAGE (10 % acrylamide) analysis of proteins isolated by HisTrap at different concentrations of Buffer B; protein fractions collected with 40% Buffer B were used for the further purification steps.

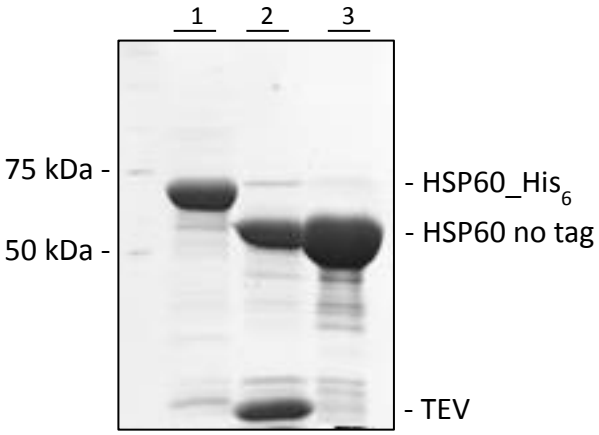

Figure 8 – Cleavage of HSP60_His_6 by TEV. Coomassie Blue-stained SDS–PAGE (10 % acrylamide) analysis of the cleavage by TEV of HSP60_His_6; line 1 is HSP60_His_6 after HisTrap and prior to cleavage by TEV; line 2 is the fraction collected in nickel beads after cleavage by TEV, it is observed that some untagged HSP60 was captured in this fraction; line 3 represents the untagged HSP60 that was in the beads' flowthrough and was used in further purification steps.

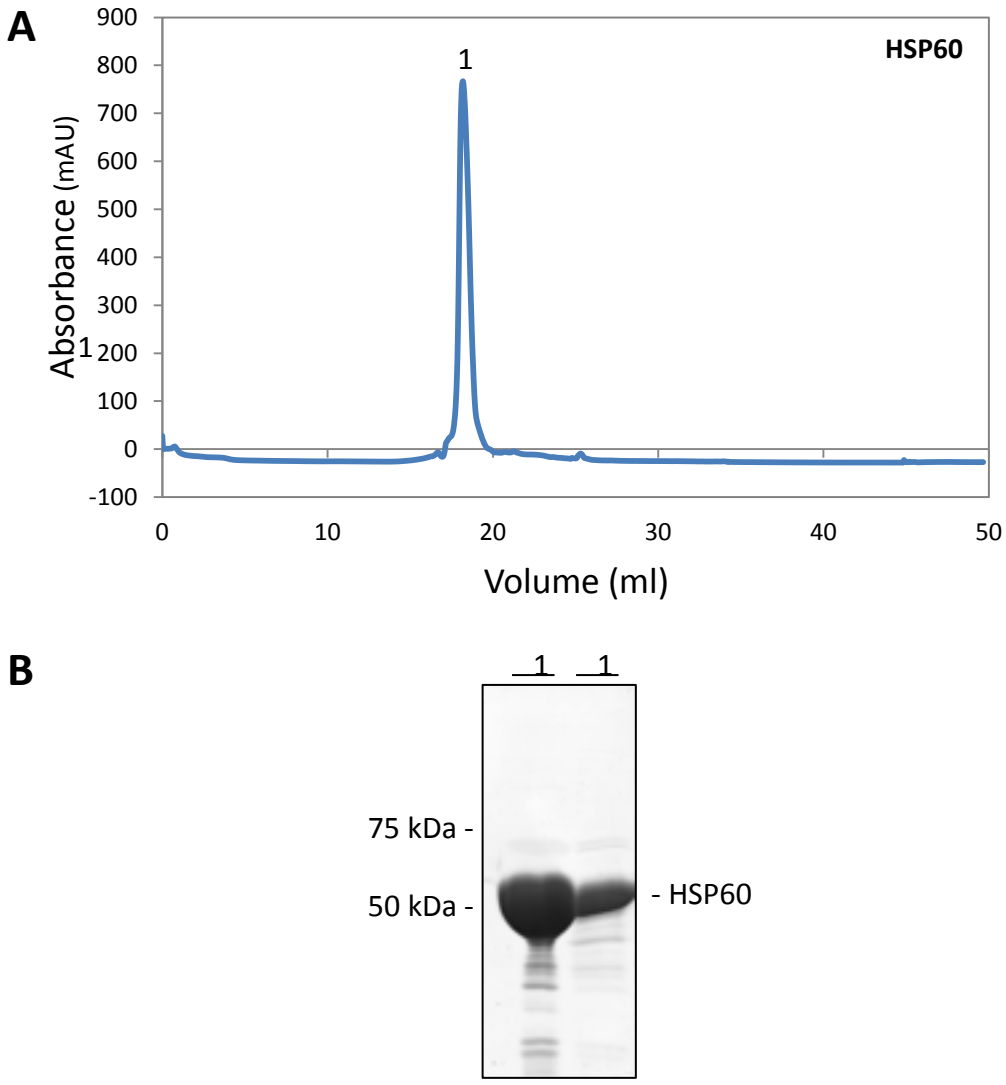

Figure 9 – Ion-exchange chromatography for HSP60 after cleavage by TEV. *A*, Analytical ion-exchange chromatography profile for HSP60 after cleavage of HSP60_His_6 by TEV; A single peak is observed. *B*, Coomassie Blue-stained SDS–PAGE (10 % acrylamide) showing different amounts of HSP60 isolated from the fraction corresponding to peak 1 collected in the Mono Q column.

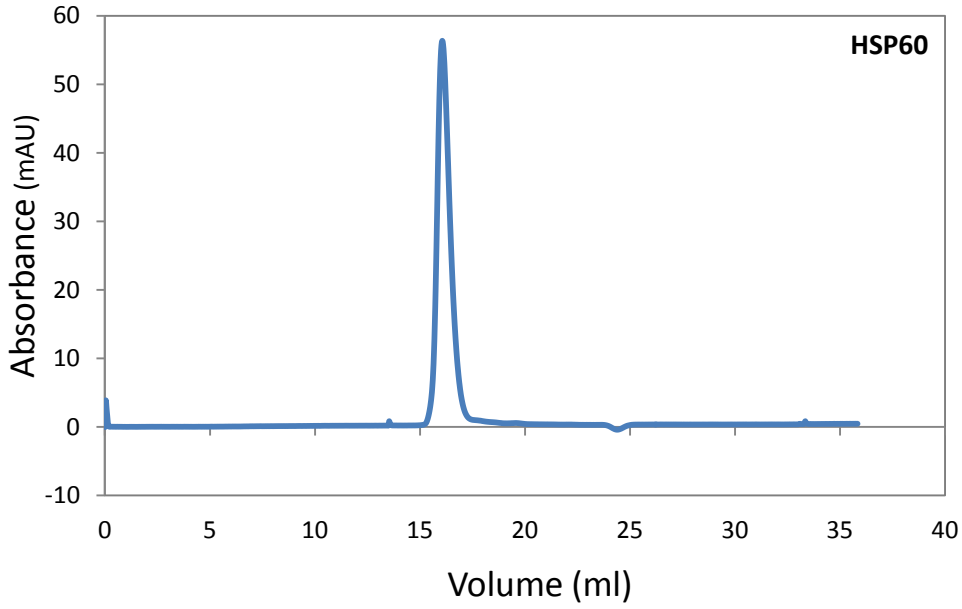

Figure 10 – Size-exclusion chromatography analysis of HSP60 after separation in ion-exchange chromatography. A single peak is observed corresponding to the non-oligomeric HSP60 that was used for the reconstitution of oligomeric HSP60.

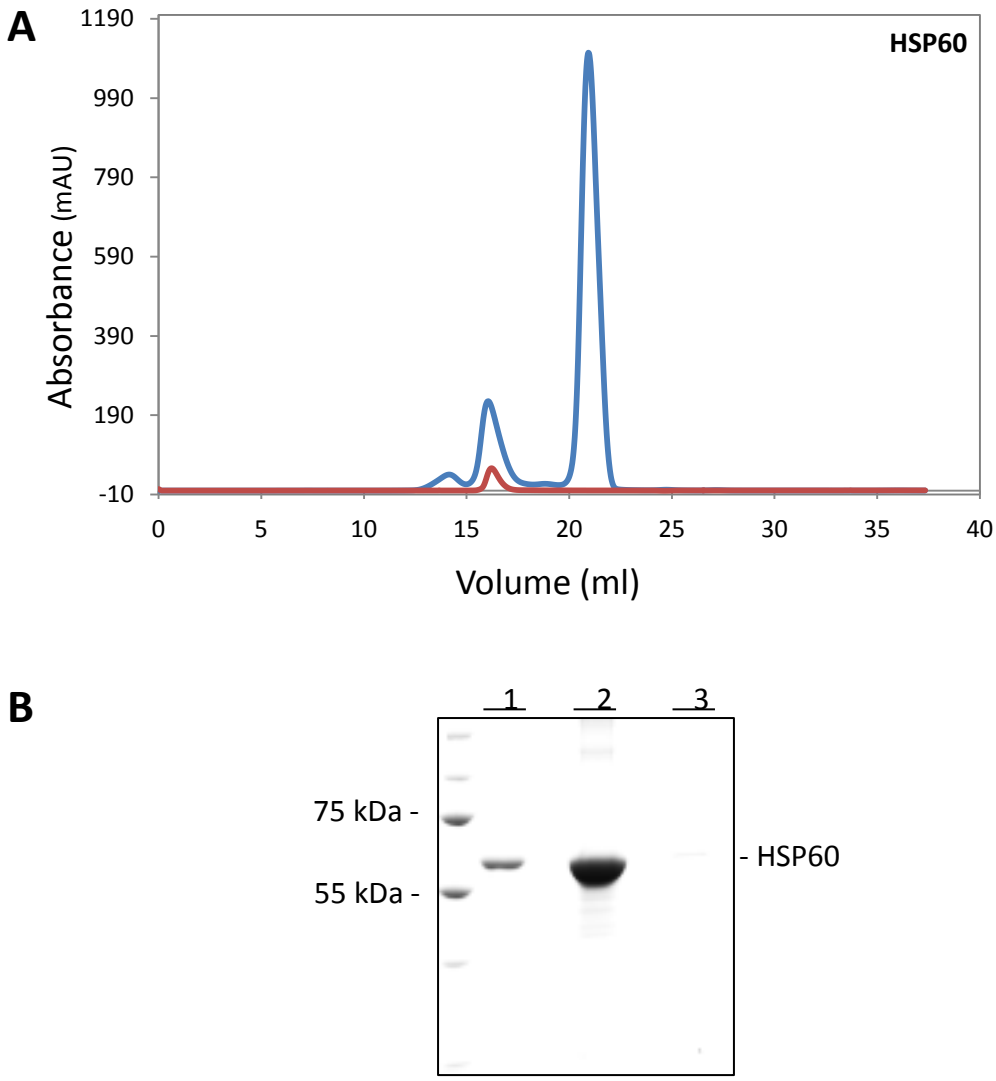

Figure 11 – Purification of Oligomeric HSP60. *A*, Analytical size-exclusion chromatography profile of after applying the oligomerization protocol to reconstitute oligomeric HSP60; peak 1 corresponding to higher molecular weight species – oligomers; peak 2 corresponds to lower molecular weight species – monomers and/or small molecular weight oligomers; peak 3 – corresponding to a compound present in the buffer with no HSP60. *B*, Coomassie Blue-stained SDS–PAGE (10 % acrylamide) representing the peaks isolated by size-exclusion chromatography.

Characterization of low molecular weight and heptameric HSP60

To evaluate the HSP60 species that we were able to isolate through the oligomerization protocol (OP) we started with the calibration of the analytical size-exclusion chromatography column (superose6 10/300) used after the OP for the determination of the molecular weight of proteins isolated. On Figure 12 panel A are the size exclusion chromatography chromatograms for standard molecular weight markers, and panel B represents the calibration curve for determination of molecular weight by analytical SEC. Applying the K_{av} (described in

"Experimental Procedures") for HSP60 species elution volumes to the calibration we inferred a molecular weight for HSP60 before OP of 95940 Da (blue dot in the calibration curve of figure 12, B), a molecular weight of 111943 Da for low molecular weight species after OP (green dot on calibration curve), and a molecular weight of 514043 Da for high molecular weight species after OP (blue dot on the calibration curve). When investigating molecular weight recurring to size exclusion chromatography numerous studies have already addressed the importance of the influence of the hydrodynamic volume and molecular shape on chromatographic behavior in a size exclusion chromatography column [346,347], consequently caution must be taken interpreting the calculated MW. Taking this in consideration, low molecular weight species isolated before and after the OP are more or less the same MW and possibly correspond to dimers of HSP60, and the high molecular weight isolated forms (514043 Da) correspond to an oligomeric structure with much higher molecular weight, possibly corresponding to the heptameric HSP60 [341].

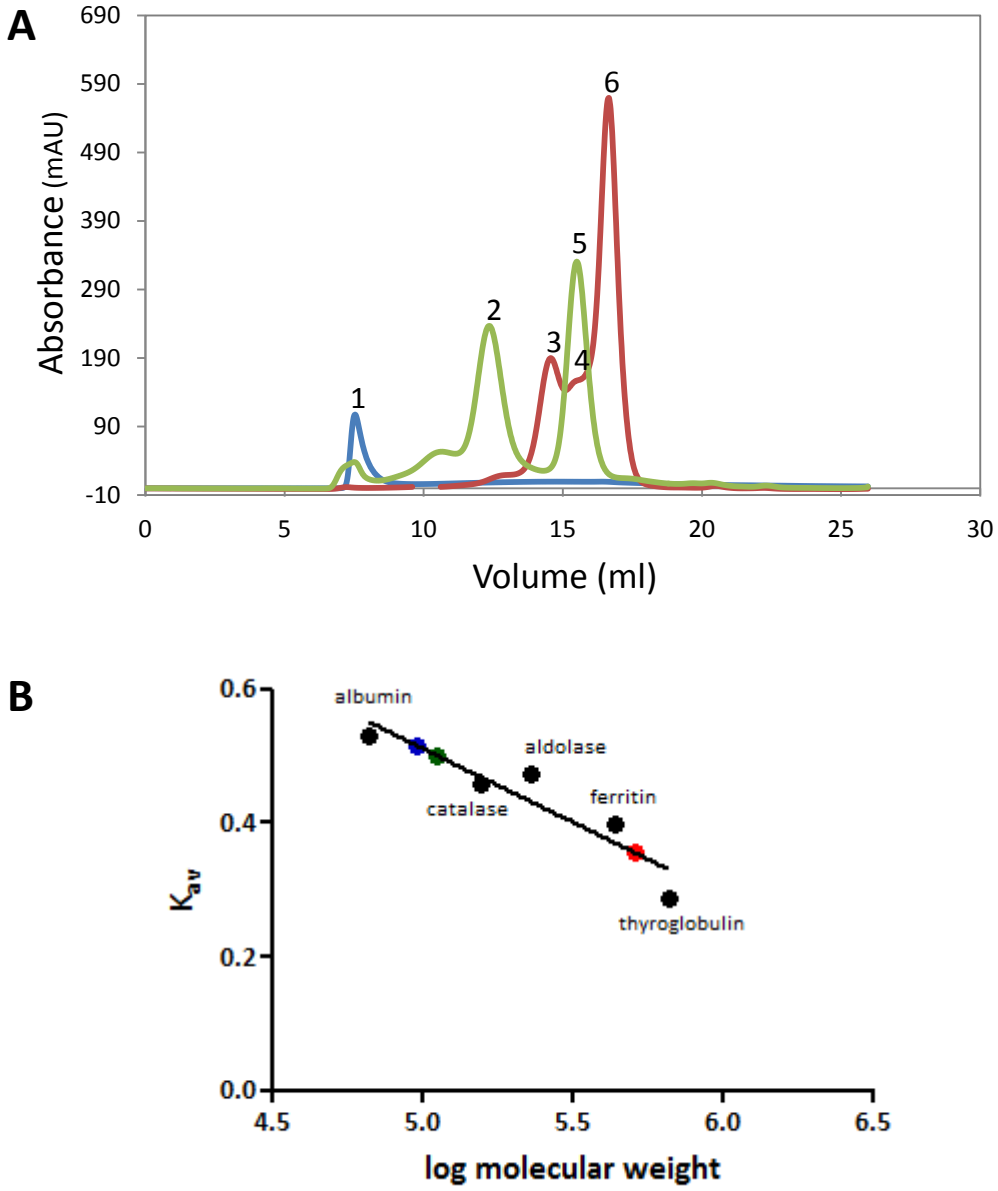

Figure 12 – Calibration of Superpose 6 10/300 column. *A*, Three analytical size exclusion chromatography (SEC) chromatograms of standard molecular weight markers are superposed; peak 1 refers to Dextran Blue that is a marker for void volume elution; peak 2 refers to thyroglobulin (Molecular weight - 669 kDa); peak 3 – ferritin (MW – 440 kDa); peak 4 – catalase (MW – 232 kDa); peak 5 – aldolase (MW – 158 kDa); peak 6 – albumin (MW – 67 kDa). *B*, Calibration curve for determination of molecular weight by analytical SEC; blue dot represents the K_{av} for the elution volume of low molecular weight HSP60 species before oligomerization protocol; green dot represents the K_{av} for the elution volume of low molecular weight HSP60 species isolated after oligomerization protocol; red dot represents K_{av} for the elution volume of oligomeric HSP60 isolated after the oligomerization protocol.

Further examining the HSP60 species obtained, we conducted a study using Dynamic Light Scattering (DLS) technique to calculate the corresponding molecular weights and the homogeneity of the pure concentrated samples. The DLS spectra of low molecular weight HSP60 (LMW_HSP60) and oligomeric HSP60 showed one major population by size (figure 13) with a polydispersity (%*Pd* = (*PdI*)1⁄2 × 100, also called relative polydispersity) of 9,5% and 4,5% respectively. As a rule, samples with % Pd <~20%, are considered to be monodisperse (Therapeutic Protein Characterization Using Light Scattering Techniques, Technical Note MRK704 01 MAN0317 Issue2. In: Zetasizer Nano Series User Manual). The R_H (hydrodynamic radius) values obtained were 6,327 nm and 8,051 nm for LMW_HSP60 and oligomeric HSP60. These values were used to estimate the molecular weight (assuming a globular protein) using an empirical calibration graph developed by Malvern Instruments available in the Nano software [348]. Accordingly, the molecular mass of LMW_HSP60 and oligomeric HSP60 were estimated to be 252,2 kDa and 443,3 kDa respectively. The value for LMW_HSP60 possibly corresponds to association of dimeric structures that were observed in analytical size exclusion chromatography, that in these conditions possibly forms a tetrameric structure. The molecular weight calculated for oligomeric HSP60 is very close to the expected molecular weight (405,74 kDa) in a heptameric ring of HSP60. Although these results are indicative, since we are assuming in the calculations that the protein is a globular structure, they closely fit with the data obtained from the size exclusion chromatography calibration curve to calculate the molecular weight, and assure us that we have monodisperse/pure samples.

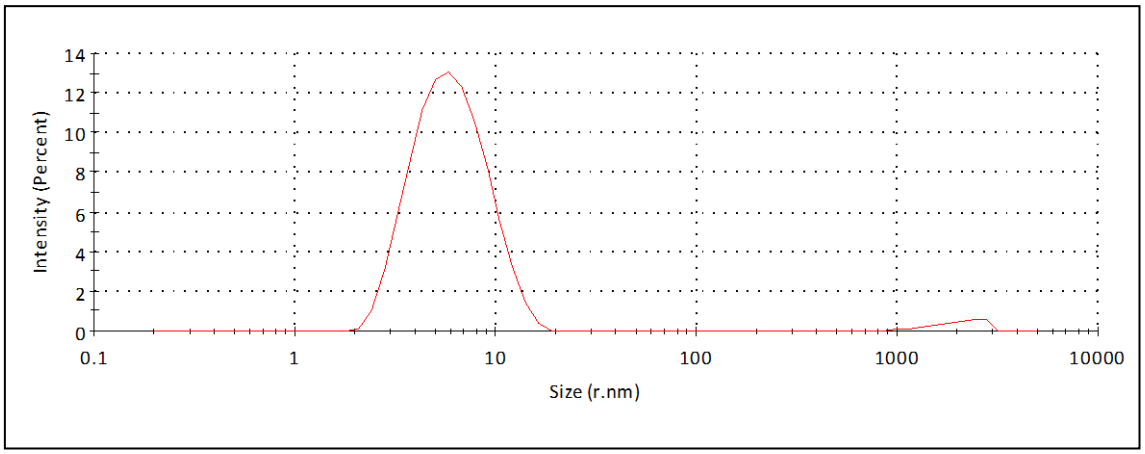

LOW MW HSP60 SPECIES: R_H= 6,327 nm ~ 252,2 kDa PdI = 0,190

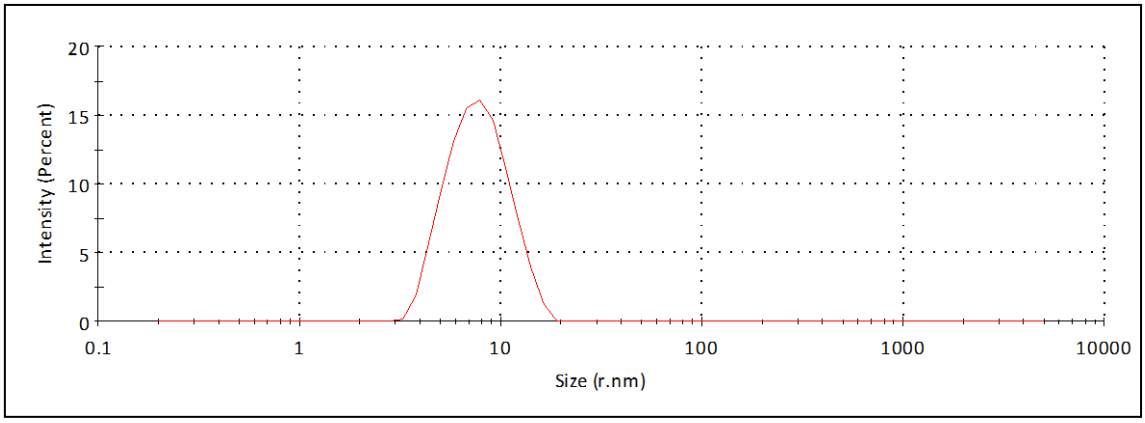

OLIGOMERS: R_H= 8,051 nm ~ 443,3 kDa PdI = 0,09

Figure 13 – Distribution of hydrodynamic radii from DLS spectrum of HSP60 forms. *A*, Low molecular weight species of HSP60 (possibly tetramers) used in the reconstitution of oligomeric HSP60, 2 mg/mL protein concentration, with a predicted molecular weight of 252,2 kDa. *B*, Oligomers of HSP60 after reconstitution protocol, 2 mg/ml protein concentration, with a predicted molecular weight of 443,3 kDa.

Proceeding with the characterization of the isolated protein we observed the protein preparations recurring to Transmission Electron Microscopy (TEM). HSP60 forms a oligomeric structure composed of seven monomers with a ring-shape structure [341] as observed in Figure 14. The TEM images obtained were similar to the ones shown in previous reports of the purification of oligomeric HSP60 [340,344]. Mammalian mitochondrial chaperonins maintain a dynamic equilibrium between the monomeric, heptameric and tetradecameric states [344]. We have no evidence of the formation of tetradecameric structures of HSP60 in our conditions which reflects not having in our oligomerization protocol the presence of co-chaperone HSP10 [325], thus favoring the formation of active single ring chaperonin [340].

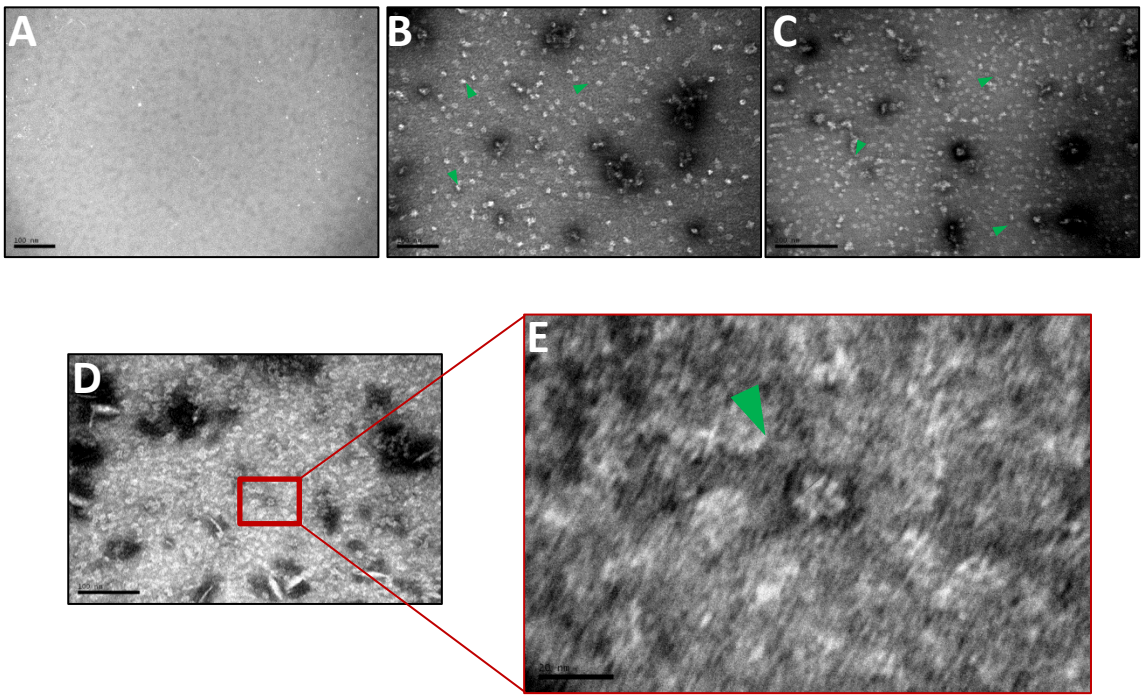

Figure 14 – Transmission Electron Microscope observation of oligomeric HSP60. *A*, Negative control, buffer used in HSP60. *B*, Ring structure of HSP60 heptamers indicated by arrowheads was observed with 150000X amplification. *C*, HSP60 heptamers observed with 200000X amplification. *D*, Ring structure of HSP60 observed with 200000X amplification. *E*, Detail of the ring structure of HSP60 heptamer using 1200000X amplification.

These results confirm the homogeneity of our purified oligomeric HSP60 (observed in DLS) and also confirm the presence in this preparation of oligomeric structures of HSP60 that correspond to heptameric rings of mitochondrial HSP60 [341].

Interaction HSP60-ATXN3

With our GST pull-down results we were able to demonstrate that monomeric HSP60 was able to interact with ATXN3. To demonstrate that HSP60 in its oligomeric form was still able to interact with ATXN3, recombinant His_6_ATXN3 was immobilized onto a biosensor chip of BiaCore X100 system, oligomers of HSP60 were injected into the cell flow and their interaction followed in real time (Figure 15). Sensorgrams indicate that oligomers of HSP60 were able to interact with full-length ATXN3 (panel A), D1_ATXN3 (panel B) or J1_ATXN3 (panel C). With this technique we were also able to identify the domain responsible for the interaction since solely the Josephin domain of ATXN3 by itself was able to establish the interaction.

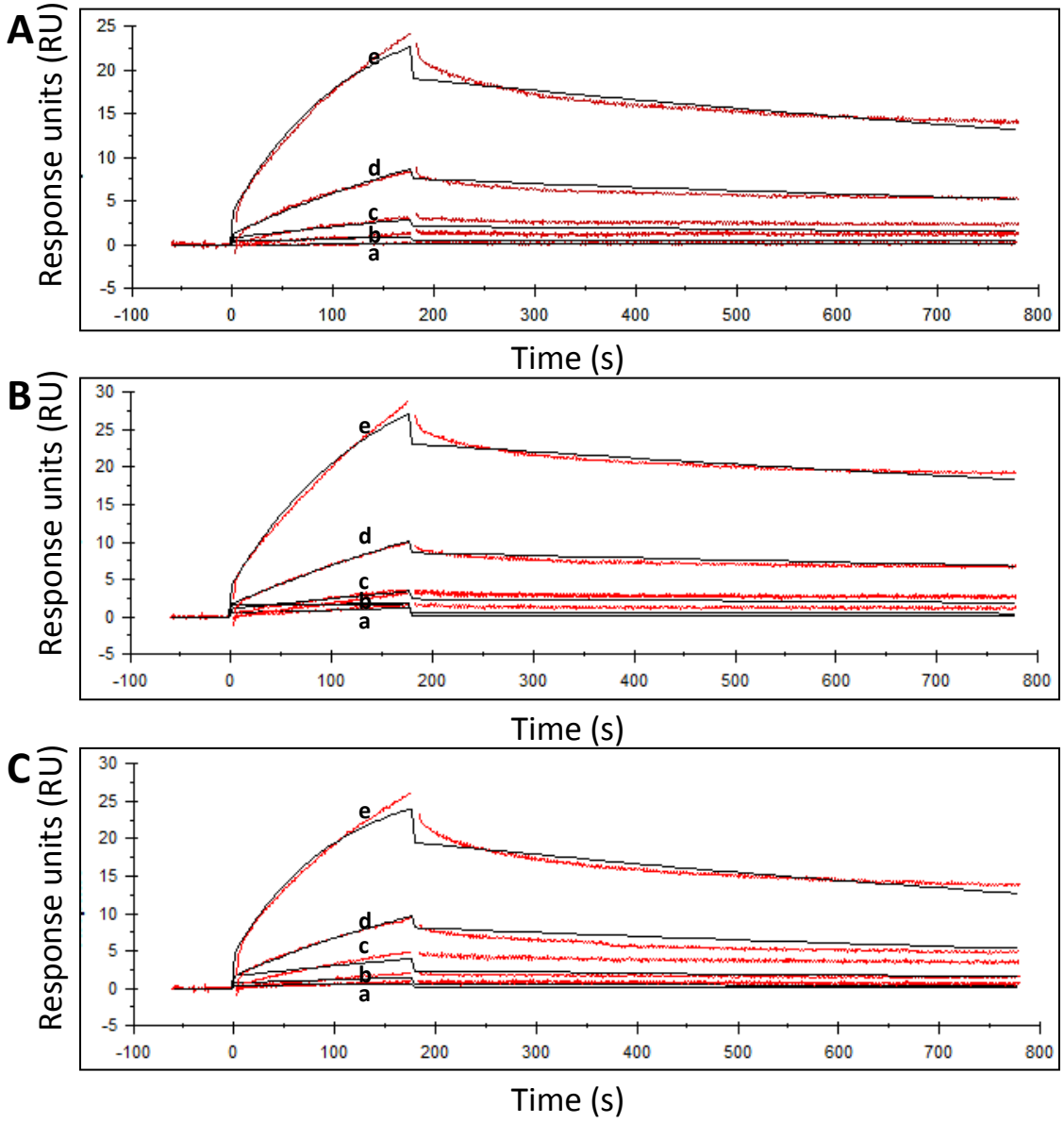

Figure 15 – Surface Plasma Resonance analysis for the interaction between HSP60 and ATXN3. Increasing amounts of HSP60 (a – 1,953 nM; b – 7,825 nM; c – 31,25 nM; d - 125 nM; e – 500 nM) were passed over ATXN3 immobilized onto a sensor chip. Specific binding is shown, sensorgrams represent each amount of analyte with subtraction of non-specific binding and is represented in resonance units. *A*, Interaction of full lenght ATXN3 with HSP60. *B*, Interaction of D1_ATXN3 (Josephin domain plus UIM1 and UIM2) with HSP60. *C*, Interaction of J1_ATXN3 (Josephin domain) with HSP60.

Discussion

Molecular chaperones facilitate and regulate proper protein folding playing a major role in cell maintenance and survival. Compared to other cell types neurons are particularly susceptible to the mechanisms of degeneration since they have a long life time, are present during the lifespan of the organism in most cases, and are not frequently replenished through cell division. To test the interaction *in vivo* between HSP60 and ATXN3 we use a model – SH-SY5Y neuroblastoma cell line - that could reproduce the neuronal environment and could lead us to take conclusions in that specific context. These cells were used in many studies of neuronal function [327–330] and in studies involving HSP60 functions, namely to study the relevance of the interaction with CLU [349], a protein expressed virtually in all tissues and involved in the modulation of carcinogenesis and tumor growth [349].

In this work we describe for the first time the interaction between the molecular chaperone HSP60 and ATXN3. Our results concerning the interaction *in vivo*, specially the sub-cellular co-localization, indicate that a significant amount of ATXN3 is interacting with HSP60 in neuronal cells, thus suggesting a relevant interaction in this context. Interactions of ATXN3 with chaperones described until now point to regulatory roles on both directions. In the case of the interaction with HSP70 [350], ATXN3 is regulating the protein levels of the chaperone through the regulation of the HSP70 promoter activity both in basal and stress conditions, and ATXN3 Knock-out animals and fibroblasts have decreased HSP70 promoter activity when compared with WT [350]. In another study, ATXN3 was proven to be an interactor and a target of regulation of the co-chaperone HSJ1, that is involved in the regulation of the ATPase activity and substrate binding of HSP70 [351]. HSJ1 is thought to be a key protein in the interplay between the chaperone machinery and the Ubiquitin Proteasome System (UPS) in the particular case of ATXN3 protein degradation [351]. While the J-domain of HSJ1 promotes the proteosomal degradation of ATXN3 in coordination with HSP70 the ubiquitin-interacting domain in the protein promotes ubiquitinated-ATXN3 accumulation. These results make HSP70 and its co-chaperone good candidates for the regulation of ATXN3 levels in cells. Previously it has also been reported that overexpression of expanded ATXN3 evokes HSP70 protein expression [352]. Since the regulation of ATXN3 by HSP70 is mediated through its co-chaperone as described above, one question that arises is whether the interaction between HSP60 and ATXN3 is direct or indirect. Chaperones and particularly HSP60 regulate protein fate sometimes through a complex network of interactions and others through a direct interaction. As an example in the case of the interaction of HSP60 with the IKK complex for its activation, the proteins do not

have any mediating partners [353], while 14-3-3 protein forms a molecular complex with cellular prion protein (PrPC) and Hsp60 [354]. Our GST pull-down results show that the interaction between ATXN3 and HSP60 is direct. In a study that demonstrates the role of HSP60 in survival of cancer cells [353], it was shown that cytosolic HSP60 regulates the levels of inhibitor of κB kinase (IKK) and it is suggested that this regulatory role is performed by monomeric HSP60 instead of single or double heptameric ring structures [353]. Our results with GST-tagged proteins and with the oligomeric HSP60 raise the possibility that ATXN3 is able to interact with both non-chaperonic monomers and with oligomers. This also raises the question about the stoichiometry of the interaction between the two proteins; if ATXN3 is able to interact with monomeric HSP60, in theory 7 molecules of ATXN3 would be able to interact with each heptameric ring of HSP60. In an attempt to clarify this question and the affinity of the interaction we analysed the interaction by Surface Plasma Resonance. Although our results confirm the direct interaction and indicate that the Josephin Domain of ATXN3 is the responsible for the interaction, our data had a standard deviation above the acceptable standards and thus we were not able to infer either the affinity of the interaction or the stoichiometry of the interaction, taking these results as qualitative and not quantitative.

Most of the studies concerning chaperonin function were made in prokaryotic *E. coli* due to the ease of the purification of the protein and the stability of the oligomeric structures. The high homology between prokaryotic and animal HSP60 [355], the fact that chaperonins can fold protein *in vitro* with similar efficiency compared to GroEL [340] and HSP60 capability to replace bacteria GroEL [356] lead to the assumption that the structure and functioning are similar in these proteins [357]. Nevertheless, there are some structural differences between the two proteins. Mammalian HSP60 is only functional in the presence of its co-chaperone - HSP10 [341] - while GroEL is able to form active complexes not only with GroES but also with HSP10 [340,356]. Relevant for our study is the fact that HSP60 occurs in mammalian cells in a dynamic equilibrium between monomers, heptamers and tetradecamers [344]. To form tetradecameric structures in major proportions the purification has to be performed in the presence of both ATP and HSP10 [344]. Although the tetradecamers represent the most similar structure to prokaryotic GroEL, studies revealed that HSP60 is active when forming just a single heptameric ring [340]. Since our objective was to test the interaction between HSP60 and ATXN3, the single ring oligomer we were able to produce represents native (although not active) conditions in cells and thus can indicate that in native conditions these proteins are indeed able to interact. The fact that HSP60 in this form, which is not active since it lacks HSP10, is able to interact with ATXN3, and the suggestion coming from GST pull-down studies that ATXN3 is also able to interact with inactive [325] HSP60 monomers suggests a regulatory role for this interaction, but it

is not possible to exclude that HSP60 is a chaperone for ATXN3 helping in the correct folding of the protein. Theoretically this is possible, since the barrel formed by GroEL heptameric rings is able to host unfolded proteins of up to 60 kDa in size [358], and the example of a protein (Mtf-1) of the exact molecular weight of ATXN3 (42 kDa) engulfed by HSP60 was suggested before [359]. To solve this question, directed mutagenesis can be used to mutate the residues responsible for enzyme-substrate interaction (which are conserved to some extent between GroEL and HSP60 [355]) and to verify if the proteins are still able to interact.

Most of the literature points regulatory roles for HSP60 in terms of altering protein localization or function, besides the known role as a chaperone. Regulating the abundance of Insulin-like Growth Factor-1 receptor β through inhibiting polyubiquitination [360], acting as a ligand for receptors in cell surface and modulating its activity as in the case of ATP synthase [361] or in Triggering receptor expressed in myeloid (TREM) cells 2 [362], or even regulating transcription through the regulation of IKK [353]. The fact that inactive HSP60 monomers are also able to interact with ATXN3 can point to a regulatory role for HSP60 in this context but further studies must be conducted to clarify the functional meaning of this interaction.

Alternatively, HSP60 could be a substrate of the DUB activity of ATXN3. HSP60 is known to regulate the immune system [363–365] and in adult cardiac myocytes is present in exosomes in a monoubiquitylated form [366]. It has been proposed that the monoubiquitylation of HSP60 is a signal for HSP60 release for the extracellular space through exosomes, so it can act as an immune system regulator. Our group has conducted experiments that also demonstrate HSP60 ubiquitylation and show that in the absence of ATXN3 in SH-SY5Y cells the levels of polyubiquitylated HSP60 are significantly decreased (unpublished data) comparing with cells that have ATXN3. This clearly points to a regulation of HSP60 ubiquitylation by ATXN3 and possibly through the last deubiquitylating activity. To capture ubiquitylated proteins Tandem Ubiquitin Binding Entities (TUBEs) [367] were used, which have preference but not exclusivity for polyubiquitylated proteins [367]. This results point to a contribution of ATXN3 to the maintenance of HSP60 polyubiquitylation. ATXN3 was described as an polyubiquitin chain editor previously [237,368]. In the particular case of the association with Hsc70-interacting protein (CHIP), ATXN3 is involved in the trimming of CHIP-associated substrates' polyubiquitin chains and possibly sending these substrates for proteosomal degradation [237], in accordance with the fact that ATXN3 knockout mice have increased levels of molecular high weight, ubiquitin-positive signal proteins [237]. To further explore the functional meaning of these results future experiments must clear if the levels of unubiquitylated HSP60 are altered or not, to check if the effect of ATXN3 KO is specific for the ubiquitylated form of HSP60.

Despite the great variety of human neurodegenerative diseases, many of these are considered

conformational diseases and characterized by the accumulation of pathological misfolded proteins, and chaperones are one of the major players in cellular maintenance and stress response. Many examples of the involvement of chaperones in neurodegeneration are available in the literature. In Parkinson´s disease HSP70 inhibits amyloid fibril formation by α-synuclein through the binding to pre-fibrillary species thus resulting in a shift from insoluble to soluble form of the protein [369]. In Alzheimer´s disease HSP27 and HSP70 co-localize with abnormal tau aggregates and regulate its hyperphosphorylation [370,371]. In SH-SY5Y cells, HSP60 and HSP70 contribute to the reduction of reactive oxygen species levels produced in the presence of β-amyloid [372], and HSP60 prevents the inhibition of complex IV in the mitochondria by β-amyloid [372]. In polyglutamine (polyQ) diseases, the relevance of HSPs was also attested: HSP40 and HSP70 reduce polyQ toxicity and inclusion body formation [352,373], and unpublished results from our group point to reduced levels of HSP60 in cerebellum and brainstem in the CMVMJD94 mouse model [374].Taking this in consideration, it is not possible to exclude that HSP60-ATXN3 interaction is relevant in terms of the etiology and pathology of Machado-Joseph disease, a hypothesis that shall be further explored.

Chapter 3

Ubiquitin C-terminal Hidrolase 1 (UBH-1) the orthologue of vertebrate UCH-L1, is not a modifier of Machado-Joseph disease in *Caenorhabditis elegans*.

Ubiquitin C-terminal Hydrolase, the orthologue of vertebrate ubiquitin carboxyl-terminal hydrolase 1, is not a modifier of Machado-Joseph disease in *Caenorhabditis elegans*

Márcio S. Baptista[1,2], Andreia Teixeira-Castro[1,2], Ana Jalles[1,2] and Patrícia Maciel[1,2*]

1. Life and Health Sciences Research Institute (ICVS), School of Health Sciences, University of Minho, Braga, Portugal
2. ICVS/3B's - PT Government Associate Laboratory, Braga/Guimarães, Portugal

*Corresponding author:

Patrícia Maciel, PhD

Life and Health Sciences Research Institute (ICVS); School of Health Sciences; University of Minho; Campus de Gualtar; 4710-057 Braga, Portugal

e-mail: pmaciel@ecsaude.uminho.pt

Tel: +351 253 604 824 Fax: +351 253 604 820

Ubiquitin C-terminal Hydrolase (UBH-1) is the orthologue of vertebrate ubiquitin carboxyl-terminal hydrolase 1, an enzyme which, besides its deubiquitylating activity also works as monoubiquitin stabilizer and ubiquitin-ligase. It has been first related with the etiology of Parkinson disease and more recently also to Alzheimer's disease. 15-deoxy-$\Delta^{12,14}$-Prostaglandin J_2 (15d-PGJ_2), a metabolite of prostaglandin D_2, specifically blocks UCH-L1 function and leads to enzyme unfolding and aggregation. In this study we analyzed the outcome of UBH-1 deletion and evaluated the impact of 15d-PGJ_2 administration in *C. elegans;* we also investigated the possible effects of UBH-1 deletion and 15d-PGJ_2 exposure as modifiers of proteostasis and enhancers of neurodegeneration in a nematode model of MJD. We concluded that deletion of UBH-1 causes no major phenotype and allows development of a globally normal nervous system. Furthermore, absence of this gene did not modify ataxin-3 (ATXN3) aggregation or neurotoxicity in an MJD transgenic model. The prostaglandin 15d-PGJ_2, either acting as an

inducer of oxidative stress or as a modulator of UBH-1, also had no effect in motor behavior or protein aggregation in the *C. elegans* model of MJD.

Introduction

Ubiqutin carboxy-terminal hydrolase L1 (UCH-L1), also denominated PARK5 or PGP9.5, is very abundant in neurons where it represents 1-2% of the total soluble protein [6]. It is thought to work mainly as a monoubiquitin stabilizer, associating with ubiquitin specifically and affecting its degradation and extending its half-life [8]. A deubiquitylating activity was also identified *in vitro* [7,116,375] for UCH-L1 but until now no substrates were identified. Ubiquitin-ligase functions have also been proposed, and *in vitro* experiments suggest a role in α-synuclein ubiquitylation[9]. A role in neurodegenerative diseases was described and two mutations in UCH-L1 were identified as PD-related. The S18Y polymorphism turns UCH-L1 ubiquitin ligase activity less effective. UCH-L1 ubiquitylates through Lysine-63, which favors the stability of α-synuclein, and thus this polymorphism turns the protein less stable reducing the risk of PD [9]. The I93M mutation was also identified in PD patients [191], evoking diminished deubiquitylase activity and changes in the secondary structure of the enzyme [376]. It was also shown that mice carrying the I93M mutation exhibit a partial loss of dopaminergic neurons, thus indicating that the mutation is relevant cause for the disease [377]. Data concerning the deletion of UCH-L1 come from the gracile axonal dystrophy [gad] mice, that carry a spontaneous mutation leading to the production of a truncated enzyme - lacking residues that are critical for enzymatic activity [378], and from UCH-L1 knock-out mice that lack the entire enzyme [379]. The latter have impaired synaptic transmission at the neuromuscular junction, with a significant reduction in synaptic vesicle content - which can explain the ataxia and paralysis phenotypes observed in both models [378,379] - and contributed to the elucidation of the physiologic role of UCH-L1 in neurons.

Inhibition of UCH-L1 hydrolase activity recurring to a specific inhibitor (LDN-57444) impairs synaptic function in mice [119], and those impairments found were similar to those found in APP/PS1 mice (Alzheimer disease (AD) mouse model) [380], which show reduced hydrolytic activity of the enzyme [119]. Restoring the UCH-L1 protein levels lead to improvements in synaptic transmission in brain slices of APP/PS1 mice and also suppressed the fear conditioning impairment, a form of learning that is deregulated in AD [10]. The restoration of the different

activities of UCH-L1 was tested and no evidences were found that restoration of ligase activity was important for the rescue of synaptic function, thus reinforcing the idea that the DUB activity of the enzyme is the one that contributes to pathology, like in the case of PD.

In *Caenorhabditis elegans*, three Ubiquitin C-terminal hydrolases are expressed (www.wormbase.org) and UBH-1 is the *C. elegans* homologue for Human UCH-L1. As shown in figure 1 and 2 the UBH-1 *C. elegans* protein is 38% identical to human UCH-L1, and 36% identical to rat UCH-L1. Studies of cellular senescence in endothelial cells showed that iRNA against *ubh-1* turned worms more susceptibe to oxidative stress [193]. In this study, a screening for *C. elegans* proteins involved in cellular senescence and in reactive oxygen species-induced state was performed, and *ubh-1* was identified as a candidate gene. Recurring to gene inactivation by RNAi accumulation of lipofuscin, a fluorescent material composed of oxidized proteins and lipids [381,382], was evaluated. UBH-1 Knock-out animals showed earlier accumulation of lipofuscin and increased sensitivity to paraquat, a known inducer of oxidative stress, thus indicating the potential role of UBH-1 in the oxidative stress response [193]. The worm UBH-1 knock-out strain is, however, poorly characterized. The only reference to some characterization comes from unpublished data available at www.wormbase.org. Here, it is described that *ubh-1* knock-out animals have a slower growth rate, smaller brood size and a longer defecation cycle. It is also referred that UBH-1 and UBH-3 showed C-terminal hydrolase activity towards *C. elegans* Ubiquitin and NEDD8.

```
1-    Rattus norvergicus (R.n)
2-    Caenorhabditis elegans (C.e)

R.n - PLESNPSVINPMIEKMGVSGV-KTVDVLFFDDESIGK---PQHAVILCFPEYKKVDEIMK
      P+E NP ++N ++ K+GV+G  +  DVL  ++E++G    P  A++L FP   + +   K
C.e - PMEINPEMLNKVLAKLGVAGQWRFADVLGLEEETLGSVPSPACALLLLFPLTAQHENFRK

R.n - PIYEQAKAADDS--VFFMKQKISNACGTFALFHSLANLEDRINLGDGSFAK-WLAEAKKV
         E+ K  + S  V+FMKQ I N+CGT  L H++AN +D++   DGS  K +L+E +K+
C.e - KQIEELKGQEVSPKVYFMKQTIGNSCGTIGLIHAVANNQDKLEFEDGSVLKQFLSETEKL

R.n - GIEERSDFLANNAELAGIHAAAATDGQTAPSGDVEHHFICFVGKNGILYEIDSRRPFARE
        E+R+     N  +   H + A +GQ      V  HFI F   +G LYE+D R PF
C.e - SPEDRAKCFEKNEAIQAAHDSVAQEGQCRVDDKVNFHFILFNNVDGHLYELDGRMPFPVN

R.n - IGPTSDATLVKDAGAACQHLIEKLD-NVSFSAIAV
       G +S+ +L++DA   C+   E+    V FSA+A+
C.e - HGASSEDSLLQDAAKVCREFTEREQGEVRFSAVAL
```

Figure 1 – BLAST with the protein sequences for Rat UCH-L1 versus *C. elegans* UBH-1.

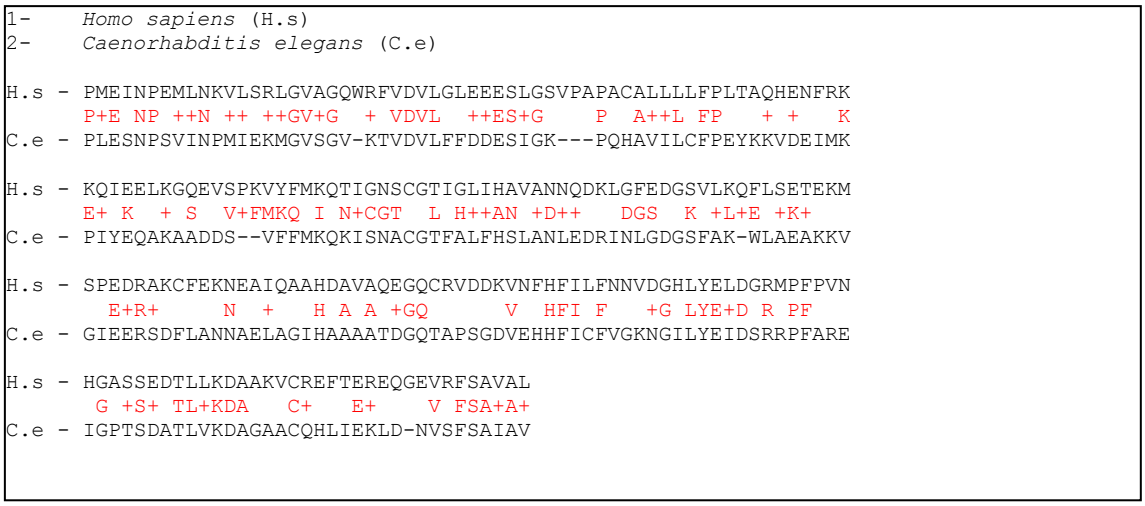

Figure 2 – BLAST with the protein sequences for Human UCH-L1 versus *C. elegans* UBH-1.

Prostaglandins (PGs) are a family of molecules derived from fatty acids that are produced by cells in response to certain stimuli to regulate cellular growth, differentiation and homeostasis [383,384]. Prostaglandin D2 (PGD2) is the most abundant prostaglandin in brain, with roles ranging from body temperature regulation, to neurotransmission regulation to modulation of the pain response [385,386]. These molecules are mediators of inflammation and inductors of oxidative stress [387–389]. Using the SH-SY5Y cell line, it was observed that intracellular ROS were upregulated upon 15-deoxy-$\Delta^{12,14}$-PGJ_2 (15d-PGJ2) treatment, through the modification of Thioredoxin 1 (Trx) enzyme - known to be protective against oxidative stress [390,391].

Cyclopentenone prostaglandins (PGs) are metabolites of prostaglandin D2. This molecule readily undergoes dehydration *in vivo* and *in vitro* to yield biologically active PGs of the J2 series, such as PGJ2, Δ12-PGJ2, and 15-deoxy-Δ12,14-PGJ2 (15d-PGJ2) [392,393]. Cyclopentenone prostaglandins, specifically 15d-PGJ2 have been described as modulators of UCH-L1 activity [394], also leading to its unfolding and aggregation [395]. In human neuroblastoma cells, cyclopentenone PGs were identified as inducers of the production of intracellular reactive oxygen species [387,388]. In *C. elegans*, a large array of prostaglandins is known to be synthesized [396–398], and specifically in sperm guide studies the F-series prostaglandin metabolism pathways have been characterized [396].

In Machado-Joseph disease (MJD), also known as spinocerebellar ataxia type 3, a neurodegenerative condition that belongs to the group of polyglutamine diseases [196], as in many neurodegenerative diseases [399], upregulation of proinflammatory genes [400] and oxidative stress plays a pivotal role [401–403]. Neuronal intranuclear inclusions (NIs) formed by the aggregation of expanded polyQ ATXN3 are a characteristic hallmark of MJD [404,405], these contain, besides molecular chaperones and components of the UPS [352,406], upregulated

mediators of inflammation [400], such as cytokine stromal cell-derived factor 1a (SDF1α), involved in cell migration during inflammation [407], or the interleukin-1 receptor-related Fos-inducible transcript (Fit-1S) that binds to proinflammatory cytokine IL1β [408]. Using cell lines that model the disease, it was found that cells with expanded ataxin-3 have decreased activity of the antioxidant enzymes, namely glutathione peroxidase (GSH-px), glutathione reductase (GSSG-R), catalase (CAT), and superoxide dismutase (SOD) [401]. The Forkhead box O transcription factor (FOXO4), involved in the response to oxidative stress [409], interacts with ATXN3 and the last is responsible for a significant increase in the FOXO4-dependent gene transcription. It was observed that co-expressing ataxin-3 with a polyglutamine (polyQ) expansion of 70 glutamines and FOXO4 results in a significant decrease in FOXO4-dependent gene transcription, namely SOD2 expression [409], which suggests that the polyQ expansion characteristic of MJD is responsible for increased susceptibility of cells to oxidative stress.

The interplay between the proinflamatory species, neurodegenerative disease and the UPS is evident in the case of UCH-L1 and PD, and to our knowledge the possible impact of this neuronal abundant deubiquitylase in Machado-Joseph disease was still not evaluated. Our aim was to address (1) the impact of an increase in proinflammatory factors (15d-PGJ2) and (2) the impact of modifying UBH-1 (orthologous to vertebrate UCH-L1), genetically or by 15d-PGJ2 exposure, in the development of MJD. We evaluated the effects on a *C. elegans* model of MJD of the deletion of UBH-1 and also the impact of 15d-PGJ2 treatment, known to compromise the function of the enzyme, thus evaluating the potential of this highly abundant neurodegenerative disease-related DUB as a modifier of the disease.

Experimental procedures

Caenorhabditis elegans strains

Nematodes were grown on NGM plates seeded with *Escherichia coli* OP50 strain at 20^{o}C, according to standard methods [410]. Populations were synchronized either by treating young adult animals with alkaline hypochlorite solution (0.5 M NaHO, ~2.6% NaClO) for 7 min [411] or by collecting embryos laid by adult animals within a 3 hours period. During the reproductive period, animals were moved to a new plate every day to avoid contamination by progeny. Experiments were repeated three to four times. All assays were performed in a blind manner. Nematodes with pan-neuronal expression of YFP - YFP-F25B3.3 - were generated as described

previously [412]. The strain expressing ATXN3 with a 130 glutamine polyQ – *Atq130*(MJD), a nematode model of Machado–Joseph disease, was previously generated and characterized in our laboratory [11]. Strain *tm526*(ubh-1 KO) was obtained from the National Bioresource Project. Strains *ld1*(skn-1::GFP) and *sj4058*(hsp60::GFP) used in this work were kindly provided by the Caenorhabditis Genetics Center (CGC). Strain *tm526*(ubh-1 KO) was crossed with *Atq130*(MJD) strain and with YFP-F25B3.3 using standard procedures, generating the double mutants *Atq130*(MJD); *tm526*(ubh-1 KO) and *Atq130*(MJD);YFP-F25B3.3. *tm526* genotyping was done using primers F_UBH-1 (5'-gctagccatctggaagctgt-3') and R_UBH-1 (5'-ggctcgtttgcgaaatgg-3'), ATq130 containing strains were selected based on YFP fluorescence. All strains were backcrossed at least 5 times with *N2*(WT) strain.

Animal treatments

For heat-shock treatment adult (day 4) animals grown at 20°C were transferred to 33°C plates for 2 h and microscopy images were immediately taken. Paraquat (Sigma) treatment consisted of transferring adult animals to plates containing paraquat 1 mM or dimethyl sulfoxide 0,1% (solvent control) (Sigma) for 2h. 15-deoxy-Δ12,14-prostaglandin J2 (15d-PGJ2) (Cayman Chemicals), treatment was performed transferring adult animals to plates containing (15d-PGJ2) 200 µM or solvent control ethyl acetate (Sigma) during 2h.

Microscopy images

Images were acquired using a Olympus BX61 (Olympus, Tokyo, Japan) microscope coupled with a DP70 digital camera. Olympus Cell^P software was used for image deconvolution and projection.

Motility assay

All assays were performed at room temperature (~20°C) using synchronized animals grown at 15°C or 20°C. Five adult animals (day 4) were placed simultaneously in the middle of a freshly seeded plate, equilibrated at 20°C. Animals remaining inside a 1 cm circle after 30 sec or 1 min were scored as locomotion-defective. A total of 150 animals were scored in at least three independent assays for each strain, and the statistical significance of the differences was assessed by Student's t-test, as described previously [413].

Confocal Imaging

All images were captured on an Olympus FV100 confocal microscope (Olympus, Tokyo, Japan), under 60X oil objective. L4, day 4 or day 6 animals were immobilized with 2 mM levamisole and mounted on a 3% agarose pad. Z-series imaging was taken of all the *C. elegans* lines generated using 514nm laser excitation for YFP fusion proteins. The pinhole was adjusted to 1.0 Airy unit of optical slice and a scan was taken every ~0.5 µm along the Z-axis. Final *images* of whole animal neuronal architecture were prepared with *Adobe Photoshop CS4 (Adobe Systems) using* flattened z-series stacks.

Quantification of aggregates

Caenorhabditis elegans fluorescent images were acquired using an Olympus FV100 confocal microscope (Olympus, Tokyo, Japan). Confocal microscope parameters were set using Hi-Lo pallet, such that protein foci and not diffuse fluorescent areas of the animals nervous system presented pixel intensity higher than 255. The z-stack was collapsed and the aggregate load of each animal (per area unit) was calculated on an imageprocessing application using MeVisLab as a platform. Details on the application and on the segmentation algorithms were described elsewhere [414]. At least eight images were analyzed per genotype and statistical assessment was performed using GraphPad Prism (GraphPad Software Inc, San Diego, CA) (ANOVA and Bonferroni mean correction tests for multiple comparisons).

Results and Discussion

The UBH-1 KO strain has a normal neurological phenotype

We studied a worm strain lacking rbr-1, the orthologue of human UCH-L1. It was observed visually that UBH-1 KO animals had no major alterations in terms of life span, size, morphology or development. Although this was not quantified, brood size appeared to be normal. Expression of YFP under the control of the promoter F25B3.3 allowed us to observe the animal's neuronal architecture. The gene product of this promoter is the *C. elegans* orthologue of $Ca2^{2+}$-regulated Ras nucleotide exchange factor (RasGRP), expressed throughout the nervous system [415], and allows a pan-neuronal expression of YFP in worms [412]. It is possible to observe in Figure 3 that the transgenic animals we generated, which besides having YFP expression throughout the nervous system are *ubh-1* knockout - YFP-F25B3.3;tm526(ubh-1 KO) – exhibit a globally normal neuronal circuitry when compared with the control animals (YFP-F25B3.3). The commissural neurons (white arrowheads) had no distinct distribution between the two animals. As seen in Figure 3 both the dorsal nerve cord neurons (green arrowheads) and the ventral nerve cord neurons (yellow arrowheads) had no observable defects in neurite extension, and the commissural branches reached both the dorsal and ventral nerve cords in UBH-1 KO. This allows us to conclude that the deletion of *ubh-1* gene does not cause any major alterations in neuronal distribution, thus any alterations eventually observed in these animals with the treatments we performed are not due to neuronal architecture defects.

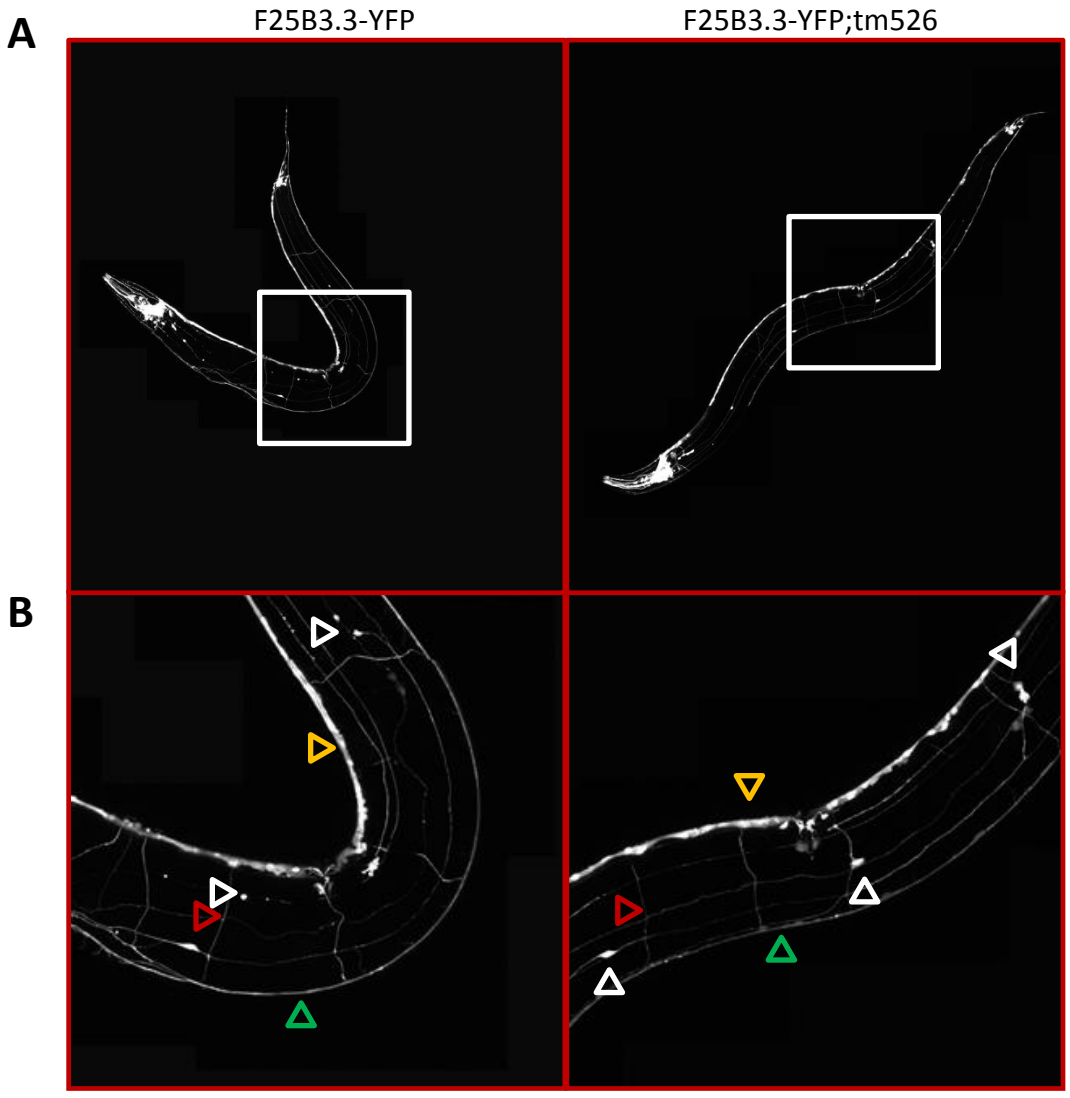

Figure 3 – UBH-1 knock-out has no major alterations in neuronal architecture. YFP-F25B3.3 or YFP-F25B3.3;tm526(ubh-1 KO) young adults (day4) harboring pan-neuronal expression of YFP under the control of the F25B3.3 promoter show no differences in global circuit architecture. *A*, Reconstruction of whole animal neuronal architecture with images obtained by confocal miscroscopy (flattened z-series stacks). *B*, Magnification of images from panel A; white head arrows indicate commissural neurons, green arrow heads indicate dorsal nerve cord neurons that send processes to ventral nerve cord neurons (yellow arrows) through neuronal commissures (red arrows).

15d-PGJ2 is able to induce oxidative stress in *C. elegans*

Normal cellular activities are possible only in a balanced redox environment, and disturbances in this equilibrium may result in oxidative stress, which is considered to be one of the causes of aging and age-related diseases, affecting numerous cellular processes [416]. Cyclopentenone prostaglandins have the ability to induce intracellular reactive oxygen species (ROS) production, demonstrated in studies using neuroblastoma cell line SH-SY5Y [387]. The intracellular ROS production was more effectively induced by 15-deoxy-$\Delta^{12,14}$-Prostaglandin J_2 (15d-PGJ2), when compared with other PGs, inducing cell death and altering the cellular redox state in these cells [387]. To our knowledge PGs have not been tested until now as potential inducers of oxidative stress in *C. elegans*. We evaluated the capability of 15d-PGJ2 to induce oxidative stress in oxidative stress reporter strains. The transcription factor SKN-1 was first identified as essential for formation of pharyngeal tissue in *C. elegans* [417]: A study to investigate the post-embryonic functions of SKN-1 identified it as an essential transcription factor for the constitutive and stress-induced expression of *gcs-1* [418], the orthologue of vertebrate γ-glutamine cysteine synthetase heavy chain [GCS(h)], a Phase II detoxification enzyme involved in the primary response to oxidative stress[419–421]. It was observed that SKN-1 is essential for oxidative stress response in worms and that, upon paraquat or heat (oxidative stress inducers), elevated SKN-1 was detected in intestinal cell nuclei [418]. In this work, upon paraquat or heat exposure, we were able to observe an increase in the expression of SKN-1 in intestine according to the results described. 15d-PGJ_2 was also able to induce, although to a smaller extent, SKN-1 expression (figure 4 panels A,B and C; white arrowheads). This indicates that 15d-PGJ_2 is able to able to induce oxidative stress in nematodes. To further evaluate 15d-PGJ_2 effects, another strain was used to assess oxidative stress. Expression of the chaperone HSP60 is known to be increased upon oxidative stress induction by paraquat administration [422]; in our experiments, paraquat was the more effective activator of HSP60 expression (Figure 4 panel D) but 15d-PGJ_2 also induced, to some extent, a response from this chaperone, confirming the potential role of 15d-PGJ_2 as a oxidative stress inducer in *C. elegans*.

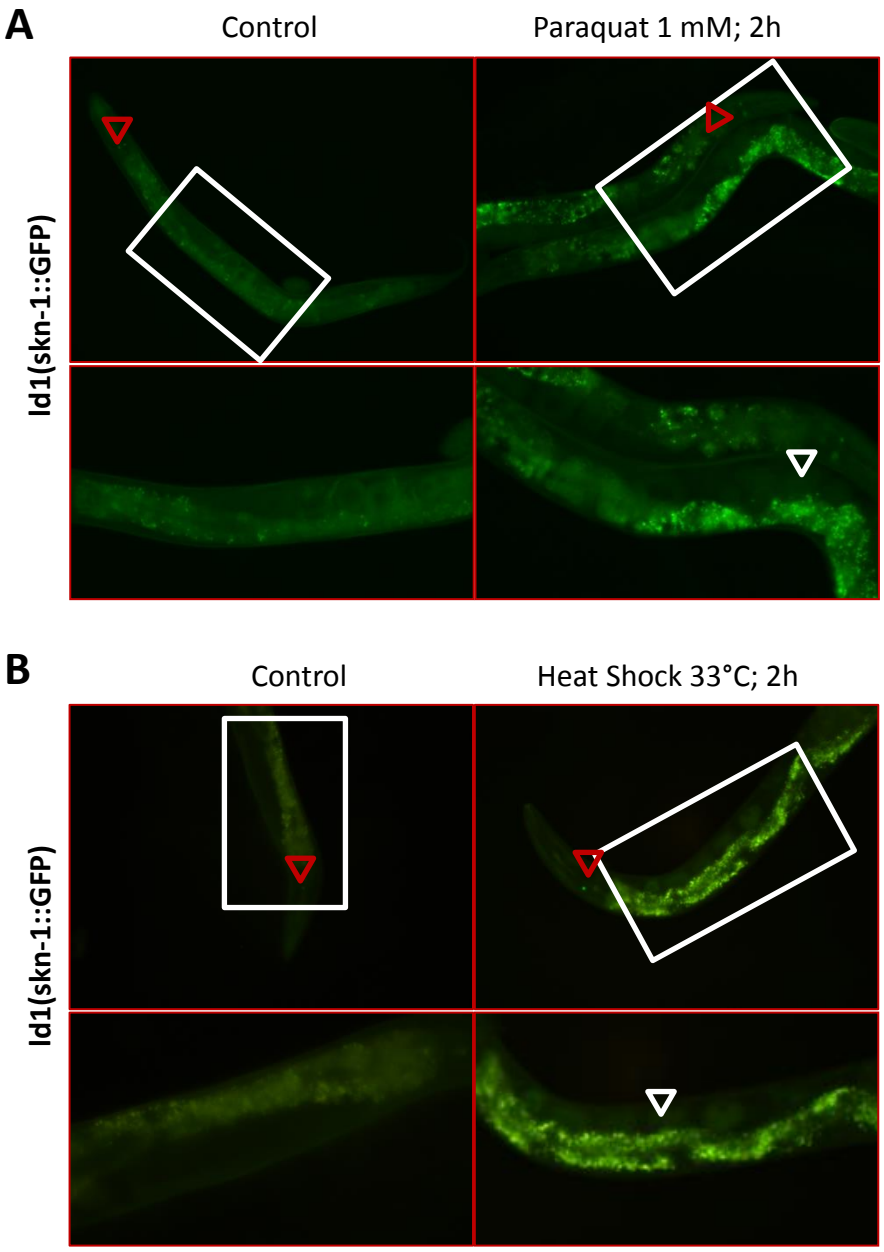
A
Control
Paraquat 1 mM; 2h
Id1(skn-1::GFP)
B
Control
Heat Shock 33°C; 2h
Id1(skn-1::GFP)
C
Control
PGJ2 200 µM; 2h
Id1(skn-1::GFP)

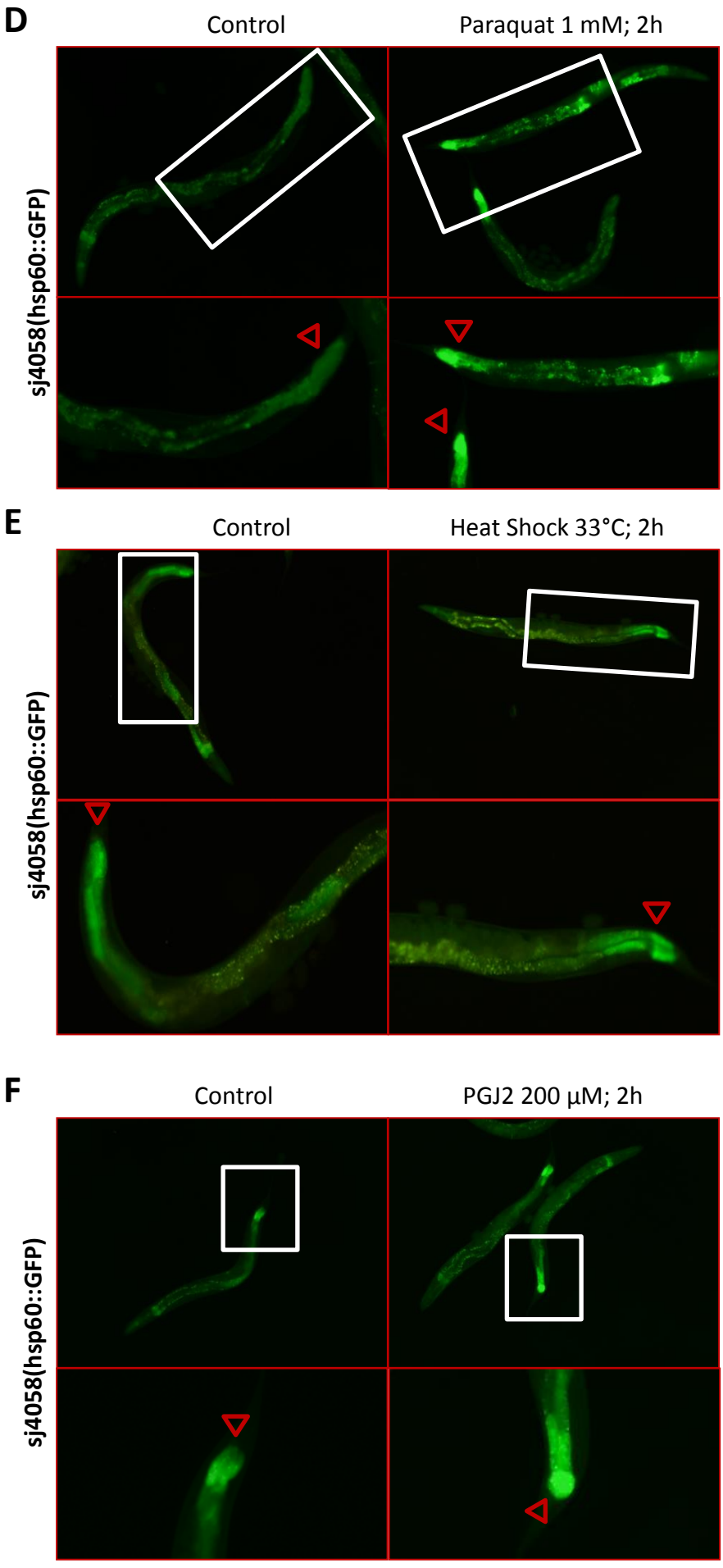
D
Control
Paraquat 1 mM; 2h
sj4058(hsp60::GFP)
E
Control
Heat Shock 33°C; 2h
sj4058(hsp60::GFP)
F
Control
PGJ2 200 µM; 2h
sj4058(hsp60::GFP)

Figure 4 – Oxidative stress reporter genes are induced by incubation with 15d-PGJ2. *A,* Incubation of paraquat 1 mM in the feeding medium induces the expression of the transcription factor SKN-1 after 2 hours of animals kept in the feeding plates ; Red arrows indicate ASI chemosensory neurons where SKN-1 is constitutively expressed; white arrows indicate stress-induced expression of SKN-1 in the intestine characteristic of SKN-1 response to oxidative stress. *B,* Upon heat-shock treatment (2 hours at 33°C) a strong SKN-1 response is observed, with expression in the intestine (white arrows). *C*, Although to a smaller extent, it is observable that 15d-PGJ2 (200 µM, 2 hours) is also able to induce an oxidative stress response in *C. elegans*, white arrows indicating the translocation of SKN-1 to intestinal cell nuclei. *D*, Paraquat incubation leads to characteristic expression of HSP-60 in *C. elegans* tail (red arrows). *E*, Induction of HSP-60 expression by heat-shock is significant, although basal expression in these conditions is also observable. *F*, Upon incubation with 15d-PGJ2 a stronger expression of HSP-60 is observed in the tail of treated animals when comparing with controls.

15d-PGJ2 and UBH-1 are not modifiers of Machado-Joseph Disease

The ubiquitin hydrolase UCH-L1 has been described to be modulated by the action of 15d-PGJ_2 in mammalian cells. It was demonstrated that 15d-PGJ_2 leads to the accumulation of ubiquitylated proteins in mouse and human neuroblastoma cells [423] and that this effect was not proteasome-mediated but rather mediated through the inhibition of UCH-L1 activity [423]. Posterior studies uncovered the mechanism by which this inhibition takes place: 15d-PGJ_2 molecules are able to directly interact with UCH-L1 and when in excess they can completely unfold this hydrolase and lead to its aggregation [395]. The roles of UCH-L1 in the pathogenesis of neurodegenerative diseases are described, namely in Parkinson Disease (PD) [9] and Alzheimer´s disease (AD) [119]. Machado-Joseph disease shares with AD and PD [424] the accumulation of reactive oxygen species, and it is known that mutant ATXN3 disrupts the oxidative stress-response through altered interaction with FOXO4 [402]; the levels of oxidative stress response enzymes: glutathione reductase, catalase, and superoxide dismutase were shown to be decreased in cells harboring mutant ataxin-3 [401]. Besides the accumulation of aggregated proteins and the proteasome inhibition characteristic of these diseases, is known to trigger the expression of cyclooxygenase (COX-2) [425], the enzyme responsible for the conversion of arachidonic acid in prostaglandins [426], suggesting an increase in the overall yield of prostaglandins in cells in these conditions. Our purpose was to evaluate the effects of 15d-PGJ_2 in Machado-Joseph disease, either as an inductor of oxidative stress *per se* or as a modulator of UCH-L1, which could act as a genetic modifier of MJD.

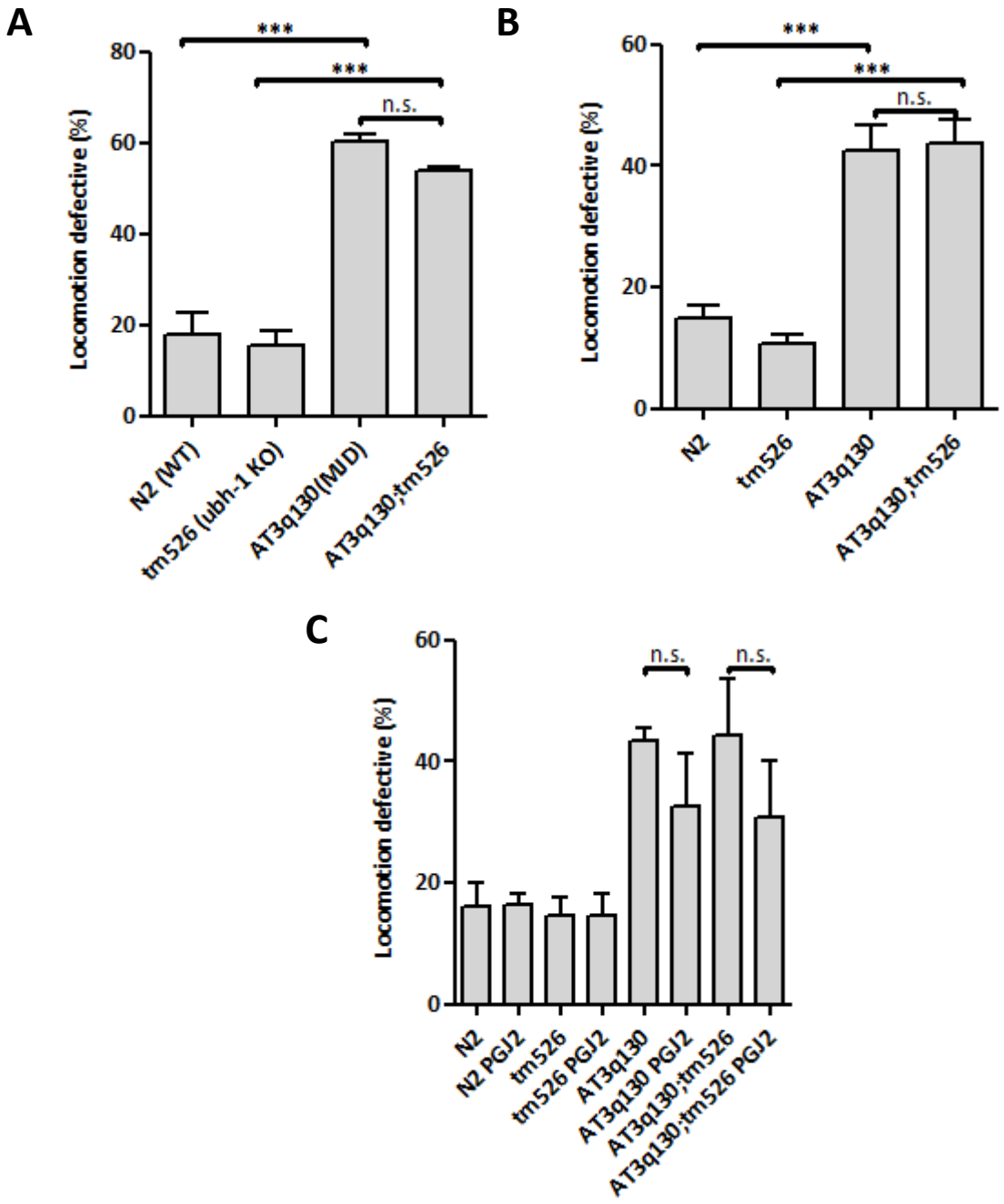

Figure 5 – Double mutant AT3q130(MJD);tm526(ubh-1 KO) shows no difference in locomotion defects when compared with the transgenic strain AT3q130(MJD). *A*, Motility analysis performed 30 seconds after placing animals in test motility plates; tm526 animals show no differences when compared with wild type animals; double mutant animals have similar motility defects when compared with AT3q130 animals. *B*, Motility analysis after 1 min show no difference in percentage of locomotion defects between single and double mutants. *C*, Upon induction of oxidative stress by 15d-PGJ2, treated animals show no significant differences compared with controls both in single and double mutant backgrounds (1 min kept in motility plates). Data are the mean ± SD, at least 150 animals per data point. Student´s *t* test, *** $P<0,0001$.

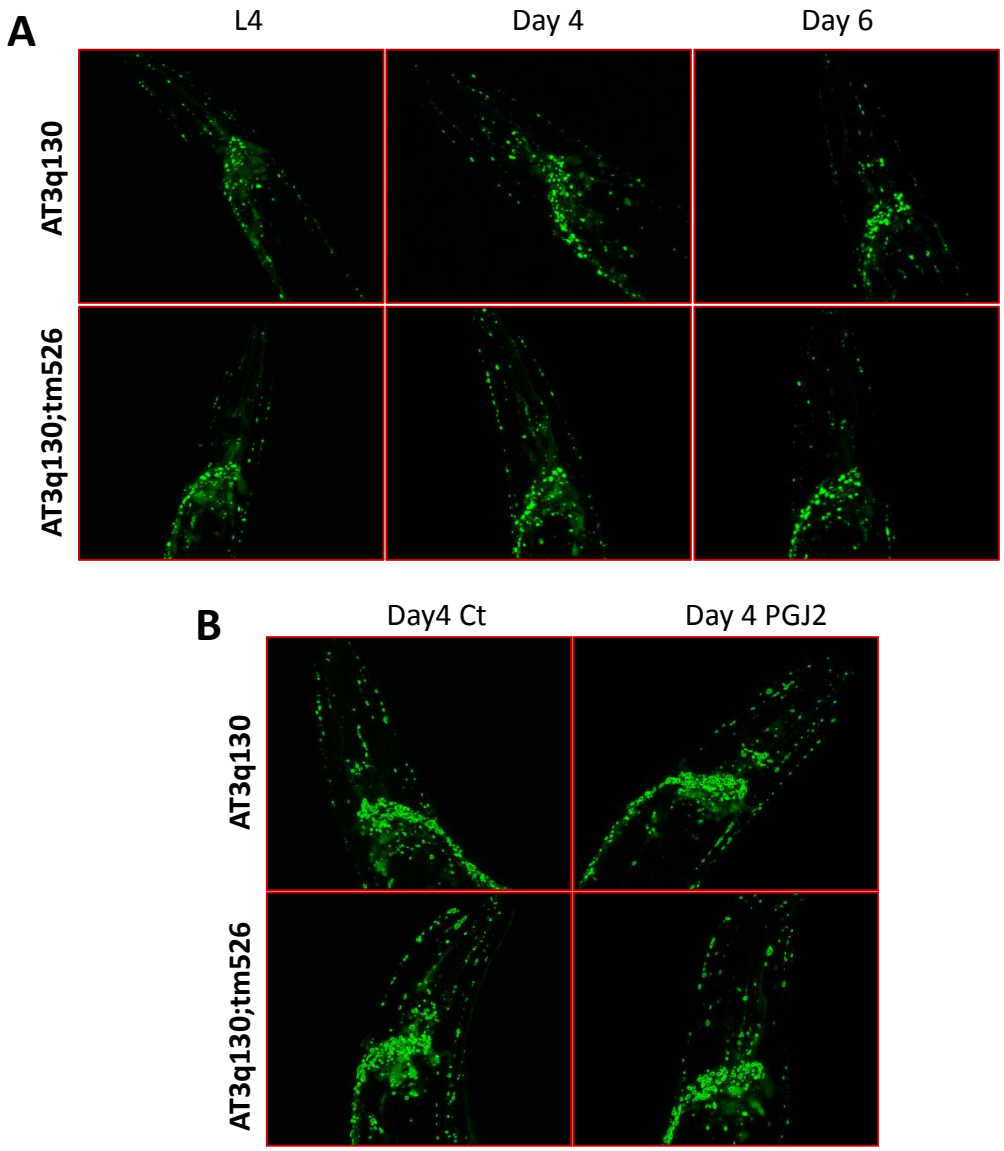
A
L4
Day 4
Day 6
AT3q130
AT3q130;tm526
B
Day4 Ct
Day 4 PGJ2
AT3q130
AT3q130;tm526

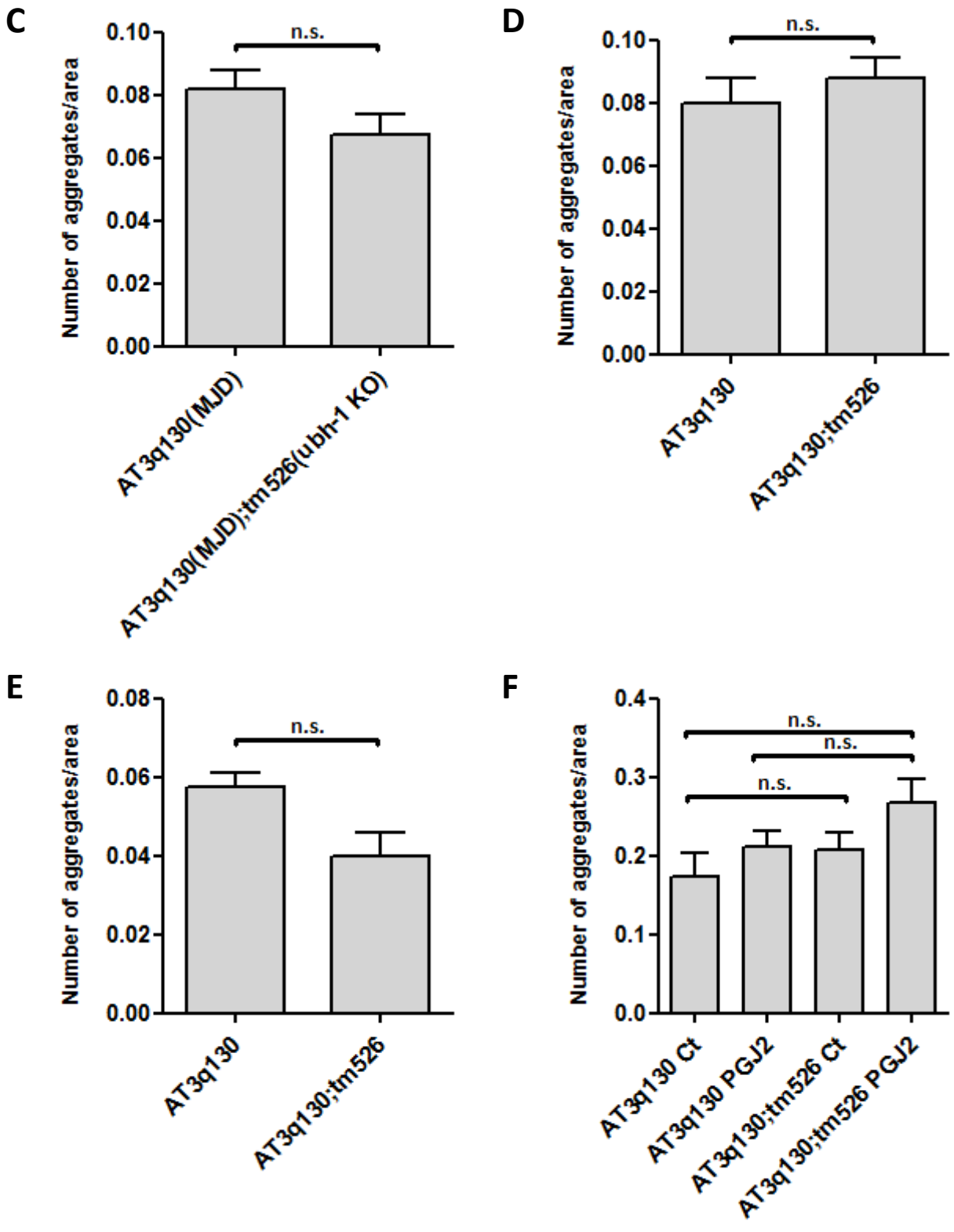

Figure 6 – **AT3q130 and double mutant animals (ATq130;tm526) show no statistically significant differences in number of aggregates per area unit at different development stages, or upon oxidative stress induction.** *A*, Confocal microscopy flattened Z-series stacks comparing aggregation pattern of single mutant animals (AT3q130) to double mutant animals (AT3q130;tm526) at different development stages (L4, day 4 and day 6). *B*, Confocal microscopy images taken after 15d-PGJ2 treatment (200 µM, 2 hours) for single and double

mutants. *C,* Quantification of number of aggregates per area unit using image processing application [5th International Conference on Practical Applications of Computational Biology & Bioinformatics (PACBB 2011). Advances in Intelligent and Soft Computing Volume 93, 2011, pp 31-38. An Image Processing Application for Quantification of Protein Aggregates in *Caenorhabditis Elegans*]shows no difference in aggregation between single and double mutant L4 animals; neither day 4 (D) or day 6 (E) animals have different aggregation pattern; upon induction of oxidative stress by 15d-PGJ2 (F) both single and double mutants do not behave differently in terms of aggregation. Values represent the mean ± SD of four or more animals per group, one way ANOVA to analyze statistical significance.

We used the MJD *C. elegans* model previously characterized in our lab [11]. We evaluated locomotion defects and observed (Figure 5) that double transgenic animals carrying the MJD mutation and defective in UBH-1 did not show any differences in locomotion when compared with MJD worms. This suggests that in this behavioral paradigm the UBH-1 protein is not a modifier of the disease. We also evaluated the ATXN3 aggregation status in single and double mutants (Figure 6) and again no differences were observed between single and double mutants. MJD worms treated with 15d-PGJ_2 showed no statistically significant differences in motility or aggregation comparing with controls (Figure 6 A,C,D and E) neither did the double mutants upon treatment with 15d-PGJ_2 (Figure 6 B,F). These results lead us to the conclusion that in spite of causing some oxidative stress, and perhaps disturbing UBH-1 activity and/or stability, 15d-PGJ_2 does not alter the neurotoxicity of mutant ATXN3. The fact that UCH-L1 and UCH-L3 share high rate of homology raises the question of whether these two enzymes have redundant roles in cells. In a study to evaluate the potential overlapping functions of UCH-L1 and UCH-L3 double mutant mice were generated (*Uch-L1*^{gad}/*Uch-L3*$^{\Delta 3\text{-}7}$), carrying the mutation present in gad mice mutation plus a targeted deletion in the *Uch-L3* gene that removes the catalytic residue, essential for hydrolase activity [375,427]. While *Uch-L3*$^{\Delta 3\text{-}7}$ mice are indistinguishable from WT [427], the double mutants show a significant more severe phenotype when compared to gad mice, namely they show earlier onset of lethality and more severe axonal degeneration of the gracile tract [428]. Although the separate and overlapping roles of these enzymes were not identified, the authors conclude that UCH-L1 and UCH-L3 have both separate and overlapping functions in the maintenance of neurons of the gracile tract. One point favoring UCH-L1 and UCH-L3 redundant functions is the shared expression in the brain and testis [7,427]. This question should be cleared in future work and assessment of the outcome in terms of MJD pathgology of double knock-out worms for UBH-1 and UBH-3 must be considered. Finally, we can conclude that activation of oxidative stress with 15d-PGJ_2, and the effects exerted by this compound on the ubiquitin hydrolase UBH-1 do not contribute to the pathology in our *C. elegans* model of MJD.

Chapter 4

Role of the proteasome in excitotoxicity-induced cleavage of Glutamic Acid Decarboxylase in cultured hippocampal neurons

This chapter is based on the published (peer-reviewed) article:

Baptista MS, Melo CV, Armelão M, Herrmann D, Pimentel DO, Leal G, Caldeira MV, Bahr BA, Bengtson M, Almeida RD and Duarte CB. "Role of the proteasome in excitotoxicity-induced cleavage of Glutamic Acid Decarboxylase in cultured hippocampal neurons". PLoS One. Apr 12;5(4):e10139. doi: 10.1371/journal.pone.0010139, 2010.

Role of the proteasome in excitotoxicity-induced cleavage of Glutamic Acid Decarboxylase in cultured hippocampal neurons.

Márcio S. Baptista[1#μ], Carlos V. Melo[1#*], Mário Armelão[1], Dennis Herrmann[1], Diogo O. Pimentel[1], Graciano Leal[1], Margarida V. Caldeira[1], Ben A. Bahr[2], Mário Bengtson[3@], Ramiro D. Almeida[1], Carlos B. Duarte[1]

1. Center for Neuroscience and Cell Biology, Department of Life Sciences, University of Coimbra, Coimbra, Portugal
2. Biotechnology Research and Training Center, University of North Carolina, Pembroke, North Carolina, USA
3. Department of Cancer and Cell Biology, Genomics Institute of the Novartis Research Foundation (GNF), San Diego, CA, USA

[#]These authors contributed equally to this work

* Current address: Department of Psychiatry and Behavioral Sciences, Nancy Priztker Laboratory, Stanford University, Palo Alto, California, USA.
[μ] Current adress: Life and Health Sciences Research Institute (ICVS); School of Health Sciences; University of Minho; Campus de Gualtar; 4710-057 Braga, Portugal
[@]Current address: Department of Cell Biology, The Scripps Research Institute, La Jolla, California, USA

*Corresponding author:

Carlos V. Melo

Department of Psychiatry and Behaviral Sciences, Nancy Priztker Laboratory, Stanford University, Palo Alto, California, 94304 USA

e-mail: cvmelo@stanford.edu
Tel: (650) 723-4913
Fax: (650) 498-7761

Abstract

Glutamic acid decarboxylase is responsible for synthesizing GABA, the major inhibitory neurotransmitter, and exists in two isoforms – GAD65 and GAD67. The enzyme is cleaved under excitotoxic conditions, but the mechanisms involved and the functional consequences are not fully elucidated. We found that excitotoxic stimulation of cultured hippocampal neurons with glutamate leads to a time-dependent cleavage of GAD65 and GAD67 in the N-terminal region of the proteins, and decrease the corresponding mRNAs. The cleavage of GAD67 was sensitive to the proteasome inhibitors MG132, YU102 and lactacystin, and was also abrogated by the E1 ubiquitin ligase inhibitor UBEI-41. In contrast, MG132 and UBEI-41 were the only inhibitors tested that showed an effect on GAD65 cleavage. Excitotoxic stimulation with glutamate also increased the amount of GAD captured in experiments where ubiquitinated proteins and their binding partners were isolated. However, no evidences were found for direct GADs ubiquitination in cultured hippocampal neurons, and recombinant GAD65 was not cleaved by purified 20S or 26S proteasome preparations. Since calpains, a group of calcium activated proteases, play a key role in GAD65/67 cleavage under excitotoxic conditions the results suggest that GADs are cleaved after ubiquitination and degradation of an unknown binding partner by the proteasome. The characteristic punctate distribution of GAD65 along neurites of differentiated cultured hippocampal neurons was significantly reduced after excitotoxic injury, and the total GAD activity measured in extracts from the cerebellum or cerebral cortex at 24h postmortem (when there is a partial cleavage of GADs) was also decreased. The results show a role of the UPS in the cleavage of GAD65/67 and point out the deregulation of GADs under excitotoxic conditions, which is likely to affect GABAergic neurotransmission. This is the first time that the UPS has been implicated in the events triggered during excitotoxicity and the first molecular target of the UPS affected in this cell death process.

Introduction

In traumatic brain injury, epilepsy, and following episodes of hypoxia-ischemia the excessive release of glutamate and the consequent overactivation of glutamate receptors leads to cell death by excitotoxicity [269-271,429]. Brain ischemia also has a strong impact in GABAergic neurotransmission. The Ca^{2+}-dependent exocytotic release of GABA appears to account for the initial phase of neurotransmitter release at the onset of ischemia, while the reversal of the plasma membrane transporters is responsible for much of the subsequent efflux [430,431]. However, the decrease in surface expression of post-synaptic GABAA receptors, in part due to their internalization, decreases GABAergic synaptic transmission [432]. Following transient focal ischemia there is also a decrease in the expression of the vesicular GABA transporter, which may have a delayed impact on the exocytotic release of the neurotransmitter [433]. The plasma membrane GABA transporter GAT1 is a calpain substrate [434], and calpain activation in the postischemic brain [435] may contribute to the deregulation of the transporter.

Glutamic acid decarboxylase (GAD) is the key enzyme in the synthesis of γ-aminobutyric acid (GABA) [436] and any alterations in the activity of the enzyme will also have an impact on the GABAergic synaptic transmission. GAD exists in two isoforms encoded by different genes, GAD65 and GAD67, with a molecular weight of 65 and 67 KDa, respectively [272]. GAD65 represents 81 % of total GAD in rat hippocampus [437], and is found predominantly in association with synaptic vesicle membranes in nerve terminals [273-275]. This GAD isoform synthesizes mainly the vesicular pool of GABA [276,277], and is responsible for the fine tuning of inhibitory transmission [278]. In contrast, GAD67 is evenly distributed throughout the cell [279], being constitutively active and accounting for the basal production of the cytosolic pool of GABA [438]. Both isoforms of GAD are cleaved in cerebrocortical neurons subjected to excitotoxic conditions by a mechanism that is sensitive to inhibitors of calpain [282-285], a non-lysosomal, calcium-activated protease that has been implicated in excitotoxic neuronal damage [439], and recombinant GAD65 and 67 are cleaved in vitro by calpain [282,283]. Cathepsin inhibitors also inhibited the cleavage of GAD65 and 67 in cerebrocortical neurons exposed to a toxic concentration of glutamate, and recombinant GAD was cleaved by cathepsin L in an in vitro assay [284]. These evidences suggest that multiple proteolytic systems are involved in the cleavage of GAD under excitotoxic conditions.

The ubiquitin-proteasome system (UPS) is the major extralysosomal system for protein degradation in the cells [51,440]. Proteins targeted to be degraded by this system are first

conjugated by polyubiquitin chains and then degraded by the proteasomes. The role of the UPS in cell death in the ischemic brain is rather complex since the activity of the proteasome is downregulated in the ischemic brain [286,441] but inhibition of the proteasome was found to be neuroprotective in focal brain ischemia [287-289]. Furthermore, the effect of proteasome deregulation on the turnover of specific proteins in the ischemic brain remains to be investigated. Hence, in the present study we investigated the putative role of the UPS in GAD cleavage under excitotoxic conditions. In particular the soluble isoform GAD67 is present mainly in the cytoplasm [442] and, therefore, may constitute a target of the UPS. We found that excitotoxic stimulation of hippocampal neurons with glutamate downregulates GADs, both at mRNA and protein levels. Our results indicate that the UPS does regulate GAD67 cleavage under excitotoxic conditions, possibly through modulation of an unknown GAD binding partner. Cleavage of GADs diminished the activity of the enzyme and the characteristic punctate distribution of GAD65 along neurites was also affected under excitotoxic conditions.

Materials and Methods

Hippocampal Cultures

Primary cultures of rat hippocampal neurons were prepared from the hippocampi of E18-E19 Wistar rat embryos, after treatment with trypsin (0.06%, for 15min at 37ºC; GIBCO-Invitrogen, Paisley, UK) and deoxyribonuclease I (5.36 mg/ml), in Ca2+- and Mg2+-free Hank's balanced salt solution (HBSS; 5.36 mM KCl, 0.44 mM KH2PO4, 137 mM NaCl, 4.16 mM NaHCO3, 0.34 mM Na2HPO4.2H2O, 5 mM glucose, 1 mM sodium pyruvate, 10 mM HEPES and 0.001% phenol red). The hippocampi were then washed with HBSS containing 10 % fetal bovine serum (GIBCO-Invitrogen), to stop trypsin activity, and transferred to Neurobasal medium (GIBCO-Invitrogen) supplemented with B27 supplement (1:50 dilution; GIBCO-Invitrogen), 25 μM glutamate, 0.5 mM glutamine and 0.12 mg/ml gentamycin. The cells were dissociated in this solution and were then plated in 6 well plates (870,000 cells/well) coated with poly-D-lysine (0.1 mg/mL), or on poly-D-lysine coated glass coverslips, at a density of 150,000 cells/well (12 well plates). The cultures were maintained in a humidified incubator of 5% CO2/95% air, at

37°C, for 7 or 10 days. Excitotoxic stimulation was performed with 125 μM glutamate in supplemented Neurobasal medium, for 20 min at 37ºC, in a humidified incubator. After stimulation with glutamate the cells were further incubated with the original culture medium for the indicated periods of time. When appropriate, 50 μM UBEI-41 (ubiquitin-activating enzyme inhibitor; Biogenova Corp., Maryland, USA), 1 μM MG132 (Calbiochem, Darmstadt, Germany), 10 μM Lactacystin (Sigma, MO, USA) or 10 μM YU102 (Biomol, Exeter, UK) were added to the incubation medium 30 min (or 1h for UBEI-41) before stimulation.

Animals used in the preparation of cell cultures and in the GAD activity experiments (see below) were handled according to National and Institutional guidelines. Experiments conducted at the Center for Neuroscience and Cell Biology were performed according to the European Union Directive 86/609/EEC on the protection of animals used for experimental and other scientific purposes. These experiments did not require approval by an Institutional Animal Care and Use Committee (IACUC). The work performed at GNF adhered to the Animal Behavior Society Guidelines for the Use of Animals in Research, and was approved by the Institutional Animal Care IACUC.

Preparation of extracts

Hippocampal neurons (DIV7) were washed twice with ice-cold PBS and once more with PBS buffer supplemented with 1 mM DTT and a cocktail of protease inhibitors (0.1 mM PMSF; CLAP: 1 μg/ml chymostatin, 1 μg/ml leupeptin, 1 μg/ml antipain, 1 μg/ml pepstatin; Sigma-Aldrich Química, Sintra, Portugal). The cells were then lysed with RIPA (150 mM NaCl, 50 mM Tris-HCl, 5 mM EGTA, 1 % Triton, 0.5 % DOC and 0.1 % SDS at a final pH 7.5) supplemented with the cocktail of protease inhibitors. After centrifugation at 16,100 g for 10 min, protein in the supernatants was quantified using the bicinchoninic acid (BCA) assay (Thermo Scientific, Rockford, IL), and the samples were denaturated with 2x concentrated denaturating buffer (125 mM Tris, pH 6.8, 100 mM glycine, 4 % SDS, 200 mM DTT, 40 % glycerol, 3 mM sodium orthovanadate, and 0.01 % bromophenol blue), at 95 ºC for 5 min.

Total RNA isolation

Total RNA was extracted from 7 DIV cultured hippocampal neurons using TRIzol® Reagent (Invitrogen), following the manufacturer's specifications. The content of 2 wells from a 6 well plate, with 870,000 cells/well (DIV7), was collected for each experimental condition. After the addition of chloroform and phase separation, the RNA was precipitated by the addition of

isopropanol. The precipitated RNA was washed once with 75 % ethanol, centrifuged, air-dried and resuspended in 60 µl of RNase-free water (GIBCO-Invitrogen). The whole procedure was performed at 4°C.

RNA Quality and RNA Concentration

RNA quality and integrity was assessed using the Experion automated gel-electrophoresis system (Bio-Rad, Amadora, Portugal), as previously described [443]. A virtual gel was created for each sample, allowing the detection of degradation of the reference markers, RNA 18S and 28S. Samples showing RNA degradation or contamination by DNA were discarded. RNA concentration was determined using both the fluorescent dye RiboGreen (Invitrogen-Molecular Probes, Leiden, The Netherlands) and NanoDrop 1000 (Thermo Scientific). The samples were aliquoted and stored at -80°C to further use.

Reverse Transcription reaction

For first strand cDNA synthesis 1000 ng of total RNA was mixed with Random Hexamer Primer p(dN)6 followed by 10 min denaturation at 65°C to ensure loss of secondary structures that may interfere with the annealing step. The samples were chilled on ice, and the template-primer mix was then supplemented with Reaction Buffer (50 mM Tris/HCl, 30 mM KCl, 8 mM MgCl2, pH 8.5), Protector RNase Inhibitor (20U), dNTPs (1 mM each) and finally AMV Reverse Transcriptase (10U; Roche, Carnaxide, Portugal), in a 20 µl final volume. The reaction was performed at 25°C for 10 min, followed by 30 min at 55°C, for primer annealing to the template and cDNA synthesis, respectively. The Reverse Transcriptase was then denatured during 5 min at 85°C, and the samples were then cooled to 4°C for 5 min, and finally stored at -80°C until further use.

Primer Design

Primers for real-time PCR were designed using the "Beacon Designer 7" software (Premier Biosoft International, CA, USA), and the following considerations were taken: (1) GC content about 50%; (2) annealing temperature (Ta) between 55 ± 5°C; (3) secondary structures and primer-dimers were avoided; (4) Primer length between 18-24 bp; (5) Final product length between 100-200 bp. The primers used for amplification of GAD65 and GAD67 were, respectively, NM 012563 (accession number to mRNA sequence) – 5'GCT CAT TGC CCG CTA

TAA G3' and 5'ATC ACG CTG TCT GTT CCG3'; NM 017007 – 5'ACA CTT GAA CAG TAG AGA C3' and 5'GCA GGT TGG TAG TAT TAG G3'. The primers used for the amplification of endogenous controls GAPDH and Tubulin alpha 1a were, respectively, NM 017008 – 5'AAC CTG CCA AGT ATG ATG3' and 5' GGA GTT GCT GTT GAA GTC3'; NM 022298 – 5'CAT CCT CAC CAC CCA CAC3' and 5'GGA AGC AGT GAT GGA AGA C3'. Following the first experiment all sets of primers were tested for their specificity in an agarose gel that allows determination of the product size and possible non-specific products.

Real-Time PCR

For gene expression analysis 2 µl of 1:100 diluted cDNA was added to 10 µl 2x SYBR Green Master Mix (Bio-Rad) and the final concentration of each primer was 250 nM in 20 µl total volume. The thermocycling reaction was initiated with activation of the Taq DNA Polymerase by heating at 95°C during 30 s, followed by 45 cycles of a 10 s denaturation step at 95°C, a 30 s annealing step, and a 30 s elongation step at 72°C. The fluorescence was measured after the extension step, using the iQ5 Multicolor Real-Time PCR Detection System (Bio-Rad). After the thermocycling reaction the melting step was performed with slow heating, starting at 55°C and with a rate of 0.5°C per 10 s, up to 95°C, with continuous measurement of fluorescence, allowing detection of possible non-specific products. The assay included a non-template control and a standard curve (in 10-fold steps) of cDNA for assessing the efficiency of each set of primers. All reactions were run in duplicate to reduce confounding variance [444].

Real Time PCR Data Processing

The threshold cycle (Ct) represents the detectable fluorescence signal above background resulting from the accumulation of amplified product, and is a proportional measure of the starting target sequence concentration. Ct was measured in the exponential phase and, therefore, was not affected by possible limiting components in the reaction. For every run performed Ct was set at the same fluorescence value. Data analysis was performed using the GenEx (MultiD Analyses, Sweden) software for Real-Time PCR expression profiling, and the results were normalized with a set of two internal control genes. Statistical analysis was performed using the Student's t test.

Immunoblotting

Protein samples were separated by SDS-PAGE, in 12% polyacrylamide gels (or 7.5% gels when spectrin products were detected), transferred to polyvinylidene (PVDF) membranes (Millipore Corp., Billerica, MA), and immunoblotted. Blots were incubated with primary antibodies (overnight at 4ºC), washed and exposed to alkaline phosphatase-conjugated secondary antibodies (1:20000 dilution; 1 h at room temperature) or exposed directly to ECL in the ubiquitin-conjugates detection which films were scanned and the optical densities of the bands were measured with appropriate software. Alkaline phosphatase activity was visualized by ECF on the Storm 860 Gel and Blot Imaging System (GE Healthcare, Buckinghamshire, UK). The following primary antibodies were used: anti-GAD65/67 (1:5000, Sigma), anti-GAD67 (1:250; BD Biosciences, Erembodegem, Belgium), antibody against calpain-mediated fragment of spectrin/fodrin nSBDP NSBDPs [1:300 [445,446]] and anti-β-Actin (1:5000, Sigma).

Recombinant GAD65 cleavage assay

0.75 µg of recombinant GAD65 (Diamyd Diagnostics, Stockholm, Sweden) were incubated with 1.5 µg of 20S or 26S proteasome (Biomol) at 37ºC for 2 h, in a total volume of 20 µl of buffer (30mM TrisHCl pH 7.6, 100 mM NaCl, 1 mM CaCl2, 2 mM MgCl2, 50 mM ATP, 1 mM DTT, 5 % (v/v) glycerol), with or without 10 µM MG132. A pre-incubation of 5 min with the proteasome inhibitor was performed. Reactions were stopped by addition of 20 µl of 2x concentrated denaturating buffer (same for immunoblot), resolved by 12 % PAGE and probed with a GAD65 antibody by Western blot.

Purified proteasome activity

To test for the activity of the purified proteasome activity, the 20S and 26S proteasome preparations were incubated in the presence of the chymotrypsin-like fluorogenic peptide suc-LLVY-MCA (Peptide Institute, Inc., Osaka, Japan). The proteasome preparations were incubated with the substrate (50 µM) in the presence or in the absence of the proteasome inhibitor MG132 (10 µM), in a medium containing 1mM EDTA, 10 mM tris-HCl (pH 7.5), 20 % glycerol, 4 mM DTT, 2 mM ATP (100 µl final volume). Substrate degradation by the proteasome was monitored every 5 min during 1 h at 37ºC in a fluorescence-luminescence detector (Synergy™ HT Multi-Mode Microplate Reader, BioTek, Winooski, VT), set to 380 and 460 nm, excitatory and emission wavelengths, respectively.

Immunoprecipitation Assay

Immunoprecipitation of ubiquitin-conjugated proteins was performed using the Ubiqapture – Q Kit (Biomol, Exeter, UK), as described by the manufacturer. A total of 50 µg lysates from cultured hippocampal neurons were used per assay. Samples were added to the tubes containing 80 µl UbiQapture-Q matrix and incubated overnight at 4ºC in an horizontal rotor mixer. The matrix was then carefully washed and the ubiquitin-protein conjugates were eluted by addition of 160 µl of PBS and 50 µl of 5X concentrated denaturating buffer (same for immunoblot). Samples were quenched by incubation during 15 min at 4ºC on an horizontal rotor and then denaturated by heating during at 95ºC for 10 min. The eluted fraction was clarified from the matrix pellet by centrifugation at 16,100 g during 10 min. Western blot analysis was performed as previously described using an anti-GAD65/67 antibody and the ubiquitin-conjugate antibody supplied by the kit, applying equal sample volumes (approximately 60 µl).

Measurement of GAD activity

Wistar adult rats were decapitated and each head was covered and kept at room temperature (approximately 21ºC) for 24 h. Brains were then dissected and placed on an ice-cold plate for dissection of the cerebellum and cerebral cortex. Samples were then resuspended in 50 mM TrisHCl and 0.02 % Triton X-100, sonicated with a probe sonicator in 5 pulses of 5 seconds, and centrifuged at 16,100 g for 10 min. The supernatants were diluted (1:30-1:100) and the protein content was measured using the BCA method. Activity of glutamate decarboxylase (GAD) was measured by the [14C]CO2 trapping method, using L-[1-14C]-glutamic acid (60 mCi/mmol, GE Healthcare, Buckinghamshire, UK) as a substrate [447]. Enzyme activity was expressed as nmol of product/h/mg of protein. Reactions contained 40 µg of extract protein and 0.5 M KH2PO4, 5mM ethylenediamineteraacetic acid (EDTA), 1 mM 2-aminoethyliso-thiouronium bromide (AET), 10 mM glutamate, 1 mM pyridoxal phosphate and L-[1-14C]-glutamic acid in a total volume of 100 µl. Samples were incubated for 1 h at 37ºC in test tubes containing #32 glass fiber filters (Schleider and Schuell, Keene, NH, USA) coated with 0.5 M Solvable (Packard Instruments, CT, USA). Each filter was suspended at the top of the tube, just underneath a rubber stopper, which sealed the tube. The reaction was stopped by the injection of 15% trichloroacetic acid through the stopper. The tubes were incubated at room temperature for another 120 min to ensure complete release and absorption of [14C]CO2 into the filter paper.

The filter papers were then removed from the tubes and placed in scintillation vials for measurement of the [14C]CO2 product in a Packard 2000 spectrometer provided with dpm correction. The scintillation cocktail used contained 5.84 g 2,5-diphenyloxazole (PPO) and 133.6 mg of 1,4-Bis(5-phenyl-2-oxazolyl)benzene (POPOP), 800 ml toluene and 200 ml of Triton X-100. Sample extracts were also analysed by Western Blot using the anti-GAD65/67 antibody.

Immunocytochemistry

For immunocytochemistry, cultured hippocampal neurons were grown on poly-D-lysine coated glass coverslips, at a density of 45x103 cells/cm2, and were then fixed in PBS supplemented with 4% paraformaldehyde/4% sucrose, for 30 min at 4ºC. After fixation the cells were permeabilized with 0.25 % Triton X-100 in PBS, for 5 min at room temperature, washed three times in PBS, and then blocked with 20% normal goat serum, for 1h at room temperature, and stained against VGLUT1 (1:1000; Synaptic Systems) + VGLUT2 (1:500; Synaptic Systems) or GABA (1:2000; SIGMA) overnight at 4ºC. Next, the cells were washed six times and incubated for 1h at room temperature with the secondary antibody (Alexa Fluor® 488 goat anti-rabbit, 1:500 to 1:1000; Barcelona, Spain). The cells were washed three times, mounted on glass slides with the Dako mounting medium and viewed on an Axiovert 200 fluorescence microscope coupled to an Axiocam HRm digital camera (Zeiss) (Figure 1).

Immunocytochemistry experiments for localization of GAD65 were performed using hippocampal neurons maintained in culture for 10 days. The cells were fixed with 4% formaldehyde, 4% sucrose in PBS for 12 min at room temperature and were subsequently permeabilized with 0.25% Triton X-100 in PBS for 3 min, washed 3 times in PBS and incubated in blocking solution (2% bovine serum albumin, 2% glycine, and 0.2% gelatin in 50mM NH4Cl) for 1 h at room temperature. Afterwards, the neurons were incubated for 1h with a mouse monoclonal antibody anti-GABAAReceptor β2/3 (Upstate Biotechnology) at a dilution of 1:200, and a rabbit polyclonal antibody anti-GAD65 (SIGMA) at a dilution of 1:1000, in blocking solution. Following the incubation with the primary antibodies, the cells were rinsed 4 times in PBS during 15 min periods, incubated for 1 h at room temperature with secondary antibodies Alexa Fluor 568 goat anti-rabbit and Alexa Fluor 488 goat anti-mouse (Invitrogen), at a dilution of 1:500 in blocking solution, rinsed 3 times in PBS followed by a final rinse in deionized water, dried, and mounted in Vectashield mounting solution (Vector Laboratories, Inc.). The neurons were imaged at the Garner Laboratory (Stanford University) with a Zeiss Axovert 200M microscope using a 63x objective. The image emission was directed through a CSU10 spinning disk confocal unit (Yokogawa) and collected by a 512B-CCD camera (Roper Scientific). Image

acquisition and analysis was conducted with Metamorph software. For each field of view, stacks of 2 images with a Z step size of 0.2 mm were collected and a Metamorph 3D reconstruction tool was used to create a projection image. For each condition, 15 images were collected from two different cover slips.

For quantitative assessment of GABAAReceptor β2/3 and GAD65 protein co-localization, the 3D reconstruction stacked images were submitted to threshold using the MetaMorph Inclusive Threshold application, in order to include only the puncta labeled by the GAD65 antibody. The total number of GAD65 puncta was determined using Integrated Morphometry Analysis of the image and selecting the Area parameter setup for measurement. After proceeding to perform an identical 3D reconstruction and threshold of the GABAAReceptor β2/3 corresponding image, the two reconstructed images were overlayed and a color threshold was set. Finally, the overlay image was used to quantify the number of puncta positive for both GABAAReceptor β2/3 and GAD65, using the Integrated Morphometry Analysis tool. This procedure was repeated for each field of view, and the ratio of GABAAReceptor β2/3 subunits and GAD65 positive puncta per total number to GAD65 puncta was determined in percentage. The average number of 15 images, per condition, was calculated for 3 independent experiments. Likewise, the number of GAD65 puncta per unit length of axon was determined by selecting the option Trace Region on MetaMorph to delineate segments of axons with at least 100 μm, and measuring the number of GAD65 puncta on the image previously submitted to a threshold, using Integrated Morphometric Analysis. The length of each axonal segment was determined selecting the Multi-line tool and uniting consecutive puncta along the delineated neurite. This procedure was repeated in each field of view, for 10-15 images per condition, in each of the 3 independent neuronal preparations.

Determination of the viability of GABAergic neurons with Hoescht 33342

Determination of cell viability was performed by fluorescence microscopy, using the indicator Hoechst 33342 as previously described [448]. The cells were stimulated with 125 μM glutamate for 20min, in Neurobasal medium supplemented with the GABA transporter inhibitor SKF89976 (10 μM). After the excitotoxic insult hippocampal neurons were further incubated in culture conditioned medium supplemented with 10 μM SKF89976 for 12 h. Incubation of the cells with SKF89976 during stimulation with glutamate and after the excitotoxic insult prevents the depletion of GABA through reversal of the plasma membrane transporter [449]. GABAergic neurons were stained using an anti-GABA polyclonal antibody (see above), and the nuclear

morphology was assessed through staining with Hoechst 33342. Analysis of the nuclear morphology was limited to GABAergic neurons, stained with the anti-GABA antibody.

Measurement of metabolic activity with CellTiter-Glow

Rat hippocampal neurons cultured in 384 micro-titter plates, coated with poly-D-lysine, at a density of 91.6x103 cells/cm2 were incubated with 125 µM glutamate in supplemented Neurobasal medium, for 20 min at 37ºC. After stimulation with glutamate, the cells were further incubated with the original culture medium, for 14 h at 37ºC. The viability of the cells was then measured by analysing the levels of ATP as an indicator of cellular metabolic activity, using CellTitter-Glo (Promega) according to manufacturer´s instructions. Briefly, in each well, 50 µl of PBS/CellTitter-Glo (1:1) were dispensed with a Multidrop 384 stacker (Titertek), after removal of the growth media, at room temperature. The plate was then placed on an orbital shaker for 2 minutes, at maximum speed and further incubated for 10 minutes at room temperature, without shaking. Luciferase luminescence was measured immediately afterwards, using an Acquest plate reader (Molecular Devices).

Statistical Analysis

Statistical analysis was performed using one-way ANOVA analysis of variance followed by the Bonferroni test, or using the Student´s t test, as indicated in the figure captions.

Results

Excitotoxic damage of cultured GABAergic hippocampal neurons

Dissociated cultures of hippocampal neurons contain glutamatergic and GABAergic neurons, expressing the vesicular glutamate transporter 1 (VGLUT1) and glutamic acid decarboxylase, respectively [450]. Immunocytochemistry experiments using antibodies against VGLUT1+VGLUT2 (Fig. 1D) and against GABA (Fig. 1E) showed that 65% of the cells present in hippocampal cultures are glutamatergic and 5% are GABAergic, respectively (Fig. 1A). Excitotoxic stimulation of cultured hippocampal neurons with 125 µM glutamate for 20 min reduced cell viability as determined using the CellTiter-Glo Luciferase chemiluminescence assay, a method based on

the quantification of the ATP present in the cells. Luciferase activity was reduced to 48% of the control 14h after the toxic insult (Fig. 1B), in agreement with the results obtained in experiments where cell survival was determined using fluorescence microscopy with the indicator Hoechst 33342 [448]. Under these conditions damaged hippocampal neurons display an apoptotic-like morphology. Since GABAergic neurons represent a minor fraction of the cells present in the cultures, we have specifically assessed the effects of excitotoxic stimulation with glutamate on the neuronal population displaying GABA immunoreactivity. In these experiments the cells were stimulated with glutamate in the presence of the GABA transporter inhibitor SKF89976 in order to prevent the release of the neurotransmitter through reversal of the plasma membrane transporter [449]. The number of GABAergic cells displaying apoptotic-like morphology 12h after glutamate stimulation was about 54% (Fig. 1C).

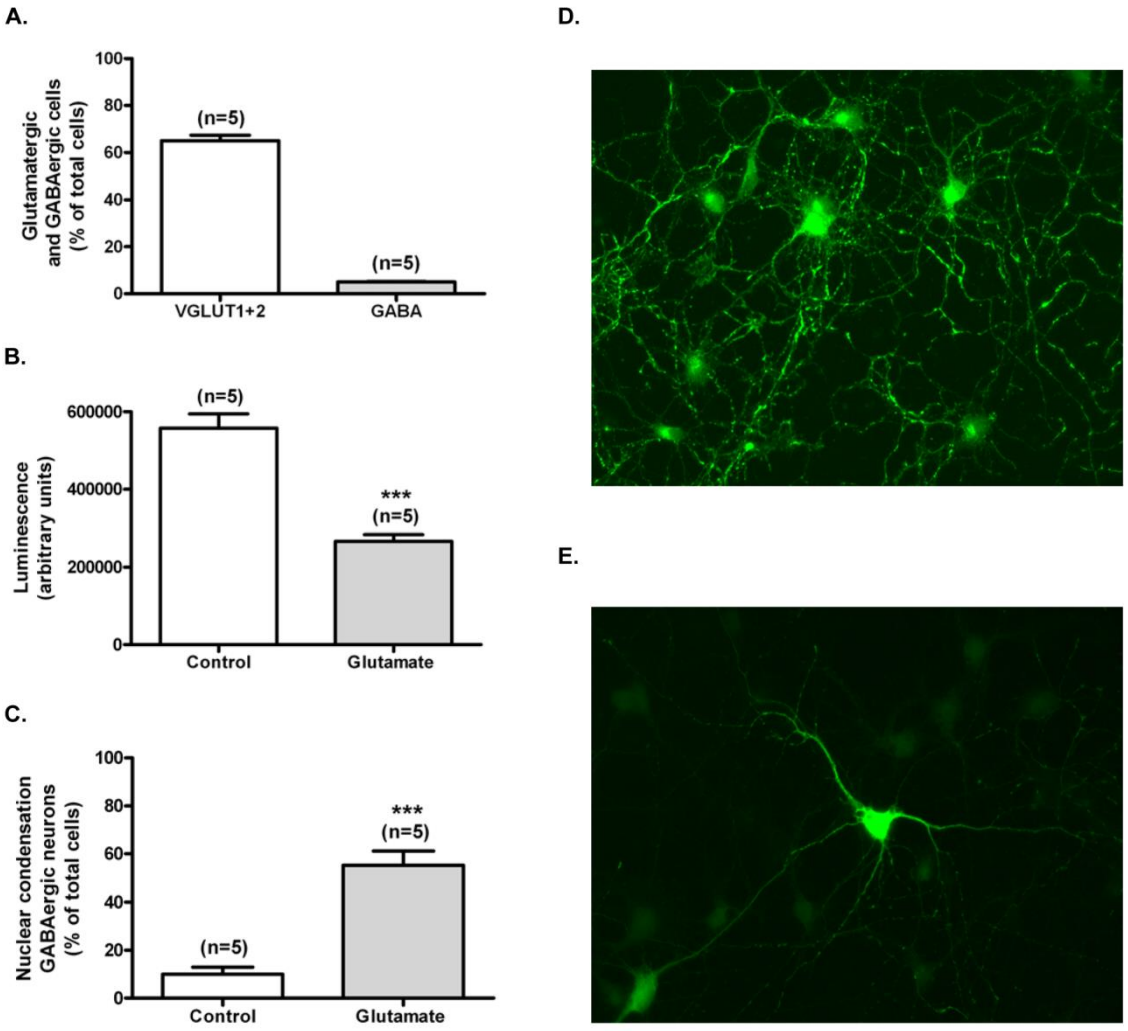

Figure 1 – Glutamate excitotoxicity decreases viability of cultured hippocampal GABAergic neurons. GABAergic and glutamatergic neurons in the cultures (DIV7) were identified by immunocytochemistry, using antibodies against GABA (A, E) and VGLUT1+2 (A, D). The total number of cells present in the analysed fields was calculated based on the number of nuclei, stained with the fluorescent dye Hoechst 33342. Data are presented as mean±SEM of 5 independent preparations (A). Excitotoxic stimulation of hippocampal neurons was performed by incubation with 125 μM glutamate, for 20 min, in fresh Neurobasal medium containing B27 supplement, and the cells were further incubated in the original medium for 14h. Cell death was assessed with the recombinant Luciferase chemoluminescence assay with CellTiterGlo (B), or by fluorescence microscopy using the fluorescence dye Hoechst 33342 (C). In the latter condition GABAergic cells were identified by immunocytochemistry, using an antibody against GABA. Data are presented as mean±SEM of 5 independent experiments. Statistical analysis was performed using Student's t-test. ***$p < 0.001$.

Excitotoxicity-induced cleavage of GAD and down-regulation of gene expression

To test the effect of glutamate stimulation on glutamic acid decarboxylase, a marker of GABAergic neurons, GAD protein levels were evaluated after the excitotoxic insult, using an antibody that recognizes both forms of the enzyme in a common C-terminal region (Fig. 2C). Under control conditions the antibody allows identifying the two GAD isoforms, with 67 kDa and 65 kDa. Glutamate stimulation induced a time-dependent decrease in the abundance of both isoforms, and this effect was correlated with the upregulation of a truncated form with an apparent molecular mass of 55-58 kDa (Fig. 2 A). The truncated form still bound the C-terminus directed antibody, but no smaller immunoreactive forms of GAD were detected in the blots (not shown). These results indicate that glutamate-induced cleavage of the two GAD isoforms occurs at the N-terminal region and gives rise to truncated forms with similar apparent molecular weights.

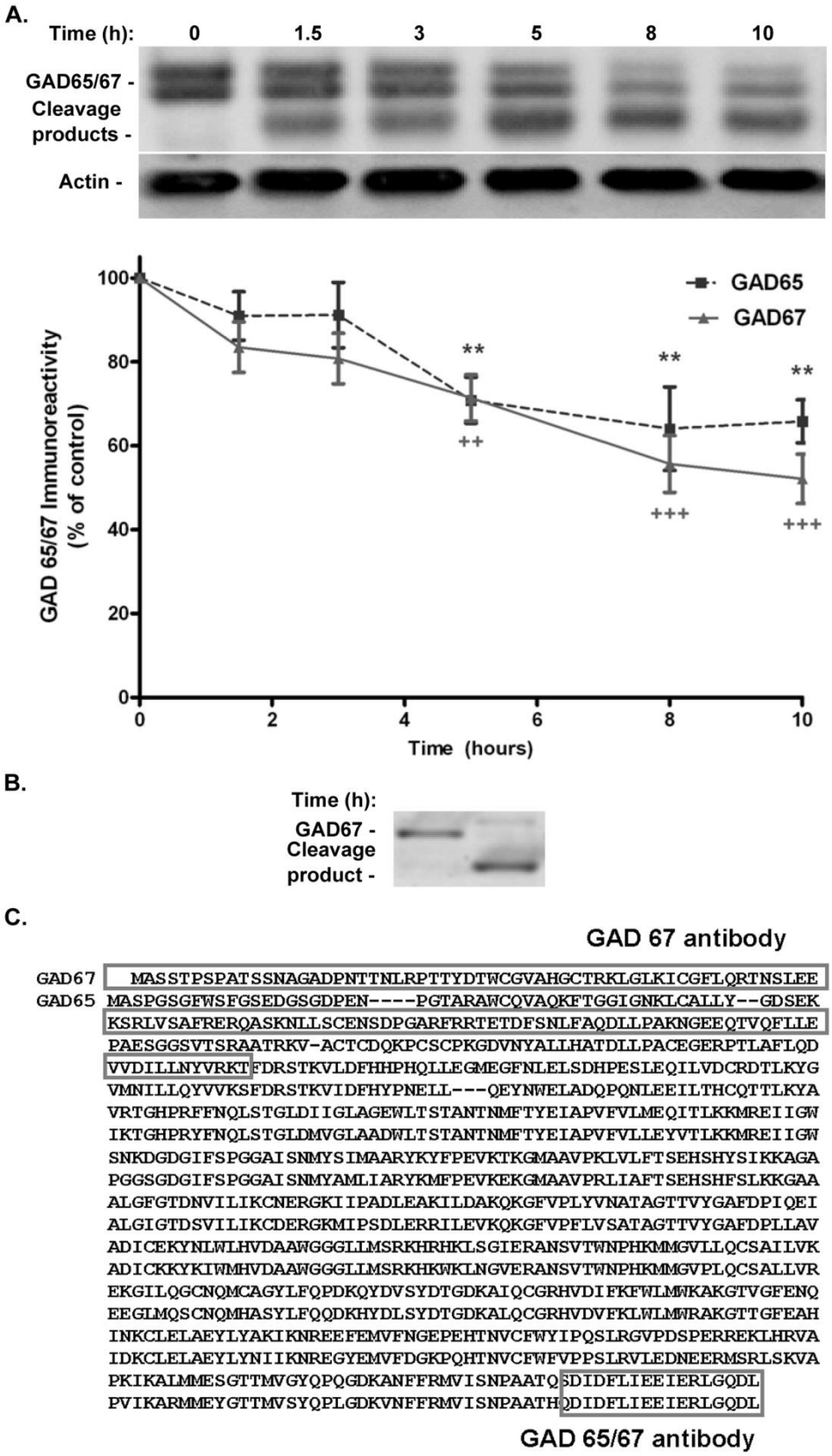

Figure 2 – Glutamate excitotoxicity induces a time-dependent decrease in GAD65 and GAD67 protein levels in cultured hippocampal neurons. Neurons were stimulated with 125 µM glutamate, for 20 min, and further incubated in culture conditioned medium for the indicated period of time. Full length GAD 65/67 protein levels were determined by Western Blot with an

antibody that recognizes both isoforms. Control protein levels of GAD65/67 were set to 100%. Actin was used as loading control (A). Panel A shows a representative experiment and mean±SEM of 9 independent experiments. The cleavage of GAD67 was also analysed with an antibody directed against amino acids 70-130 of this isoform (B). In this case the results obtained under control conditions were compared with the immunoreactivity in extracts prepared 14h after the toxic insult. The amino acid sequence of GAD65 (lower sequence) and 67 (top sequence) are aligned in panel C, which also show the binding sites for the antibodies used in this study. Statistical analysis was performed using one-way ANOVA, followed by Bonferroni´s multiple comparison test. **p < 0.01; ***p < 0.001.

In order to further characterize the cleavage of GAD under excitotoxic conditions, we tested a GAD67 specific antibody that binds its N-terminus (amino acids 17-130). The immunoreactivity pattern in extracts prepared from cells incubated for 14h after the toxic insult with glutamate was similar to that obtained using the antibody directed against the C-terminal region of GAD (Fig. 2 B). This indicates that GAD67 is cleaved before amino acid 130.

Besides its effect in inducing the cleavage of GAD, excitotoxic stimulation with glutamate may also have delayed effects on GAD by acting at the transcription level. This was tested by Real-Time PCR, in cells subjected to excitotoxic stimulation with glutamate for 20min and further incubated in culture medium for 4h. Under these conditions there was a 58% and 71% downregulation of GAD65 and GAD67 mRNA, respectively, relative to unstimulated cells (Fig. 3).

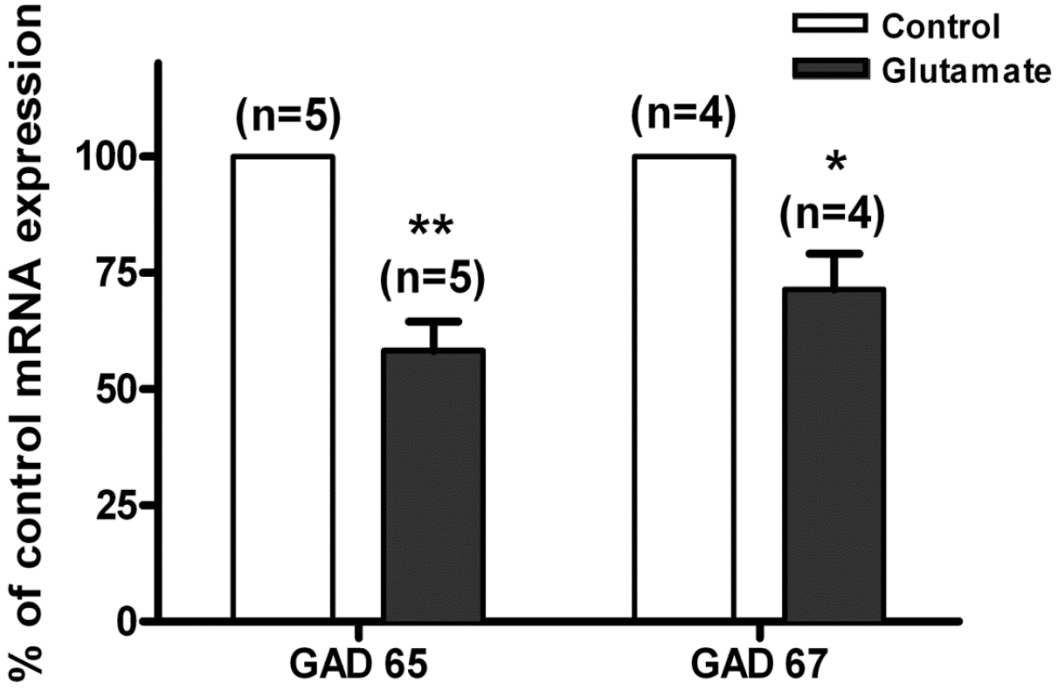

Figure 3 – Glutamate excitotoxicity decreases GAD65/67 mRNA. Gene expression was analysed in cultured hippocampal neurons (7 DIV) exposed or not to 125 µM Glutamate, for 20

min, and then returned to the original culture medium for 4h. For the reverse transcription reaction 1 μg of total RNA was used. The results were normalized with two internal control genes, GAPDH and Tubulin. Data are presented as mean±SEM of four to five independent transcription reactions, performed in independent preparations. Statistical analysis was performed using Student's t-test. *$p < 0.05$; **$p < 0.01$.

Proteasome inhibitors protect GAD65/67 from cleavage under glutamate-induced excitotoxicity in hippocampal neurons

Multiple proteolytic systems have been shown to participate in the cleavage of GAD under excitotoxic conditions, including calpains and cathepsins [282-285]. Despite the key role of the ubiquitin-proteasome system (UPS) in protein degradation in the CNS, no studies have addressed its role in the down-regulation of full-length GAD isoforms under excitotoxic conditions. To test for the effect of inhibiting different proteolytic activities of the proteasome, we used the chymotrypsin-like activity directed inhibitor MG132 and the post-glutamyl peptide hydrolyzing-activity (PGPH) directed inhibitor YU102. We also tested the effect of lactacystin which shows a slight preference for the trypsin-like and caspase-like activities [451]. MG132 is a synthetic peptide aldehyde that binds reversibly to the 20S proteasome active site forming a covalent hemiacetal adduct [452,453]. The effect of proteasome inhibitors was tested 5h after the toxic insult with glutamate since long incubation periods with these compounds causes neuronal cell death [454,455]. MG132 abrogated glutamate-induced cleavage on both isoforms of GAD, as determined 5h after the toxic insult (Fig. 4A). Lactacystin is a Streptomyces lactacystinaeus metabolite that targets the 20S proteasome by an irreversible modification of the amino terminal threonine of β-subunits, while YU102 is a α', β'-epoxyketine, the only peptidyl-glutamylpeptidehydrolyzing (PGPH)-specific peptide used in this study [453,456]. Both YU102 and lactacystin inhibited glutamate-evoked GAD65 cleavage, but were without effect on GAD67 (Fig. 4A).

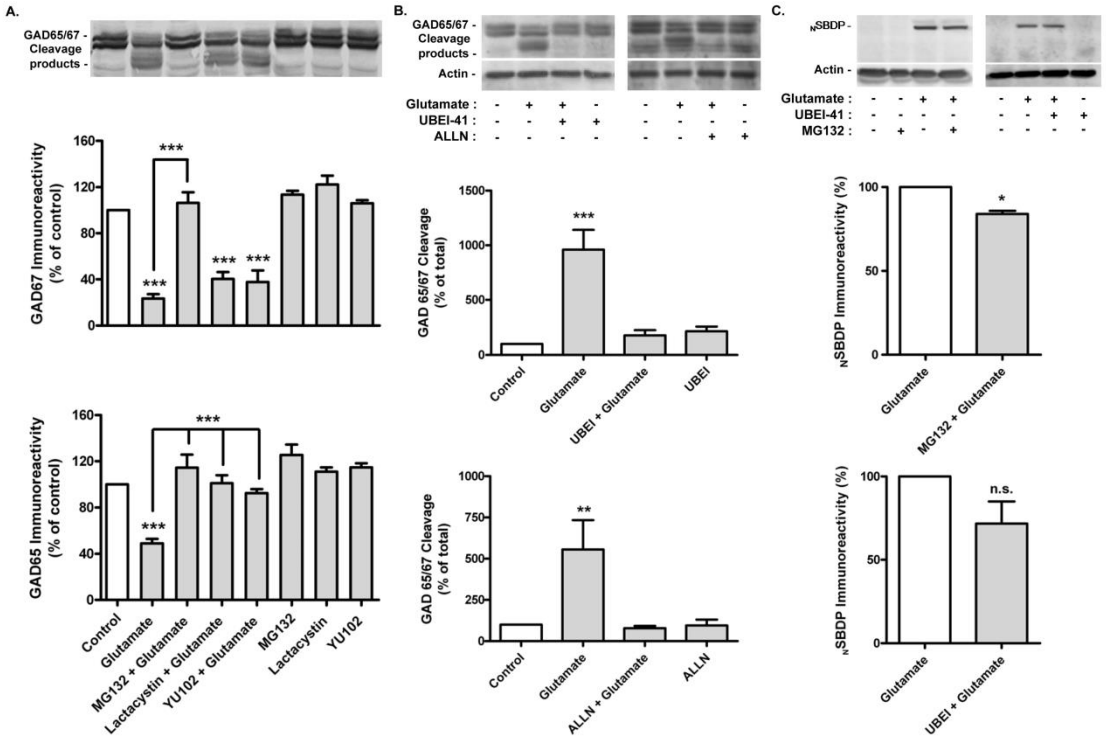

Figure 4 – Proteasome and ubiquitin-activating enzyme (E1) inhibitors prevent glutamate–induced GAD65/67 cleavage. Cultured hippocampal neurons were pre-incubated or not with 50 µM of UBEI-41 (E1 inhibitor), for 1h, or with the proteasome inhibitors MG132 (1µM), lactacystin (10 µM) or YU102 (10 µM), for 30 min, before excitotoxic stimulation with glutamate (125 µM), for 20 min. The cells were further incubated in culture conditioned medium (with or without chemical inhibitors) for 5h, and the GAD65/67 immunoreactivity was assessed by western blot (A and B). Incubation with the calpain inhibitor ALLN (10 µM) was performed under the same conditions. The average results in (A) represent the changes in GAD65 or GAD67 immunoreactivity. In panel (B) GAD cleavage was calculated as a percentage of the total enzyme content (GAD65/67). When calpain activity was evaluated through formation of N-terminal spectrin breakdown products (NSBDPs) the cells were incubated for 30 min after the toxic insult (C). The effect of MG132 and UBEI-41 on calpain activation is expressed as a percentage of the activity measured in the absence of the protease inhibitors. Results are means±SEM of 3-4 different experiments, performed in independent preparations. Statistical analysis was performed using one-way ANOVA, followed by Bonferroni´s Multiple Comparison Test (A and B) or the Student's t test (C). ***p < 0.001.

To further characterize the role of the UPS in the glutamate-evoked cleavage of GAD we tested the effect of the ubiquitin-activating enzyme (E1) inhibitor, UBEI-41 [457]. It has been assumed that only a single activating enzyme for ubiquitin exists, which operates at the initial step of the ubiquitin-proteasome pathway. Therefore, if the UPS plays a role in the cleavage of GAD, inhibitors of E1 should abrogate the excitoxicity-induced cleavage of the GAD. Accordingly, inhibition of the ubiquitin-activating (E1) enzyme prevented the effect of excitotoxic stimulation on the cleavage of GAD67 and GAD65 (Fig. 4B).

In previous studies the cleavage of GAD under excitotoxic conditions was found to be abrogated by calpain inhibitors [282-285]. Furthermore, recombinant GAD65 and 67 are cleaved in

vitro by calpain [282,283]. Accordingly, incubation of hippocampal neurons with ALLN, a chemical inhibitor that targets preferentially calpains when used at lower concentrations, prevented the glutamate-induced cleavage of GAD65/67 (Fig. 4B). Therefore, we determined whether inhibition of calpains could account for the effect of the UPS inhibitors on glutamate-induced cleavage of GADs. Activation of calpain was measured by western blot, using an antibody that binds specifically to the product resulting from the cleavage of spectrin by calpains (SBDPs) [445,446,458]. Glutamate stimulation increased the formation of N-terminal SBDPs (NSBDPs), and this effect was only slightly inhibited by MG132 (16.6%; $p<0.05$) and by UBEI-41 (28.3%; $p>0.05$) (Fig. 4C). These results indicate that calpain inhibition is not likely to account for the effects of MG132 and UBEI-41 on glutamate-evoked cleavage of GAD.

GAD65/67 interact with ubiquitinated proteins in primary hippocampal cultures

The results shown above suggest that the proteasome plays a direct role in GAD67 cleavage under excitotoxic conditions. In particular, the inhibition of GAD67 cleavage by the E1 inhibitor (Fig. 4C) suggests that the enzyme is ubiquitinated before cleavage by the proteasome. To test for the possible ubiquitination of GADs we used the UbiQapture™-Q Kit which allows isolating both mono- and poly-ubiquitinylated proteins (and their binding partners), independent of lysine residue chain linkage. Ubiquitinated proteins (and their binding partners) were isolated from extracts of hippocampal neurons stimulated or not with glutamate (with or without MG132), and the results were analysed by Western Blot with an anti-GAD65/67 antibody. GAD65/67 was immunoprecipated in similar amounts in all experimental conditions tested, but stimulation with glutamate in the presence or in the absence of MG132 increased the capture of GAD (Fig. 5A, top panel). However, in all experimental conditions the mobility of the immunoprecipitated GAD65/67 was the same as the mobility of the protein present in extracts directly loaded on the gel, suggesting that there is no change in GAD ubiquitination following glutamate stimulation. Taken together these results suggest that GAD67 interacts with another protein(s) that is ubiquitinated, and capture of this protein by an anti-ubiquitin antibody allows co-purification of the enzyme. The increased co-immunopurification of GAD67 in extracts from cells stimulated with glutamate may suggest that the excitotoxic insult increases the ubiquitination of the GAD67 interacting protein(s).

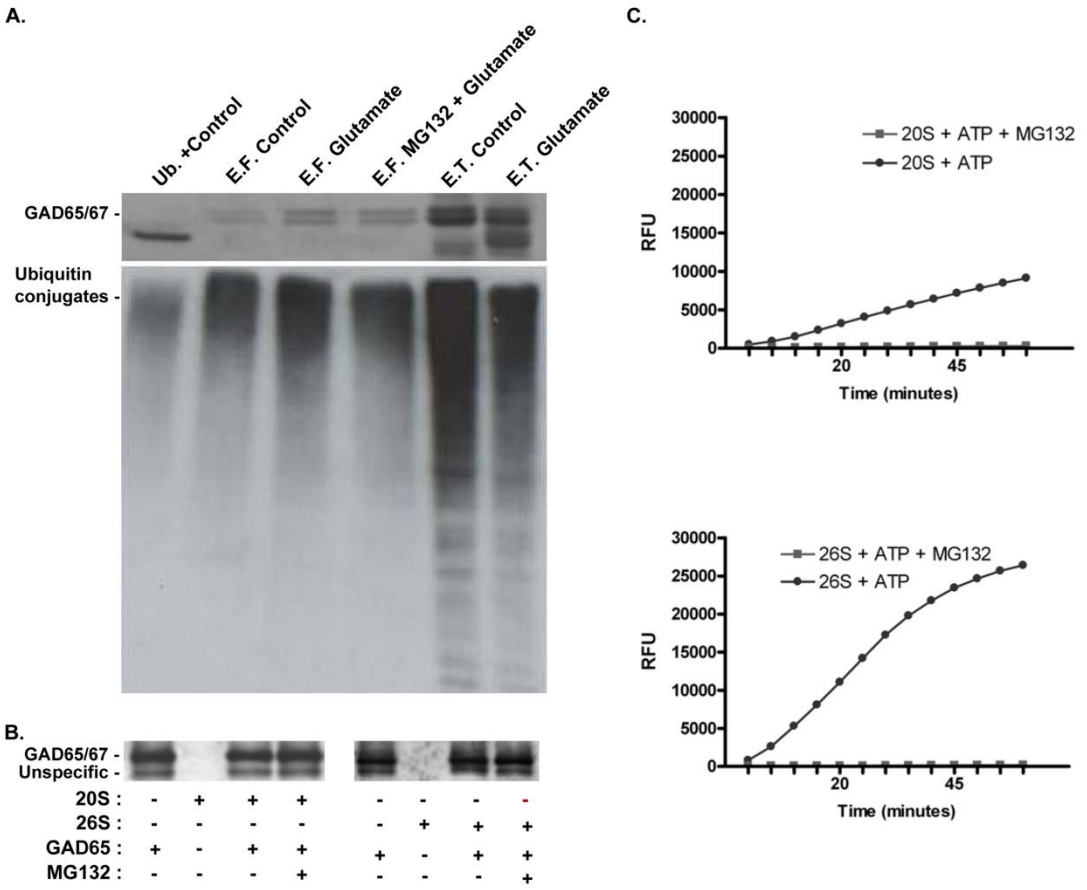

Figure 5 – GAD 65/67 are captured with an anti-ubiquitin antibody in hippocampal cultures. (A) Cultured hippocampal neurons were stimulated or not with 125 µM glutamate for 20min, in the presence or in the absence of 10 µM MG132, and the cells were further incubated with culture conditioned medium for 4h before preparation of the extracts. In the top panel, mono- and poly-ubiquitinylated proteins were isolated using the UbiQapture™-Q Kit, and the eluted fraction [454] was subjected to western blot, using an antibody against GAD65/67. GAD65/67 total immunoreactivity in the extracts prepared from control cells and from hippocampal neurons stimulated with glutamate is shown on the right (E.T.). The left lane was loaded with a control provided in the kit, consisting in ubiquitinated protein lysate. The same membranes were probed for mono- and poly-ubiquitin using an antibody included in the kit (A, middle). (B) Human recombinant GAD65 (0.75 µg) were incubated with 20/26S proteasomes (1.5 µg) for 2h at 37ºC with or without MG132. The extracts were then probed with GAD65/67 antibody. The activity of the 20S/26S proteasomes used in the experiments was confirmed using the fluorogenic substrate suc-LLVY-MCA. The increase in fluorescence resulting from the cleavage of the substrate was measured in relative fluorescence units (RFU) (C). The results of the capture of ubiquitinated proteins and the assay of the recombinant GAD65 cleavage are representative of two and three independent experiments, respectively.

Since the 20S proteasome is able to cleave substrates without ubiquitination [459,460], an in vitro system was used to determine whether this could account for the observed inhibitory effect of MG132 on the excitotoxicity-induced cleavage of GAD65. Recombinant GAD65 was incubated with 20S and 26S proteasomes using the protocol previously described [459], which allowed characterizing the ubiquitin- and ATP-independent cleavage of YB-1 (a DNA/RNA-binding nucleocytoplasmic shuttling protein) by the 20S proteasome in vitro. No cleavage of recombinant GAD65 was observed following incubation with the 20S or 26S proteasome (Fig. 5B), suggesting that this GAD isoform does not undergo a ubiquitin-independent proteasomal cleavage, as described for YB-1. Control experiments using fluorogenic substrates showed that the 20S and 26S proteasome preparations were active (Fig. 5C), further suggesting that the proteasome does not act directly on GAD65.

GADs cleavage is correlated with decreased enzyme activity and changes the subcellular distribution

Since GADs play a key role in the synthesis of GABA from glutamate, we investigated how the cleavage of the enzyme affects its activity. The assay of GAD activity using the [14C]CO2 trapping method requires the use significant amounts of protein that cannot be obtained using hippocampal cultures. Therefore, the effect of GAD cleavage on the activity of the enzyme was investigated using brain tissue from decapitated rats. Previous studies have shown that under these conditions GAD is cleaved with a pattern similar to that observed under excitotoxic conditions, particularly in the cerebellum and in the cerebral cortex [461]. The post-mortem cleavage of GAD65 and GAD67 in these brain regions was confirmed in the present study (Fig. 6B), and 24h after death there was a decrease in the total full length GAD protein levels both in the cerebellum and in the cerebral cortex (Fig. 6A). At this time point the activity of GAD was decreased to 68.8% in the cerebral cortex and to 33.1% in the cerebellum, while the total amount of full-length protein was reduced to 73% and 58%, respectively. The total GAD protein levels (full-length + cleaved protein) at 24h post-mortem was not significantly different from the amount of protein detected under control conditions (see representative western blot in the top panel of Fig. 6B).

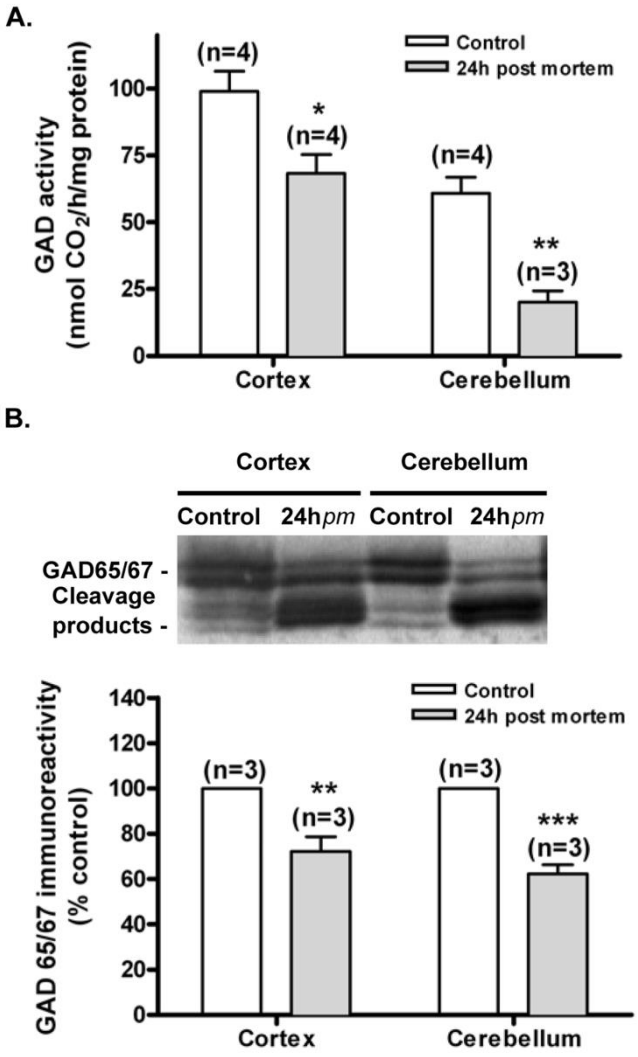

Figure 6 – Excitotoxicity-induced decrease in GAD65/67 activity. Heads of adult Wistar rats were decapitated and processed immediately or kept for 24h at room temperature. The extracts were used for both GAD activity measurements and Western Blot analysis. GAD activity was determined using a trapping technique for radiolabelled [^{14}C]CO_2 brought by GAD65/67 activity, and was expressed as nmol CO_2/hr/mg of protein (A). Full-length GAD65/67 protein levels from the same extracts were determined by Western Blot using an anti-GAD65/67 antibody, and control protein levels of GAD65/67 were set to 100%. Data are presented as mean±SEM of 3 to 4 independent experiments. Statistical analysis was performed using Student's *t*-test. *$p < 0.05$; **$p < 0.01$: ***$p<0.001$.

GAD65 is anchored to synaptic vesicles through its N-terminus [462,463]. Since glutamate stimulation cleaves GAD near the N-terminal region, we hypothesized that the cleavage of the enzyme could affect its sub-cellular localization. Under control conditions GAD65 displays a partially punctate distribution along neurites (Fig.7A, arrowheads), but this pattern is altered 4h after excitotoxic stimulation with glutamate. Under the latter conditions some neurites show a more homogeneous distribution of GAD65, diffuse along the neuronal processes (Fig. 7A, B), and the number of GAD65 puncta is significantly reduced in comparison to the control

conditions (Fig. 7C). Colocalization of GAD65 with the β2/3 GABAA receptor subunits was also significantly decreased (Fig. 7C), showing a loss of synaptic distribution of GAD65 under excitotoxic conditions.

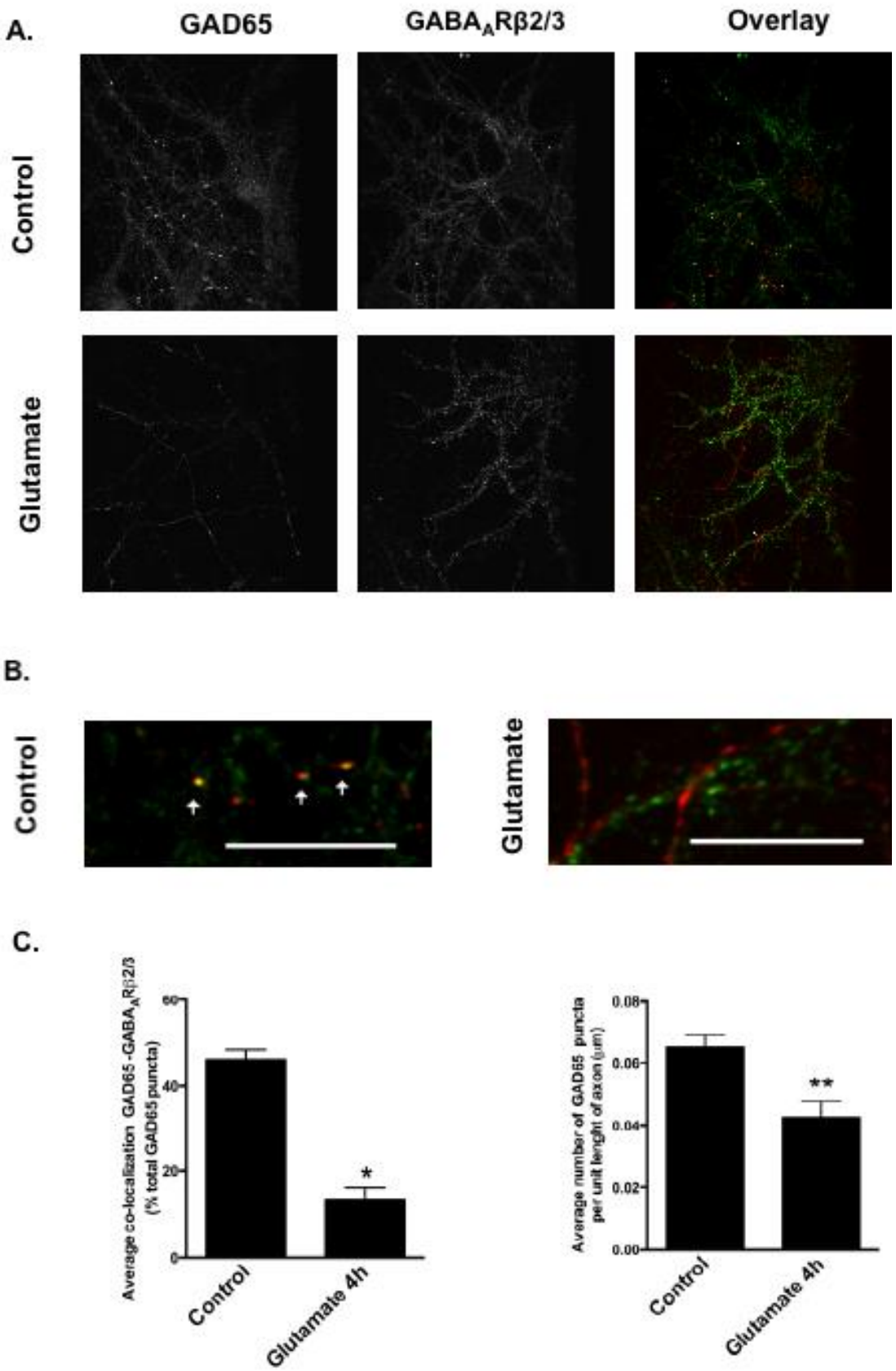

Figure 7 – Glutamate changes the subcellular distribution of GAD65 along neurites. 10 DIV hippocampal neurons were incubated with or without glutamate (125 μM) for 20 min, and then returned to the original culture medium for 4h. Cells were fixed, permeabilized and probed with specific antibodies to GAD65 and $GABA_A$ receptor subunits β2/3. (B) Arrows

indicate GAD65 clustering (red), a pattern that is changed in glutamate treated cells. Images are representative of three different experiments performed in independent preparations. Images in (B) show colocalization of the immunoreactivity for GAD65 (red) and $GABA_A$ receptor subunits β2/3 (green) under control conditions, and the redistribution of GAD65 in the axons of hippocampal neurons subjected to excitotoxic conditions. The scale bar corresponds to 10 μm. (C) Quantification of the images for the colocalization of GAD65 and $GABA_A$ subunits β2/3, expressed as percentage of total GAD65 puncta (left), and the average number of GAD65 puncta per axon unit length (right). Data are presented as mean±SEM of 3 independent experiments performed in different preparations. Statistical analysis was performed using Student's *t*-test. **p* < 0.05; ***p* < 0.01.

Discussion

Previous studies have shown the cleavage of the glutamic acid decarboxylase isoforms GAD65 and GAD67 under excitotoxic conditions [283-285], and pointed out a key role for calpains in this process [282-284]. In this work we show that the activity of E1 ubiquitin ligase and the proteasome are required for glutamate-evoked cleavage of GAD67, although no clear evidences were obtained showing a direct ubiquitination of the enzyme. Furthermore, cleavage of GAD65/67 was found to decrease enzyme activity and changed the characteristic punctate distribution of GAD65 along neurites. Both effects are likely to downregulate the activity of GABA as a neurotransmitter under excitotoxic conditions.

Glutamate-induced cleavage of GAD protein levels and downregulation of mRNA

Excitotoxic stimulation of cultured hippocampal neurons induced the cleavage of GAD65 and 67 by a mechanism sensitive to the calpain inhibitor ALLN, similarly to what was observed in neuronal cultures prepared from the whole brain or from the cerebral cortex [283,284]. The full-length proteins were cleaved into a truncated form with approximately 55-58 kDa, which was detected by an antibody directed against the N-terminal of GAD65 and GAD67. Since no immunoreactive bands with low apparent molecular weight were identified, the results indicate that both GAD isoforms are cleaved in a sequence close to the N-terminal region of the proteins. Accordingly, an antibody directed against amino acids 17-130 of GAD67 also detected the cleavage product of the enzyme, showing that the cleavage site is located before amino acid 130. The sequence after amino acid 100 in GAD67 shows high homology with GAD65 (Fig. 2C), and this explains the similarity in the apparent molecular weight of the cleavage products of GAD65 and GAD67. Much of the available evidences suggest that the N-terminal segment of GAD is exposed and flexible [464], and this may make this region available

for cleavage by proteases. In vitro studies showed that recombinant human GAD67 lacking the first 70 or the first 90 amino acids is not cleaved by calpain, in contrast with the full length protein [282], suggesting that under excitotoxic conditions GAD67 may be cleaved between amino acids 90 and 130. If this is the case, the dimerization of GADs required for their activity is likely not affected by enzyme cleavage since dimer formation occurs through interaction of C-terminal portions of GAD molecules [464]. GAD is a pyridoxal 5'-phosphate (PLP)-dependent enzyme, but the co-enzyme binding site is not contained within the N-terminal regions [465]. Therefore, changes in PLP binding are not likely to account for the changes in GAD activity following enzyme cleavage.

In addition to the cleavage of GAD we also observed a decrease in the mRNA levels for both isoforms of the enzyme in hippocampal neurons subjected to an excitotoxic insult with glutamate (Fig. 3). This is likely to limit the de novo synthesis of GAD, which could otherwise compensate for the observed dowregulation of the full-length protein. It remains to be determined whether the observed decrease in the mRNA for GAD is due to a reduction in transcription activity and/or to an active degradation of the existing transcripts. The rapid down-regulation of GAD mRNA following excitotoxic stimulation of cultured hippocampal neurons contrasts with the delayed effects of ischemic injury on GAD67 mRNA [466]; unilateral ischemic lesions of the frontoparietal cortex in adult rats increased GAD67 mRNA levels in the striatum, lasting up to 3 months after surgery. Inhibition of NMDA receptors also downregulated GAD mRNA in various brain regions, starting at day 2 after treatment [467], suggesting that glutamate receptors are directly coupled to the activation of GAD67 expression.

UPS system activity is essential for excitotoxicity-induced GAD cleavage

Previous studies have shown that calpain inhibitors fully block [283] [or inhibit to a great extent [284]] the glutamate evoked cleavage of GAD65/67 (see also Figure 4B), and in vitro experiments showed that calpains cleave recombinant GAD67 [282]. Taken together these evidences strongly suggest that calpains play a key role (if not exclusive) in GAD cleavage under excitotoxic conditions. Surprisingly, we observed that inhibition of the proteasome with MG132, lactacystin or YU102 fully abrogated the cleavage of GAD67 in hippocampal neurons subjected to excitotoxic conditions, and MG132 had the same effect on the cleavage of GAD65. Furthermore, inhibition of the ubiquitin-activating enzyme (E1) with UBEI-41 also prevented the cleavage of GAD67 and GAD65. The effects of MG132 and UBEI-41 cannot be attributed to inhibition of calpains since the inhibitors had a small (MG132) or no effect (UBEI-41) on the

glutamate-evoked calpain activation, as determined by measuring the formation of spectrin breakdown products (Fig. 4C). Since the molecular weight of the GAD truncated forms observed in the present studies is similar to that observed in previous studies where calpains were shown to participate in the cleavage of the enzyme, it is likely that the UPS and calpains act in a co-ordinated manner to cleave GADs. If this is the case, the UPS is likely to act upstream of calpains since no evidences were found for a direct effect of proteasome in GAD cleavage.

Interaction between calpains and the UPS is also physiologically relevant in other scenarios. Sequential activity of calpains and the UPS has been proposed to contribute to the degradation of myofibrils; calpains release myofibrils form the contractile apparatus, which allows initiating ubiquitination and degradation by the proteasome [468,469]. Also, degradation of IκB through phosphorylation-dependent ubiquitination or following cleavage by calpains is thought to release NFκB, and the transcription factor migrates to the nucleus where it binds DNA [470-472]. There are reports suggesting that proteasome inhibition could be neuroprotective after stroke [287,473], namely through stabilization of IκB and thereby preventing NF-κB activation. Inhibition of calpains can also provide functional neuroprotection in various animal models of cerebral ischemia [474].

The role of ubiquitination in GADs cleavage

The glutamate-evoked cleavage of GAD65/67 was sensitive to proteasome inhibition, but incubation of GAD65 with the 20S proteasome did not give rise to the cleavage product of the enzyme. Although some proteins are cleaved by the 20S proteasome without ubiquitination [459,460], this is not the case of GAD65.

Inhibition of the E1 ubiquitinating enzyme also abrogated the cleavage of GAD65/67 under excitotoxic conditions, indicating that protein ubiquitination plays a key role in the process. Separation of mono and poly-ubiquitinated proteins with the UbiQapture™-Q Kit allowed recovering GAD65 and GAD67, but although there was an increase in the amount of GAD isolated with the kit under excitotoxic conditions the apparent molecular weight of the proteins isolated was similar to that observed in whole cell extracts. This strongly suggests that GAD is not ubiquitinated, but instead interacts with a protein which state of ubiquitination is increased following excitotoxic stimulation with glutamate. This may be related with an increase in ubiquitin mRNA transcripts, as observed following ischemia [475,476], with an impairment of the proteasome activity [286,441,477], and/or to a signalling cascade induced by excitotoxicity that may ultimately leads to the ubiquitination of the GAD binding partner.

Excitotoxicity also regulates the NF-κB transcription factor after cerebral ischemia through ubiquitination and degradation of its binding partner IκB [478]. Similarly, the cleavage of GAD may follow the increase in ubiquitination and degradation of a binding partner, which may allow cleavage of the enzyme by calpains. This hypothesis explains the effect of both E1 inhibition and proteasome inhibition on GAD cleavage, and the results showing no apparent ubiquitination of the enzyme (present work), and the role of calpains [284]. The GAD binding partner that may be involved in the regulation of the protein under excitotoxic conditions remains to be identified.

Interestingly, the proteasome inhibitors showed differential effects on GAD65 and GAD67 cleavage induced by excitotoxic stimulation with glutamate. MG132 abrogated the cleavage of both GAD isoforms, in contrast with YU102 and lactacystin which were only effective against the cleavage of GAD67. The difference in the effects of the inhibitors tested may be due to their specificities: MG132 and YU102 act preferentially on the cheymotrypsin-like and caspase-like activities of the proteasome, respectively, whereas lactacystin targets preferentially the trypsin-like and caspase-like activities [451,456]. Assuming that under excitotoxic conditions the proteasome targets a GAD binding partner before cleavage of the enzymes by calpains, these results suggest that the proteasome substrates bound to each of the GAD isoforms are distinct.

Alterations of GADs activity and localization under excitotoxic conditions

The decrease in GADs activity observed in post mortem cerebral cortices to 74% was correlated with a decrease to 73% of the full-length protein found in the extracts analysed by Western Blot; in the cerebellum the GAD activity decrease to 48% in post mortem extracts relative to control, and a down-regulation of the full-length protein to 58% was observed. This decrease in enzyme activity following N-terminal cleavage is in agreement with previous results obtained using a similar experimental paradigm [461] and with the effect of calpain cleavage at the N-terminal region on the activity of recombinant GAD67 [282]. In contrast, truncation of the N-terminal region of recombinant GAD65 increased enzyme activity [479] and trypsin cleavage of recombinant GAD65 and GAD67 at their N-terminal region was shown to increase enzyme activity [464]. The difference between the effects observed in brain extracts and in in vitro experiments may be due to interaction of GAD with regulatory proteins (see below), which are absent when recombinant proteins are used. Post-translational modifications of GAD, such as phosphorylation, may also contribute to the differences in the effect of N-

terminal cleavage on the activity of the enzyme measured in brain extracts or using recombinant protein [480]. A decrease in enzyme activity in neurons subjected to excitotoxic conditions may activate compensatory mechanisms in surviving neurons since the expression of GAD is regulated by the abundance of GABA by a mechanism independent of the activation of GABA receptors [481,482]. However, within the time frame analysed after the excitotoxic insult we found no evidences for an upregulation of GAD protein levels from de novo protein synthesis (Fig. 2).

In this work we also found that excitotoxic stimulation of cultured hippocampal neurons changes the subcellular distribution of GAD65, with a loss of protein clustering along neurites. This is in agreement with the results showing a role for palmitoylation of Cys30 and Cys45 in GAD65 in the post-Golgi trafficking of the protein to presynaptic clusters [483,484]. The N-terminal truncation under excitotoxic conditions is likely to separate this targeting sequence from the catalytic domain of GAD65, dissociating the enzyme from synaptic vesicles as suggested in the results of the immunocytochemistry experiments shown in Fig. 7. Furthermore, the decrease in colocalization of GAD65 and the β2/3 GABAA receptor subunits suggests that the cleaved protein becomes more diffuse, moving away from the synapse.

It was proposed that association of GAD with membranes and the anchoring of the enzyme to synaptic vesicles occur first through formation of a complex with the heat shock protein 70 family member HSC70 (heat shock cognate 70), followed by interaction with cysteine string protein (CSP), an integral protein of the synaptic vesicle [462]. Cleavage or degradation of the GAD anchoring proteins may release the enzymes anchored to synaptic vesicles and may contribute to change the subcellular distribution of the enzyme under excytotoxic conditions. If the N-terminal region of GAD65 plays a role in the interaction with the anchoring proteins, the cleavage of the enzyme under excitotoxic conditions may also explain the observed changes in immunoreactivity after the toxic insult with glutamate. The interaction of GAD with HSC70 and synaptic vesicles also promotes the activity of the enzyme [462]. The release of GAD65 from synaptic vesicles that may occur under excitotoxic conditions would explain, at least in part, the decrease in enzyme activity observed in cerebellar and cerebrocortical extracts containing cleaved GAD.

The anchoring of GAD65 to synaptic vesicles through interaction with the vesicular GABA transporter may allow coupling the synthesis of GABA to the packaging of the neurotransmitter into the vesicles [276]. The cleavage of the N-terminal region of GAD65 and the consequent dissociation of the enzyme from synaptic vesicles and from the synapse may decrease the accumulation of GABA in the vesicles and, therefore, may deregulate GABAergic

synapses. This is particularly relevant considering that GAD65 is the isoform responsible for the synaptically released GABA [485].

In conclusion, we showed that excitotoxic conditions lead to the cleavage of GAD65/67 in cultured hippocampal neurons in a UPS-dependent manner. GAD cleavage decreased enzyme activity and changed the subcellular distribution of the 65KDa isoform, which should decrease GABA production and may affect the accumulation of the neurotransmitter in synaptic vesicles.

Chapter 5

General Discussion

General discussion

As the UPS plays a fundamental role in neurons, either during development or in fully differentiated neurons, its dysfunction has been implicated in several diseases of the nervous system and in particular concerning polyQ disorders [205–207,486,487]. In our work we have identified a possible new player in the interplay between the UPS and the chaperone machinery in the regulation of proteostasis, the molecular chaperone HSP60. We also analyzed the possible contribution of a UPS component – UBH-1 (UCH-L1 orthologue) to proteostasis in the context of MJD, using a *C. elegans* model of this disease. Finally, we tested the contribution of the UPS to one of the hallmarks of neurodegenerative diseases, and in particular of MJD, calcium deregulation. Specifically, we addressed the contribution of the UPS to the cleavage of GADs, the enzymes responsible for the synthesis of the major inhibitory neurotransmitter, in excitotoxic conditions.

In this work we identified a new interactor of ATXN3, the chaperone HSP60. In cells, proteins are exposed to stress conditions that can ultimately lead to aberrant protein conformational changes, the molecular chaperones being responsible for their correct refolding [488,489]. If the proteins' native state is not reached, misfolded proteins are targeted for degradation [490,491]. The majority of these misfolded intracellular proteins are degraded via the Ubiquitin Proteasome System (UPS) [492]. Since mitochondria are involved in the respiratory process and thus subjected to high levels of reactive oxygen species, the macromolecules present in the mitochondria, namely proteins, are highly prone to be oxidized and suffer alterations in their structure. The role of HSP60 in mitochondrial protein quality control is thus very relevant, and together with mitochondrial HSP70 it is the main responsible for protein quality control in the mitochondrial matrix [493]. The presence of ATXN3 in the mitochondria has been previously described [494] and in our work we further characterize this co-localization. Deubiquitylases such as Ubiquitin Specific Peptidase 19 (USP19) and Ubiquitin Specific Peptidase 30 (USP30) have transmembrane domains [495,496] that allow their anchoring to the outer mitochondrial membrane; ATXN3 does not have this domain and thus the mechanism by which this protein is recruited to the mitochondria remains elusive. It is possible that ATXN3 is recruited to the mitochondria by its own substrates, or alternatively through the interaction with non-substrate proteins. In this perspective, a possibility is that the interaction with HSP60 is a way of recruiting and stabilizing ATXN3 to the mitochondria to exert specific deubiquitylating activity towards its substrates. This is compatible with our results, as we have demonstrated

that the interaction between the two proteins is direct (through ATXN3's Josephin domain) and not dependent on the interaction with other proteins. To confirm this possible mechanism, experiments in knockout HSP60 cell lines can be conducted, and if the hypothesis holds true one should expect in these cells an altered distribution pattern of ATXN3, thus not localizing to the mitochondrial membrane. The Josephin domain of ATXN3 is composed of a cysteine protease sequence, which is key for the ubiquitin protease activity [246,497,498]; besides, ATXN3 can also bind histones through the Josephin domain and thus regulate transcription [499]. The fact that interaction of HSP60 with ATXN3 takes place through this particular domain of ATXN3 suggests that HSP60 is in a position to modify the function/activity of the enzyme, or modulate the transcriptional repression exerted by ATXN3. We performed DUB activity tests in vitro (data not shown) for ATXN3 in the presence versus absence of HSP60 and did not find any differences in the cleavage of a His_6-Ubiquitin construct. These results are, however, not conclusive, since it would also need to be checked if the functional HSP60 chaperone, with its co-chaperone HSP10 associated, would have any effect on ATXN3's deubiquitylating activity.

Results from our group demonstrated that upon silencing of ATXN3 by shRNA SH-SY5Y neuroblastoma-derived cells had altered patterns of HSP60 ubiquitylation (data not shown). In this cell line HSP60 polyubiquiytlation is almost abrogated, which suggests that (directly or indirectly) ataxin-3 is contributing for the maintenance of HSP60 ubiquitylation. To clarify the functional meaning of this finding, future work must clarify if the levels of unbiquitylated HSP60 are also altered in ataxin-3 KO, to check if the effect of knocking down ataxin-3 results in the regulation of total levels of the protein, or specifically of the ubiquitylated levels of the enzyme. If the latter is true this could impact on subcellular distribution, interactions or activity of HSP60. It would also be very important to check in future experiments the effect of an expanded polyQ tract in ATXN3, namely the consequences in terms of the interaction with HSP60, protein cellular distribution and activity. This would help clarify the relevance of this interaction for the pathology in MJD.

Oxidative stress and inflammation are an hallmark of MJD [400–403,407,408], and prostaglandins (PGs) are known inducers of intracellular oxidative stress [387,388]. In our work we wanted to test the contribution of (15d-PGJ2) to the pathogenesis of MJD, also through the modulation of an UPS component, the deubiquitylating enzyme UCH-L1. Our results show that exposure to 15d-PGJ2 does not alter the pathology observed in our model *C. elegans* of MJD [11], as assessed by the animals' motility and aggregation of ATXN3. Treatment with 15d-PGJ2 was able to induce oxidative stress in *C. elegans* oxidative stress reporter strains, which indicates that this prostaglandin is able to modulate stress response in these animals. Previous work demonstrated that 15d-PGJ2 treatment increases intracellular ROS through the modification of

Thioredoxin 1 (Trx) enzyme, known to be protective against oxidative stress [390,391]. In *C. elegans trx-1* encodes a thioredoxin expressed in the ASJ head sensory neurons that modulates oxidative stress response [500,501], it was demonstrated that trx-1(jh127) worms, that lack TRX-1, are more sensitive to paraquat, a known inducer of oxidative stress, comparing with WT animals [501]. It will be important to determine if 15d-PGJ2 treatment increased oxidative stress in our reporter strains through this pathway, namely by assessing the possible modifications in the structure of TRX-1 imposed by PGs, since in mammalian cell lines, this was the mechanism through which PGs induce oxidative stress [388].

The fact that 15d-PGJ2 treatment had no effect on the behavioral and biochemical parameters we tested in the *C. elegans* MJD model might indicate that the oxidative stress induced in these animals was not significantly higher than the basal stress that occurs in these conditions. Although the role of 15d-PGJ2 as a mediator of inflammation and specifically as an inducer of oxidative stress in *C. elegans* has been described [501], the roles of PGs in cells remain still elusive and sometimes seem contradictory [387,502]. Indeed, it was suggested that 15d-PGJ2 might induce the expression glutathione S-transferases (GSTs) [503] known to be responsive to oxidative stress. To clarify the specific contribution of 15d-PGJ2 to the mechanisms of oxidative stress in *C. elegans* the expression of GSTs should also be taken into account.

Another UPS-related effect that 15d-PGJ2 is known to have is the modification of the conformation and stability of the deubiquitylating enzyme UCH-L1 [394,395]. The fact that UCH-L1 has been proven to be a modifier in neurodegenerative diseases prompted us to study its possible role as a modifier in MJD. UCH-L1 has a pivotal role in Parkinson Disease (PD), and in a German family with Parkinson's disease in which the I93M mutation in the enzyme was identified [191], diminished activity and alterations in secondary structure were suggested to be the cause of disease [376]. Also in Alzheimer´s Disease, UCH-L1 was able to restore correct synaptic transmission in an animal model of the disease [119], thus suggesting a fundamental role of the enzyme in the core of neuronal communication. We started by evaluating the effects of UBH-1 deletion on motility and ATX3 aggregation in our MJD model. We found that UBH-1 KO animals show no defect in these behavioral and biochemical evaluation paradigms. Besides, the double mutant containing expanded ATX3 and deletion of UBH-1 showed no differences in these parameters when compared with single mutant carrying ATXN3 mutation. The fact that we were not able to find any alteration in our MJD model upon UBH-1 (UCH-L1 *C. elegans* orthologue) deletion might be related with the fact that in worms UBH-1 shares high homology with UBH-3 (UCH-L3 in vertebrates) (www.wormbase.org), also observable in vertebrates where UCH-L1 shares 51% sequence identity with UCH-L3 [375,504]. This high degree of homology raises the possibility of some degree of redundancy between the enzymes. To clear the

possible compensating role of UBH-3 in the absence of UBH-1 in future work double mutants carrying both enzymes deleted should be crossed with our MJD *C. elegans* model and check for possible alterations in the pathology of the disease. The fact that UBH-1 *per se* does not have an effect in the pathology of the disease, lead us to question if the alterations described in vertebrates to lead to UCH-L1 modification upon 15d-PGJ2, namely the inactivation and aggregation of the enzyme, would also have an impact in WT or MJD worms but no effect was observed. In future work the impact that 15d-PGJ2 has on endogenous UBH-1 structure and function should be evaluated, to compare with the effects observed in vertebrates and evaluate the consequences in terms of MJD pathology.

One of the mechanisms that contributes to MJD pathology is calcium signaling deregulation [264,265]. Although our study was not performed specifically in the context of MJD, our results might be relevant for the understanding of the consequences of calcium deregulation in the context of the disease. A recent study undercovered a fundamental role of calcium activated protease calpain in MJD pathology. Previous reports have demonstrated that the calcium-activated protease calpain is involved in the cleavage ATXN3 [505-507]. In that study it was demonstrated that calpains cleave both WT and polyQ expanded forms of ATXN3 being the last more susceptible to this protease, and that knocking out the inhibitor of calpains – calpastatin – in a mouse ATXN3 mice model of the disease leads to accelerated neurodegeneration, increased number of ATXN3 positive nuclear inclusions and more severe phenotype [508].

We discovered that the enzyme responsible for the synthesis of the inhibitory neurotransmitter Gamma-Amino Butyric Acid (GABA) was cleaved under excitotoxic conditions and that this cleavage was prevented in the presence of proteasome inhibitors, thus pointing to a specific role of the UPS in calcium deregulation-induced proteolytic conditions. Cleavage of GADs results in decreased enzymatic activity and altered distribution pattern in the axons of hippocampal neurons. Previously, it had been described that this cleavage was sensitive to calpain [281–285] and cathepsin [284] inhibitors. We found that UPS and E1 ubiquitin ligase inhibitors completely abrogated the excitotoxic-induced cleavage of GADs, although no evidences were found that GADs are ubiquitylated. This results point to an indirect role of the UPS in GADs cleavage, suggesting that GADs might be regulated by the UPS through a signaling cascade or that a binding partner is regulated by the UPS thus affecting GADs stability.

In summary, this work gives a contribution to addressing the molecular mechanisms through which the UPS is involved in neuronal degeneration. The increasing knowledge of ATXN3 interactome through the identification of a new molecular partner is relevant, particularly knowing the relevance of the crosstalk between the molecular chaperones and UPS for

efficient maintenance of proteostasis. The contribution that other components of the UPS machinery have to MJD is rather relevant, and further studies can address the molecular mechanisms through which this DUB is not relevant for MJD pathology in *C. elegans*, namely which are the redundant or compensatory mechanisms involved. The finding that in calcium deregulation, specifically in excitotoxicity, the UPS regulates the cleavage of the enzyme responsible for the synthesis of the main inhibitory neurotransmitter demonstrates the importance of understanding how this ubiquitous machinery is regulated and how it can be modulated to help in the finding of new therapeutic approaches for neurological diseases as MJD.

Bibliography

1. Chen H, Polo S, Di Fiore PP, De Camilli PV. Rapid Ca2+-dependent decrease of protein ubiquitination at synapses. Proc Natl Acad Sci U S A. 100(25):14908-13 (2003)

2. Realini C, Rechsteiner M. A proteasome activator subunit binds calcium. J Biol Chem. 15;270(50):29664-7 (1995)

3. Santella L, Ercolano E, Nusco GA. The cell cycle: a new entry in the field of Ca2+ signaling. Cell Mol Life Sci. 62(21):2405-13 (2005)

4. Santella L, Kyozuka K, De Riso L, Carafoli E. Calcium, protease action, and the regulation of the cell cycle. Cell Calcium. 23(2-3):123-30 (1998)

5. Martin DL, Rimvall K. Regulation of gamma-aminobutyric acid synthesis in the brain. J Neurochem. 60(2):395-407 (1993)

6. Wilson PO, Barber PC, Hamid QA, Power BF, Dhillon AP, et al. The immunolocalization of protein gene product 9.5 using rabbit polyclonal and mouse monoclonal antibodies, Br J Exp Pathol. 69(1):91-104 (1988)

7. Wilkinson KD, Lee KM, Deshpande S, Duerksen-Hughes P, Boss JM, Pohl J. The neuron-specific protein PGP 9.5 is a ubiquitin carboxyl-terminal hydrolase. Science. 246(4930):670-3 (1989)

8. Osaka H, Wang YL, Takada K, Takizawa S, Setsuie R, et al. Ubiquitin carboxy-terminal hydrolase L1 binds to and stabilizes monoubiquitin in neuron. Hum Mol Genet. 12(16):1945-58 (2003)

9. Liu Y, Fallon L, Lashuel HA, Liu Z, Lansbury PT Jr. The UCH-L1 gene encodes two opposing enzymatic activities that affect alpha-synuclein degradation and Parkinson's disease susceptibility. Cell. 111(2):209-18 (2002)

10. Gong B, Vitolo OV, Trinchese F, Liu S, Shelanski M, Arancio O. Persistent improvement in synaptic and cognitive functions in an Alzheimer mouse model after rolipram treatment. J Clin Invest. 114(11):1624-34 (2004)

11. Teixeira-Castro A, Ailion M, Jalles A, Brignull HR, Vilaça JL, et al. Neuron-specific proteotoxicity of mutant ataxin-3 in C. elegans: rescue by the DAF-16 and HSF-1 pathways. Hum Mol Genet. 1;20(15):2996-3009 (2011)

12. Gallastegui N, Groll M. The 26S proteasome: assembly and function of a destructive machine. Trends Biochem Sci. 35(11):634-42 (2010)

13. Davy A, Bello P, Thierry-Mieg N, Vaglio P, Hitti J, et al. A protein-protein interaction map of the Caenorhabditis elegans 26S proteasome. EMBO Rep. 2(9):821-8 (2001)

14. Jin, J., Li, X., Gygi, S. P. & Harper, J. W. Dual E1 activation systems for ubiquitin differentially regulate E2 enzyme charging. Nature. 447, 1135–1138 (2007).

15. Schulman, B. A. & Harper, J. W. Ubiquitin-like protein activation by E1 enzymes: the apex for downstream signalling pathways. Nat Rev Mol Cell Biol. 10, 319–331 (2009).

16. Jones, D., Crowe, E., Stevens, T. A. & Candido, E. P. M. Functional and phylogenetic analysis of the ubiquitylation system in Caenorhabditis elegans: ubiquitin-conjugating enzymes, ubiquitin-activating enzymes, and ubiquitin-like proteins. Genome Biol. 3, RESEARCH0002 (2002).

17. Kulkarni, M. & Smith, H. E. E1 ubiquitin-activating enzyme UBA-1 plays multiple roles throughout C. elegans development. PLoS Genet. 4, e1000131 (2008).

18. Burroughs, A. M., Jaffee, M., Iyer, L. M. & Aravind, L. Anatomy of the E2 ligase fold: implications for enzymology and evolution of ubiquitin/Ub-like protein conjugation. J Struct Biol. 162, 205–218 (2008).

19. Michelle, C., Vourc'h, P., Mignon, L. & Andres, C. R. What was the set of ubiquitin and ubiquitin-like conjugating enzymes in the eukaryote common ancestor? J Mol Evol. 68, 616–628 (2009).

20. Schulze E, Altmann ME, Adham IM, Schulze B, Fröde S, Engel W. The maintenance of neuromuscular function requires UBC-25 in Caenorhabditis elegans. Biochem Biophys Res Commun. 305(3):691-9, (2003)

21. Li W, Bengtson MH, Ulbrich A, Matsuda A, Reddy VA, et al. Genome-wide and functional annotation of human E3 ubiquitin ligases identifies MULAN, a mitochondrial E3 that regulates the organelle's dynamics and signaling. PLoS ONE. 3, e1487 (2008).

22. Ponts N, Yang J, Chung DW, Prudhomme J, Girke T, et al. Deciphering the ubiquitin-mediated pathway in apicomplexan parasites: a potential strategy to interfere with parasite virulence. PLoS ONE. 3, e2386 (2008).

23. Kipreos, E. T. Ubiquitin-mediated pathways in C. elegans. WormBook. 1–24 (2005). doi:10.1895/wormbook.1.36.1

24. Pickart, C. M. & Eddins, M. J. Ubiquitin: structures, functions, mechanisms. Biochim Biophys Acta. 1695, 55–72 (2004).

25. Deshaies, R. J. & Joazeiro, C. A. P. RING domain E3 ubiquitin ligases. Annu Rev Biochem. 78, 399–434 (2009).

26. Koegl M, Hoppe T, Schlenker S, Ulrich HD, Mayer TU, Jentsch S. A novel ubiquitination factor, E4, is involved in multiubiquitin chain assembly. Cell. 96(5):635-44 (1999)

27. Hoppe T. Multiubiquitylation by E4 enzymes: 'one size' doesn't fit all. Trends Biochem Sci. 30(4):183-7 (2005)

28. Peng, J. et al. A proteomics approach to understanding protein ubiquitination. Nat Biotechnol. 21, 921–926 (2003).

29. Kuhlbrodt, K., Mouysset, J. & Hoppe, T. Orchestra for assembly and fate of polyubiquitin chains. Essays Biochem. 41, 1–14 (2005).

30. Sun, L. & Chen, Z. J. The novel functions of ubiquitination in signaling. Curr Opin Cell Biol. 16, 119–126 (2004).

31. Kodadek T. No Splicing, no dicing: non-proteolytic roles of the ubiquitin-proteasome system in transcription. J Biol Chem. 285(4):2221-6 (2010)

32. Todi SV, Scaglione KM, Blount JR, Basrur V, Conlon KP, et al. Activity and cellular functions of the deubiquitinating enzyme and polyglutamine disease protein ataxin-3 are regulated by ubiquitination at lysine 117. J Biol Chem. 285(50):39303-13 (2010)

33. Treier M, Staszewski LM, Bohmann D. Ubiquitin-dependent c-Jun degradation in vivo is mediated by the delta domain. Cell. 78(5):787-98 (1994)

34. Greer SF, Zika E, Conti B, Zhu XS, Ting JP. Enhancement of CIITA transcriptional function by ubiquitin. Nat Immunol. 4(11):1074-82 (2003)

35. Brès V, Kiernan RE, Linares LK, Chable-Bessia C, Plechakova O, et al. A non-proteolytic role for ubiquitin in Tat-mediated transactivation of the HIV-1 promoter. Nat Cell Biol. (2003)

36. Ferdous A, Sikder D, Gillette T, Nalley K, Kodadek T, Johnston SA. The role of the proteasomal ATPases and activator monoubiquitylation in regulating Gal4 binding to promoters. Genes Dev. 21(1):112-23 (2007)

37. Archer CT, Kodadek T. The hydrophobic patch of ubiquitin is required to protect transactivator-promoter complexes from destabilization by the proteasomal ATPases. Nucleic Acids Res. 38(3):789-96 (2010)

38. Xu P, Duong DM, Seyfried NT, Cheng D, Xie Y, Robert J, Rush J, Hochstrasser M, Finley D, Peng J. Quantitative proteomics reveals the function of unconventional ubiquitin chains in proteasomal degradation. Cell. 137(1):133-45 (2009)

39. Bedford L, Layfield R, Mayer RJ, Peng J, Xu P. Diverse polyubiquitin chains accumulate following 26S proteasomal dysfunction in mammalian neurones. Neurosci Lett. 491(1):44-7 (2011)

40. Saeki Y, Kudo T, Sone T, Kikuchi Y, Yokosawa H, Toh-e A, Tanaka K. Lysine 63-linked polyubiquitin chain may serve as a targeting signal for the 26S proteasome. EMBO J. 28(4):359-71 (2009)

41. Kim HT, Kim KP, Lledias F, Kisselev AF, Scaglione KM, et al. Certain pairs of ubiquitin-conjugating enzymes (E2s) and ubiquitin-protein ligases (E3s) synthesize nondegradable forked ubiquitin chains containing all possible isopeptide linkages. J Biol Chem. 282(24):17375-86 (2007)

42. Jacobson AD, Zhang NY, Xu P, Han KJ, Noone S, Peng J, Liu CW. The lysine 48 and lysine 63 ubiquitin conjugates are processed differently by the 26 s proteasome. J Biol Chem. 284(51):35485-94 (2009)

43. Al-Hakim AK, Zagorska A, Chapman L, Deak M, Peggie M, Alessi DR. Control of AMPK-related kinases by USP9X and atypical Lys(29)/Lys(33)-linked polyubiquitin chains. Biochem J. 411(2):249-60 (2008)

44. Goto E, Yamanaka Y, Ishikawa A, Aoki-Kawasumi M, Mito-Yoshida M, et al. Contribution of lysine 11-linked ubiquitination to MIR2-mediated major histocompatibility complex class I internalization. J Biol Chem. 285(46):35311-9 (2010)

45. Ikeda F, Dikic I. Atypical ubiquitin chains: new molecular signals. 'Protein Modifications: Beyond the Usual Suspects' review series. EMBO Rep. 9(6):536-42 (2008)

46. Pickart CM, Cohen RE. Proteasomes and their kin: proteases in the machine age. Nat Rev Mol Cell Biol. 5(3):177-87 (2004)

47. Reyes-Turcu FE, Ventii KH, Wilkinson KD. Regulation and cellular roles of ubiquitin-specific deubiquitinating enzymes. Annu Rev Biochem. 78:363-97 (2009)

48. Winborn BJ, Travis SM, Todi SV, Scaglione KM, Xu P, et al. The deubiquitinating enzyme ataxin-3, a polyglutamine disease protein, edits Lys63 linkages in mixed linkage ubiquitin chains. J Biol Chem. 283(39):26436-43 (2008)

49. Kuhlbrodt K, Janiesch PC, Kevei É, Segref A, Barikbin R, Hoppe T. The Machado-Joseph disease deubiquitylase ATX-3 couples longevity and proteostasis. Nat Cell Biol. 13(3):273-81 (2011)

50. Nijman, S. M. B. et al. A genomic and functional inventory of deubiquitinating enzymes. Cell. 123, 773–786 (2005).

51. Hershko, A. & Ciechanover, A. The ubiquitin system for protein degradation. Annu Rev Biochem. 61, 761–807 (1992).

52. Bhat KP, Greer SF. Proteolytic and non-proteolytic roles of ubiquitin and the ubiquitin proteasome system in transcriptional regulation. Biochim Biophys Acta. 1809(2):150-5 (2011)

53. Al-Hakim A, Escribano-Diaz C, Landry MC, O'Donnell L, Panier S, et al. The ubiquitous role of ubiquitin in the DNA damage response. DNA Repair (Amst). 9(12):1229-40 (2010)

54. Grillari J, Grillari-Voglauer R, Jansen-Dürr P. Post-translational modification of cellular proteins by ubiquitin and ubiquitin-like molecules: role in cellular senescence and aging. Adv Exp Med Biol. 694:172-96 (2010)

55. Bonifacino JS, Weissman AM. Ubiquitin and the control of protein fate in the secretory and endocytic pathways. Annu Rev Cell Dev Biol. 14:19-57 (1998)

56. Meller R. The role of the ubiquitin proteasome system in ischemia and ischemic tolerance. Neuroscientist. 15(3):243-60 (2009)

57. Shang F, Taylor A. Ubiquitin-proteasome pathway and cellular responses to oxidative stress. Free Radic Biol Med. 51(1):5-16 (2011)

58. Jia L, Bickel JS, Wu J, Morgan MA, Li H, et al. RBX1 (RING box protein 1) E3 ubiquitin ligase is required for genomic integrity by modulating DNA replication licensing proteins. J Biol Chem. 286(5):3379-86 (2011)

59. Wertz IE, Dixit VM. Signaling to NF-kappaB: regulation by ubiquitination. Cold Spring Harb Perspect Biol. 2(3):a003350 (2010)

60. Kawabe H, Brose N. The role of ubiquitylation in nerve cell development. Nat Rev Neurosci. 12(5):251-68 (2011)

61. Westbrook TF, Hu G, Ang XL, Mulligan P, Pavlova NN, et al. SCFbeta-TRCP controls oncogenic transformation and neural differentiation through REST degradation. Nature. 452(7185):370-4 (2008)

62. Tuoc TC, Stoykova A. Trim11 modulates the function of neurogenic transcription factor Pax6 through ubiquitin-proteosome system. Genes Dev. 22(14):1972-86 (2008)

63. Yoon KJ, Koo BK, Im SK, Jeong HW, Ghim J, et al. Mind bomb 1-expressing intermediate progenitors generate notch signaling to maintain radial glial cells. Neuron. 58(4):519-31 (2008)

64. Zhao X, D' Arca D, Lim WK, Brahmachary M, Carro MS, et al. The N-Myc-DLL3 cascade is suppressed by the ubiquitin ligase Huwe1 to inhibit proliferation and promote neurogenesis in the developing brain. Dev Cell. 17(2):210-21 (2009)

65. Sobieszczuk DF, Poliakov A, Xu Q, Wilkinson DG. A feedback loop mediated by degradation of an inhibitor is required to initiate neuronal differentiation. Genes Dev. 24(2):206-18 (2010)

66. Simó S, Jossin Y, Cooper JA. Cullin 5 regulates cortical layering by modulating the speed and duration of Dab1-dependent neuronal migration. J Neurosci. 30(16):5668-76 (2010)

67. Feng L, Allen NS, Simo S, Cooper JA. Cullin 5 regulates Dab1 protein levels and neuron positioning during cortical development. Genes Dev. 21(21):2717-30 (2007)

68. Bryan B, Cai Y, Wrighton K, Wu G, Feng XH, Liu M. Ubiquitination of RhoA by Smurf1 promotes neurite outgrowth. FEBS Lett. 579(5):1015-9 (2005)

69. Lasorella A, Stegmüller J, Guardavaccaro D, Liu G, Carro MS, et al. Degradation of Id2 by the anaphase-promoting complex couples cell cycle exit and axonal growth. Nature. 442(7101):471-4 (2006)

70. Stegmüller J, Konishi Y, Huynh MA, Yuan Z, Dibacco S, Bonni A. Cell-intrinsic regulation of axonal morphogenesis by the Cdh1-APC target SnoN. Neuron. 50(3):389-400 (2006)

71. Schwamborn, J. C., Müller, M., Becker, A. H. & Püschel, A. W. Ubiquitination of the GTPase Rap1B by the ubiquitin ligase Smurf2 is required for the establishment of neuronal polarity. EMBO J. 26, 1410–1422 (2007)

72. Kawabe H, Neeb A, Dimova K, Young SM Jr, Takeda M, et al. Regulation of Rap2A by the ubiquitin ligase Nedd4-1 controls neurite development. Neuron. 65(3):358-72 (2010)

73. Drinjakovic J, Jung H, Campbell DS, Strochlic L, Dwivedy A, Holt CE. E3 ligase Nedd4 promotes axon branching by downregulating PTEN. Neuron. 65(3):341-57 (2011)

74. Stegmüller J, Bonni A. Destroy to create: E3 ubiquitin ligases in neurogenesis. F1000 Biol Rep. 24;2. pii: 38 (2010)

75. Nakata, K. et al. Regulation of a DLK-1 and p38 MAP kinase pathway by the ubiquitin ligase RPM-1 is required for presynaptic development. Cell. 120, 407–420 (2005)

76. Kuo CT, Zhu S, Younger S, Jan LY, Jan YN. Identification of E2/E3 ubiquitinating enzymes and caspase activity regulating Drosophila sensory neuron dendrite pruning. Neuron. 51(3):283-90 (2006)

77. Ding M, Chao D, Wang G, Shen K. Spatial regulation of an E3 ubiquitin ligase directs selective synapse elimination. Science. 317(5840):947-51 (2007)

78. Chilton, J. K. Molecular mechanisms of axon guidance. Dev Biol. 292, 13–24 (2006)

79. Dickson, B. J. Molecular mechanisms of axon guidance. Science. 298, 1959–1964 (2002)

80. Garrity, P. A. & Zipursky, S. L. Neuronal target recognition. Cell. 83, 177–185 (1995)

81. Colamarino, S. A. & Tessier-Lavigne, M. The axonal chemoattractant netrin-1 is also a chemorepellent for trochlear motor axons. Cell. 81, 621–629 (1995).

82. Kobayashi, H., Koppel, A. M., Luo, Y. & Raper, J. A. A role for collapsin-1 in olfactory and cranial sensory axon guidance. J. Neurosci. 17, 8339–8352 (1997)

83. Pascual M, Pozas E, Barallobre MJ, Tessier-Lavigne M, Soriano E. Coordinated functions of Netrin-1 and Class 3 secreted Semaphorins in the guidance of reciprocal septohippocampal connections. Mol Cell Neurosci. 26(1):24-33 (2004)

84. Saito, S. Effects of lysophosphatidic acid on primary cultured chick neurons. Neurosci Lett. 229, 73–76 (1997)

85. Campbell, D. S. & Holt, C. E. Chemotropic responses of retinal growth cones mediated by rapid local protein synthesis and degradation. Neuron. 32, 1013–1026 (2001)

86. Shen, K. & Bargmann, C. I. The immunoglobulin superfamily protein SYG-1 determines the location of specific synapses in C. elegans. Cell. 112, 619–630 (2003)

87. Zhen, M., Huang, X., Bamber, B. & Jin, Y. Regulation of presynaptic terminal organization by C. elegans RPM-1, a putative guanine nucleotide exchanger with a RING-H2 finger domain. Neuron. 26, 331–343 (2000)

88. Schaefer, A. M., Hadwiger, G. D. & Nonet, M. L. rpm-1, a conserved neuronal gene that regulates targeting and synaptogenesis in C. elegans. Neuron. 26, 345–356 (2000)

89. Li, H., Kulkarni, G. & Wadsworth, W. G. RPM-1, a Caenorhabditis elegans protein that functions in presynaptic differentiation, negatively regulates axon outgrowth by controlling SAX-3/robo and UNC-5/UNC5 activity. J. Neurosci. 28, 3595–3603 (2008)

90. Grill B, Bienvenut WV, Brown HM, Ackley BD, Quadroni M, Jin Y. C. elegans RPM-1 regulates axon termination and synaptogenesis through the Rab GEF GLO-4 and the Rab GTPase GLO-1. Neuron. 16;55(4):587-601 (2007)

91. Liao EH, Hung W, Abrams B, Zhen M. An SCF-like ubiquitin ligase complex that controls presynaptic differentiation. Nature. 430(6997):345-50 (2004)

92. Ballas N, Grunseich C, Lu DD, Speh JC, Mandel G. REST and its corepressors mediate plasticity of neuronal gene chromatin throughout neurogenesis. Cell. 121(4):645-57 (2005)

93. Huang Z, Wu Q, Guryanova OA, Cheng L, Shou W, et al. Deubiquitylase HAUSP stabilizes REST and promotes maintenance of neural progenitor cells. Nat Cell Biol. 13(2):142-52 (2011)

94. Al-Shami A, Jhaver KG, Vogel P, Wilkins C, Humphries J, et al. Regulators of the proteasome pathway, Uch37 and Rpn13, play distinct roles in mouse development. PLoS One. 5(10):e13654 (2010)

95. McCullough J, Clague MJ, Urbé S. AMSH is an endosome-associated ubiquitin isopeptidase. J Cell Biol. 166(4):487-92 (2004)

96. Ishii N, Owada Y, Yamada M, Miura S, Murata K, et al. Loss of neurons in the hippocampus and cerebral cortex of AMSH-deficient mice. Mol Cell Biol. 21(24):8626-37 (2001)

97. Mabb AM, Ehlers MD. Ubiquitination in postsynaptic function and plasticity. Annu Rev Cell Dev Biol. 26:179-210 (2010)

98. Hegde AN, Goldberg AL, Schwartz JH. Regulatory subunits of cAMP-dependent protein kinases are degraded after conjugation to ubiquitin: a molecular mechanism underlying long-term synaptic plasticity. Proc Natl Acad Sci U S A. 90(16):7436-40 (1993)

99. Fioravante D, Liu RY, Byrne JH. The ubiquitin-proteasome system is necessary for long-term synaptic depression in Aplysia. J Neurosci. 28(41):10245-56 (2008)

100. Speese SD, Trotta N, Rodesch CK, Aravamudan B, Broadie K. The ubiquitin proteasome system acutely regulates presynaptic protein turnover and synaptic efficacy. Curr Biol. 13(11):899-910 (2003)

101. Wang Y, Okamoto M, Schmitz F, Hofmann K, Südhof TC. Rim is a putative Rab3 effector in regulating synaptic-vesicle fusion. Nature. 388(6642):593-8 (1997)

102. Sudhof TC. The synaptic vesicle cycle. Annu Rev Neurosci. 27:509-47 (2004)

103. Yao I, Takagi H, Ageta H, Kahyo T, Sato S, et al. SCRAPPER-dependent ubiquitination of active zone protein RIM1 regulates synaptic vesicle release. Cell. 130(5):943-57 (2007)

104. Yao I, Takao K, Miyakawa T, Ito S, Setou M. Synaptic E3 ligase SCRAPPER in contextual fear conditioning: extensive behavioral phenotyping of Scrapper heterozygote and overexpressing mutant mice. PLoS One. 6(2):e17317 (2011)

105. Peters JM. The anaphase-promoting complex: proteolysis in mitosis and beyond. Mol Cell. 9(5):931-43 (2002)

106. an Roessel P, Elliott DA, Robinson IM, Prokop A, Brand AH. Independent regulation of synaptic size and activity by the anaphase-promoting complex. Cell. 119(5):707-18 (2004)

107. Maricq AV, Peckol E, Driscoll M, Bargmann CI. Mechanosensory signalling in C. elegans mediated by the GLR-1 glutamate receptor. Nature. 378(6552):78-81 (1995)

108. Burbea M, Dreier L, Dittman JS, Grunwald ME, Kaplan JM. Ubiquitin and AP180 regulate the abundance of GLR-1 glutamate receptors at postsynaptic elements in C. elegans. Neuron. 35(1):107-20 (2002)

109. Schwarz, L. A., Hall, B. J. & Patrick, G. N. Activity-dependent ubiquitination of GluA1 mediates a distinct AMPA receptor endocytosis and sorting pathway. J. Neurosci 30, 16718–16729 (2010)

110. Schaefer H, Rongo C. KEL-8 is a substrate receptor for CUL3-dependent ubiquitin ligase that regulates synaptic glutamate receptor turnover. Mol Biol Cell. 17(3):1250-60 (2006)

111. Juo P, Kaplan JM. The anaphase-promoting complex regulates the abundance of GLR-1 glutamate receptors in the ventral nerve cord of C. elegans. Curr Biol. 14(22):2057-62 (2004)

112. Park EC, Glodowski DR, Rongo C. The ubiquitin ligase RPM-1 and the p38 MAPK PMK-3 regulate AMPA receptor trafficking. PLoS One. 4(1):e4284 (2009)

113. Dreier L, Burbea M, Kaplan JM. LIN-23-mediated degradation of beta-catenin regulates the abundance of GLR-1 glutamate receptors in the ventral nerve cord of C. elegans. Neuron. 46(1):51-64 (2005)

114. Kowalski JR, Dahlberg CL, Juo P. The deubiquitinating enzyme USP-46 negatively regulates the degradation of glutamate receptors to control their abundance in the ventral nerve cord of Caenorhabditis elegans. J Neurosci. 31(4):1341-54 (2011)

115. Kramer LB, Shim J, Previtera ML, Isack NR, Lee MC, et al. UEV-1 is an ubiquitin-conjugating enzyme variant that regulates glutamate receptor trafficking in C. elegans neurons. PLoS One. 5(12):e14291 (2010)

116. Larsen CN, Krantz BA, Wilkinson KD. Substrate specificity of deubiquitinating enzymes: ubiquitin C-terminal hydrolases. Biochemistry. 37(10):3358-68 (1998)

117. Hegde AN, Inokuchi K, Pei W, Casadio A, Ghirardi M, et al. Ubiquitin C-terminal hydrolase is an immediate-early gene essential for long-term facilitation in Aplysia. Cell. 89(1):115-26 (1997)

118. Chain DG, Hegde AN, Yamamoto N, Liu-Marsh B, Schwartz JH. Persistent activation of cAMP-dependent protein kinase by regulated proteolysis suggests a neuron-specific function of the ubiquitin system in Aplysia. J Neurosci. 15(11):7592-603 (1995)

119. Gong B, Cao Z, Zheng P, Vitolo OV, Liu S, et al. Ubiquitin hydrolase Uch-L1 rescues beta-amyloid-induced decreases in synaptic function and contextual memory. Cell. 126(4):775-88 (2006)

120. Dindot SV, Antalffy BA, Bhattacharjee MB, Beaudet AL. The Angelman syndrome ubiquitin ligase localizes to the synapse and nucleus, and maternal deficiency results in abnormal dendritic spine morphology. Hum Mol Genet. 17(1):111-8 (2008)

121. Greer PL, Hanayama R, Bloodgood BL, Mardinly AR, Lipton DM, et al. The Angelman Syndrome protein Ube3A regulates synapse development by ubiquitinating arc. Cell. 140(5):704-16 (2010)

122. Kim J, Guermah M, McGinty RK, Lee JS, Tang Z, et al. Cell. 137(3):459-71 (2009)

123. Lu Z, Je HS, Young P, Gross J, Lu B, Feng G. Regulation of synaptic growth and maturation by a synapse-associated E3 ubiquitin ligase at the neuromuscular junction. J Cell Biol. 177(6):1077-89 (2007)

124. Colledge M, Snyder EM, Crozier RA, Soderling JA, Jin Y, et al. Ubiquitination regulates PSD-95 degradation and AMPA receptor surface expression. Neuron. 40(3):595-607 (2003)

125. Nelson RF, Glenn KA, Miller VM, Wen H, Paulson HL. A novel route for F-box protein-mediated ubiquitination links CHIP to glycoprotein quality control. J Biol Chem. 281(29):20242-51 (2006)

126. Jurd R, Thornton C, Wang J, Luong K, Phamluong K, et al. Mind bomb-2 is an E3 ligase that ubiquitinates the N-methyl-D-aspartate receptor NR2B subunit in a phosphorylation-dependent manner. J Biol Chem. 283(1):301-10 (2008)

127. Hung AY, Sung CC, Brito IL, Sheng M. Degradation of postsynaptic scaffold GKAP and regulation of dendritic spine morphology by the TRIM3 ubiquitin ligase in rat hippocampal neurons. PLoS One. 5(3):e9842 (2010)

128. Ciechanover A, Brundin P. The ubiquitin proteasome system in neurodegenerative diseases: sometimes the chicken, sometimes the egg. Neuron. 40(2):427-46(2003)

129. Hegde AN, Upadhya SC. Role of ubiquitin-proteasome-mediated proteolysis in nervous system disease. Biochim Biophys Acta. 1809(2):128-40 (2011)

130. Ehninger D, Li W, Fox K, Stryker MP, Silva AJ. Reversing neurodevelopmental disorders in adults. Neuron. 60(6):950-60 (2008)

131. Kishino T, Lalande M, Wagstaff J. UBE3A/E6-AP mutations cause Angelman syndrome. Nat Genet. 15(1):70-3 (1997)

132. Bramham CR, Alme MN, Bittins M, Kuipers SD, Nair RR, et al. The Arc of synaptic memory. Exp Brain Res. 200(2):125-40 (2010)

133. Clayton-Smith J, Laan L. Angelman syndrome: a review of the clinical and genetic aspects. J Med Genet. 40(2):87-95 (2003)

134. Sato M, Stryker MP. Genomic imprinting of experience-dependent cortical plasticity by the ubiquitin ligase gene Ube3a. Proc Natl Acad Sci U S A. 107(12):5611-6 (2010)

135. Mardirossian S, Rampon C, Salvert D, Fort P, Sarda N. Impaired hippocampal plasticity and altered neurogenesis in adult Ube3a maternal deficient mouse model for Angelman syndrome. Exp Neurol. 220(2):341-8 (2009)

136. Mulherkar SA, Jana NR. Loss of dopaminergic neurons and resulting behavioural deficits in mouse model of Angelman syndrome. Neurobiol Dis. 40(3):586-92 (2010)

137. Jiang YH, Pan Y, Zhu L, Landa L, Yoo J, et al. Altered ultrasonic vocalization and impaired learning and memory in Angelman syndrome mouse model with a large maternal deletion from Ube3a to Gabrb3. PLoS One. 5(8):e12278 (2010)

138. Nascimento RM, Otto PA, de Brouwer AP, Vianna-Morgante AM. UBE2A, which encodes a ubiquitin-conjugating enzyme, is mutated in a novel X-linked mental retardation syndrome. Am J Hum Genet. 79(3):549-55 (2006)

139. Honda S, Orii KO, Kobayashi J, Hayashi S, Imamura A, et al. Novel deletion at Xq24 including the UBE2A gene in a patient with X-linked mental retardation. J Hum Genet. 55(4):244-7 (2010)

140. Budny B, Badura-Stronka M, Materna-Kiryluk A, Tzschach A, Raynaud M, et al. Novel missense mutations in the ubiquitination-related gene UBE2A cause a recognizable X-linked mental retardation syndrome. Clin Genet. 77(6):541-51 (2010)

141. de Leeuw N, Bulk S, Green A, Jaeckle-Santos L, Baker LA, et al. UBE2A deficiency syndrome: Mild to severe intellectual disability accompanied by seizures, absent speech, urogenital, and skin anomalies in male patients. Am J Med Genet A. 152A(12):3084-90 (2010)

142. Kumar B, Lecompte KG, Klein JM, Haas AL. Ser(120) of Ubc2/Rad6 regulates ubiquitin-dependent N-end rule targeting by E3{alpha}/Ubr1. J Biol Chem. 285(53):41300-9 (2010)

143. Obin M, Mesco E, Gong X, Haas AL, Joseph J, Taylor A. Neurite outgrowth in PC12 cells. Distinguishing the roles of ubiquitylation and ubiquitin-dependent proteolysis. J Biol Chem. 274(17):11789-95 (1999)

144. Kavakebi P, Hausott B, Tomasino A, Ingorokva S, Klimaschewski L. The N-end rule ubiquitin-conjugating enzyme, HR6B, is up-regulated by nerve growth factor and required for neurite outgrowth. Mol Cell Neurosci. 29(4):559-68 (2005)

145. Mulugeta Achame E, Wassenaar E, Hoogerbrugge JW, Sleddens-Linkels E, Ooms M, et al. The ubiquitin-conjugating enzyme HR6B is required for maintenance of X chromosome silencing in mouse spermatocytes and spermatids. BMC Genomics. 11:367 (2010)

146. Park CC, Gale GD, de Jong S, Ghazalpour A, Bennett BJ, et al. Gene networks associated with conditional fear in mice identified using a systems genetics approach. BMC Syst Biol. 5:43 (2011)

147. Hwang CS, Shemorry A, Auerbach D, Varshavsky A. The N-end rule pathway is mediated by a complex of the RING-type Ubr1 and HECT-type Ufd4 ubiquitin ligases. Nat Cell Biol. 12(12):1177-85 (2010)

148. Elting M, Kariminejad A, de Sonnaville ML, Ottenkamp J, Bauhuber S, et al. Johanson-Blizzard syndrome caused by identical UBR1 mutations in two unrelated girls, one with a cardiomyopathy. Am J Med Genet A. 146A(23):3058-61 (2008)

149. Alkhouri N, Kaplan B, Kay M, Shealy A, Crowe C, et al. Johanson-Blizzard syndrome with mild phenotypic features confirmed by UBR1 gene testing. World J Gastroenterol. 14(44):6863-6 (2008)

150. Zenker M, Mayerle J, Lerch MM, Tagariello A, Zerres K, et al. Deficiency of UBR1, a ubiquitin ligase of the N-end rule pathway, causes pancreatic dysfunction, malformations and mental retardation (Johanson-Blizzard syndrome). Nat Genet. 37(12):1345-50 (2005)

151. Fallahi GH, Sabbaghian M, Khalili M, Parvaneh N, Zenker M, Rezaei N. Novel UBR1 gene mutation in a patient with typical phenotype of Johanson-Blizzard syndrome. Eur J Pediatr. 170(2):233-5 (2011)

152. Eisele F, Wolf DH. Degradation of misfolded protein in the cytoplasm is mediated by the ubiquitin ligase Ubr1. FEBS Lett. 582(30):4143-6 (2008)

153. Nillegoda NB, Theodoraki MA, Mandal AK, Mayo KJ, Ren HY, et al. Ubr1 and Ubr2 function in a quality control pathway for degradation of unfolded cytosolic proteins. Mol Biol Cell. 21(13):2102-16 (2010)

154. Heck JW, Cheung SK, Hampton RY. Cytoplasmic protein quality control degradation mediated by parallel actions of the E3 ubiquitin ligases Ubr1 and San1. Proc Natl Acad Sci U S A. 107(3):1106-11(2010)

155. Kume K, Iizumi Y, Shimada M, Ito Y, Kishi T, et al. Role of N-end rule ubiquitin ligases UBR1 and UBR2 in regulating the leucine-mTOR signaling pathway. Genes Cells. 15(4):339-49 (2010)

156. An JY, Seo JW, Tasaki T, Lee MJ, Varshavsky A, Kwon YT. Impaired neurogenesis and cardiovascular development in mice lacking the E3 ubiquitin ligases UBR1 and UBR2 of the N-end rule pathway. Proc Natl Acad Sci U S A. 103(16):6212-7 (2006)

157. Tarpey PS, Raymond FL, O'Meara S, Edkins S, Teague J, et al. Mutations in CUL4B, which encodes a ubiquitin E3 ligase subunit, cause an X-linked mental retardation syndrome associated with aggressive outbursts, seizures, relative macrocephaly, central obesity, hypogonadism, pes cavus, and tremor. Am J Hum Genet. 80(2):345-52 (2007)

158. Lee J, Zhou P. DCAFs, the missing link of the CUL4-DDB1 ubiquitin ligase. Mol Cell. 26(6):775-80 (2007)

159. Higa LA, Zhang H. Stealing the spotlight: CUL4-DDB1 ubiquitin ligase docks WD40-repeat proteins to destroy. Cell Div. 2:5 (2007)

160. Miranda-Carboni GA, Krum SA, Yee K, Nava M, Deng QE, et al. A functional link between Wnt signaling and SKP2-independent p27 turnover in mammary tumors. Genes Dev. 22(22):3121-34 (2008)

161. Kerzendorfer C, Whibley A, Carpenter G, Outwin E, Chiang SC, et al. Mutations in Cullin 4B result in a human syndrome associated with increased camptothecin-induced topoisomerase I-dependent DNA breaks. Hum Mol Genet. 19(7):1324-34 (2010)

162. Francke U. Williams-Beuren syndrome: genes and mechanisms. Hum Mol Genet. 8(10):1947-54 (1999)

163. Micale L, Fusco C, Augello B, Napolitano LM, Dermitzakis ET, Meroni G, Merla G, Reymond A. Williams-Beuren syndrome TRIM50 encodes an E3 ubiquitin ligase. Eur J Hum Genet. 16(9):1038-49 (2008)

164. Froyen G, Corbett M, Vandewalle J, Jarvela I, Lawrence O, et al. Submicroscopic duplications of the hydroxysteroid dehydrogenase HSD17B10 and the E3 ubiquitin ligase HUWE1 are associated with mental retardation. Am J Hum Genet. 82(2):432-43 (2008)

165. Besche HC, Haas W, Gygi SP, Goldberg AL. Isolation of mammalian 26S proteasomes and p97/VCP complexes using the ubiquitin-like domain from HHR23B reveals novel proteasome-associated proteins. Biochemistry. 48(11):2538-49 (2009)

166. Tai HC, Besche H, Goldberg AL, Schuman EM. Characterization of the Brain 26S Proteasome and its Interacting Proteins. Front Mol Neurosci. 3. pii: 12 (2010)

167. Liu Z, Oughtred R, Wing SS. Characterization of E3Histone, a novel testis ubiquitin protein ligase which ubiquitinates histones. Mol Cell Biol. 25(7):2819-31 (2005)

168. Gu J, Ren K, Dubner R, Iadarola MJ. Cloning of a DNA binding protein that is a tyrosine kinase substrate and recognizes an upstream initiator-like sequence in the promoter of the preprodynorphin gene. Brain Res Mol Brain Res. 24(1-4):77-88 (1994)

169. Hall JR, Kow E, Nevis KR, Lu CK, Luce KS, et al. Cdc6 stability is regulated by the Huwe1 ubiquitin ligase after DNA damage. Mol Biol Cell. 18(9):3340-50 (2007)

170. Zhong Q, Gao W, Du F, Wang X. Mule/ARF-BP1, a BH3-only E3 ubiquitin ligase, catalyzes the polyubiquitination of Mcl-1 and regulates apoptosis. Cell. 121(7):1085-95 (2005)

171. Stankiewicz AR, Livingstone AM, Mohseni N, Mosser DD. Regulation of heat-induced apoptosis by Mcl-1 degradation and its inhibition by Hsp70. Cell Death Differ. 16(4):638-47 (2009)

172. Zhao X, Heng JI, Guardavaccaro D, Jiang R, Pagano M, et al. The HECT-domain ubiquitin ligase Huwe1 controls neural differentiation and proliferation by destabilizing the N-Myc oncoprotein. Nat Cell Biol. 10(6):643-53 (2008)

173. D'Arca D, Zhao X, Xu W, Ramirez-Martinez NC, Iavarone A, Lasorella A. Huwe1 ubiquitin ligase is essential to synchronize neuronal and glial differentiation in the developing cerebellum. Proc Natl Acad Sci U S A. 107(13):5875-80 (2010)

174. Glessner JT, Wang K, Cai G, Korvatska O, Kim CE, et al. Autism genome-wide copy number variation reveals ubiquitin and neuronal genes. Nature. 459(7246):569-73 (2009)

175. Marshall CR, Noor A, Vincent JB, Lionel AC, Feuk L, et al. Structural variation of chromosomes in autism spectrum disorder. Am J Hum Genet. 82(2):477-88 (2008)

176. McInnes LA, Nakamine A, Pilorge M, Brandt T, Jiménez González P, et al. A large-scale survey of the novel 15q24 microdeletion syndrome in autism spectrum disorders identifies an atypical deletion that narrows the critical region. Mol Autism. 1(1):5 (2010)

177. Cukier HN, Salyakina D, Blankstein SF, Robinson JL, Sacharow S, et al. Microduplications in an autism multiplex family narrow the region of susceptibility for developmental disorders on 15q24 and implicate 7p21 Am J Med Genet B Neuropsychiatr Genet. 156B(4):493-501 (2011)

178. Seo H, Isacson O. The hAPP-YAC transgenic model has elevated UPS activity in the frontal cortex similar to Alzheimer's disease and Down's syndrome. J Neurochem. 114(6):1819-26 (2010)

179. Berto G, Camera P, Fusco C, Imarisio S, Ambrogio C, et al. The Down syndrome critical region protein TTC3 inhibits neuronal differentiation via RhoA and Citron kinase. J Cell Sci. 120(Pt 11):1859-67 (2007)

180. Valero R, Bayés M, Francisca Sánchez-Font M, González-Angulo O, Gonzàlez-Duarte R, Marfany G. Characterization of alternatively spliced products and tissue-specific isoforms of USP28 and USP25. Genome Biol. 2(10):RESEARCH0043 (2001)

181. Nalepa G, Rolfe M, Harper JW. Drug discovery in the ubiquitin-proteasome system. Nat Rev Drug Discov. 5(7):596-613 (2006)

182. Hol EM, Fischer DF, Ovaa H, Scheper W. Ubiquitin proteasome system as a pharmacological target in neurodegeneration. Expert Rev Neurother. 6(9):1337-47 (2006)

183. Bedford L, Lowe J, Dick LR, Mayer RJ, Brownell JE. Ubiquitin-like protein conjugation and the ubiquitin-proteasome system as drug targets. Nat Rev Drug Discov. 10(1):29-46 (2011)

184. Edelmann MJ, Nicholson B, Kessler BM. Pharmacological targets in the ubiquitin system offer new ways of treating cancer, neurodegenerative disorders and infectious diseases. Expert Rev Mol Med. 13:e35 (2011)

185. Driscoll JJ, Dechowdhury R. Therapeutically targeting the SUMOylation, Ubiquitination and Proteasome pathways as a novel anticancer strategy. Target Oncol. 5(4):281-9 (2010)

186. Jia L, Sun Y. SCF E3 ubiquitin ligases as anticancer targets. Curr Cancer Drug Targets. 11(3):347-56 (2011)

187. Maeda I, Kohara Y, Yamamoto M, Sugimoto A. Large-scale analysis of gene function in Caenorhabditis elegans by high-throughput RNAi. Curr Biol. 11(3):171-6 (2001)

188. Zhong W, Feng H, Santiago FE, Kipreos ET. CUL-4 ubiquitin ligase maintains genome stability by restraining DNA-replication licensing. Nature. 423(6942):885-9 (2003)

189. Springer W, Hoppe T, Schmidt E, Baumeister R. A Caenorhabditis elegans Parkin mutant with altered solubility couples alpha-synuclein aggregation to proteotoxic stress. Hum Mol Genet. 14(22):3407-23 (2005)

190. Kitada T, Asakawa S, Hattori N, Matsumine H, Yamamura Y, et al. Mutations in the parkin gene cause autosomal recessive juvenile parkinsonism. Nature. 392(6676):605-8 (1998)

191. Leroy E, Boyer R, Auburger G, Leube B, Ulm G, et al. The ubiquitin pathway in Parkinson's disease. Nature. 395(6701):451-2 (1998)

192. Harrington AJ, Hamamichi S, Caldwell GA, Caldwell KA. C. elegans as a model organism to investigate molecular pathways involved with Parkinson's disease. Dev Dyn. 239(5):1282-95 (2010)

193. Ha MK, Soo Cho J, Baik OR, Lee KH, Koo HS, Chung KY. Caenorhabditis elegans as a screening tool for the endothelial cell-derived putative aging-related proteins detected by proteomic analysis. Proteomics. 6(11):3339-51 (2006)

194. Cornejo Castro EM, Waak J, Weber SS, Fiesel FC, Oberhettinger P, et al. Parkinson's disease-associated DJ-1 modulates innate immunity signaling in Caenorhabditis elegans. J Neural Transm. 117(5):599-604 (2010)

195. Gitler AD, Chesi A, Geddie ML, Strathearn KE, Hamamichi S, et al. Alpha-synuclein is part of a diverse and highly conserved interaction network that includes PARK9 and manganese toxicity. Nat Genet. 41(3):308-15 (2009)

196. Kawaguchi Y, Okamoto T, Taniwaki M, Aizawa M, Inoue M, et al. CAG expansions in a novel gene for Machado-Joseph disease at chromosome 14q32.1. Nat Genet. 8(3):221-8

197. Rodrigues AJ, Coppola G, Santos C, Costa Mdo C, Ailion M, et al. Functional genomics and biochemical characterization of the C. elegans orthologue of the Machado-Joseph disease protein ataxin-3. FASEB J. 21(4):1126-36 (2007)

198. Lappe-Siefke C, Loebrich S, Hevers W, Waidmann OB, Schweizer M, et al. The ataxia (axJ) mutation causes abnormal GABAA receptor turnover in mice. PLoS Genet. 5(9):e1000631 (2009)

199. Dohm CP, Kermer P, Bähr M. Aggregopathy in neurodegenerative diseases: mechanisms and therapeutic implication. Neurodegener Dis. 5(6):321-38 (2008)

200. Taylor JP, Hardy J, Fischbeck KH. Toxic proteins in neurodegenerative disease. Science. 296(5575):1991-5 (2002)

201. Fink AL. The aggregation and fibrillation of alpha-synuclein. Acc Chem Res. 39(9):628-34 (2006)

202. Bruijn LI, Becher MW, Lee MK, Anderson KL, Jenkins NA, et al. ALS-linked SOD1 mutant G85R mediates damage to astrocytes and promotes rapidly progressive disease with SOD1-containing inclusions. Neuron. 18(2):327-38 (1997)

203. Chen S, Ferrone FA, Wetzel R. Huntington's disease age-of-onset linked to polyglutamine aggregation nucleation. Proc Natl Acad Sci U S A. 99(18):11884-9 (2002)

204. Thorpe JR, Tang H, Atherton J, Cairns NJ. Fine structural analysis of the neuronal inclusions of frontotemporal lobar degeneration with TDP-43 proteinopathy. J Neural Transm. 115(12):1661-71 (2008)

205. Mayer RJ, Lowe J, Lennox G, Doherty F, Landon M. Intermediate filaments and ubiquitin: a new thread in the understanding of chronic neurodegenerative diseases. Prog Clin Biol Res. 317:809-18 (1989)

206. Lowe J, Blanchard A, Morrell K, Lennox G, Reynolds L, et al. Ubiquitin is a common factor in intermediate filament inclusion bodies of diverse type in man, including those of Parkinson's disease, Pick's disease, and Alzheimer's disease, as well as Rosenthal fibres in cerebellar astrocytomas, cytoplasmic bodies in muscle, and mallory bodies in alcoholic liver disease. J Pathol. 155(1):9-15 (1988)

207. Layfield R, Cavey JR, Lowe J. Role of ubiquitin-mediated proteolysis in the pathogenesis of neurodegenerative disorders. Ageing Res Rev. 2(4):343-56 (2003)

208. Bennett EJ, Bence NF, Jayakumar R, Kopito RR. Global impairment of the ubiquitin-proteasome system by nuclear or cytoplasmic protein aggregates precedes inclusion body formation. Mol Cell. 17(3):351-65 (2005)

209. Bence NF, Sampat RM, Kopito RR. Impairment of the ubiquitin-proteasome system by protein aggregation. Science. 292(5521):1552-5 (2001)

210. David DC, Ollikainen N, Trinidad JC, Cary MP, Burlingame AL, Kenyon C. Widespread protein aggregation as an inherent part of aging in C. elegans. PLoS Biol. 8(8):e1000450 (2010)

211. Keller JN, Dimayuga E, Chen Q, Thorpe J, Gee J, Ding Q. Autophagy, proteasomes, lipofuscin, and oxidative stress in the aging brain. Int J Biochem Cell Biol. 36(12):2376-91 (2004)

212. Ferrington DA, Husom AD, Thompson LV. Altered proteasome structure, function, and oxidation in aged muscle. FASEB J. 19(6):644-6 (2005)

213. Gavilán MP, Castaño A, Torres M, Portavella M, Caballero C, et al. Age-related increase in the immunoproteasome content in rat hippocampus: molecular and functional aspects. J Neurochem. 108(1):260-72 (2009)

214. Williams AJ, Paulson HL. Polyglutamine neurodegeneration: protein misfolding revisited. Trends Neurosci. 31(10):521-8 (2008)

215. Jana NR, Nukina N. Recent advances in understanding the pathogenesis of polyglutamine diseases: involvement of molecular chaperones and ubiquitin-proteasome pathway. J Chem Neuroanat. 26(2):95-101 (2003)

216. Gatchel JR, Zoghbi HY. Diseases of unstable repeat expansion: mechanisms and common principles. Nat Rev Genet. 6(10):743-55 (2005)

217. Ortega Z, Díaz-Hernández M, Maynard CJ, Hernández F, Dantuma NP, Lucas JJ. Acute polyglutamine expression in inducible mouse model unravels ubiquitin/proteasome system impairment and permanent recovery attributable to aggregate formation. J Neurosci. 30(10):3675-88 (2010)

218. DiFiglia M, Sapp E, Chase KO, Davies SW, Bates GP, et al. Aggregation of huntingtin in neuronal intranuclear inclusions and dystrophic neurites in brain. Science. 277(5334):1990-3 (1997)

219. Paulson HL. Protein fate in neurodegenerative proteinopathies: polyglutamine diseases join the (mis)fold. Am J Hum Genet. 64(2):339-45 (1999)

220. Zhou H, Cao F, Wang Z, Yu ZX, Nguyen HP, et al. Huntingtin forms toxic NH2-terminal fragment complexes that are promoted by the age-dependent decrease in proteasome activity. J Cell Biol. 163(1):109-18 (2003)

221. Li X, Wang CE, Huang S, Xu X, Li XJ, et al. Inhibiting the ubiquitin-proteasome system leads to preferential accumulation of toxic N-terminal mutant huntingtin fragments. Hum Mol Genet. 19(12):2445-55 (2010)

222. Maynard CJ, Böttcher C, Ortega Z, Smith R, Florea BI, et al. Accumulation of ubiquitin conjugates in a polyglutamine disease model occurs without global ubiquitin/proteasome system impairment. Proc Natl Acad Sci U S A. 106(33):13986-91 (2009)

223. Mitra S, Tsvetkov AS, Finkbeiner S. Single neuron ubiquitin-proteasome dynamics accompanying inclusion body formation in huntington disease. J Biol Chem. 284(7):4398-403 (2009)

224. Godin JD, Poizat G, Hickey MA, Maschat F, Humbert S. Mutant huntingtin-impaired degradation of beta-catenin causes neurotoxicity in Huntington's disease. EMBO J. 29(14):2433-45 (2010)

225. Anderson C, Crimmins S, Wilson JA, Korbel GA, Ploegh HL, Wilson SM. Loss of Usp14 results in reduced levels of ubiquitin in ataxia mice J Neurochem. 95(3):724-31 (2005)

226. Wilson SM, Bhattacharyya B, Rachel RA, Coppola V, Tessarollo L, et al. Synaptic defects in ataxia mice result from a mutation in Usp14, encoding a ubiquitin-specific protease. Nat Genet. 32(3):420-5 (2002) Transgenic rescue of ataxia mice with neuronal-specific expression of ubiquitin-specific protease 14. J Neurosci. 32(3):420-5 (2002)

227. Crimmins S, Jin Y, Wheeler C, Huffman AK, Chapman C, et al. Transgenic rescue of ataxia mice with neuronal-specific expression of ubiquitin-specific protease 14. J Neurosci. 26(44):11423-31 (2006)

228. Lee BH, Lee MJ, Park S, Oh DC, Elsasser S, et al. Enhancement of proteasome activity by a small-molecule inhibitor of USP14. Nature. 467(7312):179-84 (2010)

229. Hardy J, Selkoe DJ. The amyloid hypothesis of Alzheimer's disease: progress and problems on the road to therapeutics. Science. 297(5580):353-6 (2002)

230. van Leeuwen FW, de Kleijn DP, van den Hurk HH, Neubauer A, Sonnemans MA, et al. Frameshift mutants of beta amyloid precursor protein and ubiquitin-B in Alzheimer's and Down patients. Science. 279(5348):242-7 (1998)

231. Tan Z, Sun X, Hou FS, Oh HW, Hilgenberg LG, et al. Mutant ubiquitin found in Alzheimer's disease causes neuritic beading of mitochondria in association with neuronal degeneration. Cell Death Differ. 14(10):1721-32 (2007)

232. Berke SJ, Chai Y, Marrs GL, Wen H, Paulson HL. Defining the role of ubiquitin-interacting motifs in the polyglutamine disease protein, ataxin-3. J Biol Chem. 280(36):32026-34 (2005)

233. Nijman, S. M. B. et al. A genomic and functional inventory of deubiquitinating enzymes. Cell 123, 773–786 (2005).

234. Ouyang H, Ali YO, Ravichandran M, Dong A, Qiu W, et al. Protein aggregates are recruited to aggresome by histone deacetylase 6 via unanchored ubiquitin C termini. Biol Chem. 287(4):2317-27 (2012)

235. Burnett BG, Pittman RN. The polyglutamine neurodegenerative protein ataxin 3 regulates aggresome formation. Proc Natl Acad Sci U S A. 102(12):4330-5 (2005)

236. Durcan TM, Kontogiannea M, Bedard N, Wing SS, Fon EA. Ataxin-3 deubiquitination is coupled to Parkin ubiquitination via E2 ubiquitin-conjugating enzyme. J Biol Chem. 287(1):531-41 (2012)

237. Scaglione KM, Zavodszky E, Todi SV, Patury S, Xu P, et al. Ube2w and ataxin-3 coordinately regulate the ubiquitin ligase CHIP. Mol Cell. 43(4):599-612 (2011)

238. Rodrigues AJ, Neves-Carvalho A, Teixeira-Castro A, Rokka A, Corthals G, et al. Absence of ataxin-3 leads to enhanced stress response in C. elegans. PLoS One. 6(4):e18512 (2011)

239. Schmitt I, Linden M, Khazneh H, Evert BO, Breuer P, et al. Inactivation of the mouse Atxn3 (ataxin-3) gene increases protein ubiquitination. Biochem Biophys Res Commun. 362(3):734-9 (2007)

240. do Carmo Costa M, Bajanca F, Rodrigues AJ, Tomé RJ, Corthals G, et al. Ataxin-3 plays a role in mouse myogenic differentiation through regulation of integrin subunit levels. PLoS One. 5(7):e11728 (2010)

241. Durcan TM, Kontogiannea M, Thorarinsdottir T, Fallon L, Williams AJ, et al. The Machado-Joseph disease-associated mutant form of ataxin-3 regulates parkin ubiquitination and stability. Hum Mol Genet. 20(1):141-54 (2011)

242. Burnett B, Li F, Pittman RN. The polyglutamine neurodegenerative protein ataxin-3 binds polyubiquitylated proteins and has ubiquitin protease activity. Hum Mol Genet. 12(23):3195-205 (2003)

243. Chow MK, Mackay JP, Whisstock JC, Scanlon MJ, Bottomley SP. Structural and functional analysis of the Josephin domain of the polyglutamine protein ataxin-3. Biochem Biophys Res Commun. 322(2):387-94 (2004)

244. Ferro A, Carvalho AL, Teixeira-Castro A, Almeida C, Tomé RJ, et al. NEDD8: a new ataxin-3 interactor. Biochim Biophys Acta. 1773(11):1619-27 (2007)

245. Hirabayashi M, Inoue K, Tanaka K, Nakadate K, Ohsawa Y, et al. VCP/p97 in abnormal protein aggregates, cytoplasmic vacuoles, and cell death, phenotypes relevant to neurodegeneration. Cell Death Differ. 8(10):977-84 (2001)

246. Doss-Pepe EW, Stenroos ES, Johnson WG, Madura K. Ataxin-3 interactions with rad23 and valosin-containing protein and its associations with ubiquitin chains and the proteasome are consistent with a role in ubiquitin-mediated proteolysis. Mol Cell Biol. 23(18):6469-83 (2003)

247. Wang G, Sawai N, Kotliarova S, Kanazawa I, Nukina N. Ataxin-3, the MJD1 gene product, interacts with the two human homologs of yeast DNA repair protein RAD23, HHR23A and HHR23B. Hum Mol Genet. 9(12):1795-803 (2000)

248. Doss-Pepe EW, Stenroos ES, Johnson WG, Madura K. Ataxin-3 interactions with rad23 and valosin-containing protein and its associations with ubiquitin chains and the proteasome are consistent with a role in ubiquitin-mediated proteolysis. Mol Cell Biol. 23(18):6469-83 (2003)

249. Zhong X, Pittman RN. Ataxin-3 binds VCP/p97 and regulates retrotranslocation of ERAD substrates. Hum Mol Genet. 15(16):2409-20 (2006)

250. Rodrigues AJ, Neves-Carvalho A, Ferro A, Rokka A, Corthals G, et al. ATX-3, CDC-48 and UBXN-5: a new trimolecular complex in Caenorhabditis elegans. Biochem Biophys Res Commun. 386(4):575-81 (2009)

251. Connell P, Ballinger CA, Jiang J, Wu Y, Thompson LJ, et al. The co-chaperone CHIP regulates protein triage decisions mediated by heat-shock proteins. Nat Cell Biol. 3(1):93-6 (2001)

252. Jana NR, Dikshit P, Goswami A, Kotliarova S, Murata S, et al. Co-chaperone CHIP associates with expanded polyglutamine protein and promotes their degradation by proteasomes. J Biol Chem. 280(12):11635-40 (2005)

253. Cemal CK, Carroll CJ, Lawrence L, Lowrie MB, Ruddle P, et al. YAC transgenic mice carrying pathological alleles of the MJD1 locus exhibit a mild and slowly progressive cerebellar deficit. Hum Mol Genet. 11(9):1075-94 (2002)

254. Hasegawa T, Treis A, Patenge N, Fiesel FC, Springer W, Kahle PJ. Parkin protects against tyrosinase-mediated dopamine neurotoxicity by suppressing stress-activated protein kinase pathways. J Neurochem. 105(5):1700-15 (2008)

255. Ulusoy A, Kirik D. Can overexpression of parkin provide a novel strategy for neuroprotection in Parkinson's disease? Exp Neurol. 212(2):258-60 (2008)

256. Yasuda T, Hayakawa H, Nihira T, Ren YR, Nakata Y, et al. Parkin-mediated protection of dopaminergic neurons in a chronic MPTP-minipump mouse model of Parkinson disease. J Neuropathol Exp Neurol. 70(8):686-97 (2011)

257. Nandhu MS, Paul J, Kuruvilla KP, Malat A, Romeo C, Paulose CS. Enhanced glutamate, IP3 and cAMP activity in the cerebral cortex of unilateral 6-hydroxydopamine induced Parkinson's rats: effect of 5-HT, GABA and bone marrow cell supplementation. 18:5 (2011)

258. Perego C, Vanoni C, Bossi M, Massari S, Basudev H, et al. The GLT-1 and GLAST glutamate transporters are expressed on morphologically distinct astrocytes and regulated by neuronal activity in primary hippocampal cocultures. J Neurochem. 75(3):1076-84 (2000)

259. Shehadeh J, Fernandes HB, Zeron Mullins MM, Graham RK, Leavitt BR, et al. Striatal neuronal apoptosis is preferentially enhanced by NMDA receptor activation in YAC transgenic mouse model of Huntington disease. Neurobiol Dis. 21(2):392-403 (2006)

260. Tang TS, Slow E, Lupu V, Stavrovskaya IG, Sugimori M, et al. Disturbed Ca2+ signaling and apoptosis of medium spiny neurons in Huntington's disease. Proc Natl Acad Sci U S A. 102(7):2602-7 (2005)

261. Taylor-Robinson SD, Weeks RA, Bryant DJ, Sargentoni J, Marcus CD, et al. Proton magnetic resonance spectroscopy in Huntington's disease: evidence in favour of the glutamate excitotoxic theory. Mov Disord. 11(2):167-73 (1996)

262. Benn CL, Slow EJ, Farrell LA, Graham R, Deng Y, et al. Glutamate receptor abnormalities in the YAC128 transgenic mouse model of Huntington's disease. Neuroscience. 147(2):354-72(2007)

263. Zhang H, Li Q, Graham RK, Slow E, Hayden MR, Bezprozvanny I. Full length mutant huntingtin is required for altered Ca2+ signaling and apoptosis of striatal neurons in the YAC mouse model of Huntington's disease. Neurobiol Dis. 31(1):80-8 (2008)

264. Dueñas AM, Goold R, Giunti P. Molecular pathogenesis of spinocerebellar ataxias. Brain. 129(Pt 6):1357-70 (2006)

265. Polyglutamine diseases: where does toxicity come from? what is toxicity? where are we going? Takahashi T, Katada S, Onodera O. J Mol Cell Biol. 2(4):180-91 (2010)

266. Orrenius S, Zhivotovsky B, Nicotera P. Regulation of cell death: the calcium-apoptosis link. Nat Rev Mol Cell Biol. 4(7):552-65 (2003)

267. Patterson RL, Boehning D, Snyder SH. Inositol 1,4,5-trisphosphate receptors as signal integrators. Annu Rev Biochem. 73:437-65 (2004)

268. Chen X, Tang TS, Tu H, Nelson O, Pook M, et al. Deranged calcium signaling and neurodegeneration in spinocerebellar ataxia type 3. J Neurosci. 28(48):12713-24 (2008)

269. Choi DW. Glutamate neurotoxicity and diseases of the nervous system. Neuron. 1(8):623-34 (1988)

270. Lipton SA, Rosenberg PA. Excitatory amino acids as a final common pathway for neurologic disorders. N Engl J Med. 330(9):613-22 (1994)

271. Lewén A, Li GL, Olsson Y, Hillered L. Changes in microtubule-associated protein 2 and amyloid precursor protein immunoreactivity following traumatic brain injury in rat: influence of MK-801 treatment. 719(1-2):161-71 (1996)

272. Erlander MG, Tillakaratne NJ, Feldblum S, Patel N, Tobin AJ. Two genes encode distinct glutamate decarboxylases. Neuron. 7(1):91-100 (1991)

273. Nathan B, Floor E, Kuo CY, Wu JY. Synaptic vesicle-associated glutamate decarboxylase: identification and relationship to insulin-dependent diabetes mellitus. J Neurosci Res. 40(1):134-7 (1995)

274. Hsu CC, Thomas C, Chen W, Davis KM, Foos T, et al. Role of synaptic vesicle proton gradient and protein phosphorylation on ATP-mediated activation of membrane-associated brain glutamate decarboxylase. J Biol Chem. 274(34):24366-71 (1999)

275. Reetz A, Solimena M, Matteoli M, Folli F, et al. GABA and pancreatic beta-cells: colocalization of glutamic acid decarboxylase (GAD) and GABA with synaptic-like microvesicles suggests their role in GABA storage and secretion. EMBO J. 10(5):1275-84 (1991)

276. Jin H, Wu H, Osterhaus G, Wei J, Davis K, et al. Demonstration of functional coupling between gamma -aminobutyric acid (GABA) synthesis and vesicular GABA transport into synaptic vesicles. Proc Natl Acad Sci U S A. 100(7):4293-8 (2003)

277. Wu H, Jin Y, Buddhala C, Osterhaus G, Cohen E, et al. Role of glutamate decarboxylase (GAD) isoform, GAD65, in GABA synthesis and transport into synaptic vesicles-Evidence from GAD65-knockout mice studies. 1154:80-3 (2007)

278. Asada H, Kawamura Y, Maruyama K, Kume H, Ding R, et al. Mice lacking the 65 kDa isoform of glutamic acid decarboxylase (GAD65) maintain normal levels of GAD67 and GABA in their brains but are susceptible to seizures. Biochem Biophys Res Commun. 229(3):891-5 (1996)

279. Kaufman DL, Houser CR, Tobin AJ. Two forms of the gamma-aminobutyric acid synthetic enzyme glutamate decarboxylase have distinct intraneuronal distributions and cofactor interactions. J Neurochem. 56(2):720-3 (1991)

280. Lernmark A. Glutamic acid decarboxylase--gene to antigen to disease. J Intern Med. 240(5):259-77 (1996)

281. Tatsuta T, Langer T. Quality control of mitochondria: protection against neurodegeneration and ageing. EMBO J. (2008)

282. Sha D, Jin Y, Wu H, Wei J, Lin CH, et al. Role of mu-calpain in proteolytic cleavage of brain L-glutamic acid decarboxylase. Brain Res. 1207:9-18 (2008)

283. Wei J, Lin CH, Wu H, Jin Y, Lee YH, Wu JY. Activity-dependent cleavage of brain glutamic acid decarboxylase 65 by calpain. J Neurochem. 98(5):1688-95 (2006)

284. Monnerie H, Le Roux PD. Glutamate alteration of glutamic acid decarboxylase (GAD) in GABAergic neurons: the role of cysteine proteases. Exp Neurol. 213(1):145-53 (2008)

285. Monnerie H, Le Roux PD. Reduced dendrite growth and altered glutamic acid decarboxylase (GAD) 65- and 67-kDa isoform protein expression from mouse cortical GABAergic neurons following excitotoxic injury in vitro. Exp Neurol.205(2):367-82 (2007)

286. Ge P, Luo Y, Liu CL, Hu B. Protein aggregation and proteasome dysfunction after brain ischemia. Stroke. 38(12):3230-6 (2007)

287. Phillips JB, Williams AJ, Adams J, Elliott PJ, Tortella FC. Proteasome inhibitor PS519 reduces infarction and attenuates leukocyte infiltration in a rat model of focal cerebral ischemia. Stroke. 31(7):1686-93 (2000)

288. Williams AJ, Hale SL, Moffett JR, Dave JR, Elliott PJ, et al. Delayed treatment with MLN519 reduces infarction and associated neurologic deficit caused by focal ischemic brain injury in rats via antiinflammatory mechanisms involving nuclear factor-kappaB activation, gliosis, and leukocyte infiltration. J Cereb Blood Flow Metab. 23(1):75-87 (2003)

289. Zhang L, Zhang ZG, Zhang RL, Lu M, Adams J, et al. Postischemic (6-Hour) treatment with recombinant human tissue plasminogen activator and proteasome inhibitor PS-519 reduces infarction in a rat model of embolic focal cerebral ischemia. Stroke. 32(12):2926-31 (2001)

290. Caldeira MV, Curcio M, Leal G, Salazar IL, Mele M, et al. Excitotoxic stimulation downregulates the ubiquitin-proteasome system through activation of NMDA receptors in cultured hippocampal neurons. Biochim Biophys Acta. 1832(1):263-74 (2013)

291. Adams J, Kauffman M. Development of the proteasome inhibitor Velcade (Bortezomib). Cancer Invest. 22(2):304-11 (2004)

292. Chen FT, Yang CM, Yang CH. The protective effects of the proteasome inhibitor bortezomib (velcade) on ischemia-reperfusion injury in the rat retina. PLoS One. 8(5):e64262 (2013)

293. Yu X, Kem DC. Proteasome inhibition during myocardial infarction. Cardiovasc Res. 85(2):312-20 (2010)

294. Sanduja S, Kaza V, Dixon DA. The mRNA decay factor tristetraprolin (TTP) induces senescence in human papillomavirus-transformed cervical cancer cells by targeting E6-AP ubiquitin ligase. Aging (Albany NY). 1(9):803-17 (2009)

295. Eldridge AG, O'Brien T. Therapeutic strategies within the ubiquitin proteasome system. Cell Death Differ. 17(1):4-13 (2010)

296. Ardley HC, Robinson PA. The role of ubiquitin-protein ligases in neurodegenerative disease. Neurodegener Dis. 1(2-3):71-87 (2004)

297. Dikshit P, Jana NR. Role of ubiquitin protein ligases in the pathogenesis of polyglutamine diseases. Neurochem Res. 33(5):945-51 (2008)

298. Katsuno M, Sang C, Adachi H, Minamiyama M, Waza M, et al. Pharmacological induction of heat-shock proteins alleviates polyglutamine-mediated motor neuron disease. Proc Natl Acad Sci U S A. 102(46):16801-6 (2005)

299. Yasuda H, Shichinohe H, Kuroda S, Ishikawa T, Iwasaki Y. Neuroprotective effect of a heat shock protein inducer, geranylgeranylacetone in permanent focal cerebral ischemia. Brain Res. 1032(1-2):176-82 (2005)

300. Herbst M, Wanker EE. Small molecule inducers of heat-shock response reduce polyQ-mediated huntingtin aggregation. A possible therapeutic strategy. Neurodegener Dis. 4(2-3):254-60 (2007)

301. Bukau B, Weissman J, Horwich A. Molecular chaperones and protein quality control. Cell. 125(3):443-51 (2006)

302. Hartl FU, Hayer-Hartl M. Molecular chaperones in the cytosol: from nascent chain to folded protein. Science. 295(5561):1852-8 (2002)

303. Parcellier A, Gurbuxani S, Schmitt E, Solary E, Garrido C. Heat shock proteins, cellular chaperones that modulate mitochondrial cell death pathways. Biochem Biophys Res Commun. 304(3):505-12 (2003)

304. Levy-Rimler G, Bell RE, Ben-Tal N, Azem A. Type I chaperonins: not all are created equal. FEBS Lett. 529(1):1-5 (2002)

305. Gupta RS, Venner TJ, Chopra A. Genetic and biochemical studies with mutants of mammalian cells affected in microtubule-related proteins other than tubulin: mitochondrial localization of a microtubule-related protein. Can J Biochem Cell Biol. 63(6):489-502 (1985)

306. Picketts DJ, Mayanil CS, Gupta RS. Molecular cloning of a Chinese hamster mitochondrial protein related to the "chaperonin" family of bacterial and plant proteins. J Biol Chem. 264(20):12001-8 (1989)

307. Singh B, Patel HV, Ridley RG, Freeman KB, Gupta RS. Mitochondrial import of the human chaperonin (HSP60) protein. Biochem Biophys Res Commun. 169(2):391-6 (1990)

308. Itoh H, Kobayashi R, Wakui H, Komatsuda A, Ohtani H, et al. Mammalian 60-kDa stress protein (chaperonin homolog). Identification, biochemical properties, and localization. J Biol Chem. 270(22):13429-35 (1995)

309. Hartl FU, Hayer-Hartl M. Converging concepts of protein folding in vitro and in vivo. Nat Struct Mol Biol. 16(6):574-81 (2009)

310. Mayhew M, da Silva AC, Martin J, Erdjument-Bromage H, Tempst P, Hartl FU. Protein folding in the central cavity of the GroEL-GroES chaperonin complex. Nature. 379(6564):420-6 (1996)

311. Horwich AL, Farr GW, Fenton WA. GroEL-GroES-mediated protein folding. Chem Rev. 106(5):1917-30 (2006)

312. Horovitz A. Structural aspects of GroEL function. Curr Opin Struct Biol. 8(1):93-100 (1998)

313. Paulson HL, Perez MK, Trottier Y, Trojanowski JQ, Subramony SH, et al. Intranuclear inclusions of expanded polyglutamine protein in spinocerebellar ataxia type 3. Neuron. 19(2):333-44 (1997)

314. Chiti F, Dobson CM. Protein misfolding, functional amyloid, and human disease. Annu Rev Biochem. 75:333-66 (2006)

315. Lim J, Crespo-Barreto J, Jafar-Nejad P, Bowman AB, Richman R, et al. Opposing effects of polyglutamine expansion on native protein complexes contribute to SCA1. Nature. 452(7188):713-8 (2008)

316. Schiffer NW, Céraline J, Hartl FU, Broadley SA. N-terminal polyglutamine-containing fragments inhibit androgen receptor transactivation function. Biol Chem. 389(12):1455-66 (2008)

317. Broadley SA, Hartl FU. The role of molecular chaperones in human misfolding diseases. FEBS Lett. 583(16):2647-53 (2009)

318. Barral JM, Broadley SA, Schaffar G, Hartl FU. Roles of molecular chaperones in protein misfolding diseases. Semin Cell Dev Biol. 15(1):17-29 (2004)

319. Muchowski PJ, Wacker JL. Modulation of neurodegeneration by molecular chaperones. Nat Rev Neurosci. 6(1):11-22 (2005)

320. Bross P, Naundrup S, Hansen J, Nielsen MN, Christensen JH, et al. The Hsp60-(p.V98I) mutation associated with hereditary spastic paraplegia SPG13 compromises chaperonin function both in vitro and in vivo. J Biol Chem. 283(23):15694-700 (2008)

321. Hansen JJ, Dürr A, Cournu-Rebeix I, Georgopoulos C, Ang D, et al. Hereditary spastic paraplegia SPG13 is associated with a mutation in the gene encoding the mitochondrial chaperonin Hsp60. 70(5):1328-32 (2002)

322. Magen D, Georgopoulos C, Bross P, Ang D, Segev Y, et al. Mitochondrial hsp60 chaperonopathy causes an autosomal-recessive neurodegenerative disorder linked to brain hypomyelination and leukodystrophy. Am J Hum Genet. 83(1):30-42 (2008)

323. Parnas A, Nadler M, Nisemblat S, Horovitz A, Mandel H, Azem A. The MitCHAP-60 disease is due to entropic destabilization of the human mitochondrial Hsp60 oligomer. J Biol Chem. 284(41):28198-203 (2009)

324. Gales L, Cortes L, Almeida C, Melo CV, Costa MC, et al. Towards a structural understanding of the fibrillization pathway in Machado-Joseph's disease: trapping early oligomers of non-expanded ataxin-3. J Mol Biol. 353(3):642-54 (2005)

325. Viitanen PV, Lorimer G, Bergmeier W, Weiss C, Kessel M, Goloubinoff P. Purification of mammalian mitochondrial chaperonin 60 through in vitro reconstitution of active oligomers. Methods Enzymol. 290:203-17 (1998)

326. Biedler JL, Roffler-Tarlov S, Schachner M, Freedman LS. Multiple neurotransmitter synthesis by human neuroblastoma cell lines and clones. Cancer Res. 38(11 Pt 1):3751-7 (1978)

327. Kaplan DR, Matsumoto K, Lucarelli E, Thiele CJ. Induction of TrkB by retinoic acid mediates biologic responsiveness to BDNF and differentiation of human neuroblastoma cells. Eukaryotic Signal Transduction Group. Neuron. 11(2):321-31 (1993)

328. Cuende J, Moreno S, Bolaños JP, Almeida A. Retinoic acid downregulates Rae1 leading to APC(Cdh1) activation and neuroblastoma SH-SY5Y differentiation. Oncogene. 27(23):3339-44 (2008)

329. Miloso M, Villa D, Crimi M, Galbiati S, Donzelli E, et al. Retinoic acid-induced neuritogenesis of human neuroblastoma SH-SY5Y cells is ERK independent and PKC dependent. J Neurosci Res. 75(2):241-52. (2004)

330. Rossino P, Defilippi P, Silengo L, Tarone G. Up-regulation of the integrin alpha 1/beta 1 in human neuroblastoma cells differentiated by retinoic acid: correlation with increased neurite outgrowth response to laminin. Cell Regul. 2(12):1021-33 (1991)

331. Chakravarthy B, Gaudet C, Ménard M, Atkinson T, Brown L, et al. Amyloid-beta peptides stimulate the expression of the p75(NTR) neurotrophin receptor in SHSY5Y human neuroblastoma cells and AD transgenic mice. J Alzheimers Dis. 19(3):915-25 (2010)

332. Cao W, Huang J, Wu J, Cao G, He Y, et al. Study of 99mTc-annexin V uptake in apoptotic cell models of Parkinson's disease. Nucl Med Commun. 28(12):895-901 (2007)

333. Min HJ, Ko EA, Wu J, Kim ES, Kwon MK, et al. Chaperone-like activity of high-mobility group box 1 protein and its role in reducing the formation of polyglutamine aggregates. J Immunol. 190(4):1797-806 (2013)

334. Soltys BJ, Gupta RS. Immunoelectron microscopic localization of the 60-kDa heat shock chaperonin protein (Hsp60) in mammalian cells. Exp Cell Res. 222(1):16-27 (1996)

335. Tait D, Riccio M, Sittler A, Scherzinger E, Santi S, et al. Ataxin-3 is transported into the nucleus and associates with the nuclear matrix. Hum Mol Genet. 7(6):991-7 (1998)

336. Landry SJ, Taher A, Georgopoulos C, van der Vies SM. Interplay of structure and disorder in cochaperonin mobile loops. Proc Natl Acad Sci U S A. 93(21):11622-7 (1996)

337. Landry SJ, Zeilstra-Ryalls J, Fayet O, Georgopoulos C, Gierasch LM. Characterization of a functionally important mobile domain of GroES. Nature. 364(6434):255-8 (1993)

338. Ellis RJ. Molecular chaperones. Opening and closing the Anfinsen cage. Curr Biol. 4(7):633-5 (1994)

339. Bukau B, Horwich AL. The Hsp70 and Hsp60 chaperone machines. Cell. 92(3):351-66 (1998)

340. Nielsen KL, Cowan NJ. A single ring is sufficient for productive chaperonin-mediated folding in vivo. Mol Cell. 2(1):93-9 (1998)

341. Viitanen PV, Lorimer GH, Seetharam R, Gupta RS, Oppenheim J, et al. Mammalian mitochondrial chaperonin 60 functions as a single toroidal ring. J Biol Chem. 267(2):695-8 (1992)

342. Todd MJ, Walke S, Lorimer G, Truscott K, Scopes RK. The single-ring Thermoanaerobacter brockii chaperonin 60 (Tbr-EL7) dimerizes to Tbr-EL14.Tbr-ES7 under protein folding conditions. Biochemistry. 34(45):14932-41 (1995)

343. Dickson R, Weiss C, Howard RJ, Alldrick SP, Ellis RJ, et al. Reconstitution of higher plant chloroplast chaperonin 60 tetradecamers active in protein folding. J Biol Chem. 275(16):11829-35 (2000)

344. Levy-Rimler G, Viitanen P, Weiss C, Sharkia R, Greenberg A, et al. The effect of nucleotides and mitochondrial chaperonin 10 on the structure and chaperone activity of mitochondrial chaperonin 60. Eur J Biochem. 268(12):3465-72 (2001)

345. Jindal S, Dudani AK, Singh B, Harley CB, Gupta RS. Primary structure of a human mitochondrial protein homologous to the bacterial and plant chaperonins and to the 65-kilodalton mycobacterial antigen. Mol Cell Biol. 9(5):2279-83 (1989

346. Potschka M. Universal calibration of gel permeation chromatography and determination of molecular shape in solution. Anal Biochem. 162(1):47-64 (1987)

347. Cabré F, Canela EI, Canela MA. Accuracy and precision in the determination of Stokes radii and molecular masses of proteins by gel filtration chromatography. J Chromatogr. 472(2):347-56 (1989)

348. in Zetasizer Nano Series User Manual.

349. Chaiwatanasirikul KA, Sala A. The tumour-suppressive function of CLU is explained by its localisation and interaction with HSP60. Cell Death Dis. 2:e219 (2011)

350. Reina CP, Nabet BY, Young PD, Pittman RN. Basal and stress-induced Hsp70 are modulated by ataxin-3. Cell Stress Chaperones. 17(6):729-42 (2012)

351. Gao XC, Zhou CJ, Zhou ZR, Zhang YH, Zheng XM, et al. Co-chaperone HSJ1a dually regulates the proteasomal degradation of ataxin-3. PLoS One. 6(5):e19763 (2011)

352. Chai Y, Koppenhafer SL, Bonini NM, Paulson HL. Analysis of the role of heat shock protein (Hsp) molecular chaperones in polyglutamine disease. J Neurosci. 19(23):10338-47 (1999)

353. Chun JN, Choi B, Lee KW, Lee DJ, Kang DH, et al. Cytosolic Hsp60 is involved in the NF-kappaB-dependent survival of cancer cells via IKK regulation. PLoS One. 5(3):e9422 (2010)

354. Satoh J, Onoue H, Arima K, Yamamura T. The 14-3-3 protein forms a molecular complex with heat shock protein Hsp60 and cellular prion protein. J Neuropathol Exp Neurol. 64(10):858-68 (2005)

355. Brocchieri L, Karlin S. Conservation among HSP60 sequences in relation to structure, function, and evolution. Protein Sci. 9(3):476-86 (2000)

356. Nielsen KL, McLennan N, Masters M, Cowan NJ. A single-ring mitochondrial chaperonin (Hsp60-Hsp10) can substitute for GroEL-GroES in vivo. J Bacteriol. 181(18):5871-5 (1999)

357. Hartl FU. Molecular chaperones in cellular protein folding. Nature. 381(6583):571-9 (1996)

358. Brinker A, Pfeifer G, Kerner MJ, Naylor DJ, Hartl FU, Hayer-Hartl M. Dual function of protein confinement in chaperonin-assisted protein folding. Cell. 107(2):223-33 (2001)

359. Sun W, Wang L, Jiang H, Chen D, Murchie AI. Targeting mitochondrial transcription in fission yeast with ETB, an inhibitor of HSP60, the chaperone that binds to the mitochondrial transcription factor Mtf1. Genes Cells.17(2):122-31 (2012)

360. Shan YX, Yang TL, Mestril R, Wang PH. Hsp10 and Hsp60 suppress ubiquitination of insulin-like growth factor-1 receptor and augment insulin-like growth factor-1 receptor signaling in cardiac muscle: implications on decreased myocardial protection in diabetic cardiomyopathy. J Biol Chem. 278(46):45492-8 (2003)

361. Alard JE, Hillion S, Guillevin L, Saraux A, Pers JO, et al. Autoantibodies to endothelial cell surface ATP synthase, the endogenous receptor for hsp60, might play a pathogenic role in vasculatides. PLoS One. 6(2):e14654 (2011)

362. Stefano L, Racchetti G, Bianco F, Passini N, Gupta RS, et al. The surface-exposed chaperone, Hsp60, is an agonist of the microglial TREM2 receptor. J Neurochem. 110(1):284-94 (2009)

363. Burian K, Kis Z, Virok D, Endresz V, Prohaszka Z, et al. Independent and joint effects of antibodies to human heat-shock protein 60 and Chlamydia pneumoniae infection in the development of coronary atherosclerosis. Circulation. 103(11):1503-8 (2001)

364. Ohashi K, Burkart V, Flohé S, Kolb H. Cutting edge: heat shock protein 60 is a putative endogenous ligand of the toll-like receptor-4 complex.J Immunol. 164(2):558-61 (2000)

365. Farsi A, Domeneghetti MP, Brunelli T, Gori AM, Fedi S, et al. Activation of the immune system and coronary artery disease: the role of anti-endothelial cell antibodies. Atherosclerosis. 154(2):429-36 (2001)

366. Gupta S, Knowlton AA. HSP60 trafficking in adult cardiac myocytes: role of the exosomal pathway. Am J Physiol Heart Circ Physiol. 292(6):H3052-6 (2007)

367. Hjerpe R, Aillet F, Lopitz-Otsoa F, Lang V, England P, Rodriguez MS. Efficient protection and isolation of ubiquitylated proteins using tandem ubiquitin-binding entities. EMBO Rep. 10(11):1250-8 (2009)

368. Wang H, Ying Z, Wang G. Ataxin-3 regulates aggresome formation of copper-zinc superoxide dismutase (SOD1) by editing K63-linked polyubiquitin chains. J Biol Chem. 287(34):28576-85 (2012)

369. Dedmon MM, Christodoulou J, Wilson MR, Dobson CM. Heat shock protein 70 inhibits alpha-synuclein fibril formation via preferential binding to prefibrillar species. J Biol Chem. 280(15):14733-40 (2005)

370. Jinwal UK, Akoury E, Abisambra JF, O'Leary JC 3rd, Thompson AD, et al. Imbalance of Hsp70 family variants fosters tau accumulation. FASEB J. 27(4):1450-9 (2013)

371. Petrucelli L, Dickson D, Kehoe K, Taylor J, Snyder H, et al. CHIP and Hsp70 regulate tau ubiquitination, degradation and aggregation. Hum Mol Genet. 13(7):703-14 (2004)

372. Veereshwarayya V, Kumar P, Rosen KM, Mestril R, Querfurth HW. Differential effects of mitochondrial heat shock protein 60 and related molecular chaperones to prevent intracellular beta-amyloid-induced inhibition of complex IV and limit apoptosis. J Biol Chem. 281(40):29468-78 (2006)

373. Jana NR, Tanaka M, Wang Gh, Nukina N. Polyglutamine length-dependent interaction of Hsp40 and Hsp70 family chaperones with truncated N-terminal huntingtin: their role

in suppression of aggregation and cellular toxicity. Hum Mol Genet. 9(13):2009-18 (2000)

374. Silva-Fernandes A, Costa Mdo C, Duarte-Silva S, Oliveira P, Botelho CM, et al. Motor uncoordination and neuropathology in a transgenic mouse model of Machado-Joseph disease lacking intranuclear inclusions and ataxin-3 cleavage products. Neurobiol Dis. 40(1):163-76 (2010)

375. Larsen CN, Price JS, Wilkinson KD. Substrate binding and catalysis by ubiquitin C-terminal hydrolases: identification of two active site residues. Biochemistry. 35(21):6735-44 (1996)

376. Nishikawa K, Li H, Kawamura R, Osaka H, Wang YL, et al. Alterations of structure and hydrolase activity of parkinsonism-associated human ubiquitin carboxyl-terminal hydrolase L1 variants. Biochem Biophys Res Commun. 304(1):176-83 (2003)

377. Setsuie R, Wang YL, Mochizuki H, Osaka H, Hayakawa H, et al. Dopaminergic neuronal loss in transgenic mice expressing the Parkinson's disease-associated UCH-L1 I93M mutant. Neurochem Int. 50(1):119-29 (2007)

378. Saigoh K, Wang YL, Suh JG, Yamanishi T, Sakai Y, et al. Intragenic deletion in the gene encoding ubiquitin carboxy-terminal hydrolase in gad mice. Nat Genet. 23(1):47-51 (1999)

379. Chen F, Sugiura Y, Myers KG, Liu Y, Lin W. Ubiquitin carboxyl-terminal hydrolase L1 is required for maintaining the structure and function of the neuromuscular junction. Proc Natl Acad Sci U S A. 107(4):1636-41 (2010)

380. Trinchese F, Liu S, Battaglia F, Walter S, Mathews PM, Arancio O. Progressive age-related development of Alzheimer-like pathology in APP/PS1 mice. Ann Neurol. 55(6):801-14 (2004)

381. Double KL, Dedov VN, Fedorow H, Kettle E, Halliday GM, et al. The comparative biology of neuromelanin and lipofuscin in the human brain. Cell Mol Life Sci. 65(11):1669-82 (2008)

382. Höhn A, Grune T. Lipofuscin: formation, effects and role of macroautophagy. Redox Biol. 1(1):140-144 (2013)

383. Smith WL. Prostanoid biosynthesis and mechanisms of action. Am J Physiol. 263(2 Pt 2):F181-91 (1992)

384. Smith WL. The eicosanoids and their biochemical mechanisms of action. Biochem J. 259(2):315-24 (1989)

385. Abdel-Halim MS, Lundén I, Cseh G, Anggård E. Prostaglandin profiles in nervous tissue and blood vessels of the brain of various animals. Prostaglandins. 19(2):249-58 (1980)

386. Chiu EK, Richardson JS. Behavioral and neurochemical aspects of prostaglandins in brain function. Gen Pharmacol. 16(3):163-75 (1985)

387. Kondo M, Oya-Ito T, Kumagai T, Osawa T, Uchida K. Cyclopentenone prostaglandins as potential inducers of intracellular oxidative stress. J Biol Chem. 276(15):12076-83 (2001)

388. Shibata T, Yamada T, Ishii T, Kumazawa S, Nakamura H, et al. Thioredoxin as a molecular target of cyclopentenone prostaglandins. J Biol Chem. 278(28):26046-54 (2003)

389. Ricciotti E, FitzGerald GA. Prostaglandins and inflammation. Arterioscler Thromb Vasc Biol. 31(5):986-1000 (2011)

390. Nakamura H, Nakamura K, Yodoi J. Redox regulation of cellular activation. Annu Rev Immunol. 15:351-69 (1997)

391. Yodoi J, Uchiyama T. Diseases associated with HTLV-I: virus, IL-2 receptor dysregulation and redox regulation. Immunol Today. 13(10):405-11 (1992)

392. Kikawa Y, Narumiya S, Fukushima M, Wakatsuka H, Hayaishi O. 9-Deoxy-delta 9, delta 12-13,14-dihydroprostaglandin D2, a metabolite of prostaglandin D2 formed in human plasma. Proc Natl Acad Sci U S A. 81(5):1317-21 (1984)

393. Fitzpatrick FA, Wynalda MA. Albumin-catalyzed metabolism of prostaglandin D2. Identification of products formed in vitro. J Biol Chem. 258(19):11713-8 (1983)

394. Liu H, Li W, Ahmad M, Miller TM, Rose ME, et al. Modification of ubiquitin-C-terminal hydrolase-L1 by cyclopentenone prostaglandins exacerbates hypoxic injury. Neurobiol Dis. 41(2):318-28 (2011)

395. Koharudin LM, Liu H, Di Maio R, Kodali RB, Graham SH, Gronenborn AM. Cyclopentenone prostaglandin-induced unfolding and aggregation of the Parkinson disease-associated UCH-L1. Proc Natl Acad Sci U S A. 107(15):6835-40 (2010)

396. Hoang HD, Prasain JK, Dorand D, Miller MA. A heterogeneous mixture of F-series prostaglandins promotes sperm guidance in the Caenorhabditis elegans reproductive tract. PLoS Genet. 9(1):e1003271 (2013)

397. Kubagawa HM, Watts JL, Corrigan C, Edmonds JW, Sztul E, et al. Oocyte signals derived from polyunsaturated fatty acids control sperm recruitment in vivo. 8(10):1143-8 (2006)

398. Prasain JK, Hoang HD, Edmonds JW, Miller MA. Prostaglandin extraction and analysis in Caenorhabditis elegans. J Vis Exp. (76)(2013)

399. Beal MF. Aging, energy, and oxidative stress in neurodegenerative diseases. Ann Neurol. 38(3):357-66 (1995)

400. Evert BO, Vogt IR, Kindermann C, Ozimek L, de Vos RA, et al. Inflammatory genes are upregulated in expanded ataxin-3-expressing cell lines and spinocerebellar ataxia type 3 brains. 21(15):5389-96 (2001)

401. Yu YC, Kuo CL, Cheng WL, Liu CS, Hsieh M. Decreased antioxidant enzyme activity and increased mitochondrial DNA damage in cellular models of Machado-Joseph disease. J Neurosci Res. 87(8):1884-91 (2009)

402. Araujo J, Breuer P, Dieringer S, Krauss S, Dorn S, et al. FOXO4-dependent upregulation of superoxide dismutase-2 in response to oxidative stress is impaired in spinocerebellar ataxia type 3. Hum Mol Genet. 20(15):2928-41 (2011)

403. Pacheco LS, da Silveira AF, Trott A, Houenou LJ, Algarve TD, et al. Association between Machado-Joseph disease and oxidative stress biomarkers. Mutat Res. pii: S1383-5718(13)00229-5 (2013)

404. Paulson HL, Das SS, Crino PB, Perez MK, Patel SC, et al. Machado-Joseph disease gene product is a cytoplasmic protein widely expressed in brain. 41(4):453-62 (1997)

405. Schmidt T, Landwehrmeyer GB, Schmitt I, Trottier Y, Auburger G, et al. An isoform of ataxin-3 accumulates in the nucleus of neuronal cells in affected brain regions of SCA3 patients. Brain Pathol. 8(4):669-79 (1998)

406. Warrick JM, Chan HY, Gray-Board GL, Chai Y, Paulson HL, Bonini NM. Suppression of polyglutamine-mediated neurodegeneration in Drosophila by the molecular chaperone HSP70. Nat Genet. 23(4):425-8 (1999)

407. Bajetto A, Bonavia R, Barbero S, Piccioli P, Costa A, et al. Glial and neuronal cells express functional chemokine receptor CXCR4 and its natural ligand stromal cell-derived factor 1. J Neurochem. 73(6):2348-57 (1999)

408. Reikerstorfer A, Holz H, Stunnenberg HG, Busslinger M. Low affinity binding of interleukin-1 beta and intracellular signaling via NF-kappa B identify Fit-1 as a distant member of the interleukin-1 receptor family. 270(30):17645-8 (1995)

409. Furukawa-Hibi Y, Kobayashi Y, Chen C, Motoyama N. FOXO transcription factors in cell-cycle regulation and the response to oxidative stress. Antioxid Redox Signal. 7(5-6):752-60 (2005)

410. Brenner S. The genetics of Caenorhabditis elegans. Genetics. 77(1):71-94 (1974)

411. Lewis JA, Fleming JT. Basic culture methods. Methods Cell Biol. 48:3-29 (1995)

412. Brignull HR, Moore FE, Tang SJ, Morimoto RI. Polyglutamine proteins at the pathogenic threshold display neuron-specific aggregation in a pan-neuronal Caenorhabditis elegans model. J Neurosci. 26(29):7597-606 (2006)

413. Gidalevitz T, Ben-Zvi A, Ho KH, Brignull HR, Morimoto RI. Progressive disruption of cellular protein folding in models of polyglutamine diseases. Science. 311(5766):1471-4 (2006)

414. An image processing aplication for quantification of protein aggregates in Caenorhabditis elegans. In 5thInternational Conference on Pratical Applications of Computional Biology and Bioinformatics. Advances in Soft Computing. Springer, Vol. 93, pp. 31-38

415. Kawasaki H, Springett GM, Toki S, Canales JJ, Harlan P, et al. A Rap guanine nucleotide exchange factor enriched highly in the basal ganglia. Proc Natl Acad Sci U S A. 95(22):13278-83 (1998)

416. Halliwell B. Oxidative stress and cancer: have we moved forward? Biochem J. 401(1):1-11 (2007)

417. Bowerman B, Eaton BA, Priess JR. skn-1, a maternally expressed gene required to specify the fate of ventral blastomeres in the early C. elegans embryo. Cell. 68(6):1061-75 (1992)

418. An JH, Blackwell TK. SKN-1 links C. elegans mesendodermal specification to a conserved oxidative stress response. Genes Dev. 17(15):1882-93 (2003)

419. Toone WM, Jones N. AP-1 transcription factors in yeast. Curr Opin Genet Dev. 9(1):55-61 (1999)

420. Hayes JD, McMahon M. Molecular basis for the contribution of the antioxidant responsive element to cancer chemoprevention. Cancer Lett. 174(2):103-13 (2001)

421. Thimmulappa RK, Mai KH, Srisuma S, Kensler TW, Yamamoto M, Biswal S. Identification of Nrf2-regulated genes induced by the chemopreventive agent sulforaphane by oligonucleotide microarray. 62(18):5196-203 (2002)

422. Yoneda T, Benedetti C, Urano F, Clark SG, Harding HP, Ron D. Compartment-specific perturbation of protein handling activates genes encoding mitochondrial chaperones. J Cell Sci. 117(Pt 18):4055-66 (2004)

423. Li Z, Melandri F, Berdo I, Jansen M, Hunter L, et al. Delta12-Prostaglandin J2 inhibits the ubiquitin hydrolase UCH-L1 and elicits ubiquitin-protein aggregation without proteasome inhibition. Biochem Biophys Res Commun. 319(4):1171-80 (2004)

424. Pimentel C, Batista-Nascimento L, Rodrigues-Pousada C, Menezes RA. Oxidative stress in Alzheimer's and Parkinson's diseases: insights from the yeast Saccharomyces cerevisiae. Oxid Med Cell Longev. 2012:132146 (2012)

425. Rockwell P, Yuan H, Magnusson R, Figueiredo-Pereira ME. Proteasome inhibition in neuronal cells induces a proinflammatory response manifested by upregulation of cyclooxygenase-2, its accumulation as ubiquitin conjugates, and production of the prostaglandin PGE(2). Arch Biochem Biophys. 374(2):325-33 (2000)

426. Simmons DL, Botting RM, Hla T. Cyclooxygenase isozymes: the biology of prostaglandin synthesis and inhibition. Pharmacol Rev. 56(3):387-437 (2004)

427. Kurihara LJ, Semenova E, Levorse JM, Tilghman SM. Expression and functional analysis of Uch-L3 during mouse development. Mol Cell Biol. 20(7):2498-504 (2000)

428. Kurihara LJ, Kikuchi T, Wada K, Tilghman SM. Loss of Uch-L1 and Uch-L3 leads to neurodegeneration, posterior paralysis and dysphagia. Hum Mol Genet. 10(18):1963-70 (2001)

429. Gardoni F, Di Luca M. New targets for pharmacological intervention in the glutamatergic synapse. Eur J Pharmacol. 545:2-10 (2006)

430. Carvalho AP, Ferreira IL, Carvalho AL, Duarte CB. Glutamate receptor modulation of [3H]GABA release and intracellular calcium in chick retina cells. Ann N Y Acad Sci. 757:439-456 (1995)

431. Saransaari P, Oja SS GABA release under normal and ischemic conditions. Neurochem Res. 33:962-969 (2008)

432. Schwartz-Bloom RD, Sah R. gamma-Aminobutyric acidA neurotransmission and cerebral ischemia. J Neurochem. 77:353-371 (2001)

433. Vemuganti R. Decreased expression of vesicular GABA transporter, but not vesicular glutamate, acetylcholine and monoamine transporters in rat brain following focal ischemia. Neurochem Int. 47:136-142 (2005)

434. Baliova M, Knab A, Franekova V, Jursky F. Modification of the cytosolic regions of GABA transporter GAT1 by calpain. Neurochem Int. 55:288-294 (2009)

435. Bevers MB, Neumar RW. Mechanistic role of calpains in postischemic neurodegeneration. J Cereb Blood Flow Metab. 28:655-673 (2008)

436. Martin DL, Rimvall K. Regulation of gamma-aminobutyric acid synthesis in the brain. J Neurochem. 60:395-407 (1993)

437. Sheikh SN, Martin SB, Martin DL. Regional distribution and relative amounts of glutamate decarboxylase isoforms in rat and mouse brain. Neurochem Int. 35:73-80 (1999)

438. Lernmark A. Glutamic acid decarboxylase--gene to antigen to disease. J Intern Med. 240:259-277 (1996)

439. Vanderklish PW, Bahr BA. The pathogenic activation of calpain: a marker and mediator of cellular toxicity and disease states. Int J Exp Pathol. 81:323-339 (2000)

440. Herrmann J, Lerman LO, Lerman A. Ubiquitin and ubiquitin-like proteins in protein regulation. Circ Res. 100:1276-1291 (2007)

441. Asai A, Tanahashi N, Qiu JH, Saito N, Chi S, et al. Selective proteasomal dysfunction in the hippocampal CA1 region after transient forebrain ischemia. J Cereb Blood Flow Metab. 22:705-710 (2002)

442. Solimena M, Dirkx Jr. R, Radzynski M, Mundigl O, De Camilli P. A signal located within amino acids 1-27 of GAD65 is required for its targeting to the Golgi complex region. J Cell Biol. 126:331-341 (1994)

443. Santos AR, Duarte CB. Validation of internal control genes for expression studies: effects of the neurotrophin BDNF on hippocampal neurons. J Neurosci Res. 86:3684-3692 (2008)

444. Kubista K, Sindelka R, Tichopad A, Bergkvist A, Lindh D, et al. The prime technique: real-time PCR data analysis, G.I.T. Laboratory Journal. 9: 2 (2007)

445. Bahr BA. Integrin-type signaling has a distinct influence on NMDA-induced cytoskeletal disassembly. J Neurosci Res. 59: 827-832 (2000)

446. Munirathinam S, Rogers G, Bahr BA. Positive modulation of alpha-amino-3-hydroxy-5-methyl-4-isoxazolepropionic acid-type glutamate receptors elicits neuroprotection after trimethyltin exposure in hippocampus. Toxicol Appl Pharmacol. 185:111-118 (2002)

447. Frick KM, Burlingame LA, Delaney SS, Berger-Sweeney J. Sex differences in neurochemical markers that correlate with behavior in aging mice. Neurobiol Aging 23:145-158 (2002)

448. Almeida RD, Manadas BJ, Melo CV, Gomes JR, Mendes CS, et al. Neuroprotection by BDNF against glutamate-induced apoptotic cell death is mediated by ERK and PI3-kinase pathways. Cell Death Differ. 12: 1329-1343 (2005)

449. Duarte CB, Ferreira IL, Santos PF, Oliveira CR, Carvalho AP. Glutamate increases the [Ca2+]i but stimulates Ca2+-independent release of [3H]GABA in cultured chick retina cells. Brain Res. 611: 130-138 (1993)

450. Swanwick CC, Harrison MB, Kapur J. Synaptic and extrasynaptic localization of brain-derived neurotrophic factor and the tyrosine kinase B receptor in cultured hippocampal neurons. J Comp Neurol. 478:405-417 (2004)

451. Kisselev AF, Goldberg AL. Proteasome inhibitors: from research tools to drug candidates. Chem Biol. 8:739-758 (2001)

452. Rock KL, Gramm C, Rothstein L, Clark K, Stein R, et al. Inhibitors of the proteasome block the degradation of most cell proteins and the generation of peptides presented on MHC class I molecules. Cell 78:761-771 (1994)

453. Myung J, Kim KB, Crews CM. The ubiquitin-proteasome pathway and proteasome inhibitors. Med Res Rev. 21: 245-273 (2001)

454. Rideout HJ, Stefanis L Proteasomal inhibition-induced inclusion formation and death in cortical neurons require transcription and ubiquitination. Mol Cell Neurosci. 21:223-238 (2002)

455. Butts BD, Hudson HR, Linseman DA, Le SS, Ryan KR, et al. Proteasome inhibition elicits a biphasic effect on neuronal apoptosis via differential regulation of pro-survival and pro-apoptotic transcription factors. Mol Cell Neurosci. 30:279-289 (2005)

456. Myung J, Kim KB, Lindsten K, Dantuma NP, Crews CM. Lack of proteasome active site allostery as revealed by subunit-specific inhibitors. Mol Cell. 7:411-420 (2001)

457. Yang Y, Kitagaki J, Dai RM, Tsai YC, Lorick KL, et al. Inhibitors of ubiquitin-activating enzyme (E1), a new class of potential cancer therapeutics. Cancer Res. 67:9472-9481 (2007)

458. Caba E, Brown QB, Kawasaki B, Bahr BA. Peptidyl alpha-keto amide inhibitor of calpain blocks excitotoxic damage without affecting signal transduction events. J Neurosci Res 67:787-794 (2002)

459. Sorokin AV, Selyutina AA, Skabkin MA, Guryanov SG, Nazimov IV, et al. Proteasome-mediated cleavage of the Y-box-binding protein 1 is linked to DNA-damage stress response. EMBO J. 24:3602-3612 (2005)

460. Baugh JM, Pilipenko EV. 20S proteasome differentially alters translation of different mRNAs via the cleavage of eIF4F and eIF3. Mol Cell. 16:575-586 (2004)

461. Martin SB, Waniewski RA, Battaglioli G, Martin DL. Post-mortem degradation of brain glutamate decarboxylase. Neurochem Int. 42:549-554 (2003)

462. Hsu CC, Davis KM, Jin H, Foos T, Floor E, et al. Association of L-glutamic acid decarboxylase to the 70-kDa heat shock protein as a potential anchoring mechanism to synaptic vesicles. J Biol Chem. 275:20822-20828 (2000)

463. Esclapez M, Tillakaratne NJ, Kaufman DL, Tobin AJ, Houser CR. Comparative localization of two forms of glutamic acid decarboxylase and their mRNAs in rat brain supports the concept of functional differences between the forms. J Neurosci. 14:1834-1855 (1994)

464. Battaglioli G, Liu H, Hauer CR, Martin DL. Glutamate decarboxylase: loss of N-terminal segment does not affect homodimerization and determination of the oxidation state of cysteine residues. Neurochem Res. 30, 989-1001 (2005)

465. Fenalti G, Law RH, Buckle AM, Langendorf C, Tuck K, et al. GABA production by glutamic acid decarboxylase is regulated by a dynamic catalytic loop. Nat Struct Mol Biol. 14:280-286 (2007)

466. Salin P, Chesselet MF Expression of GAD (Mr 67,000) and its messenger RNA in basal ganglia and cerebral cortex after ischemic cortical lesions in rats. Exp Neurol. 119:291-301 (1993)

467. Qin ZH, Zhang SP, Weiss B. Dopaminergic and glutamatergic blocking drugs differentially regulate glutamic acid decarboxylase mRNA in mouse brain. Brain Res Mol Brain Res. 21:293-302 (1994)

468. Jackman RW, Kandarian SC. The molecular basis of skeletal muscle atrophy. Am J Physiol Cell Physiol. 287:C834-843 (2004)

469. Bartoli M, Richard I. Calpains in muscle wasting. Int J Biochem Cell Biol. 37:2115-2133 (2005)

470. Alkalay I, Yaron A, Hatzubai A, Orian A, Ciechanover A, et al. Stimulation-dependent I kappa B alpha phosphorylation marks the NF-kappa B inhibitor for degradation via the ubiquitin-proteasome pathway. Proc Natl Acad Sci U S A. 92:10599-10603 (1995)

471. Scherer DC, Brockman JA, Chen Z, Maniatis T, Ballard DW. Signal-induced degradation of I kappa B alpha requires site-specific ubiquitination. Proc Natl Acad Sci U S A. 92:11259-11263 (1995)

472. Chen F, Lu Y, Kuhn DC, Maki M, Shi X, et al. Calpain contributes to silica-induced I kappa B-alpha degradation and nuclear factor-kappa B activation. Arch Biochem Biophys. 342:383-388 (1997)

473. Di Napoli M, McLaughlin B. The ubiquitin-proteasome system as a drug target in cerebrovascular disease: therapeutic potential of proteasome inhibitors. Curr Opin Investig Drugs. 6:686-699 (2005)

474. Ray SK. Currently evaluated calpain and caspase inhibitors for neuroprotection in experimental brain ischemia. Curr Med Chem. 13:3425-3440 (2006)

475. Noga M, Hayashi T. Ubiquitin gene expression following transient forebrain ischemia. Brain Res Mol Brain Res. 36:261-267 (1996)

476. Vannucci SJ, Mummery R, Hawkes RB, Rider CC, Beesley PW. Hypoxia-ischemia induces a rapid elevation of ubiquitin conjugate levels and ubiquitin immunoreactivity in the immature rat brain. J Cereb Blood Flow Metab. 18:376-385 (1998)

477. Liu CL, Martone ME, Hu BR. Protein ubiquitination in postsynaptic densities after transient cerebral ischemia. J Cereb Blood Flow Metab. 24:1219-1225 (2004)

478. Shah IM, Lees KR, Pien CP, Elliott PJ. Early clinical experience with the novel proteasome inhibitor PS-519. Br J Clin Pharmacol. 54:269-276 (2002)

479. Wei J, Jin Y, Wu H, Sha D, Wu JY. Identification and functional analysis of truncated human glutamic acid decarboxylase 65. J Biomed Sci. 10:617-624 (2003)

480. Wei J, Wu JY. Post-translational regulation of L-glutamic acid decarboxylase in the brain. Neurochem Res. 33:1459-1465 (2008)

481. de Almeida OM, Gardino PF, Loureiro dos Santos NE, Yamasaki EN, de Mello MC et al. Opposite roles of GABA and excitatory amino acids on the control of GAD expression in cultured retina cells. Brain Res. 925:89-99 (2002)

482. de Mello FG, Hokoc JN, Ventura AL, Gardino PF. Glutamic acid decarboxylase of embryonic avian retina cells in culture: regulation by gamma-aminobutyric acid (GABA). Cell Mol Neurobiol. 11:485-496 (1991)

483. Kanaani J, el-Husseini Ael-D, Aguilera-Moreno A, Diacovo JM, Bredt DS, et al. A combination of three distinct trafficking signals mediates axonal targeting and presynaptic clustering of GAD65. J Cell Biol. 158:1229-1238 (2002)

484. Kanaani J, Patterson G, Schaufele F, Lippincott-Schwartz J, Baekkeskov S. A palmitoylation cycle dynamically regulates partitioning of the GABA-synthesizing

enzyme GAD65 between ER-Golgi and post-Golgi membranes. J Cell Sci. 121:437-449 (2008)

485. Soghomonian JJ, Martin DL. Two isoforms of glutamate decarboxylase: why? Trends Pharmacol Sci. 19:500-505 (1998)

486. de Pril R, Fischer DF, Maat-Schieman ML, Hobo B, de Vos RA, Brunt ER, Hol EM, Roos RA, van Leeuwen FW. Accumulation of aberrant ubiquitin induces aggregate formation and cell death in polyglutamine diseases. Hum Mol Genet. 13(16):1803-13 (2004)

487. Li XJ, Li S. Proteasomal dysfunction in aging and Huntington disease. Neurobiol Dis. 43(1):4-8 (2011)

488. Bar-Lavan Y, Kosolapov L, Frumkin A, Ben-Zvi A. Regulation of cellular protein quality control networks in a multicellular organism. FEBS J. 279(4):526-31 (2012)

489. Hartl FU, Bracher A, Hayer-Hartl M. Molecular chaperones in protein folding and proteostasis. Nature. 475(7356):324-32 (2011)

490. Kettern N, Dreiseidler M, Tawo R, Höhfeld J. Chaperone-assisted degradation: multiple paths to destruction. Biol Chem. 391(5):481-9 (2010)

491. Powers ET, Morimoto RI, Dillin A, Kelly JW, Balch WE. Biological and chemical approaches to diseases of proteostasis deficiency. Annu Rev Biochem. 78:959-91 (2009)

492. Gaczynska M, Rock KL, Goldberg AL. Role of proteasomes in antigen presentation. Enzyme Protein. 47(4-6):354-69 (1993)

493. Bender T, Lewrenz I, Franken S, Baitzel C, Voos W. Mitochondrial enzymes are protected from stress-induced aggregation by mitochondrial chaperones and the Pim1/LON protease. 22(5):541-54 (2011)

494. Pozzi C, Valtorta M, Tedeschi G, Galbusera E, Pastori V, Bigi A, Nonnis S, Grassi E, Fusi P. Study of subcellular localization and proteolysis of ataxin-3. Neurobiol Dis. 30(2):190-200 (2008)

495. Nakamura N, Hirose S. Regulation of mitochondrial morphology by USP30, a deubiquitinating enzyme present in the mitochondrial outer membrane. Mol Biol Cell. 19(5):1903-11 (2008)

496. Hassink GC, Zhao B, Sompallae R, Altun M, Gastaldello S, Zinin NV, Masucci MG, Lindsten K. The ER-resident ubiquitin-specific protease 19 participates in the UPR and rescues ERAD substrates. 10(7):755-61 (2009)

497. Nicastro G, Menon RP, Masino L, Knowles PP, McDonald NQ, Pastore A. The solution structure of the Josephin domain of ataxin-3: structural determinants for molecular recognition. Proc Natl Acad Sci U S A. 102(30):10493-8 (2005)

498. Mao Y, Senic-Matuglia F, Di Fiore PP, Polo S, Hodsdon ME, De Camilli P. Deubiquitinating function of ataxin-3: insights from the solution structure of the Josephin domain. 102(36):12700-5 (2005)

499. Li F, Macfarlan T, Pittman RN, Chakravarti D. Ataxin-3 is a histone-binding protein with two independent transcriptional corepressor activities. J Biol Chem. 277(47):45004-12 (2002)

500. Miranda-Vizuete A, Fierro González JC, Gahmon G, Burghoorn J, Navas P, Swoboda P. Lifespan decrease in a Caenorhabditis elegans mutant lacking TRX-1, a thioredoxin expressed in ASJ sensory neurons. FEBS Lett. 580(2):484-90 (2006)

501. Jee C, Vanoaica L, Lee J, Park BJ, Ahnn J. Thioredoxin is related to life span regulation and oxidative stress response in Caenorhabditis elegans. Genes Cells. 10(12):1203-10 (2005)

502. Uchida K, Shibata T. 15-Deoxy-Delta(12,14)-prostaglandin J2: an electrophilic trigger of cellular responses. Chem Res Toxicol. 21(1):138-44 (2008)

503. Kawamoto Y, Nakamura Y, Naito Y, Torii Y, Kumagai T, Osawa T, Ohigashi H, Satoh K, Imagawa M, Uchida K. Cyclopentenone prostaglandins as potential inducers of phase II detoxification enzymes. 15-deoxy-delta(12,14)-prostaglandin j2-induced expression of glutathione S-transferases. J Biol Chem. 275(15):11291-9 (2000)

504. Johnston SC, Larsen CN, Cook WJ, Wilkinson KD, Hill CP. Crystal structure of a deubiquitinating enzyme (human UCH-L3) at 1.8 A resolution. EMBO J. 16(13):3787-96 (1997)

505. Simões AT, Gonçalves N, Koeppen A, Déglon N, Kügler S, Duarte CB, Pereira de Almeida L. Calpastatin-mediated inhibition of calpains in the mouse brain prevents mutant ataxin 3 proteolysis, nuclear localization and aggregation, relieving Machado-Joseph disease. Brain. 135(Pt 8):2428-39 (2012)

506. Koch P, Breuer P, Peitz M, Jungverdorben J, Kesavan J, Poppe D, Doerr J, Ladewig J, Mertens J, Tüting T, Hoffmann P, Klockgether T, Evert BO, Wüllner U, Brüstle O. Excitation-induced ataxin-3 aggregation in neurons from patients with Machado-Joseph disease. Nature. 480(7378):543-6 (2011)

507. Haacke A, Hartl FU, Breuer P. Calpain inhibition is sufficient to suppress aggregation of polyglutamine-expanded ataxin-3. J Biol Chem. 282(26):18851-6 (2007)

508. Hübener J, Weber JJ, Richter C, Honold L, Weiss A, Murad F, Breuer P, Wüllner U, Bellstedt P, Paquet-Durand F, Takano J, Saido TC, Riess O, Nguyen HP. Calpain-mediated ataxin-3 cleavage in the molecular pathogenesis of spinocerebellar ataxia type 3 (SCA3). Hum Mol Genet. 22(3):508-18 (2013)